UNIVERSITY OF SOUTHAMPTON
CIVIL ENGINEERING DEPARTMENT

DEVELOPMENT OF COMPUTER AIDED DESIGN FOR THE EFFECTIVE DESIGN OF MICRO-CATCHMENTS IN ARID CLIMATES

BY

NADER NOURA

A THESIS SUBMITTED TO THE FACULTY OF ENGINEERING AND APPLIED SCIENCE IN CANDIDACY FOR THE DEGREE OF DOCTOR OF PHILOSOPHY

SOUTHAMPTON, UK
(August, 2002)

UNIVERSITY OF SOUTHAMPTON

ABSTRACT

FACULTY OF ENGINEERING AND APPLIED SCIENCE

CIVIL AND ENVIRONMENTAL ENGINEERING

Doctor of Philosophy

DEVELOPMENT OF COMPUTER AIDED DESIGN FOR THE EFFECTIVE DESIGN OF MICRO-CATCHMENTS IN ARID CLIMATES

By Nader Noura

In arid regions, where water-harvesting techniques can be applied to use surface runoff for agricultural production, long term meteorological records of data are often scarce. micro-catchment systems have attracted significant developments in design and operation of water delivery in arid climate areas. In contrast, advances in exploiting the potential of methods to conserve water and increase crop yield by accurate control of rain water and moisture regime through the soil were made at a much slower pace.

An attempt is made to model and calculate actual runoff water received in infiltration basins from runoff areas based on changes in rainfall intensity, infiltration, size and slope of a Micro-Catchment system. A soil moisture simulation model is developed, relating to fundamental physical principles, to provide the necessary data for evaluating the potential success of rainfed agriculture in infiltration basins of. The model considers infiltration, evaporation, redistribution, and water uptake by plant roots. Based on a survey of existing techniques and their limitations, a generalised water balance model is proposed as a tool to analyse the performance of the system, and to locate problems in the water harvesting process. The combined models are interpreted numerically by finite difference methods and a number of numerical techniques are developed to treat time-dependent, none linear and moving boundary conditions. When tested by comparison with analytical solutions and field experiments that have been published in recent literature, the results were favourable.

The proposed water balance model is used to obtain an insight into the generation of actual runoff, the dynamics of moisture movement in the root zone and to examine the role of crop water demands in controlling the size of Micro-Catchment systems. The numerical investigation has significance implications on micro-catchment system design and estimates of actual evapotranspiration and water use (yield relations).

The application of the proposed model to practical problems in the present study, demonstrates its usefulness as a viable alternative to expensive experimental set-ups. Aided by the model, methods of moisture regime control in arid climates are examined to seek optimum utilisation of scarce water resources in Micro-Catchment systems.

Contents

List of Figures:

List or Tables:

Notation

The following symbols are used in the text. Symbols, which are, not included, fall outside the main line of argument and are defined in the respective section.

Symbols	Interpretation
a, b	approximate values
A, A_r	micro catchment size, runoff area
A, B	Green and Ampt abbreviated parameters
ADW	amount of deficit water
Ap, Alt	applied water, sum of rainfall and runoff, altitude
b and c	constant coefficient
C	soil water capacity, adjustment factor in calculation of reference evapotranspiration
CN	curve number
D, D_r, D_i	diffusivity, maximum retention capacity, deep percolation, total root extraction, root extraction at node i
D_d	volumetric root extraction
DRZ	depth of root zone
DW	deficit water
d_r, d_i	root zone depth (fraction of potential), maximum root depth, daily rainfall in the ith day
e, e_s	runoff efficiency, runoff coefficient, vapour pressure, base of natural logarithm, storage efficiency
e_s, e_d,	saturation vapour pressure, actual vapour pressure
e_{use}	water use efficiency
exp	exponential
E, Eto, E_{ac}	evaporation, Reference evapotranspiration, actual evaporation
E_s, E_t, Et_c,	potential soil surface evaporation, actual transpiration, evapotranspiration, crop evapotranspiration
E_a, E_I, E_o	aerodynamic term, incoming radiation, outgoing radiation
E_r	root extraction

f, f_p, $f(r, z)$	infiltration, allowable moisture depletion fraction ($f \leq 1$), potential infiltration, function or fraction (≤ 1)
f_{ac}, f_{pre}, f_{ini}	actual infiltration, predicted infiltration, initial infiltration
F, $F(t)$, F_p,	cumulative infiltration at ponding time, cumulative infiltration, cumulative infiltration at time t
G, $G(t)$	surface pondage, surface pondage at time t
h, h_{pond}	depth, humidity, pond water
h, h_1, h_2,	pressure head, pressure head at saturated conditions, pressure head at field capacity
h_3, h_4	pressure head as a reduction factor, pressure head at wilting point
I	infiltration
K, K_s	hydraulic conductivity, saturated hydraulic conductivity
$(K_e)c$, $(K_e)o$	crop proportionality factor, reference crop coefficient
K_s, K_e	crop coefficient and evaporation coefficient
K_{cb}, K_c, K_e	basal crop coefficient, crop coefficient, reference crop coefficient
k and k_1	constant coefficient, number of iteration
ln	natural logarithm
log	common logarithm
L, L_{Gro}, Lai,	length, length of growing season, leaf area index
L_{ini} L_{dev}, L_{mid},	initial growth length, developed and mid season growth length
M, MAD	Initial soil water deficit, maximum allowable deficiency
N, N_s	maximum daily sunshine duration, duration (days)
n	number
P	rainfall depth, atmospheric pressure
P_{ab}, pdf, $P_A(x_I)$	probability, probability distribution, exponential distribution
Q	storm runoff
q, q_{eva}, $q_{ac,eva}$	flux (moisture or heat), evaporation flux, actual flux evaporation
q_{apl}, q_{run}, q_i	potential applied flux, runoff from surface, actual infiltration rate
q_b	flux at the bottom
R, Ri, $Ri(t_p)$	resistance of flow in the pathway, runoff, rainfall intensity, rainfall intensity at time of ponding
$R(t_{int})$, $Ri(t_{int})$,	rainfall in time interval, rainfall intensity in time interval

$R(t_{ste})$, $R_i(t_{ste})$ rainfall in time step, rainfall intensity in time step

R_c, $R_c(t_n)$, $R_c(t_{n-1})$, cumulative rainfall, Cumulative rainfall at time n and at time n-1

R_{exc}, $R(t)$ rainfall excess, cumulative rainfall as a function of time

R_n, R_s, R_u net solar radiation, solar radiation, random number

R_a, extraterrestrial radiation

$Run_{(p)}$ potential runoff

RH_{max}, RH_{min} maximum relative humidity, mean air humidity

r radial distance, crop albedo (=0.25 for grass)

S, SW, S_{av}, potential maximum retention, sink term of root extraction, soil water balance, average soil suction

S(h), S_{max}, S_{ac} root extraction as a function of pressure head, maximum possible root extraction, actual root extraction

S_i, S_d sink term, stress day factor

T_{ac}, T_p T_k actual transpiration, potential transpiration, absolute air temperature

t, t_p, t_{int}, t_{ste} time, time of ponding, time interval, time step

t_{del}, t_{ac}, T_{ste} time delay, actual time, time step duration

U_d, U_r, mean wind velocity, ratio between daytime and nighttime win speed

V, V_i the amount of water to be applied in irrigation, volume of two node distance

V_{ac} actual volume of runoff

W volume

W_{min}, W_{max}, W_{av}, minimum water requirement, maximum water requirement, average water requirement

y_{ac}, y_{max}, actual yield per tree, maximum yield per tree

Z_r, Z_L maximum depth of the rooting system,

α, m and n shape parameters, inverse of pressure head

α, β coefficient in regression relationship

α, β, γ, λ, a, b matrices (conductance properties)

α (h) coefficient dependent on pressure head

λ Parameter of statistical distribution

γ Psychrometric constant

ν Volume

δ, δ_h, δ_θ,	solar declination, Threshold value, equals 1 cm, quals 0.0001 cm^3/cm^3
Δ, ΔW,	Increment, slope, factor for vapour flow, soil moisture storage
θ, θ_{air}, θ_s	Volumetric content, air dry moisture content, saturated moisture content
θ_{fc}, θ_r, θ_{wp},	Field capacity moisture content, residual water content, moisture content at wilting point
π	3.14159265
σ	Stefan Boltzmann's constant
ϕ	potential (total)
ψ	Suction head
ω,	Sunset hour angle
$\int$	Integration sign
* or x	multiplication sign
∂	Partial differential operator
Σ	Summation sign
∇ (del)	operator

Acknowledgements

Acknowledgements are due to the Ministry of Culture and Higher Education of the Islamic Republic of Iran for awarding me their scholarship, which gave me the opportunity to do my PhD at the University of Southampton.

The author is indebted to Professor W. Poweri, head of Civil Engineering Department, Southampton University for advice and encouragement during this study.

Sincere appreciation goes to Dr. D.W. Raycroft, Director of the Institute of Irrigation studies, for the valuable discussions he provided to complement the topics in this research.

And of course my sincere thanks and gratitude to my supervisor Professor Trevor Tanton who has very helpful and supportive throughout the work. I really enjoyed working with Trevor who was a friend as well as an academic advice.

Thanks to my research colleagues at the University of Southampton for being supportive and for exchanging ideas on our work, and indeed on other matter as well, which proved to be invaluable.

Last but by no means least, thanks are due to all the staff members of the Civil and Environmental Engineering Department at the University of Southampton for being there for us when we needed them.

The author remains deeply indebted to his wife whose support and patience were abundant throughout the preparation of this thesis.

Chapter 1 Introduction

1.1 The Problem

Agriculture, which accounts for 70% of global water use and nearly all-consumptive use, is increasingly competing with cities and industry for diminishing supplies. The use of fossil water supplies, with extraction rates greater than recharge, means that falling water tables are widespread throughout the world. Over the next few decades, agriculture will not be able to rely on vast increases in irrigated areas to maintain the required growth in output necessary to match increases in population. This means that, unless some revolutionary boost in yields is discovered, much of the world's future food increase will have to come from the dry land regions, where productivity is currently low. In these areas, rainfall is often unpredictable and in short supply, and crop production is often oriented towards reliability of yields rather than maximising production (Fisher; 1995).

Managed micro-catchment systems (figure 1.1) can be effective for the water management and utilisation of water resources to meet crop water requirements in arid climates. They are a method of collecting surface runoff from a small runoff area and storing it in the root zone of an adjacent infiltration basin to meet water requirements. In the infiltration basin there may be planted a single type of tree or annual crop (Ben-hur; 1991). Thesystem stores enough water in the root zone during the storms, to cover the water requirement of the crop or trees during the growing season (Ciuff, 1989. Kahlown et al., 1996; Pandey Sushil; 1991; Karl Wood, et al, 1995; Rodriguez. et al, 1996).

Micro-catchment systems (figure 1.1) are not a potential replacement of all methods, but have the greatest advantages in arid regions, where water resources are scarce, and rainfall distribution is too poor to sustain conventional agriculture (Boers, et al., 1986). The land needs to have an appropriate slope and soil texture such that it readily supplies runoff, but at the same time absorbs and stores water in the cropping zone. Micro-catchment systems have numerous benefits, such as improving the depth of water penetration on many problem soils, reducing total evaporation and maximisation of surface runoff generation, and increasing crop yield (Rodriguez; 1996. Kronen. 1994; Yair; 1983) Currently, the use of small

catchments has received increased attention due to shortage of conventional water sources, in many dry regions. Some of the advantages of micro-catchments as compared with large catchments are as follows:

I. They allow a high percentage of precipitation to be harvested and stored in the root zone
II. They allow agriculture to develop in areas too dry to support crop or conventional irrigation
III. Water does not need further transportation, as it is stored in the root zone where the trees and crops can utilise it close to the runof generation site.
IV. Construction and maintenance expenses can be relatively low as they do not require high technology.
V. The possibility of the system's destruction in the event of heavy storms is low compared with large catchment system.
VI. Due to their simplicity, farmers can construct the micro-catchments themselves, if it can be demonstrated that the crops grown make it worth their while.

The advances in micro-catchment system design and operation have been primarily in improving methods of water harvesting and delivery systems (Tabor, Joseph; 1995); with much less attention being placed on matching the runoff to the soil moisture depletion replenishment in the root zone.

A number of models have been developed for expanding water-harvesting design (Van Dijk, Ahmed Mohamed Hassan, 1993). A review of these models indicates that they all have considerable technical weakness that limit their general applicability. This work identifies their weaknesses and develops and tests a general model for micro-catchment design, which overcomes many of them.

The approach adopted in this work is to develop a micro-catchment model that is capable of:

I. Assessing the reliability of rainfall in a runoff catchment

II. Assessing the reliability of runoff that will result from a given soil type and slope from a given runoff area and given rainfall patterns.

III. Identifing the area of cropping land that the runoff from a given micro-catchment can reliably support for cropping.

IV. Testing the robustness of the model.

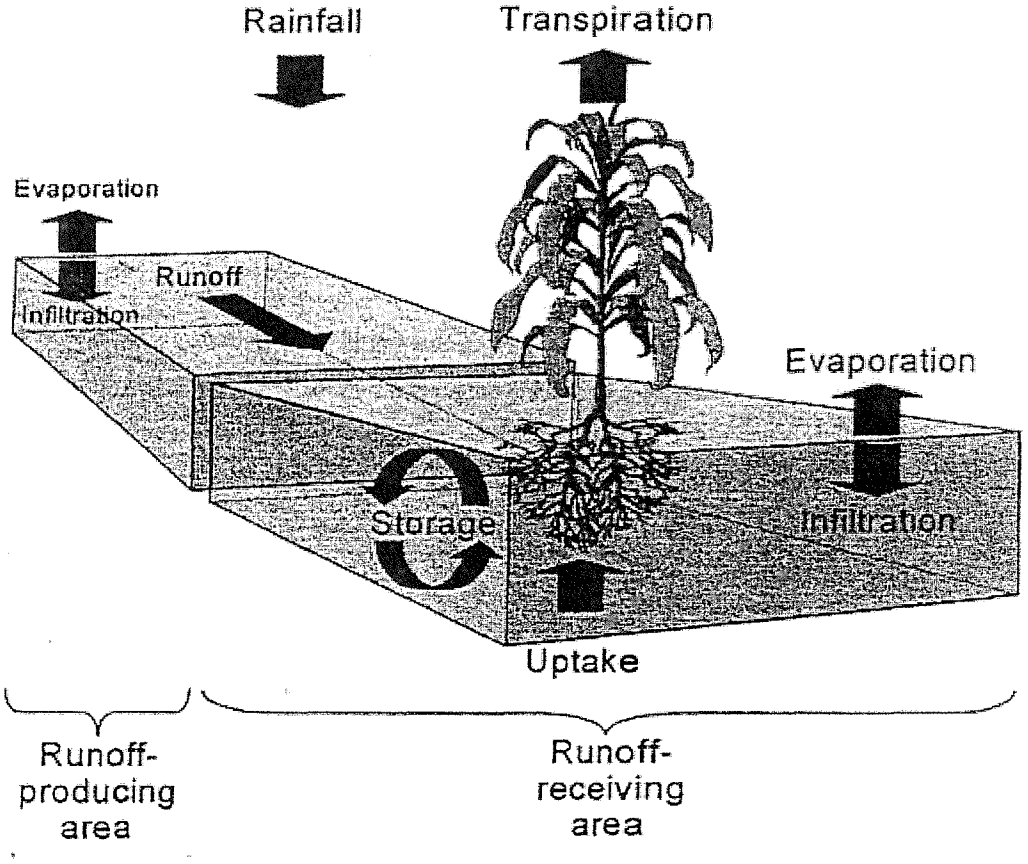

Figure 1.1:Micro-catchment water harvesting system consisting runoff area and infiltration basin

Chapter 2 Micro-catchment systems design in arid climates: variables and design principles

2.1 Introduction

This chapter, examins existing theories of the rainfall-runoff process in the runoff area and examins the theories of moisture movement that are most relevant to study the infiltration in the infilteration basin. The various variables and modelling processes that are important in micro-catchment system design in arid climatic conditions are also briefly reviewed.

2.2. Rainfall and runoff process in a micro-catchment system

Storm rainfall has many characteristics that affect rainfall and runoff processes in a micro-catchment system. The relative amount of rain, seasonalality, and the size and intensities of individual storms all affect seasonal runoff forecasting for design. The most important characteristic features of the precipitation in arid regions are its unpredictability and its high temporal and spatial variation (FAO 1981; Rodier, 1985 and Yair et al, 1985. Temporal variability in arid regions is such that, according to Rodier (1985), describing rainfall in terms of annual precipitation is meaningless. He states that in some arid regions the daily total precipitation might approach or even exceed the mean annual precipitation. Seasonal or monthly rainfall may be more variable than annual rainfall. The likelihood of receiving a specific rainfall for a period of one month or less can seldom be derived from the records at a single gauge site (FAO, 1981).

Surface runoff is the result of a complex interaction between rainfall and the soil surface. Engineers and hydrologists frequently encounter the problem of estimating the magnitude and timing of direct runoff from ungaged basins. The methods adopted range from simple and empirical procedures such as the rational method developed originally by Chow (1988), to mathematical models such as those of Ye et. al. (1997) and Wang (1996). Mathematical models can satisfactorily simulate rainfall-runoff linkages; however, they do have some limitations in micro-catchment systems in terms of time and resource demands. Such limitations are the reason to turn back to the simpler proposed models, which will be

described in the next chapters (chapters 3 & 4) and analysed in chapter 7.

2.2.1 Rainfall-runoff processes

Precipitation and its relationship with runoff has been studied by engineering to enable them to design structures and water supply systems, and by scientists to develop an understanding of the processes involved. Concepts such as interception, infiltration, surface storage, interflow and surface flow characteristics are described in hydrology textbooks (O'Loughlin et al, 1997). The various concepts and processes are given in Fig. 2.1 as following:

(A) Figure 2.1(a), shows the processes that are involved in a natural or rural catchment. The real processes are quite complex, however, the concepts combine and gloss over the many different mechanisms. Processes are frequently simplified to the forms shown in Fig 2.1 (b) and 2.1 (c).

(B) The black box process in Fig 2.1 (b) focuses upon inputs and outputs and does not deal explicitly with the physical workings of the transformation process. This process may be described by relatively simple relationships between rainfall and the runoff process (such as the rational method), or a complex, statistical time-series procedure. In both cases the processes can be calibrated by establishing a statistical regression relationship between the rainfall input and runoff output (O'Loughlin et. al, 1997).

(C) The process shown in Fig. 2.1 (c) has two parts. The loss process involves describe the removal or abstraction of losses, those portions of the rainfall which are infiltrated or evaporated, and so are not directly converted to runoff. The remaining "rainfall excess" is then inputted to a routing process, which concentrates and transports it from various parts of a catchment. The calculations involved are usually based on concepts or analogues of real processes, and are not intended to be physically realistic in any detailed sense.

(D) In Fig. 2.1 (d), A physical process is shown in Fig. 2.1 (d), which is intended to represent the real processes mathematically. This identifies and closely describes particular mechanisms, such as the interception of rainfall on grass and the leaves of trees. These processes are operated over a number of time steps, converting continuous periods of months or years (O'Loughlin et. al, 1997).

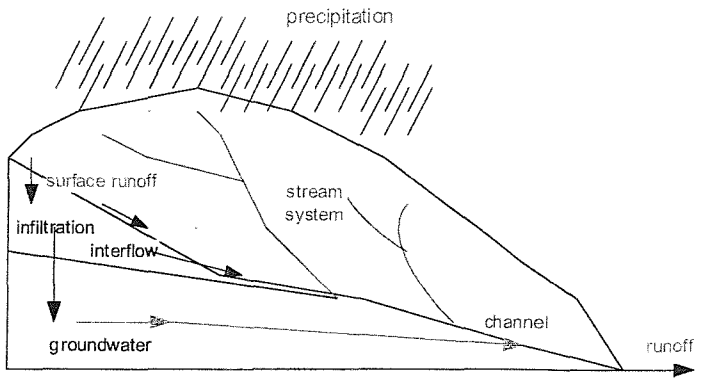

(A): Cross-section of a rural catchment showing hydrological processes

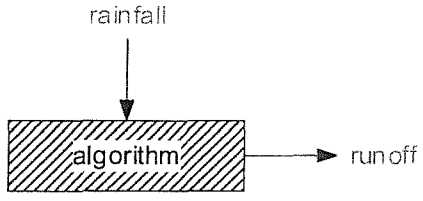

B: A simple "black box" process

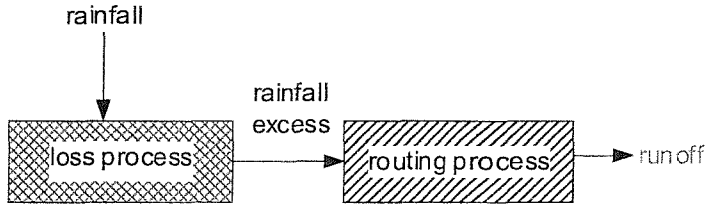

C: A two-stage loss-routing process

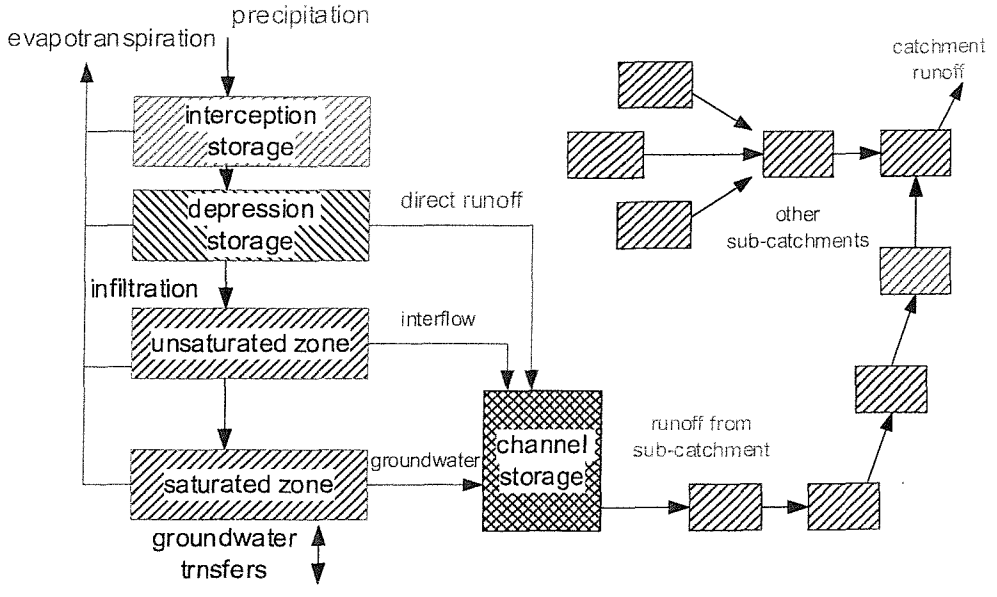

D: A physical process

Fig 2.1: General Rainfall-Runoff Processes

To allow for the real distribution of flow, catchments can be divided into sub-catchments arranged as a cascade or series, or as a branched network. The hydrological process is described in many texts (such as Diskin, 1995; Singh, 1988, 1989).

2.2.2 Factors affecting the rainfall and runoff process in a micro-catchment system

In arid and semi-arid regions two distinctive factors, storm type and micro-catchment characteristics, are affect the rainfall and runoff process. For example, a detailed description of two types of storm in arid regions and their spatial variability has been given by Yair et al (1985).

I Convective storms

Convective storms are common in arid regions. They are characterised by high intensity and short duration, and are localised (Osborn et al, 1972. and Yair, 1985). According to Yair (1985), the spatial organisation of convective cells on any rainy day is not random and the relative position of localised showers on a given day seems to follow a fixed systematic pattern. He states that the cells that are 3-10 km in diameter tend to be spaced uniformly. Sharon (1981) carried out a study in central Namibia with the purpose of finding possible spatial patterns of storms in this area. The results showed that convective storms are not randomly scattered in space but tend to form at preferred distances from each other, around 40-50 and 80-100 km.

II Frontal storms

Frontal storms may also occur in arid regions. They are developed in humid areas and extend into the adjoining arid or semi arid areas. This type of rainfall covers large areas (Rodier, 1985). According to Yair et al (1985), frontal storms have medium to low intensity and their duration may be a few hours or even a day. The amount of rain in such storms may vary from a few millimetres to more than 50 mm, depending on the distance from the frontal rain centre.

The spatial variation of rainfall in frontal storms is more complex than that of the convective type. Two causes for spatial variation during frontal storms have been described

by Yair et al (1985) as follows:

(A) Spatial variation is caused because the duration is long and the storms extend over large areas where synoptic conditions are not uniform. This type of spatial variation, as with convective cells, is independent of the earth's topography.

(B) Spatial variability occurs even within areas of uniform synoptic conditions, due to the interaction between incoming rainfall and local topography. This type of spatial variation can be found at all scales. The influence of topography in causing differences between rainfall levels is an example of this kind of effect. The effect of slope aspect in relation to the direction of incoming rainfall is also recognised.

III Micro-catchment characteristics

The available water in the infiltration basin of a micro-catchment system in arid zones depends both on the size and the geometry of the runoff area as well as on the related characteristics (size, slope and antecedent moisture conditions) and the nature of precipitation. It is well known that the micro-catchment characteristics are an important factor in the generation of runoff in arid regions. Ben Asher et al (1985) pointed out that the larger the size of a basin, the smaller percentage of runoff produced by a given storm. The average depth of precipitation that is likely to occur with a given frequency decreases with the area of the basin. This is due to the limited area extension of storms, especially those of high intensity, which are typical to arid areas.

A major factor in designing micro-catchment water-harvesting systems is runoff efficiency, which is dependent upon the micro-catchment characteristics (size, slope and antecedent moisture conditions). Flug (1982) defined the term "runoff efficiency" as the percentage of precipitation, which is collected as runoff. According to this, the suggested value of runoff efficiency is determined from a single plot next to the area planned for agriculture cultivation.

In large micro-catchment systems, more water infiltrates into the runoff area because the residence time of rainfall is longer as compared to small micro-catchments. Hence large micro-catchments have less runoff.

2.3 `Moisture movement processes in a micro-catchment system

2.3.1 Soil water relations and governing flow equations

The most general equation for describing soil water movement is an analogue of OHM'S law (Hillel, 1980).

$$q = \frac{\Delta\phi}{R} \qquad 2.1$$

Where:

q is soil water flux,

$\Delta\phi$ is change in potential, and

R is resistance of flow by various parts in the pathway.

Soil water potential differences give rise to water flow, either in liquid or in vapour form. Either of these modes would be expected to produce soil water flow proportion or to the corresponding potential gradient.

Darcy's law (1956) expresses this as:

$$q = K(\theta)\frac{\partial\phi}{\partial z} \qquad 2.2$$

Where:

q is the flow (alternative flux),

K is hydraulic conductivity a function of soil moisture and

$\partial\phi$ is the potential gradient.

θ is soil moisture content

To describe the transient nature of soil water infiltration, it is esential to include the time factor:

$$\frac{\partial\theta}{\partial t} = -\nabla q \qquad 2.3$$

Where:

∇q is the flux gradient, which may include both soil moisture content and time components

θ is volumetric moisture content and

t is time.

Most of the processes of soil-water flow can occur, however, while the soil has varying water content.

Equation 2.2 may be described by the equations of diffusion conditions as:

$$q = -D(\theta)\frac{\partial \theta}{\partial z} + K(\theta) \qquad 2.4$$

Where: $D(\theta) = K(\theta).\frac{\partial \psi}{\partial \theta}$ (difusion), and

$K(\theta)$ is soil hydraulic conductivity as a function of soil moisture content (θ)

ψ is matric suction

Then the equation 2.4 can be expressed by the one-dimensional form of the Darcy-Richard equation appropriate to many applications in the infiltration basin of a micro-catchment system.

$$q = -K\left(\frac{\partial h}{\partial z} + 1\right) \qquad 2.5$$

Where:

the notation z for the (vertical positive) upward is used.

Having defined the flux q, the expression for conservation of mass can be written as:

$$q = -\frac{\partial \theta}{\partial t} - S \qquad 2.6$$

Where:

θ = the volumetric soil moisture content

t = time

S = the sink (or negative source) of soil water (e.g. water extraction by roots)

For one-dimensional vertical flow, equation 2.6 reads as:

$$\frac{\partial \theta}{\partial t} = \frac{\partial Q}{\partial z} - S \qquad 2.7a$$

Or $$\frac{\partial Q}{\partial z} = -\frac{\partial \theta}{\partial t} - S \qquad 2.7b$$

Where:

θ is volumetric soil water content (fraction),

S is root water uptake ($cm^{-}d^{-}$), and

Q is the downward flux ($cm\ d^{-}$) with depth z (cm).

The combination of mass conservation and Darcy's equation leads to the partial differential equation of unsaturated flow. The combination of equation 2.4 and 2.7 yields:

$$\frac{\partial}{\partial z}\left(K\frac{\partial \theta}{\partial z}\right) = \frac{\partial \theta}{\partial t} + S \qquad 2.8$$

It should be mentioned that hydraulic conductivity (K) depends on soil moisture content. Substituting equation 2.7 into equation 2.8, equation 2.8 then reduces to:

$$\frac{\partial}{\partial z}\left[K(\theta)\frac{\partial h}{\partial z}\right] + \frac{\partial K(\theta)}{\partial z} = \frac{\partial \theta}{\partial t} + S \qquad 2.9$$

When we consider flow in the absence of a groundwater table, we deal with unsaturated flow only. For the transient movement of water in the root zone, we can restrict ourselves to vertical flow and introducing the differential soil water capacity $C(h) = \partial\theta/\partial h$, equation 2.9 can be written in terms of soil metric head h as:

$$\frac{\partial h}{\partial t} = \frac{1}{C(h)}\frac{\partial}{\partial z}[K(h)]\left(\frac{\partial h}{\partial z} + 1\right) - \frac{S}{C(h)} \qquad 2.10$$

Equation 2.10 has the advantage of being applicable for an entire flow region in the root zones of micro-catchment systems, including saturated and unsaturated flow. The use of (h) instead of water content (θ) as the depth variable has the advantage of being applicable in layered soils of root zones, where (h) remains continuous at the boundaries between the layers.

2.3.2 Moisture transfer systems

2.3.2.1 Infiltration

Infiltration is a process of water entry through the soil surface. This process is of great practical importance, since its rate often determines the amount of runoff in a Micro-Catchment system, which will occur over the soil surface during rainstorms, and can determine the depth of the infiltration basin. Infiltration generally decreases with time to a steady state. The decrease is primarily due to the reduction of hydraulic gradients at the surface but may also be affected by other factors such as surface sealing and crusting. If infiltration is continued for a sufficiently long time, the infiltration rate will approach a minimum or constant rate (f_c). The constant infiltration rate is generally assumed to be the saturated hydraulic conductivity. In a micro-catchment system, water enters the soil from the surface and in this case the infiltration process can be generally described by existing theories. When the application rate exceeds the ability of the soil to absorb water, infiltration proceeds at a maximum rate, commonly termed the potential infiltration rate. Conversely, if the application rate is lower than the ability of the soil to absorb water, the infiltration rate is equal to the actual infiltration rate and is lower than the potential infiltration rate. Both the potential infiltration rate and the actual or real infiltration rates vary during and for some time after each rainfall event. These variations are usually described as a function of time and the moisture content of the upper layer of the soil. The process of infiltration under rainfall was studied by Green-Ampt (1911); Horton (1940), Kostiakov (1932), Philip (1969), Smith et al(1993), Diskin and Nazimov (1996), Ogden and Saghafian (1997).

2.3.2.1.1 Factors affecting infiltration

I Rainfall intensity

Generally, the actual infiltration rate is the volume of water entering the soil per unit area in a unit time. The potential infiltration rate of the soil at a given location and a specified time is defined as the highest rate of water entry into the soil.

In the surface of a micro-catchment system, if rainfall intensity is less than the saturated hydraulic conductivity, the actual infiltration rate is lower than the final infiltration rate and soil will absorb all the rain water as fast as it is applied without ever reaching saturation. If rainfall intensity is less than the potential infiltration rate, but greater than the saturated hydraulic conductivity, the actual infiltration rate is below its potential infiltration rate and all application will be absorbed by the soil surface. However, if the rainfall at a given time interval is continued at the same intensity, and as soil infiltration decreases, the soil surface will eventually become saturated and the potential and actual infiltration rate and saturated hydraulic conductivity will become equal and rainfall excess becomes runoff. If the rainfall intensity is greater than the potential infiltration rate, excess rainfall runs off the catchment area.

Moldenhauer et al (1960) examined rainfall and runoff records from plots during natural rainstorms. They defined the ∅ index [(total storm rainfall - total storm runoff)/(duration of runoff)] to be strongly dependent upon rainfall intensity. Hawkins (1982) and Dunne et al (1991) reviewed other published interpretations of rainfall and runoff records, which concluded that the proportion of a drainage basin generating overland flow would increase as rainfall intensity increased.

Hawkins (1982) postulated that for one soil type or experimental plot there are spatial variations of unspecified scale in saturated hydraulic conductivity (K). At a given rainfall intensity (I), only those small areas with K< I generate runoff. Other areas of the soil surface absorb rainfall only at the rate I, which is less than their respective values of K. As the intensity increases, it exceeds the hydraulic conductivity (K) values for an increasing proportion of the surface which is brought to saturation and generates runoff. The spatially averaged infiltration rate increases with rainfall intensity until all parts of the plots are saturated (Dunne et al, 1991).

II Soil properties

Coarse-textured soils such as sands have large pores down which water can easily drain, while the exceedingly fine pores in clays retard drainage. If the soil particles are held together in aggregates by organic matter or a small amount of clay, the soil will have a loose,

friable structure that will allow rapid infiltration and drainage. The infiltration rate of a soil in a micro-catchment system can only be maintained if the system of coarser pores is maintained. The zone where this system is most likely to collapse is in the surface of the soil, since wet soil crumbs are weak and can easily be broken by the impact of raindrops. This can cause soil particles to become detached from the crumbs and block the coarser surface pores. The crumbs and the walls of the coarser pores in some soils may collapse spontaneously on wetting, and this is particularly liable to happen if a dry soil is suddenly flooded; or they may collapse slowly if the soil becomes waterlogged for any reason. The maintenance of permeability in the surface layer of the infiltration basin of micro-catchment systems is one of the major problems of good soil management in soils of low structured stability. Failure to maintain permeability can lead to the loss of crops through poor aeration, and to a loss of water or whole collapse of a micro-catchment system. Most theoretical analyses of infiltration have used the equation for vertical flow through a simple soil profile with a planar, unvegetated surface (Rubin, 1966). The results illuminate the effects of soil texture and initial moisture content of infiltration commonly observed in field measurements. The effects of soil structure on infiltration received less theoretical attention until the advent of recent interest in macropore flow (Dunne and Leopold, 1978); Russell 1998).

III Vegetation

Vegetation generally increases the rate and amount of infiltration from storm rainfall in a micro-catchment system. Although the impact of different vegetation may vary according to the tillage system, soil type, and climatic conditions, vegetation may increase infiltration through the following mechanisms.

1 Prevention of surface sealing: Clearly, seal prevention by vegetation is increased by no till management that retains residues on the surface for longer periods of the year (Vandervaere, et al, 1998). It prevents raindrop impact damage to the soil surface across the surface area for infiltration and retards runoff. However, by increasing soil aggregate stability, plants can increase water infiltration and decrease runoff, even when residuals are incorporated with conventional tillage.

2 Increased available water storage capacity: Meisinger et al (1991) estimated that transpiration reduces percolation and leaching losses and thus increases capacity in the soil for infiltration of subsequent rains and reduction of runoff (Dabney, 1998).

3 Increasing soil macroporosity: Vegetation may increase soil macroporosity both directly through root growth and death and indirectly by improving the habitat and activity of micro fauna that, in turn, create macroporosity (Tomlin et al, 1995). Plants in the infiltration basin of a micro-catchment system create short-term macroporosity until subsequent rainfall causes consolidation

The understanding of how vegetation affects infiltration in micro-catchment systems has not been quantified, which may explain why the empirical literature on this topic is confusing. Dunne et al (1991), Johnson and Niederhof (1941), and Marston (1952), failed to discover any simple relationship between vegetation cover density and infiltration capacity measured with infiltrometers. Dabney (1998) documented large changes in infiltration with only modest changes in vegetation density.

2.3.2.2 Redistribution

Redistribution can be viewed as a continuous process aiming to accomplish equilibrium of soil-water potential in the entire soil profile. In fact redistribution is a process of movement of moisture from zones of high potential to zones of low potential, notably the movement of moisture from the water entry zone at the soil surface to the surrounding soil. Also, there are continuous movements of moisture near the wetting front in response to very steep suction gradients that prevail during water entry into the soil profile. Redistribution therefore, results in further penetration of the wetted zone into surrounding soil beyond the limits of the zone intended for replenishment by irrigation or rainfall runoff. Moisture redistribution rates necessarily decrease in time due to the continuous reduction of the suction gradients and hydraulic conductivity. Consequently, the rate of advance of the wetting front into the surrounding soil falls rapidly.

Ogden and Saghafian (1997) stated that, if the rainfall intensity is less than the potential infiltration rate, the actual infiltration rate is equal to the rainfall intensity. A

rainfall break period begins when the rainfall intensity is less than the saturated hydraulic conductivity (*K*s), all ponded surface water is infiltrated, and soil water redistribution occurs. During a rainfall break period, the water content at the soil surface (θ_0) becomes less than the water content of the soil at natural saturation (θs). As the depth to the wetting front (Z) increases during redistribution, the water content along the entire depth of the profile is assumed to decrease uniformly.

During redistribution, the water content in the soil is expected to be characterised by a smooth but time-varying profile, particularly for moderately long redistribution periods. However the amount of water contained in the profile at any time during redistribution is equal to the cumulative infiltration (F), which is equal to $Z(\theta o-\theta_i)$ (Ogden and Saghafian, 1997).

2.3.2.3 Soil Surface Evaporation

A key process in evaporation is the movement of water vapour from the liquid surface to the bulk atmosphere. Evaporation from the surface of bare soils represents a sizeable proportion of water loss in micro-catchment systems. Evaporation from bare soil, is an unsteady process, and can be described in three stages. The initial stage takes place when the soil is wet and conductive enough to supply water to the sites of evaporation at a rate equal to evaporative demand. Being controlled by external conditions, this stage is commonly desvribed as "weather controlled". This is followed by a falling rate stage, during which the actual evaporation falls progressively below the potential rate and the process is controlled by the ability of the profile to conduct water. This stage is known as the "soil profile controlled stage" and usually persists for long periods. When the surface soil layers are dried, such that liquid-water conduction almost ceases, a third stage, known as the "slow-rate stage," begins. During this stage, evaporation is primarily due to vapour movement by diffusion (Idso et al, 1974; Brutsaert and Chen, 1995). It is limited by:

(A) the ability of the atmosphere to diffuse water vapours away from the surface.

(B) the radiative energy available to both vaporises water and maintains surface temperatures large enough to produce gradients of vapour density in the near surface atmosphere.

Evaporation of water from the soil surfaces of a micro-catchment system can be estimated using the general equations of flow, the same as for infiltration and redistribution. The only difference is the boundary conditions; instead of water being applied at the soil surface, water is being removed.

The first stage of evaporation, quantitatively, can be approximated by a steady state expression. Thus, a potential evaporation rate is needed to determine how much water could be lost from the soil if water was freely available. In this stage and micro-catchment system conditions, because of having specific conditions in the arid climate as discussed above, soil surface evaporation is estimated using the expression suggested by Ritchie (1979). According to Ritchie, the potential evaporation can be estimated in relation to the leaf area index (LAI); the fraction of net radiation that reaches soil surface through plant cover (R_n) is known by:

$$E_s = \left[\frac{\Delta}{\Delta + \gamma}\right] R_n e^{-0.39(Lai)} \qquad 2.11$$

Where:

E_s = Potential soil surface evaporation (mm/d)

R_n = Net solar radiation in flux in evaporation units (mm/d)

Δ = Slope of the saturation vapour pressure curve versus temperature curve (millibars/ ^{o} C)

Lai = leaf area index

γ = Psychrometric constant (kpa / C)

These equations must be lacking when the canopy is small at the beginning of the growing season because of the neglect of the wind and vapour pressure deficit term. This method is generally accepted for irrigation methods that wet the entire soil profile. Thus, theoretically, they can only be used in wetted area of a micro-catchment system or in an infiltration basin area. This method is needed to accurately assess the net radiation reaching the soil surface in relation to the variable degree of shading in the micro-catchment system, where the source of water delivered to the system is rainfall and runoff.

In the second and third stage, since water is not available or cannot be moved to the soil surface fast enough to meet potential demand, actual evaporation is smaller than

potential evaporation. In this period the surface soil water has decreased below a threshold value, so that soil evaporation depends on the flux of water through the upper layer of the soil. In this stage, evaporation can be calculated as described in section 4.4.1.1 (see chapter 4).

2.4 Soil moisture depletion by root extraction

2.4.1. Introduction

A general description of moisture extraction by roots can be approached within the framework in equation (2.10). Water uptake by plant roots generally has one of two purposes. Either it produces estimates of transpirational water loss for the water budget, or it provides estimates of plant water status for predicting water stress. Moisture uptake by plant roots can be traced back to Philip (1957) and Chang (1997). However, the more detailed studies of moisture uptake by plant root date back to studies by Mathur and Rao (1999).

The driving forces for the uptake of water into roots is a result of the difference between the water potential of the soil solution adjacent to the root and the root xylem. In the case of transpiring plants, this driving force is mainly due to the suction (negative pressure) produced in the root xylem. A number of researchers in the past have investigated the problem of water flow to plant roots. The literature classifies these studies into two categories. The first category depends on the microscopic approach, which deals with the convergent radial flow of soil-water to a single root. In this approach, the plant root is idealised as an infinitely long hollow cylindrical sink of uniform characteristics along its length. This microscopic model has contributed significantly to the understanding of the root extraction process.

The microscopic model requires knowledge of the resistance along the flow path, which can be separated into resistance to absorption and resistance to conditions. The extent of the root system is variable, since the rooting depth and the total root length change with time, environmental conditions and the irrigation regime. This variability cannot be quantitatively described by the microscopic approach, and an active root system with various

extraction rates at various locations can only be described macroscopically. Microscopic models are not effective due to the following reasons:

I In reality, steady-state conditions hardly exist, as the living root system is a dynamic system. The geometry of the root system is time dependent; thus, the root grows in different directions.

II The permeability of the root varies with position along the root and with time.

III The root water uptake is most effective in young root material. Since the length of the young root is not directly related to the total length, there will be differential absorption activities depending upon the age and location of the roots while using the microscopic approach.

IV The experimental evaluation of root properties is not practical because of the inherent difficulty in taking root measurements, particularly in the conditions of micro-catchment systems.

V The main limitation of the microscopic models is that they cannot be experimentally tested, and boundary conditions cannot be easily defined and applied to such models.

The second category follows a macroscopic approach. In this approach, the root ystem is treated as a single unit that does not take into account the effect of individual roots because of the difficulty in measuring the time-dependent geometry of the root system. The entire root zone is assumed to extract moisture from each differential volume of the root zone at some rate, and the water uptake by roots is represented by a volumetric sink term in the unsaturated flow equation. In micro-catchment systems conditions and in this study, as the assumptions of some researchers have assumed the rate of water extraction by root systems for the entire depth of the root zone to be constant, the boundary conditions are specified at the soil surface of the composite soil plant system and at the water table. These macroscopic models allow natural interaction with the transpiration process.

Some researchers have classified the water uptake model into a third category as a hybrid approach to take into account root density, root permeability, and root water extraction in the extraction relationship.

2.4.2 Factors affecting soil moisture extraction by root system

I Climatic factors

Many atmospheric factors directly or indirectly influence evaporative demands. Incoming radiation, wind, temperature and humidity, as well as exposure of the dry surface have an effect on the evapotranspiration rate. The climatic effects on crop water requirements have been discussed by many authors (Jenson et al; 1997; Allen 1996; Hatfield and Allen 1996). A universally applicable and practical method of linking evapotranspiration to atmospheric properties is provided by the energy balance method or water balance method by (Hanks in Hanks and Ritchie, 1991).

With low evaporative demand, plant-water potentials need not to be much different from soil-water potential, even if resistance to water flow due to lower soil conductivity is high. Conversely, under conduction of high evaporative demand, plant-water potentials may become much greater than the soil-water potential, even if the soil conductivity is high. This suggests that the limiting soil suction, beyond which the actual transpiration falls below potential demand, and the soil suction at which plants wilt, are not universal values, but are evaporative demand dependent. It is therefore noted that the relation between the relative plant water uptake (actual / potential transpiration) and average soil suction is not unique and cannot be described by a single relationship independent of the evaporative demand.

II Soil factors

The drying rate of a bare soil is controlled by water content and the hydraulic conductivity of the soil. When the capacity of the soil to conduct water to the surface does not equal the evaporative demand, the surface dries.

Soil texture, surface configuration and profile stratification dominate the control of soil water storage. Coarse-texture soils retain less water than do fine-textured ones. The lower water content in coarse-textured soils results in a smaller supply of water near the surface readily available for delivery to the evaporative site than that occuring in fine-textured soils. Coarse-textured soils generally have higher hydraulic conductivity at low

water suction (near saturation) than do fine-textured soils. Thus, in coarse-textured soil in comparison with fine-textured ones, added water moves more rapidly downward when soil is wet and upward more slowly to the drier surface layers. Coarse-textured soils, as a result, generally lose less water by surface evaporation than do fine-textured ones. Profile stratification usually results in retention of more water after wetting that if the profile were uniform in conductivity with depth. The structural conditions of the surface soil layers in the infiltration basin may also alter water transmission to the surface and promote self-mulching. Salvucci (1997) provides further discussion about evaporation under soil-limited conditions.

The soil suction head difference between soil and root, which is required to maintain a steady flow rate, depends on soil conductivity, as equation 2.3 suggests. An additional complication that arises in the near surface zones is the active role of root water uptake. As soil water potential decreases, its conductivity to water decreases and the suction gradient between soil and root, which is needed to maintain a certain rate of flow, becomes larger and larger (Ritchie and Johnson, 1990).

III Plant Factors

Many properties of the plant community influence evaporation and root extraction (transpiration) in a micro-catchment system. Plant species, light reflected from plants, plant cover, plant height, rooting depth and distribution, and the stage of growth are some of the important ones that influence evaporative demands in the infiltration basin of a micro-catchment system.

Soil water absorption by roots in the infiltration basin of a micro-catchment system is related to root density, root spatial distribution, and root capacity for soil water absorption. In general, higher plant moisture uptake by root results from high root densities. However, more rapid uptake results in rapid depletion of available moisture in the vicinity of the dense roots and the extraction rate does not remain constant. Root spatial distribution depends on plant species, requirement for support, as well as on moisture distribution. A plant with growing roots can reach continuously into moist regions of soil rather than depend entirely on the conduction of water over appreciable distances against increasing hydraulic resistance. The mean daily water uptake by the root system of a crop depends on

transpiration per unit surface of soil, the total length of root in the column of soil and distribution (Chang and Corapciouglu, 1997).

The soil will deliver water to plant roots as long as the water potential in the soil is greater than in the roots and, due to the finiteness of the volume of water available, the soil suction will gradually increase and equal that in roots. When this condition is reached, plant water uptake will cease unless the soil water is replenished. Recent experimental and theoretical studies provide some evidence and, in certain cases, quantitative descriptions of the various factors that influence moisture extraction by roots (Mathur and Rao.1999); those characteristics and their implications on the quantitative aspects of root extraction are discussed in the next chapter.

2.5 Existing methods of evaluation in relation to design of a micro-catchment system

To design a micro-catchment system needs analysis of hydrological information, soil surface infiltration, soil water storage capacity and crop water requirements. Sometimes there may not be adequate hydrological, meteorological, and biophysical data available at locations of interest, and even when data are available, it can be difficult to decide which is the most appropriate method to use.

Selecting the appropriate hydrological method requires careful consideration of:

1. The type and accuracy of information required
2. Available data
3. The physical and biological characteristics of the catchment
4. The technical capabilities of individuals performing the study
5. Time and economic constraints

2.5.1 Current methods of rainfall-runoff evaluation at estimating runoff from ungaged catchments

The estimation of flow characteristics of catchments can be carried out in several ways, ranging from simple runoff coefficient methods to a flow frequency analysis and estimation of the probability of occurrence of a specific flow. Most analyses of rainfall

runoff need stream flow records of sufficient length to represent the long-term variation of catchment runoff. Only in rare cases are sufficient measurements of stream flow available, because the majority of catchments are ungaged. For ungaged catchments, using rainfall records can be one of the ways to assess runoff. Excess rainfall in the runoff area of a Micro-Catchment system is that rainfall which is neither retained on the surface nor infiltrated into the soil. After flowing across the surface of the runoff zone it will be collected on the surface of the infiltration basin or root zone of a micro-catchment system. Existing methods of analysing rainfall-runoff can be classified into three groups:

2.5.1.1 Empirical methods

An example of empirical methods to relate rainfall to runoff is the average runoff coefficient method (Pandit et al; 1996). The method is an empirical technique, which relates rainfall to runoff with a certain probability. These methods are quite crude and attempt to lump several parameters into a single factor that is a gross approximation to reality, and should be avoided where possible (Hotchkiss, et al, 1995). The curve number method is one of the most used empirical methods, which was developed by the United States soil conservation service (SCS,) for estimating the volume and rate of runoff from agricultural catchments in the US (US SCS National Engineering Handbook, 1985). The curve number method has achieved world wide acceptance, as it uses only one parameter, potential maximum retention (S) or curve number (CN), a constant which is evaluated from the soils, land use and vegetation of the catchment. However, compared with other popular models, it does not treat the antecedent condition adequately. Even so, it is one of the most widely used methods for estimating runoff from rainfall, its main shortcoming is that much work is necessary to verify the form of rainfall runoff curves and the parameters for use in the method under regional conditions. The method is subject to large errors but these tend to be compensated for by changing the parameters, and the effect on the estimation of storage requirements is not as great as would be expected. The results are very sensitive to the value of the curve number. The initial accumulation of rainfall represents interception, depression storage, and infiltration before the start of runoff and is called initial abstraction. After runoff has started, some additional rainfall is lost, mainly in the form of infiltration; this is called

actual retention. With increasing rainfall, the actual retention also increases up to the potential maximum retention. This is described as:

$$Q = \left[\frac{(P-0.2S)^2}{P+0.8S}\right] \qquad For\ P > 0.2S \qquad 2.12a$$

$$Q=0 \qquad For\ P < 0.2S \qquad 2.12b$$

Where:

Q is storm runoff

P is rainfall depth

S is potential maximum retention after runoff begins, in inches. S is related to the curve number (CN) of the catchment by

$$S = \left(\frac{1{,}000}{CN}\right) - 10 \qquad 2.13a$$

Where:

CN = a dimensionless number, having a range from 0 to 100; ($100 \geq CN \geq 0$)

S = in inches. Equation 2.13a, in metric units, can be written as

$$S = \left(\frac{2{,}540}{CN}\right) - 2.54 \qquad 2.13b$$

Where: S is in centimetres.

The factors used to determine CN values are the hydrologic soil group, cover type, treatment, hydrologic conditions, and antecedent moisture conditions (AMS). Soil is classified into four hydrologic soil groups (A, B, C, and D) according to their minimum infiltration rate, Pandit et, al (1996.

Ponce and Hawkins (1996) explained some disadvantages of the curve number method namely:

1. It's marked sensitivity to the choice of curve number
2. The absence of clear guidance on how to vary antecedent moisture
3. The method's varying accuracy for different biomes
4. The absence of an explicit provision for spatial effects

5. The fixing of the initial abstraction ratio at $\lambda = 0.2$

The method is described in practically all recent textbooks and other sources, for example, by Chow et al (1988), M_C Cuen (1989), Soil conservation service (SCS, 1986), Hawkins (1993), Steenhuis et al (1995), Pandit and Gopalakrishnan (1996), Ponce and Hawkins (1996), and Bonta (1997).

2.5.1.2 Statistical methods

The statistical methods include probabilistic methods, regression and statistical techniques. If sufficient past records are available and there is no appreciable change in the regime of out- put water in a catchment, these methods can be used. Regression techniques essentially determine the functional relationship between rainfall and runoff. The stochastic approach is designed in hydrology to extend hydrologic forecasts and improve decision-making capability. The statistical and stochastic properties of the observed time series are assumed to represent the population properties, and the synthetic long-term time series are assumed to come from the same population. In fact, these methods try to model the hydrologic series using persistence (stochastically deterministic factors) and random factors. An example of this method is the regression model between rainfall and runoff created by Schreiber and Kincaid (1967), Diskin et al (1972) and Ben-Aher, et al (1985).

2.5.1.3 Simulation methods

These methods include direct simulation using physical models, semi-direct simulation using analogue models and indirect simulation using digital models. Most of the catchment simulation methods are quite diverse in their structure and operation, and are effective under a variety of different conditions. Obviously, a rainfall runoff model is a simplified representation of a complex catchment system. Field rainfall runoff modelling can be divided into two main categories, including stochastic and deterministic models. Stochastic catchment models are those which aim to produce an output with certain statistical properties or certain probabilities of occurrence. Deterministic models have no stochastic components and thus for a given input can be accurately predicted (Sharifi, 1997).

Deterministic models can be subdivided into conceptual (deterministic-conceptual) and process models (deterministic-empirical models). The distinction between conceptual

and empirical depends on whether or not the functional relationship between the variables is derived from consideration of the physical processes. This distinction is, however, artificial since many physical laws contain empirical constants. The conceptual models are those structures make little attempt to represent the movement of water through the catchment (Black box types) (e.g. Ye, et al, 1997). Process models are those where some effort is made to simulate the hydrologic components of a catchment. There is no known model, which is entirely free from empiricism. Physically based models, though more complex than simple models still cannot adequately describe the dynamics of nature (Scoging et al, 1992). A deterministic model can be either a continuous (producion a continuous flow record) or an event model (producing a hydrograph for particular storm input). Some models are defined as one dimensional or lumped parameter models, which assumes a uniformity of processes over the entire catchment (like the curve number method). Other models provide the spatial variability of parameters and accept the concept of saturation for overland flow or subdivid the catchment into a number of small sub catchments (distributed models), (Wang, and Chen, 1996). The internal time step of the models depends on the accuracy of the output required. Daily rainfall and runoff data are more readily available than data on shorter time steps. Thus daily models with daily time steps are usually preferred. This kind of modelling has better applicability for ungaged catchments. Many hydrological models have been developed that use rainfall data as input and runoff as outputs. An example is given by Wang et al (1992).

2.5.2 Current methods of estimating the evapotranspiration and crop water requirement

Methods of estimating evapotranspiration and crop water requirement can be estimated within three general categories, direct and indirect methods, and simulation of the soil water balance (Hatfield, 1990).

2.5.2.1 Direct methods

Evapotranspiration can be directly calculated from the residual of the soil water balance when all other terms have been measured, and is given as:

$$ET = SW + P + I - D - R \qquad 2.14$$

Where:

ET = evapotranspiration

P = rainfall

SW = soil water balance

I = infiltration

D = deep percolation

R = runoff

This method has been successfully used in a number of hydrological scale studies, where entire drainage basins have been studied. In small field studies, this method has been used to determine soil water use by crops for periods of 7 to 10 days (Burman et al, 1981).

2.5.2.2 Indirect methods

Indirect methods of estimating evapotranspiration are provided through theoretical and empirical methods. The process of calculating the evaporative demand and crop water requirements in order to utilize rainwater is very important and frequently repeated in many technical irrigation activities. It includes dealing with large quantities of data and mathematical calculation that can be difficult to explain. Estimation of the removal of water in the infiltration basin of a micro-catchment system requires an accurate evapotranspiration (ET_{ac}) estimate. Several forms of evapotranspiration equations have been developed and tested, ranging from the Thornthwaite model, with only monthly temperature as input, to the Penman-monteith model, which can accept monthly meteorological inputs (Monteith 1965).

Penman (1948) developed an equation that combines the two factors influencing the rate of water vapour loss from a surface: energy input and the rate of aerodynamic exchange from the surface. The general form of the equation is

$$ET_o = \frac{\Delta Rn + \gamma E_a}{\Delta + \gamma} \qquad 2.15$$

Where:

ET_o = Reference evapotranspiration (mm/day)

Rn = net radiation (mm/day)

E_a = Aerodynamic term (mm/day)

Δ = Slope of the saturation vapour pressure temperature curve (kPa/°C) at mean air temperature

γ = Psychrometric constant ($KPa/^{o}C$)

When reference evapotranspiration is adopted, transforming ET_o into the crop evapotranspiration ET_c requires the use of crop coefficient K_c (Doorenbons and Pruitt, 1977 in Pereira et al, 1999). The reference evapotranspiration can be written as a function of the equilibrium evapotranspiration (climatic data)

$$ET_o = (K_e)_o * E_e \qquad 2.16$$

While the actual evapotranspiration (ET_c) of a crop may be expressed by

$$ET_c = (K_e)_c * E_e \qquad 2.17$$

Where:

$(K_e)_o$ and $(K_e)_c$ are proportionality factors relative to the reference crop and the crop under study, respectively.

E_e evaporation

Finally crop water requirement can be expressed by

$$ET_c = K_c * ET_o \qquad 2.18$$

Other suggestions and tables for K_c were also given by Allen et al (1998), who presented the procedure for predicting the effects of specific wetting events on the value for the crop coefficient K_c. The solution consists of splitting K_c into two separate coefficients, one for crop transpiration, i.e., the basal crop coefficient (K_{cb}), and one for soil evaporation (K_e):

$$ET_c = (K_{cb} + K_e)ET_o \qquad 2.19$$

Where the soil is wet, evaporation from the soil occurs at maximum rate. However, the crop coefficient ($K_c = K_{cb} + K_e$) can never exceed a maximum value, K_c max. When the top soil dries out, less water is available for evaporation and a reduction in evaporation begins to occur in proportion to the amount of water remaining in the surface soil layer even reaching

zero when no water remains near the soil surface for evaporation. The basal crop coefficient (K_{cb}) is defined as the ratio of the crop evapotranspiration over the reference evapotranspiration (ET_c / ET_o), when the soil surface is dry, but transpiration occurrs at a potential rate, i.e., water does not limiting transpiration. Therefore, '$K_{cb}ET_o$' represents primarily the transpiration component of ET_C. The $K_{cb}ET_o$ does include a residual diffusive evaporation component supplied by soil water below the dry surface and by soil water beneath dense vegetation. Recommended values for K_{cb} are listed in tables by Allen et al (1998).

Numerous investigators of micro-catchments have suggested that direct evaporation from the soil surface should be less in micro-catchments because of the reduction of the fraction of wetted soil surface. In evaluating actual evapotransporation, major problems encountered in arid and semi arid regions and in micro-catchment system conditions are that the water loss is controlled more by plant and soil factors than by the atmosphere. In fact, actual daily evapotranspiration is usually much less than the potential (atmospheric) evapotranspiration in arid regions (Parton et al, 1981; Nichols, 1992 in Kempt et al 1997). Existing methods for estimating evaporative demand cannot be transposed to micro-catchment systems, particularly in arid zones. Most of these methods relate to conditions of crop cover of soil surface and uniform wetness of the field in non-limiting moisture conditions. Both conditions are rarely satisfied in the root zone of micro conditions, except perhaps in humid areas. These two characteristics estimating actual evapotranspiration by existing methods lead to over estimation of the actual values, as they necessarily include a higher fraction due to soil evaporation. Very recent experimental work by Kempe et al (1997) strongly supports this observation.

Taking into consideration the micro-climatological effects in micro-catchment system, it can be deduced that crop water requirements significantly differ in all cases. This points to the possibility that the actual reduction in evaporative demand in arid climates is not just due to the specific conditions in the system, but may also be due to other reasons that influence the quantitative comparison of micro-catchment systems with other methods of water management in arid regions.

2.5.2.3 Soil-plant-atmosphere relationship method

This method is being developed in parallel with rapid progress of computer languages and computer science. It is used to evaluate a variety of crops and conditions. The current method provides a mechanism for estimating actual evapotranspiration and also the separation of soil water evaporation and plant transpiration.

Most models used for estimating soil evaporation and transpiration are deterministic and can be further categorised as mechanistic or functional. Mechanistic models for evapotranspiration are usually based on dynamic rate concepts. They incorporate basic mechanisms of process such as Darcy's law and the appropriate continuity equations for water and heat flux, respectively. Functional models are usually based on capacity factors and treat processes in a more simplified manner, reducing the amount of input required. Mechanistic models are useful primarily as research tools for better understanding of an integrated system, and are usually not used by non authors due to their complexity, the functional models have modest input requirements making them useful for management purposes. Because of their simplicity, functional models are more widely used and independently validated than mechanistic models (Ritchie and Johnson, 1990).

Ritchie (1972) first proposed a functional model in which soil water evaporation (E_s) could be separated from total evapotranspiration (ET). This model is currently used as a subroutine in many more complex models. The structure of the model includes the physics of soil water evaporation as a function of surface soil water content and the amount of crop cover (for more information see Hatfield, 1990 and Ritchie, 1990).

2.5.3 Current methods for the evaluation of soil moisture movement and depletion

A primary task in irrigation scheduling in a micro-catchment system is to define the extent of the wetting zone. The current practice, based upon empirical rules, is to select a fraction of the potential rooting zone, when no control on its size by the moisture regime is imposed. The most common value of this fraction is (1/3) in arid zones with widely spaced plants Mathur et al (1999).

Existing methods to define the wetted zone can be classified into three groups:

I Field Measurements of Moisture Distribution

This method relies on direct measurement of moisture content in a sample area by excavation, auger, tensiometers or moisture sensor. The horizontal and vertical extents of the wetted zone are defined when the required quantity of water has been applied and redistribution of moisture is completed.

II Empirical Predictions

From limited numbers of field experiments, relationships between the total volume of water applied and the distance of the wetting front from the surface water resource are established. Tan and O'Connor (1996) give an example.

III Mathematical Modelling

Based on Basha (1999), an appropriate analytical solution of one–dimensional non-linear steady infiltration into a finite medium, which is subject to an arbitrary root–uptake function was provided. He derived and expressed the pressure head distribution explicitly for arbitrary values of the exponent n. Marino and Tracy (1988), described a macroscopic root soil water flow model to develop and verify a macroscopic root soil water flow model that simulates the vertical movement of water through a root system.

To complete the irrigation schedule design, the depletion of moisture from the root zone is estimated using a simple inventory or more detailed mathematical models.

I Moisture depletion inventory models

The amount of water to be applied by irrigation is computed from an inventory type model of the form

$$V = (\theta_{fc} - \theta_{wp}) * d_r * f \qquad 2.20$$

Where:

V is the amount of water to be applied

θ_{fc} moisture content at field capacity

θ_{wp} moisture content at wilting point

d_r is root zone depth (fraction of potential depth) and

f is allowable moisture depletion fraction ($f \leq 1$)

II Prediction of moisture depletion based on soil-water flow modelling

Recent mathematical models are based on solving the mass conservation equation in a one-dimensional or a steady-state form. Katul et al (1997) developed a soil water transport model based on the solution of a one-dimensional mass conservation equation with a term representing plant water uptake. The result shows that the root water uptake component that resulted from a covariance between the root water uptake and moisture content is comparable to the contribution from soil hydraulic properties and soil water redistribution.

2.6 Discussion

Existing methods used for establishing the amount of runoff from micro-catchments have a number of drawbacks. Perhaps the greatest weakness of existing models, is their inadequacy to describe complex and non-linear flows in infiltration in response to changes in rainfall intensity and soil surface saturation, as they do not include any relationship with time.

The majority of existing empirical methods like the curve number method have no clear or fully defined expression for spatial scale effects. For example, Ponce and Hawkins (1996) stated that in the absence of clear guidelines, the runoff curve number is assumed to apply to small and midsize catchments. Its application to large catchments (greater than 100 sq. m. or 250 sq. km) should be viewed with greater care and attention. On the other hand, Ponce and Hawkins (1996) have shown that curve numbers for areas less than 227ha in southern Arizona tend to decrease with increasing catchment size. The size of the Micro-Catchment is likely to be less than 0.5 ha and hence the value of the curve number method is thrown into question without recalibration.

In order to explain the performance drawback of distributed models and overland flow models in the conditions of micro-catchment systems, there is an example of an overland flow model, which was designed and tested by Scoging (1992). She states that there are some drawbacks regarding the performance of this model in in conditions of micro-catchment systems. Commonly these kinds of models are related to macro flowlines, slope parameters and complex flow line directions, which at the site scale; may converge, diverge or remain parallel. Since at the micro-catchment size routing can and must only occur as a

converging flow, and because of the greater distance of the overland flow lines, a lower quantity of water reaches the infiltration zone. In spite of other drawbacks, it also places high demands on field data collection.

Treatment of the moisture regime as a sorption dominant process with little attention to the process of root extraction and evaporation from the surface, which interact to produce complex moisture distribution patterns cannot be predicted by studying the infiltration process alone. The complex flow and root zones geometric in micro-catchment systems, which are time dependent, are not catered for in existing modeling techniques. It is therefore concluded that a primary target of any improvement would be to devise a technique by which accurate analysis of rainfall runoff in runoff zone and moisture depletion in the root zone of a micro-catchment system can be accomplished. In such a technique, the complex process of runoff generation and the complex flow and root zone geometrics should be considered. Additionally, improved methods to emulate the dynamic nature of the conditions in micro-catchment systems is required. The prediction of moisture depletion should be based on realistic models of root extraction. Ideally, improved methods that finally predict a micro-catchment system area should provide the posibility for exploring the statistical implications of the various system design stages. They should make it possible to examine, mathematically, the many runoff zone areas that influence the generation of the surface runoff and consequently, water availability in the root zone of a micro-catchment system.

Chapter 3 Modelling micro-catchment runoff and cropping

3.1 Introduction

The discussion in the previous chapter highlighted the need for better methods for prediction of rainfall excess and runoff and crop water requirements. A transient one-dimensional finite difference water balance model relating micro-catchment size to both rainfall runoff and crop water requirement in infiltration basin was developed. In this chapter the proposed model is linked in to the transient one-dimensional finite difference water balance frame, to apply to design and operation problems in these systems. Using computer programming, numerous rainfall and runoff models, involving crop water requirements consisting of soil surface evaporation and transpiration via root extraction were adapted. These models can be a viable alternative to expensive field experimentation and replace simplistic techniques not skilfully developed or properly finished in current practice. The description of model components is given.

3.2 Description of model components

The basic components of the model are given in figure 3.1. There are three major components, the calculation of runoff from the catchment area, the calculation of the soil water balance in the crop zone and the calculation of the optimum size of the catchment and infiltration area to ensure reliable crop production.

3.2.1 Potential runoff calculation:

Potential runoff is calculated from data of daily rainfall, soil type, cover, and depression storage and slope and catchment size. The model first calculates potential runoff before taking account of transmission and storage losses. Details of the methodology are given in 3.3.1. The water balance in the root zone is calculated from:

(Runoff + direct precipitation) – (Drainage losses + Evapotranspiration)

Potential infiltration in the catchment is calculated from the total daily runoff and precipitation minus any loss due to lack of storage in the infiltration basin (See 3.3.1.1).

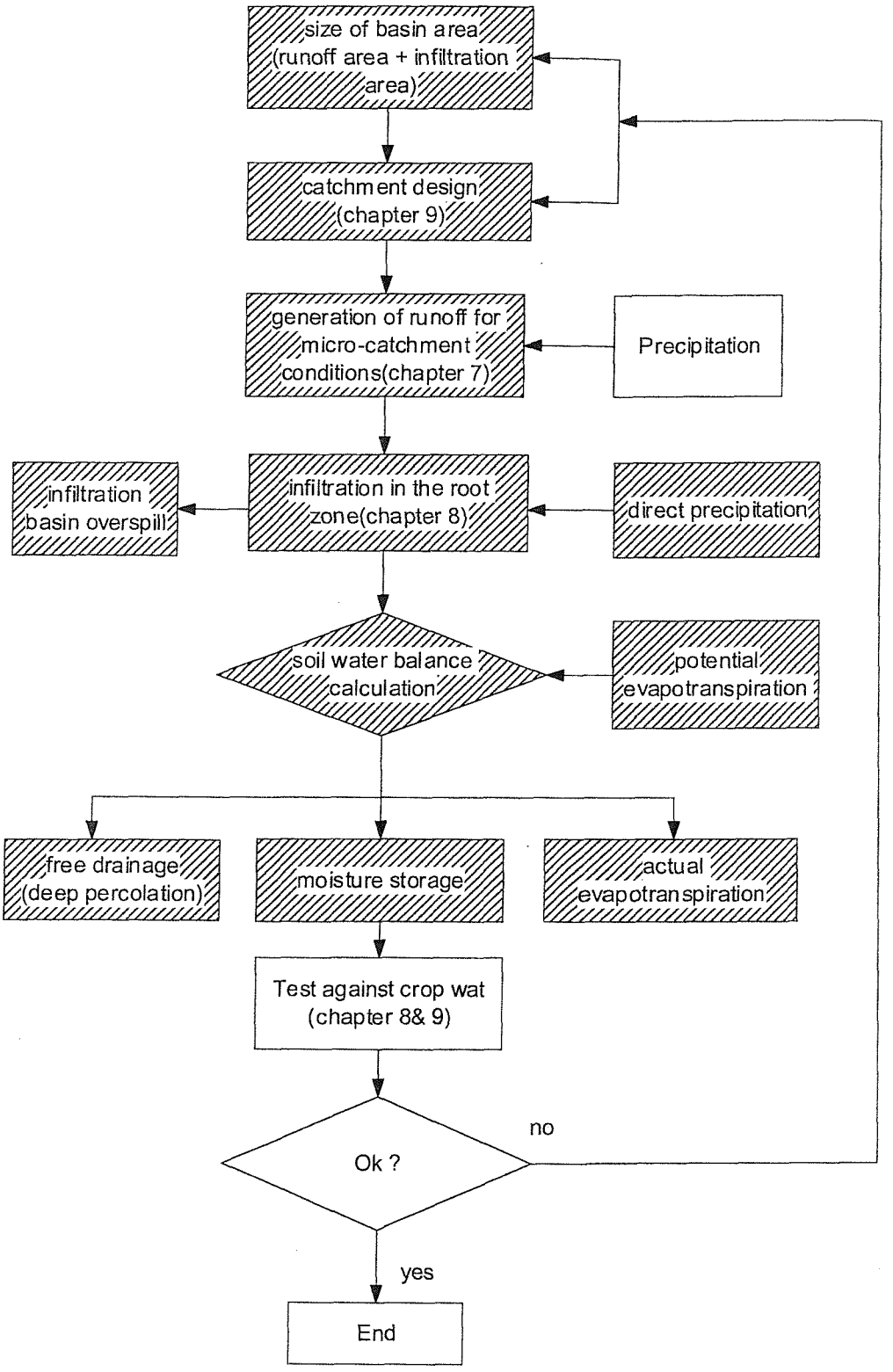

Fig 3.1: Micro-catchment design model components

3.2.2 Water balance:

The actual water balance model was calculated by the finite difference method proposed by Belmans et al (1983). The methodology calculates soil water balance by calculating the stored water at different depths within the root zone. The amount of water at different levels is calculated from:

Recharge – (drainage + evaporation from the soil surface + transpiration losses via the roots)
Details of the methodology are given in section 4.3.

The design of the system is calculated by optimising the size of the catchment and infiltration area to ensure over 90% probability of achieving acceptable crop water requirements (see chapter 9).

3.3 Development of a transient one-dimensional soil water balance model in micro-catchment systems

To select a numerical technique to model transient one-dimensional finite difference soil-water movement, and a water balance model in the root zone of a micro-catchment system, the following approaches were adopted:

I. A regression rainfall-runoff model to assess potential micro-catchment rainfall-runoff was developed based on a system approach (as discussed in section 3.3.1). In this model the rainfall excess is considered as a function of rainstorm intensity and the actual infiltration rate. The value of runoff, obtained from rainfall excess and an experimental slope coefficient will be linked by a numerical technique to the model described in (II).

II. A crop water requirement model was formulated based on soil surface evaporation and transpiration (see section 3.3.2), making use of the experimental evidence available, and comparing the merits and suitability of the available approaches.

III. A transient one-dimensional finite-difference soil water model was developed capable of predicting soil moisture storage and movement in the root zones of micro-catchments under different climatic and runoff conditions.

IV The various micro-catchment conditions, and rainfall-runoff flow geometry in runoff area were defined based on various soil properties and climatic conditions. Soil moisture flow geometry in the infiltration zone was based on the plant root system to be simulated by the model as a major constraint in selecting a particular numerical technique.

V Based on I, II, III and IV, a numerical technique can be selected (as discussed in chapter 2, section, 2.6) and a water balance procedure is developed to define and design a micro-catchment system as will be described in chapter 4 (see 4.6).

3.3.1. Rainfall excess model

Rain falling in the runoff zone is temporarily stored in depressions or runs out of the catchment as runoff. Runoff water in a micro-catchment will normally drain into the growing basin except in exceptional storms when the excess will be discharged out of the micro-catchment. For practical purposes however, evaporation can be considered as negligible during a rainfall event. The water budget equation, which describes the balance of water quantity in the runoff area of a micro-catchment, for the variables involved in a soil surface infiltration process, is:

$$R_{exc} = R_{exc}(t) = R(t) - [F(t) + G(t)] \qquad 3.1$$

Where:

R_{exc} is cumulative rainfall excess, which is source of runoff, in millimetres

$R(t)$ is the cumulative rainfall in millimetres, a continuous function of time

t is the time in minutes measured from a standard time which can be the beginning of a rain;

$G(t)$ is the amount of surface pondage in millimetres, which will infiltrate in that time

$F(t)$ as cumulative infiltration

3.3.1.1 Infiltration of rainfall:

The Green and Ampt (1911) equation describes the infiltration process under a ponded surface as follows:

$$f_p = K_s\left(1+\frac{MS_{av}}{F}\right)=\frac{dF}{dt} \qquad 3.2$$

Where: f_p is potential infiltration rate

S_{av} = average soil suction

M = initial soil water deficit

F = cumulative infiltration

K_s = saturated hydraulic conductivity

Although the original derivation by Green and Ampt assumed total saturation behind the wetting front, this requirement was in effect relaxed by Philip (1957). He assumed that the water content θ_S was constant, but not necessarily equals to total porosity. Likewise, K_S is expected to be less than the water content, so equation 3.2 may be written as,

$$f_p = \frac{A}{F}+B \qquad 3.3$$

Where:

$A = K_s * M * S_{av}$, *and*

$B = K_S$

The two parameters of the model depend on the soil are physical properties, initial water content and distribution, and surface conditions such as cover, crusting, etc.

Three cases or stages of infiltration can be considered when a rainfall intensity (Ri) is applied to a soil having a saturated conductivity (K_s) and an infiltration capacity (f_p).

Case A: $R_i < K_s$. For this condition, runoff will not occur, since all the rainfall infiltrates, but it is still important as the soil moisture level is being altered.

Case B: $K_s < R_i \leq f_p$. During this stage, all the rainfall infiltrates into the soil, and the soil moisture level near the soil surface increases.

Case C: $K_s < f_p \leq R_i$. The infiltration rate is maximum and rainfall runoff is generated.

Where:

R_i is rainfall intensity

K_s is saturated hydraulic conductivity

f_p infiltration capacity

Infiltration in the case *B* is infiltration prior to runoff. As was described earlier, the moisture content at the surface increases during rainfall until surface saturation is reached. And rainfall excess is generated as in case C.

We imagine that t_p is the time of starting surface ponding, from a stage without surface ponding. F_0 is the cumulative infiltration at $t = t_p$, and F_p is the cumulative infiltration under ponding. Integration of equation 3.2 from $t = t_p$ to t (any time after ponding) and from $F = F_0$ to F_p, and rearrangement, yield:

$$\frac{F_p}{S_{av}M} - \ln\left(1+\frac{f_p}{S_{av}M}\right) - \frac{F_0}{S_{av}M} + \ln\left(1+\frac{F_0}{S_{av}M}\right) = \frac{K_s\left(t-t_p\right)}{S_{av}M} \qquad 3.4$$

In practice, calculation of excess rainfall using the Green and Ampt equation against rainfall intensity is used in the following stages:

The duration of the rainfall event is divided into many short periods in such a way that within each period, the rainfall intensity is essentially considered constant under the following condition:

$$R_i(t) = \frac{R_C(t_n) - R_C(t_{n-1})}{t_n - t_{n-1}} = R_i = Constant \qquad 3.5$$

Where:

$R_i(t)$ = rainfall intensity at time t,

t_n-t_{n-1} = nth time interval (short),

$R_c(t_n)$ = Cumulative rainfall at the end of the nth time interval, and

$R_C(t_{n-1})$ = cumulative rainfall in millimetres at the beginning of the nth time interval.

The variable cumulative rainfall $R_C(t)$ within a short period can be written as:

$$R_C(t) = R_C(t_{n-1}) + \int_{t_{n-1}}^{t} R_i(t)dt = R_C(t_{n-1}) + (t - t_{n-1})R_i \qquad 3.6$$

Combining 3.3, 3.4 and 3.6, and letting $t = t_p$, we obtain the ponding time for this special case as:

If rainfall intensity is smaller than the potential infiltration, infiltration is equal to rainfall and in this period rainfall excess is zero, as follows:

$$R_i < f_p \text{ then, } f(t) = R_i \text{ and in this conditions } \frac{dR_{exc}}{dt} = 0.$$

Where:

R_{exc} =Rainfall excess

The infiltration process during rainfall can now be separated into two stages:

In the first stage, there is no surface ponding for period from t_{n-1} to t_n.. In this period, the infiltration rate and cumulative rainfall excess $R_{exc}(t)$ satisfy

$$R_{exc}(t) = R_{exc}(t_{n-1}), \qquad t_{n-1} \le t \le t_n \qquad 3.7$$

The cumulative infiltration can be obtained by the mass-balance principle as:

$$F(t) = F(t_{n-1}) + f(t) \quad \text{or } F(t) = R(t) - R(t_{n-1}) \qquad 3.8$$

In the second stage, there is surface ponding for the period from t_{n-1} to t_n. In this period, the infiltration rate is given by 3.3, and the rainfall excess R_{exc} can be obtained using the mass-balance principles:

$$R_{exc}(t) = R_C(t) - F_p, \qquad t_{n-1} \le t \le T_n \tag{3.9}$$

Surface ponding occurs when rainfall intensity equals the infiltration capacity, which is defined as the rate of infiltration that reaches its maximum capacity for a given type of soil and moisture conditions, so that

$$R_i(t_p) = f_p \tag{3.10}$$

With use of 3.10, 3.2 becomes

$$f_p = \frac{K_s(F_P + S_{av}M)}{F_P} \quad \text{and} \quad F_P = \frac{K_s(F_P + S_{av}M)}{R_i(t_p)} \quad \text{because } f_p = R_i(t_p) \tag{3.11}$$

$F_p * R_i(t_p) - K_s * F_p = K_s S_{av} M$. On the other hand based on equation 3.8, we can write

$$R_C(t_p) - R_{exc}(t_{n-1}) = F_p = \frac{K_s S_{av} M}{R_i(t_p) - K_s}, \tag{3.12}$$

and cumulative infiltration at ponding time can be calculated from:

$$F_P = \frac{K_s S_{av} M}{R_i(t_p) - K_s} \tag{3.13}$$

The ponding time can be obtained simply by combining equations 3.6 and 3.11 and letting $t = t_P$ as follows:

$$R_C(t_p) = R_C(t_{n-1}) + (t_p - t_{n-1}) * R_i, \text{ And } t_p = \frac{R_C(t_P) - R_C(t_{n-1})}{R_i} + t_N \tag{3.14}$$

The combination of equations 3.14 and 3.12 yields:

$$t_p = \frac{\frac{K_s S_{av} M}{R_i(t_p) - K_s} + R_{exc}(t_{n-1}) - R_C(t_{n-1})}{R_i(t_p)} + t_n \qquad 3.15$$

If we refer to the coefficient of: $A = K_s S_{av} M$, and B = K_s, consequently the equation 3.15 changes to the equation:

$$t_p = \frac{\frac{A}{R_i(t_p) - B} + R_{exc}(t_{n-1}) - R(t_{n-1})}{R_i(t_p)} + t_n \qquad 3.16$$

Details of performance and analysis of the rainfall- runoff model is provided in chapter seven.

3.3.1.2 Conversion of rainfall excess into runoff:

The surface runoff volume from a single storm event is expected to be less than the volume of rainfall. Indeed, in previously and developed models of rainfall excess in micro-catchment systems, surface runoff is generated from the rainfall intensity in excess of the infiltration rate. The precipitation measurement of rain gage stations is examined in terms of the relationship between rainfall depth and rainfall excess depth, as explained in the previous model. In the analysis of storm data in runoff, simple linear relations between rainfall and rainfall excess are examined. Firstly, for each soil group, data for cumulative excess rainfall are plotted versus data for cumulative rainfall in each storm to see how these data points approach straight lines (for more information see chapter 7), then simple bivariate regression equations between rainfall and runoff are derived. In fact, regression techniques essentially determine the functional relationship between rainfall to runoff, such as the following simplest linear regression equation.

$$R = a + bP \qquad 3.17$$

Where:

R is runoff per storm,

P is storm size,

a ,and, *b*, are the coefficients of the linear regression equation.

The threshold value obtained from the P- axis intercept (-*a*/b) is denoted as P_0. The coefficient *b* represents runoff efficiency after the threshold rainfall has been exceeded. Linear regression analyses of storms on water harvesting in micro-catchment systems have been used to obtain threshold values (minimal rainfall necessary to produce runoff).

3.3.2. Philosophy of crop evapotranspiration and the water requirements model

In micro-climatic environments and conditions of micro-catchment systems, crop water requirements are controlled by soil surface evaporation and crop transpiration in the root zone. Crop water demand is strongly controlled by radiation, turbulence and vapour pressure deficit, and by the nature of the overall plant canopy. In arid and semi-arid regions, water loss under rainfall conditions is likely to be controlled more by plant and soil factors than by atmosphere (Meshkat et al; 1999). In fact, actual daily evapotranspiration (ET_{ac}) is usually much less than the potential (atmospheric) evapotranspiration (ET_P). Plant factors, including species composition and cover, phonology, stometal response, and rooting patterns as well as soil factors such as texture, interaction with rainfall-runoff and climatic conditions produce particular patterns of evaporation and transpiration in micro-catchment systems. Potential crop evapotranspiration could be computed directly from the Penman-Monteith or modified Penman equation (empirical methods described in chapter 2 section, 2.5.3 and appendix A), if the crop specific surface and aerodynamic resistance are known (Pereira et al, 1999). The challenge in applying the Penman-Monteith equation is in the prediction of parameters during periods of partial ground cover soil moisture content and partial surface wetness. Relatively experienced multilayer models are available for simulating evaporation and transpiration from partial cover crops (Shuttleworth and Gurney, 1990 cited in Pereira et al 1999). However, widespread application of these models will require the accumulation and calibration of expensive sets of background parameters, which will represent the various agricultural crops and the standardisation of the computational solution. This was supported by a number of experimental findings, as discussed in chapter two in section, 2.5.3.

3.3.2.1 Soil evaporation model:

As discussed in chapter 2 (section 2.3.2.3) an adopted functional model developed by Ritchie (1972) calculates potential soil evaporation from a soil with incomplete cover on a daily basis (Lockington. 1994, Ritchie and Johnson, 1990).

During the constant rate stage (E_S), it is assumed that the first layer of soil surface in the infiltration zone is sufficiently wet for the water to be transported to the surface at the potential rate. In this study of micro-catchment conditions, the first stage of soil evaporation (E_S, mm) has been calculated using the modified Penman equation (Doorenbos and Pruitt 1977, Kotsopoulos and Babajimopoulos, 1997) for calculation of reference evaporation (E_o mm), and the Ritchie (1972) equation, as in Appendix A:

During stage 2 (E_S), soil evaporation from below a tree canopy planted in the infiltration zone is assumed to be the same as evaporation of bare soil, because soil evaporation is less dependent on the available energy and more dependent on the hydraulic properties of the soil. The soil evaporation in this stage (Es, mm) is calculated as explained in chapter 4 (section 4.4.1.2).

3.3.2.2 Transpiration model (root extraction)

Modelling of transpiration is much more complex than soil surface evaporation because plants extract water throughout the soil profile, where plant roots may be growing with time; thus transpiration is not only a function of climate, but of both changing soil wetness and time boundary conditions (Hanks. 1991). The basic equation for one-dimensional water flow, as shown in equation 3.30, which is sufficient for infiltration and redistribution, must also take account of root extraction. The transpiration or water uptake rate by plant roots can be included in the continuity equation, as macroscopic sink terms (Markar and Mein, 1987), shown as, S, in equation 3.18. In this, the root water extraction rate is given by

$$S(h) = \alpha(h) S_{max} \qquad 3.18$$

Where:

$\alpha(h)$ is a coefficient, function of the water extraction at the particular soil suction value, h (value varies between 0 and 1)

S_{max} is the maximum possible water uptake rate to the roots.

If Z_r is the maximum depth of the rooting system, the actual transpiration rate (T_{ac}) at any given instant time and root depth is given by:

$$T_{ac} = \int_0^{z_r} S(h)dz \qquad 3.19$$

Substituting 3.18 Into 3.19 obtains

$$T_{ac} = S_{max} \int_0^{z_r} \alpha(h)dz \qquad 3.20$$

When the actual transpiration rate is equal to the potential transpiration rate (T_p), $a(h)$ should be equal to 1.0.

To seek a relation between soil moisture availability and the rate of root extraction in a root zone, the water balance of a root zone of depth (d_r) is considered, with soil moisture variability in any time interval as a function of root extraction. In the following equation it is assumed that there is no water input or output except for plant water uptake.

$$\Delta\theta = \frac{T_{ac} * \Delta t}{d_r} = S * \Delta t \qquad 3.21$$

Where:

$\Delta\theta$ is change of moisture content in a time interval (Δt),

S is rate of root extraction and

T_{ac} is actual transpiration.

d_r is maximum root depth

In a short time period, moisture content gradient in the root zone is constant and equal to root extraction, which in the above equation can be written as:

$$\frac{\partial \theta}{\partial t} = S \qquad 3.22$$

If it is further assumed that the actual transpiration represents a moisture flux across the boundaries of a root then the variability of moisture content in a short period of time can be explained in the equation below:

$$\frac{\partial \theta}{\partial t} = -K_p * \nabla \theta \qquad 3.23$$

Thus, a mass conservation equation is obtained relating the actual rate of root extraction to moisture availability in soil through a coefficient (K_P), which in turn is similar to soil hydraulic conductivity.

In the root zone of a micro-catchment infiltration basin, K_P, can be viewed as the ability of the soil water to transport moisture to the roots for transpiration, similar to hydraulic conductivity. This coefficient is dependent on the moisture content of the system. In quantitative terms, both sides of equation 3.18 are divided by the maximum possible root extraction, S_{max}, which is defined by Belmans and Feddes (1983) in the following equation:

$$S_{\max} = \frac{T_P}{d_r} \qquad 3.24$$

Then the coefficient of relative root extraction, $\alpha(h)$, is explained by:

$$\alpha(h) = \frac{S_{ac}}{S_{\max}} = \frac{K_P}{S_{\max}} * \nabla \theta = \hat{K}_P * \nabla \theta \qquad 3.25$$

Where:

T_P = Potential transpiration

$\alpha(h)$ = Relative rate of root extraction (actual/Potential)

S_{ac} = Actual root extraction

S_{max} = Maximum or potential root extraction, and

$\hat{K}_p$ = Coefficient dependent on moisture content and magnitude of evaporative demand.

$\nabla\theta$ = Moisture content gradient

d_r = maximum root depth

The equation is in fact a form of stress model, which that is related to the relative rate of plant water uptake; on the other hand, it is a function of soil moisture availability in the root zone. The consequence of this is that estimates of irrigation intervals in a micro-catchment system and other field conditions do not relate to soil hydraulic properties, except in defining the range of moisture availability. Thus by considering equation 3.25, a point is reached when ($\hat{K}_p$) is a function of all micro-catchment system components (soil & crop) in infiltration basin. In fact it is a function of soil and water interaction and is influenced by their physical characteristics. Thus ($\hat{K}_p$) is dependent on soil, water, plants and atmospheric characteristics. This then leads to defining a further feature of the model. That is, it should account for soil hydraulic properties, and changes in rooting depth.

First, a relationship between soil moisture content (soil pressure head) and root extraction for a given evaporative demand is sought. Experimental data by a number of researchers aids this search and in particular the works of Katul et al (1997), and Kempt et al (1997). They suggest that the search for a general relationship should consider that:

I Plant transpiration will continue at the potential rate until a critical value of soil suction is reached. Beyond this value, the potential transpiration could no longer be continued over a long period and the transpiration rate falls below the potential value.

II The critical soil suction or pressure head is not a unique value, but depends on the evaporative demand.

III A plant's wilting point at certain soil suction is a variable that depends on the evaporative demand.

IV When soil moisture content is close to saturation, specific conditions will occur such that root activities are stopped or delayed and root extraction might cease.

As discussed, above with adaptation of some of the published results, Mathur and Rao, (1999) make it possible to obtain a relationship between the soil moisture content and relative function of root extraction coefficient '$\alpha(h)$' (see equation 3.26). This relationship shows that, at optimal soil moisture conditions, root water extraction will be equal to the potential transpiration rate. When soil moisture is limited, root water extraction will reduce by a factor, $a(h)$, which is a function of pressure head. The reduction function is obtained by establishing the three conditions listed below:

$$\alpha(h) = \frac{h - h_4}{h_3 - h_4} \quad \text{for} \quad h_4 \le h_3 \qquad 3.26a$$

$$\alpha(h) = 1 \quad \text{for} \quad h_3 \le h < h_2 \qquad 3.26b$$

$$\alpha(h) = \frac{h - h_1}{h_2 - h_1} \qquad \text{for} \qquad h_2 \le h < h_1 \qquad 3.26c$$

Where:

h is pressure head at the time of estimating

h_1 is pressure head at saturated conditions

h_2 is pressure head at soil field capacity

h_3 is pressure head beyond which relative transpiration is less than unity for high and low potential transpiration

h_4 is pressure head at zero transpiration or soil wilting point moisture content

The pressure head h being less than or greater than h_4 indicates a condition of oxygen deficiency and wilting point, respectively; and h_3 depends on evaporative demand. Thus, the optimal uptake takes place when h lies between h_2 and h_3.

Water extraction is assumed to be zero when the soil is wetter than the saturated point (h_1) and when the soil is drier than the wilting point (h_4). Water uptake is constant and maximum when the water potential ranges between h_2 and h_3.

3.3.2.3 Explanation of the root extraction model

As discussed in section 2.4.1.Two models of microscopic and macroscopic for root extraction can be undertaken. To adopt a microscopic model would be impractical, as the detailed geometry and hydraulic properties of the root system are difficult to measure and are time dependent. In addition, the parameters that are required in the model, such as the permeability of roots, vary with position along the root, as Mathur and Rao (1999) point out. In this work and in micro-catchment systems, for practical purposes, a macroscopic scale model is approached.

3.3.2.4. Plant rooting characteristics in micro-catchment systems:

A micro-catchment water harvesting system in the root zone consists of a wetting pattern in three-dimensions, where the distribution and shape of the wetted volume depends on gravitational forces and root distributions. The distribution of water and nitrates and the shape of the wetted soil volume in the profile are influenced by:

I Root system distribution (i.e. density profile and pattern), and root system effectiveness (i.e. maximum inflow rates for nitrate and water);

II Soil types (soil hydraulic properties, dispersivity, nitrate-diffusion coefficient, etc.)

III Climatic conditions (i. e. potential transpiration rate), as supported by Habib and Lafolie (1991).

The shape of the wetted zone decides the limits of root activities, which are naturally limited where moisture availability is high. The limited water design of Micro-Catchment systems in arid climate will give this opportunity, with plants capable of utilising the available water and nutrient resources efficiently.

The three-dimensional geometry of a root zone in a micro-catchment system is difficult to describe in mathematical terms, because of moisture dynamics complexity in the soil, and this complex geometry is also related to the unsuitable distribution of the rainfall runoff regime in arid climates. The one-dimensional geometry assumption in solving the set

of equations has some limitations in modelling water uptake by root systems differing only by their densities. This suggests two modifications, which should be included in the water uptake model:

I Root resistance to internal water flow; and

II Soil resistance terms accounting for higher potential gradients in a soil layer for a low root density. The water uptake by the root system appears to be very sensitive to the distribution of the root system. This indicates that the identification of active parts of the root system by means of mathematical identification techniques should be possible (Habib and Lafolie, 1991). The complex pattern in the root zone of a micro-catchment system requires a search for the possible root zone boundaries and root distribution, before quantitative assessment of root extraction can be achieved realistically.

An exact definition of the optimal size of the wetting zone in the soil is not possible for all field conditions, particularly in a Micro-Catchment system and conditions of arid climate. However, many researchers feel that under arid conditions, a minimum of 33% of the potential root zone size is needed, and up to 66% may be preferred for better margins of safety and nutrient availability. In humid climates, 25% to 50% is considered adequate for most crops.

3.3.2.5. Root extraction model in a micro-catchment system:

Up to this stage, we have defined two main required features of the model as follows:

I. First: The model should be of the macroscopic type, and

II. Second: The model should be able to relate root extraction to soil moisture availability in soil.

III. A third feature of the model, which needs to be discussed here, is that the model should be flexible, such that if data are available on root effectiveness or distribution,

these could be incorporated into the model with ease. A review of the literature lists various extraction models suggested by researchers when soil moisture is not limiting. For cases when soil moisture is limiting, the extraction term is reduced by a factor that is a function of the soil water pressure head and the hydraulic conductivity in the root zone. From the various available extraction models, a macroscopic linear root water uptake model is adopted in this study.

To obtain a mathematical interpretation of the root extraction model, assume that the entire root zone is divided into (n node) concentric finite cylinders of nodal points in the vertical direction. If the root extraction of subdivided root depth is denoted (D_i), then the total volumetric root extraction (D_r) to extract this amount can be expressed by:

$$D_r = \sum_{i=1}^{n} D_i \qquad i = 1, 2, 3, \ldots\ldots n \qquad 3.27$$

The first limits in equation 3.27 require that the total volumetric root extraction from each of the finite root depths should not exceed the potential volumetric transpiration. If the rate of extraction from each node (i) is represented by a sink term (S_i) then

$$D_i = \sum_{i=1}^{n} S_i * V_i \qquad 3.28$$

Where:

V_i is the volume of two node distance (i and i+1);

To satisfy the first constraint, (S_i) should not exceed an upper value (i.e. $S_i \leq S_{max}$).

To define (S_{max}), two options can be considered.

I. Firstly, similar to that suggested by Hoogland in Belmans et al (1983), in this approach, the extraction under non-limiting moisture conditions could be related to the depth in the root zone from soil surface in a linear relation.

$$S_{max} = a - b|z| \qquad 3.29$$

Where:

a and b are constants in principle and have to be determined from measured data. Values of $0.01 \leq a \leq 0.03d^{-1}$ (per day) with a mean of a =0.02, were used by Belmans et al (1983).

II. The second option or approach to define S_{max}, perhaps more generally applicable, is defined by:

$$S_{max} = \frac{T_p}{d_r} * f(r,z) \qquad 3.30$$

Where:

f(r,z) is a function of spatial co-ordinates. f(r,z), which can be viewed as a weighting function,and used to introduce known root effectiveness in both the radial and vertical directions.

Considering that in a micro-catchment system and arid climatic conditions the range of moisture variation in the root zone is commonly small, the second approach (eq 3.30) is considered more appropriate. The function $f(r,z)$ allows a high degree of flexibility, but the value of (S_{max}) must be constrained, if the value of $f(r,z)$ is not unity.

To define the limits of (S_{max}), the experimental evidence suggests that when root extraction is not controlled by the irrigation regime, the maximum possible rate of extraction is in the range suggested by Belmans et al (1983). The experimental evidence, which was discussed in section 3.3.2.2, shows that in low frequency irrigation, the roots are capable of

extracting the same amount of moisture from a smaller root zone. Quantitatively, it is possible to define an acceptable upper limit for S_{max} by:

$$S_{max} = \hat{S}_{max} * F_1 \qquad 3.31$$

Where:

$\hat{S}_{max}$ is the value of (S_{max}) when potential root depth is attained and

F_1 is a factor. This value is only required when value of f(r, z) departs from unity. Thus, the constraint can be expressed by:

$$\sum_{i=1}^{n_1} S_i * V_i < D^i_{max} \qquad 3.32$$

Or simply:

$S_i < S_{max}$ $\qquad$ i = 1,2,....., n

Based on the suggestion of Prasad (1988), a linear root water extraction term varies with time and equals zero at the bottom of the root zone. Prasad (1988) validated the model using the experimental results of Erie et al (1965) and the model results were found to agree well with the experimental data. It is for this reason that the sink term developed by Prasad (1988) is adopted in this study. The water extraction function based on this suggestion is

$$S(z,t) = \frac{2T_p(t)}{z_r}\alpha(h)\left(1 - \frac{z}{z_r}\right) \qquad 3.33$$

Where:

z_r = maximum rooting depth;

z = root depth on jth depth

$S(z,t)$ = extraction rate, considered positive from the soil into the root;

$T_p(t)$ = Potential transpiration rate on the tth day; and $\alpha(h)$ = pressure head-dependent reduction factor.

In the water extraction expression of 3.33, the water extraction rate is proportional to the root depth (z), which in turn is a function of time.

3.3.2.6 Calculation of stress days from soil moisture data

The most important aspect of growing tree crops in arid climates is to ensure that the number of stress days in a season never get to a level where it will kill the trees. Poor yield can be tolerated in a season, but dead trees cannot. This section describes the methodology for calculating the number of stress days based on daily soil moisture conditions in the root zone.

Several simulation runs were made in order to evaluate soil moisture conditions for crop growth in arid regions. The decision factors used were stress day and minimum amount of supplementary water requirement (Phien et al., 1984). The stress day is defined as a day when the soil water content is less than a minimum value, $\theta_{\min}$

$$\theta_{\min} = \theta_{FC} - (\theta_{FC} - \theta_{WP}).MAD \qquad 3.34$$

Where:

MAD is the dimensionless maximum allowable deficiency (James, 1988). In this study, MAD is taken as 0.75 of the available soil moisture-holding capacity of the soil.

θ_{FC} is soil moisture content at field capacity

θ_{WP} is soil moisture content at wilting point

For stress day, all-important descriptions (namely, the total number, time of occurrence and severity) were considered. The severity is represented by a dimensionless stress day factor, S_d, defined as (Hiler and Clark, 1971):

$$S_d = 1 - \frac{\theta - \theta_{WP}}{\theta_{\min} - \theta_{WP}} \qquad 3.35$$

Where:

θ_{min} is the critical value of soil water content for crop growth calculated with equation 3.35

The amount of deficit water (ADW) corresponding to duration of stress day is also evaluated.

$$ADW = \text{maximum } [DW_k] \quad k = 1,\ldots\ldots,N_S \qquad 3.36$$

Where:

$$DW_k = (\theta_{min} - \theta_k).DRZ$$

N_S is the duration (in days) of the spell of stress days being considered and DRZ is the depth of the root zone.

This may be treated as the minimum amount of supplementary water required in order avoiding the corresponding stress spell. The minimum amount of supplementary water required in a month or during the entire growing season may be computed accordingly by summing up the individual amounts needed in the different spells, if any, covered by that month or the growing season.

3.3.3 Soil moisture movement, the infiltration model, in the infiltration zone of a micro-catchment system

The numerical approximation of equation 2.10 leads to a solution by the finite-difference expression, which is valid for all nodal points, except the top and bottom points of unsaturated soil in the infiltration zone of a micro-catchment. A popular method to solve equation 2.10 has been the implicit, finite difference scheme, with explicit linearization of hydraulic conductivity (K), water capacity (C), and root extraction (S), as described by Binh et al. (1994), Belmans et al. (1983) and Haverkamp et al. (1977). They divided the entire flow domain into grid intervals Δz, Δl, Δu, and the time domain is similarly divided into intervals Δt. The two-dimensional grid of the equations is given in the next chapter (chapter 4) and it is applied to the design of micro-catchment systems (chapter 9). Equation 2.10, can be expressed in finite difference form as:

$$\frac{h_i^{j+1} - h_i^{j}}{\Delta t^{j}} =$$

$$\frac{K^{j}_{i-(1/2)}\left(\frac{\Delta h^{j+1}_{i-(1/2)}}{\Delta Z_i} + 1\right) - K^{j}_{i+(1/2)}\left(\frac{\Delta h^{j}_{i+(1/2)}}{\Delta Z_i} + 1\right)}{C_i^{j}\Delta Z_i} - \frac{S_i^{j}}{C_i^{j}} \qquad 3.37$$

Where:

h^j denotes the appropriate value of h, (pressure head) at the nth discrete time level ($t-t^j$)

$\Delta t = t^{j+1} - t^j$ is the time steps

Subscript (i) is the node number (increasing downward), and

Superscript (j) is the time level.

(K) is the hydraulic conductivity taken at the old time level (explicit linearization). The spatial averages of K were calculated as geometrical means. The scheme can be solved without iteration.

C is specific moisture capacity evaluated using h^j, as defined in hydraulic conductivity (explicit linearization).

The solution is assumed to be known at time level, j, and unknown at time level j+1

The applied equation by Belmans, et al (1983) accommodated three scheme adaptations as proposed by van Dam and Feddes (2000) in equation 3.37 as follows:

I. The first adaptation is the handling of the differential water capacity, C, in equation 3.37, put in the dominator of a fraction. As we know, the water capacity (C) in the saturated zone equals zero, limiting the numerical scheme to the unsaturated zone. Based on Belmans (1983), the saturated zone and fluctuations in the groundwater table had to be modelled separately. The numerical scheme was adapted in such a way that only multiplication with C occurs. However, In this variability, the flow equation can be solved for both unsaturated and saturated zones simultaneously.

II. Secondly, because of high the non-linearity of the water content (C), in the Belmans model, averaging during a time step results in serious errors when highly transient conditions are simulated. In order to control these errors, a simple but effective adaptation was suggested by Milly (1985) and further analyzed by Celia et al. (1990), followed by van Dam (2000). Instead of applying during a time step as follows:

$$\theta_i^{j+1} - \theta_i^j = C_i^{j+(1/2)}(h_i^{j+1} - h_i^j) \qquad 3.38$$

Where:

$C_i^{j+(1/2)}$ = The average of water capacity during the time step,

They applied at each iteration step:

$$\theta_i^{j+1} - \theta_i^j = C_i^{j+1,k-1}(h_i^{j+1,k} - h_i^{j+1,k-1}) + \theta_i^{j+1,,k-1} - \theta_i^j \qquad 3.39$$

Where:

k is the iteration level

$C_i^{j+1,k-1}$ is the water capacity evaluated at the pressure head value of the last iteration,

$\left(h_i^{j+1,k-1}\right)$ is the last pressure head iteration

At convergence the term $(h_i^{j+1,k} - h_i^{j+1,k-1})$ will be small, which effectively eliminates water capacity (C). Implementation of this mass conservation property requires an iterative solution of the equation matrix (chapter 4).

III. The third adaptation concerns the averaging of hydraulic conductivity (K) between the nodes. Haverkamp and Vauclin (1977) and Belmans et al. (1983) proposed using the geometric mean of hydraulic conductivity in the model.

$$K_{i-1/2}^j = \sqrt{K_{i-1}^j K_i^j} \qquad 3.40$$

In their simulations the geometric mean increased the accuracy of calculated fluxes in nodal distance (van Dam and Feddes, 2000). However, the geometric mean has serious disadvantages too. When simulating infiltration in arid regions and dry soils or high

evaporation from wet soils, the geometric mean severely underestimates the water fluxes (Warrick, 1991). Other researchers proposed using the harmonic mean of hydraulic conductivity (K) or various kinds of weighted averages (Hills, 1989, van Dam and Feddes, 2000). In this study and micro-catchment design system, and based on experience of van Dam (2000) arithmetic mean of hydraulic conductivity used.

$$K_i^j = K\left(h_i^j\right) \quad \text{and} \qquad K_{i+(1/2)}^j = \frac{K_i^j + K_{i+1}^j}{2} \tag{3.41}$$

Equation 3.34, incorporating three adaptations above, may be rewritten in the following equation form.

$$C_i^{j+1,k-1}\left(h_i^{j+1,k} - h_i^{j+1,k-1}\right) \tag{3.42}$$

$$= \frac{\Delta t^j}{\Delta z_l}\left[K_{i-(1/2)}^j\left(\frac{h_{i-1}^{j+1,k} - h_i^{j+1,k}}{\Delta z_u}\right) + K_{i-(1/2)}^j - K_{i+(1/2)}^j\left(\frac{h_i^{j+1,k} - h_{i+1}^{j+1,k}}{\Delta z_l}\right) - K_{i+(1/2)}^j\right] - \Delta t^j S_i^j$$

Where:

$\Delta t^j = t^{j+1} - t^j$

$\Delta z_u = z_{i-1} - z_i$

$\Delta z_l = z_i - z_{i+1}$

Δz_i is the compartment thickness

K and S are evaluated at the old time level j

Application of equation 3.39 to each node in the infiltration basin of a micro-catchment system, including the prevailing boundary conditions, results in a tri-diagonal system of equations, which will be solved efficientey in chapter 4 (Press et al., 1989 and Remson et al, 1971).

3.4 Potential evapotranspiration and estimating potential transpiration

The Penman-Monteith equation will not be specifically presented here since it appears in many references (e.g., Allen et al., 1998). Based on Kotsopoulos and Banajimopoulos (1997), the Penman (1984) equation which is modified states the daily evaporative demand in appendix A. The modified Penman method is the most comprehensive approach to estimating reference crop evapotranspiration, because it takes into account all the factors that influence the evapotranspiration rate. Thus

$$ET_0 = C * \left[\frac{\Delta}{\Delta + \gamma} * Rn + \frac{\Delta}{\Delta + \gamma} * Ea \right] \qquad 3.43$$

Where:

ET_0 = reference evapotranspiration (mm/d)

C = the adjustment factor that compensated for the effect of day and night weather conditions;

Δ = The slope of saturation vapour pressure curve at mean air temperature (Millibars/°C)

γ = Psychrometric constant (millibars/°C)

Rn = net solar radiation in evaporation units (mm/d)

Ea = aerodynamic term (mm/d)

The functional model of Ritchie (1972), as used in CERES-Maize, is used to calculate soil evaporation (E_s) ,as described in a separated model in 2.11 (section 2.3.2.3). The difference in the estimated potential evapotranspiration and estimated potential evaporation (equation 3.40 and 2.11 respectively) gives the potential transpiration (T_P) that is used in the calculation of crop water requirements in a micro-catchment system in an arid climate.

3.5 Micro-catchment characteristics and their relation to model components

The micro-catchment characteristics to be provided by the proposed model represent limitations on design in micro-catchment systems. The amount of water which is available from runoff in a micro-catchment water harvesting system in arid climate regions depends upon rainfall characteristics (amount, intensity and distribution) and micro-catchment characteristics (size, slope and antecedent moisture conditions). The consumption of available water in the infiltration basin of this system depends on the geometry of the root zone. For practical problems of design, the following characteristics of a micro-catchment should be accommodated.

3.5.1 Size of the micro-catchment

It is commonly accepted that runoff efficiency, which is defined as the percentage of rainfall converted into runoff, is a decreasing function of the size of the catchment area. Although for a large catchment area the absolute amount of water collected is greater, the relative amount of water per unit area received by trees in the infiltration zone is less for a smaller area. This can be explained by the longer distance of flow between the runoff generation area and the infiltration basin and the related higher water losses at the outside edge of the infiltration basin area. For a larger size of micro-catchment system, the opportunity time for rainwater to infiltrate is longer, and relatively smaller amounts of water will reach the infiltration basin. It is therefore reasonable to design a micro-catchment in a such a way that, for a given infiltration size, the size of the runoff area surrounded between the infiltration zone and any point on the outline of the micro-catchment is minimal, subject to the plant's water requirements.

3.5.2 Slope of runoff area

Based on the objective of this project, the only resource of water that could answer to all water needs is rainfall and runoff. The amounts of water available in the infiltration basin depend both on the size and the geometry of the contributing area as well as on the related characteristics of the micro-catchment and the nature of the precipitation. The size of the micro-catchment area and precipitation has previously been discussed. The geometry of the

runoff area depends on slope and it's relation to runoff efficiency that sometimes can be affected by over 30% regarding runoff efficiency and water delivery in the infiltration basin.

3.6 Discussion

The rainfall-runoff relationship is a complex function of soil surface infiltration and rainfall intensity in the runoff zone of a micro-catchment system. On the other hand the soil hydraulic properties in the infiltration zone, which appear in the equations, are functions of the independent variables (moisture content or suction head). The solution of these equations can be approached analytically or numerically. The most appropriate conditions to be found in micro-catchment systems are discussed below.

The non-linear mass conservation equation was difficult to solve analytically. Analytical models require restrictive assumptions and resorting to linearisation of rainfall runoff and soil infiltration governing equations, or to eliminating the time element (i.e. Zarmi et al, 1983) thus presuming steady-state conditions which rarely occur in a Micro-Catchment system (Nieber and Feddes (1999). For some problems in non-linear equations and in particular when the coupled rainfall and infiltration in the runoff zone and soil moisture movement in the infiltration zone of Micro-Catchment systems is considered, no analytical solution exists. Perhaps the most serious drawback of analytical based models is their inadequacy to describe complex rainfall-runoff geometry, coupling available water to evaporation, root extraction of plants, infiltration and soil moisture movement through the soil, such as those which occur in the root zone of micro-catchment systems.

The numerical methods for solving the equations of continuum mechanics in many areas of engineering have also been adapted to the solution of the governing equations of surface runoff generation, infiltration and crop water requirements in micro-catchment systems conditions (Nieber and Feddes1999). Numerical methods are based on subdividing a rainfall regime into finite time segments represented by a series of time intervals at which infiltration and rain excess can be obtained. This solution is neither independent of the solution at the surrounding segments, nor the boundary conditions. These methods which have been used in recent years, include finite difference methods (explicit or implicit),

integrated finite difference methods, finite element methods, and boundary element methods. Of these methods the finite difference and the finite element methods have the most applications for modelling soil conditions of a micro-catchment system. Nieber and Feddes (1999) adopted models based on this technique.

The advantage of the numerical solution approach, in comparison to the analytical solution approach, is the flexibility in handling arbitrary and initial conditions, arbitrary spatial parameter distributions, and non-linearity in the governing equations. Numerical models, on the other hand, provide a high degree of flexibility in treating complex, and in some techniques, time dependent boundary conditions and provide the opportunity to vary the operating conditions of the model with relative ease. Some classes of numerical methods allow simulation of complex rainfall runoff and water infiltration geometry (Feddes, 1988). Some numerical models of rainfall-runoff involve extensive data preparation, particularly for time dependent and soil condition problems (Cundy and Tento, 1985 Yen and Lee, 1997), and are commonly more expensive to use then analytical models.

Existing numerical models for design of micro-catchment systems have a number of serious drawbacks, namely:

I. The majority consider the moisture regime in micro-catchments to be sorption dominant, and do not allow moisture depletion by root extraction and surface evaporation.

II. In addition, modelling root extraction was, in many cases, based on the availability of certain information regarding root effectiveness or root hydraulic properties. Macroscopic root extraction models were generally characterised by the exclusion of evaporative demand effect on moisture availability in the root zone.

No numerical models exist for coupling all hydrological factors, which are affected in the design of a micro-catchment system. In fact it is better to design a system based on a logical relationship between water, soil and atmosphere and daily validity of data.

Chapter 4 Description of a finite difference model in boundary conditions for predicting soil water states in the infiltration basin of a micro-catchment system

4.1. Introduction

Chapter 3 described the process involved in runoff and infiltration in a micro-catchment system. This chapter describes how these physical components and relationships can be built into a finite difference model to describe the water stress of the soil in an infiltration basin of a micro-catchment system.

The first part of this chapter describes how the runoff from the model can be calculated and the data presented in a format to meet an infiltration basin model. The second part of the chapter describes a numerical model that can calculate the water balance in an infiltration basin

The basic finite difference model describes the water balance in the root zone over time. The model gives a mass balance of water in different soil layers as:

$$\text{Soil water} = P - I - E_t - E_s$$

Where:

I = infiltration

P = rainfall

E_t = transpiration or root extraction

E_s = soil evaporation

E_r and E_S are driven by potential evapotranspiration

The actual model and the components of the model boundary conditions are described below.

4.2. Description of the runoff model in a micro-catchment system

A physical based model that simulates the hydrological response of a catchment subject to spatially and temporally varied storm rainfall is described in section 3.3.1. According to the model, the relationship between daily rainfall and potential runoff is linear. Since the basin is small, the potential runoff is given as:

$$Run_{(Pi)} = cd_i - b \qquad i = 1,2,\ldots\ldots,m \qquad 4.1$$

Where:

$Run_{(Pi)}$ = Potential runoff (the amount of rain d_i converted into potential runoff in the ith day, in millimetres)

d_i = the total daily rain depth in the ith day of the year (in millimetres),

m = the number of the day under consideration (this study uses 365 days),

c and b = constant coefficient

The expression for Potential runoff ($Run_{(Pi)}$) can be transformed as follows:

$$Run_{(Pi)} = c(d_i - \delta) \qquad i = 1,2,\ldots\ldots,m \text{ (days)} \qquad 4.2$$

Where:

$\delta = b/c$ is interpreted as the threshold value for runoff production for a rainstorm in the area considered (in millimetres),

If during a specific storm d_i, no potential runoff is generated (that is, the depth is less than the threshold value or the intensity is not "high enough"), then the threshold value is equal to rainfall ($\delta = d_i$). For storms that produce potential runoff it is shown that the threshold value is independent of separate rainstorm characteristics and can be written as:

$$Run_{(Pi)} = c(d_i - \delta) \qquad i = 1,2....m \text{ (days of year)} \qquad 4.3$$

Where:

δ = A constant threshold value, independent of the single event this amount of rainfall can be calculated by the rainfall-runoff model described in section 3.3.1. $Run_{(Pi)}$ represents the sum of runoff from a catchment for days (i) when rainfall exceeds the threshold value, see section (3.3.1).

The hydraulic response characteristics of the catchment to rainfall and potential runoff can be described using the concept of micro-catchment size and slope. The two additional factors affect both the travel time from the point, where water falls to the ground until it reaches the outlet of the runoff area, and the volume of water received by the infiltration zone. The volume of water collected in an infiltration basin is evaluated as a function of the micro-catchment's physical and geometrical properties, which for an engineered catchment is the size and slope of the runoff area. In micro-catchments that have similar shape and slope, as discussed in 2.2.2 (chapter 2), runoff efficiency is a function of micro-catchment area (Oron et al, 1983, Frasier 1989, Sharma, 1986, 1982). Therefore the potential runoff in equations 4.1, 4.2, and 4.3 has to be changed into actual runoff as a variable, depending on the micro-catchment size on a specific slope.

The potential runoff can be transformed to actual runoff using a simple regression model form such as:

$$e = \alpha + \beta(A) \qquad 4.4$$

Where:

e = Runoff efficiency or percent of potential runoff calculated from equation 4.3

α = Constant coefficient of regression

β = Coefficient in relation to the slope of regression and slope of micro-catchment

A = Micro-catchment size (square meter)

Multiplying runoff coefficient (as a percentage of potential runoff) by potential runoff yields the actual runoff

In order to estimate the volume of water received by an infiltration basin, equation 4.4 has to be transformed into actual runoff volume, rather than a value in millimetres. If the potential runoff calculated by equation 4.3 is multiplied by the runoff coefficient (e = % of $Run_{(Pi)}$) and micro-catchment size (A), the volume of harvested water will be given in the considered period (in this study, the period of calculation is daily) as follows:

$$(Run_{(Pi)}/1000)eA = V_{act} \qquad 4.5$$

Where:

V_{ac} = actual volume of runoff (m^3)

Trial values for the volume of runoff are computed using equation 4.5 with the recent value of the micro-catchment size. At this stage, known slope percent of runoff area and its effectiveness on runoff generation is already defined, otherwise a value of unity for runoff coefficient (e) is assumed.

4.3 Soil water balance description in a micro-catchment system

4.3.1 Formulation of moisture flow and initial conditions in an infiltration basin

Finite difference approximation can be applied to partial derivatives, with appropriate initial and boundary conditions in a micro-catchment system. The initial and boundary conditions represent the field conditions to be emulated. The soil water movement model was given in equation 3.39, and based on the solution of this equation (in appendix C), a statement of the numerical problem, can be summarized with soil moisture content (θ, cm^3/cm^3) and pressure head (h, cm) as the independent variables for micro-catchment conditions, as follows:

$$\alpha_i h_{i-1}^{j+1,k-1} + \beta_i h_i^{j+1,k-1} + \gamma_i h_{i+1}^{j+1,k-1} = f_i \qquad 4.6$$

Consider a one-dimensional unsaturated flow system bounded by linear drains at

Z =0 and Z_r in a micro-catchment system with the initial conditions:

$$\theta(z,t_0)=\theta_0 \qquad t \le 0 \qquad 4.7$$

Or

$$\theta(z\ ,t_0)=\theta_0(z,t_0) \qquad \text{For } z_0 \le z_i \le Z_r \qquad 4.7a$$

$$h(z,t_0)=h_0 \qquad t_0 \le 0 \qquad 4.7b$$

Or

$$h(z,t_0) = h_0(z,t_0) \qquad \text{for } z_0 \le z \le Z_r \qquad 4.8$$

and the following general boundary conditions:

$$\theta(z_0,t)=\theta_i(t) \qquad \text{For} \quad 0 \le t \le t_i \qquad 4.9$$

$$h(z_0,t)=h_i(t) \qquad \text{For} \quad 0 \le t \le t_i \qquad 4.10$$

Where:

$h_0(z,t_0)$ = initial pressure head

$\theta_0(z,t_0)$ = initial moisture content

$h_i(t)$ = applied water (head) pre-specified value of pressure head

$\theta_i(t)$ = soil moisture content

t_i = irrigation or rainfall runoff application time

z = depth of soil layer steps (soil layers or sub divided parts of maximum soil profile depth)

Z_r = Maximum depth of soil profile

The above equations are time dependent and highly nonlinear (Romano et al, 1998). The independent variables are the moisture content, and the pressure head. The coefficient

appearing in equation 4.6 (α, β, and γ), are functions of the independent variables. The field conditions to be simulated represent the boundary conditions for the mass conservation equations in the infiltration basin (see appendix C). They are also time dependent and non-linear, since the transpiration, evaporation and surface infiltration can, for most periods, be moisture content (or soil pressure head) dependent. The flow geometry is multidimensional and the geometry of the root zone can be complex, so that, in this study, it is assumed that flow geometry is one-dimensional.

4.3.2 Evaluation and description of the coefficients of the moisture flow model

As can be seen in appendix C, the coefficient matrix associated with the finite difference solution of differential equations is sparse; that is, they contain a large number of zero elements. To be efficient, a method involving tridiagonal system was selected for solution of the equations. Triangular elements can be used effectively, not only to represent difficult geometries, but also to concentrate co-ordinate functions in those regions where rapid changes are expected, such as near the soil surface or wetting fronts. For one symmetric element in one dimensional soil moisture flow, the approximation functions of both soil moisture content and pressure head are identical to plane triangular elements. The properties of the selected method are described in many textbooks (Gottardi and Venutelli, 1992; Dunavant. 1985; Remson; 1971; Salvadori and Baron, 1961).

Application of equation 3.39 in relation to soil water movement, as solved in appendix C, has given a set of of equations (see appendix C). Each of these equations depends on each node in a tridiagonal matrix, for which we may define the following coefficients. The system of equation (C4) can be written in a matrix notation as

$$Ah_i^{j+1,k-1} = f_i \qquad 4.11$$

The system is solved and the equations 4.11 are in the form: of

$$\begin{bmatrix} \beta_1 & \gamma_1 & 0 & 0 & \cdots & & \\ \alpha_2 & \beta_2 & \gamma_2 & 0 & & & \\ 0 & \alpha_3 & \beta_3 & \gamma_3 & 0 & & \\ 0 & & & & & & \\ 0 & & & & & & \\ 0 & \cdots & & \alpha_{n-1} & \beta_{n-1} & \gamma_{n-1} & \\ 0 & \cdots & & 0 & \alpha_n & \beta_n & \end{bmatrix} \begin{bmatrix} h_1^{j+1,k-1} \\ h_2^{j+1,k-1} \\ h_3^{j+1,k-1} \\ \\ \\ h_{n-1}^{j+1,k-1} \\ h_n^{j+1,k-1} \end{bmatrix} = \begin{bmatrix} f_1 \\ f_2 \\ f_3 \\ \\ \\ f_{n-1} \\ f_n \end{bmatrix} \qquad (4.12)$$

It is useful to seek a factorization of matrix A into matrix L multiplied by matrix U. Because of the special nature of A, however, L and U have the forms

A= L * U

$$A = LU = \begin{bmatrix} b_1 & & & \\ \alpha_2 b_2 & & & \\ 0 & \alpha_3 b_3 & & \\ & & & \\ & & & \\ & & & \\ & & & \alpha_n b_n \end{bmatrix} \begin{bmatrix} 1 & \lambda_1 & & & \\ & 1 & \lambda_2 & & \\ & & 1 & \lambda_3 & \\ & & & & \\ & & & & \lambda_{n-1} \\ & & & & 1 \end{bmatrix} = \qquad 4.13$$

Where:

A is the coeficient section (first section) of matrics in equation 4.12. Coeficient of matrics A subdivided in two matrics of L and U that multiplication of these two matrics resulted in a matrics in equation 4.14.

L and U are two sections of matrics in equation 4.13

On multiplying out LU, we obtain a matrix of the following form:

$$A = LU = \begin{bmatrix} b_1 & b_1\lambda_1 & 0 & 0 & \cdots & 0 \\ \alpha_2 & \alpha_2\lambda_1 + b_2 & b_2\lambda_2 & 0 & \cdots & 0 \\ 0 & \alpha_3 & \alpha_3\lambda_2 + b_3 & b_3\lambda_3 & \cdots & 0 \\ 0 & & & & & \\ 0 & & & & & \\ 0 & & & \alpha_{n-1} & \alpha_{n-1}\lambda_{n-1} + b_{n-1} & b_{n-1}\lambda_{n-1} \\ 0 & & & \alpha_n & & \alpha_n\lambda_{n-1} + b_n \end{bmatrix} \qquad 4.14$$

For this to equal A, it is required that:

$$\beta_1 = b_1$$

$$b_i \lambda_i = \gamma_i \qquad \text{i} = 1, 2, \ldots\ldots\text{n-1}$$

$$\alpha_i \lambda_{i-1} + b_i = \beta_i \qquad \text{i} = 2, 3, \ldots\ldots\text{n} \qquad 4.15$$

Equation 4.15 is obtained by comparing the respective terms in 4.10 and 4.14. Solving for the λ_i and b_i

$$b_1 = \beta_1$$

$$\lambda_i = \frac{\gamma_i}{b_i} \qquad \text{i} = 1, 2, \ldots\ldots\text{n-1} \qquad 4.16$$

$$b_i = \beta_i - \alpha_i \lambda_{i-1} \qquad \text{i} = 2, 3, \ldots\ldots, \text{n}$$

These are the values of b_i and λ_i that are the entries of L and U (two matrics) in equation 4.13 giving the factorization of A. For the above computations to be valid, $b_i \neq 0$ for all node i. This is true in the cases considered herein.

Finally the solution can now be found for different depths to establish the pressure head:

I. First: L*y = f is solved by forward substitution giving

$$y_1 = \frac{f_1}{b_1}$$

$$y_i = \frac{f_i - \alpha_i y_{i-1}}{b_i} \qquad i = 2, 3, \ldots\ldots\ldots, n \qquad 4.17$$

II. Second: $Uh_i^{j+1,k-1} = y$ is solved by backward substitution to give

$$h_n^{j+1,k-1} = y_n$$

$$h_i^{j+1,k-1} = y_i - \lambda_i h_{i+1}^{j+1,k-1} \qquad i = n-1, n-2, \ldots\ldots..1 \qquad 4.18$$

In this application the expressions for the coefficients $\alpha_i, \beta_i, \gamma_i$ and f_i are listed for each node and for both flux and head controlled boundary conditions.

4.3.3. Description of root extraction (transpiration)

This section describes how transpiration losses from different soil depths are calculated. At the beginning of each time step, moisture content value, or pressure head at each nodal point in the root zone are computed, by extrapolation from previous values.

Root extraction (S_i) is computed using equation 3.33 with the conditional values of $a(h)$ as defined in equation 3.26. At this stage, known functions of effectiveness of root absorption, f(r,z) in each nodal point are introduced; otherwise a value of unity is assumed.

Two important features of crop root systems affect water uptake in the profile of the root zone. The first is that high root densities can result in the rapid depletion of available water in surface soil layers. The second is that deep root penetration can make available a much larger volume of soil water for plant extraction than provided by the surface layers of soil. Water uptake by deep roots is in part influenced by the density of roots in the soil and by resistance incurred by the long length of xylem-involved transport of water to the soil surface. Numerical trail values for the sink term requires the definition of the volume of influence of each sink in the root zone. This in turn requires the limitation of the root zone boundaries. In one-dimensional problems, horizontal planes representing the root zone

depth, which may vary with time, easily accomplish this limitation. In micro-catchment systems, limitation of root zone is far more complex, however. In order to reduce the complex relationship between root extraction and root growth, it is assumed that tree root growth in the infiltration basin is the maximum possible growth. The technique used here is as follows.

In order to control the possibility of the sink term being active at unrealistic depths or radial distances, a time dependent control zone is defined representing the maximum possible radial and vertical distances at which roots may be present. In practice, the presented control zone could be defined from known rooting characteristics and maturity in relationship with time. This relationship was provided by Mathure and Rao (1999) and can also be established by sampling techniques, such as angle profile sampling or trench profile techniques (Atkinson., 1991). A sample area in an infiltration zone can provide valuable information not only on the exact extent of the root zone, but also on root density distribution, to evaluate the root effectiveness fraction in both the radial and vertical direction ($f_{r,z}$). The sampling methods in the infiltration zone of a micro-catchment system in specific conditions are simple, as the depth required is not too deep and relatively equal to maximum root growth in a profile (maximum about 2 metres). In this study, in order to restrict unrealistic depth or radial distance of soil moisture in the root zone, it is imagined that for mature trials the root growth is at maximum possible depth and constant fixed distribution in any time period of a year.

The estimates of error, which may result in selecting the control zone (fixed root distribution), are typically expected to be small as, in spite of the uncontinuous dispersion of moisture from the root zone, steep gradients are expected to remain close to the boundaries of the wetting zone. This fact, coupled with the weighting given to root depth in the sink terms in this study, further reduces the likelihood of error.

In most cases, the radial extent of the root zone can be defined with reasonable accuracy in the infiltration basin, as the site of the basin should correspond to root zone development. The sink term can then be integrated over the one-dimensional finite difference grid as follows:

$$D_d = \sum_{i=1}^{i=n} \int_{r=0}^{r=n} S_i dr \qquad 4.19$$

Where:

D_d = volumetric root extraction per day

S_i = root extraction or sink term defined in equation (3.33)

r_i = radial distance to the centre of the axi-symmetric of root length

To evaluate the integral using the axi-symetric finite difference elements, would require that sink term (S_i) varies in the radial direction within a vertical direction of node distance (z_i). In this study, as shown in figure 4.1, it can be assumed that sink term (S_i) is representative of a finite volume of radial thickness (Δr), and the integration is carried out in the vertical direction only. Then the root extraction is calculated as:

$$D_d = \sum_{i=1}^{i=n} 2\pi r_i S_i \Delta z_i = \sum_{i=1}^{i=n} 2\pi r_i \frac{2T_p}{z_i} \alpha(h) \left(1 - \frac{z_i}{z_L}\right) \Delta z_i \qquad 4.20$$

Where:

r_i is effective radial thickness of node i,

z_i is vertical depth of root length in node i,

Δz_i is average vertical thickness of node i,

z_L is maximum possible root length

$2 \pi r$ is area of soil layer in node i

T_p is potential transpiration

$\alpha(h)$ is a coefficient dependent on pressure head in node i

The total root extraction in a daily time step, finally, is calculated as:

$$D_d = \sum_{i=1}^{i=n} D_i \qquad 4.21$$

Where:

n is the number of concentric soil layers in the root zone,

i is the node code order

At this stage, the balance with the volumetric potential transpiration ($T_p = D_{i,Max}$) is checked by reference to eq 3.32:

$$D_i \leq D_{i,Max}$$

Otherwise, the trial sink terms are modified by:

$$\hat{S}_i = S_i \frac{D_{i,Max}}{D_i} \qquad 4.22$$

The new values ($\hat{S}_i$) are used to obtain a modified solution by introducing the extraction term in the matrix formulation in equation (4.6).

4.3.4 Moisture flow in the time domain and convergence

The equations of 4.6 and C3 must be calculated for each time step selected; thus time needs to be included as a derivative dependence and as a second dimension to the transient-flow problems. Selection of a suitable method to discrete the time domain needs to consider accuracy and the need to store results from a previous time step. From numerical experiments, a number of investigators (e.g. Hills and Porro, 1989) concluded that a finite difference approximation is the most viable. A number of finite difference schemes can be used, each with various properties, depending on stability and the amount of information to be retained at each time level. In this study, a time centred version, which is also known as "tridiagonal", was adopted. The matrix formulation in equation (4.6) based on this method is transformed into the following form:

$$\frac{1}{2} A\left[\left(h_i^{j+1}\right) + \left(h_i^{j}\right)\right] = f_i \qquad 4.23$$

Where:

A is a Matrix of coefficients

It remains to decide at what time level the matrix coefficients should be computed.

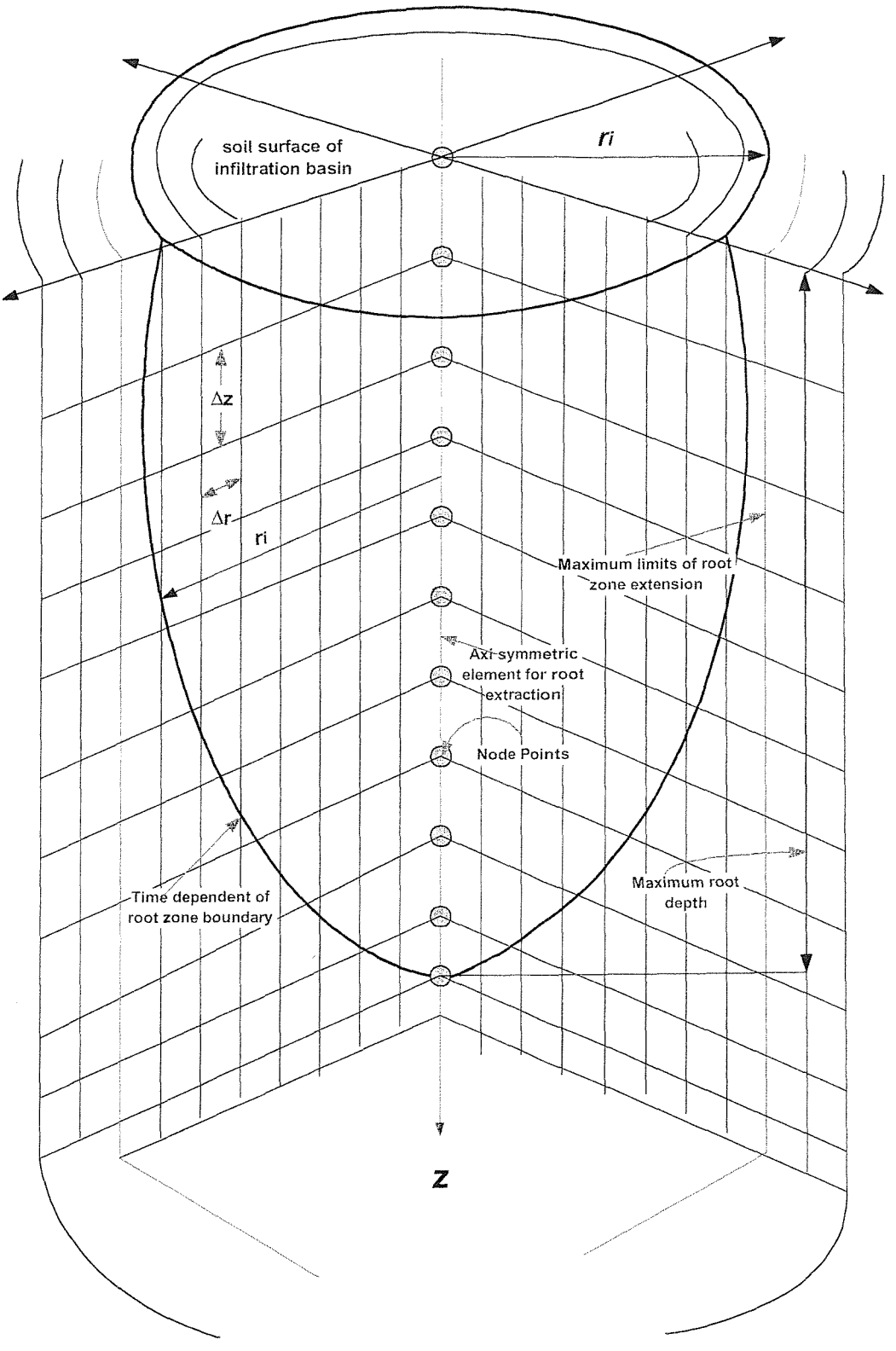

Figure 4.1 Schematic diagram of geometry of root zone and definition of terms in the infiltration basin of a micro-catchment system

When uncoupled flow problems of moisture or pressure head are considered, standard solution methods could be applied to equation 4.24. When a coupled flow problem is considered, both sets of equations have to be solved simultaneously. In this study, a scheme is used by which alternate solutions of equations for ($\theta_i^{t+\Delta t}$), or $\left(h_i^{t+\Delta t}\right)$ are carried out. The matrix coefficient is updated at each iteration, until convergence is achieved. This is accomplished by guessing values for the independent variables (pressure head and soil moisture content) at half the time step, using linear extrapolation from previous known or computed values.

$$h_i^{j+1,k-1} = h_i^{j+1,k} \pm \frac{\Delta t_i^{j+1,k-1}}{\Delta t_i^{j+1,k}} * \left(h_i^{j+1,k-1} - h_i^{j+1,k}\right) \qquad 4.24$$

or

$$\theta_i^{j+1,k} = \theta_i^{j+1,k-1} \pm \frac{\Delta t_i^{j+1,k-1}}{\Delta t_i^{j+1,k}} \left(\theta_i^{j+1,k-1} - \theta_i^{j+1,k}\right) \qquad 4.25$$

The system of equations is then solved to obtain new values for the independent variables (pressure head and moisture content) by the alternating scheme. The highly non-linear nature of the governing equations requires continuous improvements of the results. This is accomplished by an iterative process leading to a convergence solution (e.g. Galarza et al, 1999, Huang et al 1996, Botta and Wubs, 1993).

In numerical simulation, using the pressure head based (h) form of a Richard equation, the value of the pressure head at a new time level is usually guessed at first, and subsequently improved iteratively (Davey and Rosindale, 1994). The iterative process continues until the difference between the calculated values of the pressure head between two successive iteration levels becomes less than present tolerance (δ_a). Since the last iteration of the minimization problem provides the optimum set of parameter values, these lead to the final solution of the simulation problem, until the following inequality is satisfied at all nodes (Huang et al, 1996):

$$\left|\delta_m\right| = \left|h^{j+1,k+1} - h^{j+1,k}\right| \le \delta_h \qquad 4.26$$

or

$$C^{j+1,k}\left|\delta^{m}\right| = \left|\theta^{j+1,k+1} - \theta^{j+1,k}\right| \leq \delta_{\theta} \qquad 4.27$$

In fact, the convergence criterion used is the maximum pressure head or soil moisture content difference $\left|h_i^{j+1,k+1} - h_i^{j+1,k}\right|$ in the iteration solution of equation 4.6.

Improvement to the solution is achieved by:

$$h_i^{j+1,k+1} = \frac{1}{2}\left(h_i^{j+1,k+1} + h_i^{j+1,k}\right) \qquad 4.28$$

$$\theta_i^{j+1,k+1} = \frac{1}{2}\left(\theta_i^{j+1,k+1} + h_i^{j+1,k}\right) \qquad 4.29$$

Then the equations are re-solved until pre-defined convergence criteria are satisfied. The convergence criteria is satisfied when:

$$\left|h_i^{j+1,k+1} - h_i^{j+1,k}\right| \leq \delta_h \qquad 4.30$$

Or

$$\left|\theta_i^{j+1,k+1} - h_i^{j+1,k}\right| \leq \delta_{\theta} \qquad 4.31$$

Where:

$\delta_h = 1.0$ cm (for pressure head)

$\delta_{\theta} = 0.0001\,\text{cm3 cm}^{-3}$ (for soil moisture content)

4.4 Boundary conditions

Micro-catchment systems are by definition small and runoff areas or contributing areas typically have a maximum size of about1000 square metres. Availability of rainfall-runoff and the crop water requirement of the planted crop in the infiltration basin restrict the size of runoff area. Infiltration basins may typically be about 10 square metres, where trees are grown (Boers and Ben-Asher, 1982). Precipitation characteristics and the amount of runoff and soil characteristics restrict water supply in a micro-catchment system. Losses of water from the infiltration basin consist of seepage losses from the bottom of the root zone and water vapour losses from the upper boundary to the atmosphere. The change in the

volume of stored water in the soil profile mainly occurs because of evaporation and plant transpiration or root extraction and rainfall runoff.

The infiltration area is at the lowest point of the micro-catchment and is typically about 9 square metres. The infiltration zone typically has a maximum depth of water of 20 centimeters. The actual design of the basin depends on the slope of the land, the depth of the soil and precipitation. In the case of trees, the rooting area and depth of the different species is documented or can be established experimentally. These characteristics dictate the minimum size and shape of infiltration basins. The boundaries of a micro-catchment system are defined as follows:

4.4.1 Boundary conditions of soil-atmosphere during rainfall and runoff periods

4.4.1.1 Boundary conditions of soil surface evaporation in a micro-catchment system

An appropriate procedure for top boundary conditions during the iterative solution of the Richard equation may determine the success or failure of a numerical scheme. The soil water pressure heads may change very rapidly near the soil surface. For instance, in the case of rainfall and runoff after a dry period, the soil water pressure head may increase in a few minutes from -10^6 to 0 cm. Also, when saturated soils become unsaturated, the pressure head distribution near the soil surface changes rapidly because of the small differential water capacity of most soils near saturation level. Moreover, the top boundary condition may switch from head control to flux-control and vice versa during the iterative solution of the Richard's equation.

Evaporation from the soil surface varies throughout the day in response to changes in environmental considerations. In practice, only the mean daily evaporation data is available for modeling purposes. Since it is the total daily flux of water from the soil surface that is important for modeling purposes the daily evaporation has been distributed equally between the time steps in any one given day.

Rainfall and runoff generally occur in direct storms in any oneday. The model adds daily recharge from the runoff area to the amount of direct precipitation falling on the area

from rainfall to give a total depth of recharge for the day. In the model, the total daily precipitation/ runoff is spread uniformly throughout the day's time steps.

There are two factors that influence the numerical treatment of the soil surface evaporation process in the infiltration basin of a micro-catchment system:

I. Firstly, the phenomenon of the drying front outlined in section 2.3.2. The result is that soil moisture from underlying layers can move to the surface by vapour diffusion. The soil moisture moves continuously in the soil profile as the drying process continues. The implication of the presence of the drying front on the numerical treatment of the evaporation processes is that the soil profile becomes a two-phase system. Within the upper dry region, water loss can be in the vapour phase only, whereas in the lower regions it may contain vapour and liquid water. The vapour leaving the system is assumed to take no appreciable amount of heat, and the problem is reduced to a simultaneous pure heat conduction in one region, and an unsteady coupled moisture and heat flow in the other.

II. Secondly, the evaporative demand is never strictly constant, and variations of such demand, particularly on a daily scale, depends on time. For t>0, the soil moisture content on the soil surface, $\theta(0,t)$, declines instantaneously from initial condition, (θ_i), to air-dry moisture content (θ_{air}). The constant boundary condition is given by

$$q_{eva}(0,t) = E_P \qquad 4.32$$

Where:

q_{eva} is evaporation flux and E_p is potential evaporation

E_P (E_P>0) is termed the potential evaporation rate. The dependence of the surface θ on time in this problem is of critical importance since it determines when the "energy limited" drying stage is replaced by the "soil-limited" stage (Lockington, 1994). The exact boundary condition during this transition is quite complex, being a nonlinear function of soil moisture content (θ) and moisture variation on the soil layers, $\partial\theta/\partial z$ (Staple, 1971, Reynolds, Walker, 1984 and Salvucci, 1997). An approximate condition is that potential evaporation is maintained until soil moisture on the surface

equals air dry moisture content or $\theta(0,t) = \theta_{air,}$ after which time surface moisture content remains at air dry moisture content. In any event, soil-surface moisture content, $\theta(0, t)$, cannot fall bellow air-dry moisture content (θ_{air}). Both factors point to the importance of careful selection of the finite difference mesh size on the soil surface. Thus, the mesh size on the soil surface should be fine enough to track the movement of the drying front and account for the rapid moisture content variations in those layers.

To search for the appropriate boundary conditions, a process of evaporation surface flux is carried out as follows:

At the commencement of each time step, the surface node is fixed to potential soil surface evaporation, which is calculated by the equation in section 2.3.2.3. The model seeks to be convergent at half the time-step. The evaporation mass flux at the soil surface node is calculated by the following equation:

$$q_{eva}(0,t) = K_{1/2}\left(\frac{h_1^{k-1} - h_2^{k-1}}{\Delta z} - 1\right) \qquad 4.33$$

The actual soil surface evaporation rate for a given soil depends only on atmospheric conditions. The actual flux cross the surface, $q_{ac,eva}(0,t)$, is determined by the ability of the soil to transit water through the soil surface. Thus the exact flux at the soil surface cannot be predicted a priori but is subject to the condition that its magnitude is as large as possible, but not greater than the magnitude of the potential rate, and that the resulting water content profile does not violate the air dry and saturation limits of the equation.

$$\theta_{air} \le \theta(z,t) \le \theta_S \qquad 4.34$$

Where:

θ_{air} is air-dry soil moisture content

θ_S is saturation moisture content

$\theta(z, t)$ is soil moisture content at time t and z depth

If the water content at the soil surface is greater than the air dry soil moisture content and smaller or equal soil to the moisture of the field capacity, the evaporation rate per time step is a fraction of potential evaporation (Zhang, et al 1996), as follows:

$$q_{ac,eva} = E_P * \left(\frac{\theta_i - \theta_{air}}{\theta_f - \theta_{air}} \right) \qquad \theta_{air} < \theta_i \leq \theta_f \qquad 4.35a$$

$$q_{ac,eva} = 0 \qquad \theta_i \leq \theta_{air} \qquad 4.35b$$

$$q_{ac,eva} = E_P \qquad \theta_i > \theta_f \qquad 4.35c$$

Where:

$q_{ac,eva}$ is actual soil surface evaporation

E_P is potential soil surface evaporation

θ_i, water content at the soil surface

θ_{air} the air dry water content of the top soil, and

θ_f, the field capacity of the top soil

If computed evaporation flux (q_{eva}) is greater than the potential soil surface evaporation, then the specified flux at surface node (i=1) is increased to a high value (qi) by:

Subject to:

$$q_{ac,eva} = q_i * \frac{\theta_i}{\theta_{air}} \qquad 4.36a$$

$$q_{ac,eva} \leq E_P \qquad 4.36b$$

On the other hand, if the moisture content of the soil surface node is approaching air dry moisture content, then the soil surface evaporation is effectively equal to zero. If actual evaporation is calculated using equation 4.35, then it is able to specify the boundary conditions for the soil surface node (i =1)

4.4.1.2 Surface flux infiltration and boundary conditions

Under normal weather conditions and ranged soil wetness, the soil surface boundary condition is flux controlled. Under rainfall conditions that causes the head of the water to collect on the soil surface governs the infiltration flux. With runoff conditions, the infiltration of water into the soil surface of an infiltration basin is controlled by the depth of

precipitation falling on the basin and the depth of runoff water. The rate of infiltration is calculated by soil properties and antecedent moisture conditions. In these cases, the controlled conditions in section 4.4.1.1 are modified, to apply to infiltration rather than evaporation flux.

The upper boundary condition in the model treats the arrival of a given depth of water as a single input and takes no account of the non-uniform distribution and duration of flooding that occurs in practice in the field. At the moment of rainfall and runoff, as water infiltrates into the soil, the actual infiltration capacity in the infiltration basin diminishes with time, as each layer becomes saturated, and when the soil surface itself saturated, a constant rate of infilteration occurs. This means that the boundary conditions, which must be satisfied at the soil surface, are not constant.

The technique proposed here makes full use of the high degree of flexibility that the finite difference numerical method offers, and is performed as shown for three different boundary conditions at the soil surface to characterize different stages of the infiltration process.

Stage 1. When the soil surface is not ponded and the soil can be described as unsaturated, the flux boundary condition is used as:

$$q_{apl} = -K(h)\left(\frac{\partial h}{\partial z} + 1\right) = -K_{1/2}\left(\frac{h_1^{j+1,k-1} - h_2^{j+1,k-1}}{\Delta z} + 1\right) \qquad 4.37$$

Where:

q_{apl} = the potential applied surface flux following from:

$$q_{apl} = +E_{ac} - P - Run \qquad 4.38$$

Where:

P = precipitation rate at the soil surface

Run = the actual runoff received by the infiltration basin

E_{ac} = actual soil surface evaporation on the surface of the infiltration basin

Stage 2. When the soil surface is saturated but not ponded: At the first time step, the depth of rainfall runoff is assumed to represent the flux at the soil surface of the infiltration basin. To test the validity of this assumption, the values of soil moisture content at time ($\Delta t_{1/2}$) are approximated for the soil surface node and a convergent solution is obtained. Once convergence is achieved, comparing the computed flux at the soil surface node (qi) with the discharge (q_{apl}) tests the boundary condition on the surface.

If:

$$q_i = K_{1/2}\left(\frac{\partial h}{\partial z}+1\right)+E_{ac} \leq Z \qquad 4.39$$

then the assumed boundary conditions are valid at the node on the soil surface.

When the surface is saturated and the surface water layer is either being formed or depleted, a surface reservoir boundary condition is used (Novak et al, 2000 and Mls 1982).

$$q_i = -K_s\left(\frac{\partial h}{\partial z}+1\right) = q_{apl}(t) - \frac{dh}{dt} \qquad \text{For} \quad 0 < h < h_{pond} \qquad 4.40$$

Where:

q_i = actual soil surface infiltration

K_s = saturated hydraulic conductivity of the soil matrix

h_{pond} = the critical thickness of the water layer on the soil surface when surface runoff is initiated

The surface reservoir boundary condition (4.40) permits a water layer to either build up at the soil surface or be used up for infiltration. The left-hand side represents the actual infiltration rate into the soil profile through the soil surface. The first term on the right side, q_{top}, represents the applied surface flux, and the second term is the change in the thickness of the water layer at the soil surface.

The boundary condition in equation (4.40) applies when the soil surface is already saturated, but the value of the critical head (h_{pond}) is not yet reached. During this time, the surface water layer is being formed, depending upon the actual infiltration rate and the applied surface flux. The boundary condition is also used after precipitation and runoff

events have ended (or when the precipitation and runoff rate is or has become lower than the sum of the actual infiltration rate and evaporation), and surface water is being used for infiltration and evaporation.

Stage 3. When the surface ponding of the infiltration basin reaches the critical thickness (h_{pond}) a boundary condition is used that specifies the flow rate of runoff. In that case,

$$\text{If} \quad |q_{apl}(t)| > |q_i(t)| \qquad h = h_{\text{pond}} \qquad 4.41$$

Where:

q_i(t) = actual infiltration rate.

The flow of runoff from soil surface of infiltration basin is calculated as follows:

$$q_{run}(t) = q_{apl}(t) + K_s\left(\frac{\partial h}{\partial z} + 1\right) \qquad 4.42$$

The boundary onditions of three stages of infiltration are tested (chapter 6 section 6.4.1) and performed in chapter 8 section 8.4.3.

4.4.1.3 Lower boundary conditions (base of root zone)

The variety of lower boundary conditions, the same as those used by Mathure and Rao (1999), and Novak et al (2000) or van Dam (2000), can be prescribed at the lower boundary. The conditions can be either assumed as a zero flux or the prescribed flux across the lower boundary (Numan boundary condition) or the prescribed pressure heads at the bottom of the profile (Dirichlet boundary condition). The equations are solved in appendix C; thus

$$K(h)\left(\frac{\partial h}{\partial z} - 1\right)\Big|_{z=L} = 0 \qquad \text{For } t \geq 0 \qquad 4.43a$$

Or

$$K(h)\left(\frac{\partial h}{\partial z} - 1\right)\Big|_{z=L} = q_n^j \qquad \text{For } t \geq 0 \qquad 4.34b$$

Or

$$h(z,t)\Big|_{z=L} = h_n^j \qquad \text{For } t \geq 0 \qquad 4.43c$$

Where:

q_n^j = Specified soil-water flux at the bottom of the soil profile; and

h_n^j = Specified soil-water pressure head

When the bottom of the infiltration basin of a micro-catchment system is allowed to drain fully, $\frac{\partial h}{\partial z}$ is set equal one so that:

$$q_n^j = -K\left(h_n^j\right) \qquad 4.44$$

The amount of water depletion from lower boundary of soil profile is an effective factor in soil moisture storag. The soil moisture storage and depletion simulated in in chapter 8 (8.3.2)

4.5 Direct problems of the model and procedures of controlling in a micro-catchment system

4.5.1 Selection of time step

Selection of time step sizes is very important. A common feature of most numerical solutions is their sensitivity to both the size of time step (Δt) and space increments (Δz). On the other hand, the numerical features (accuracy, stability and convergence) of the problem also constrain the choice of time steps. In fact, time step size is usually chosen on the basis of numerical requirements. Selection of time steps is based on the fact that difficulties in convergence often occur just after solving the equations at observation times. This is a consequence of the fact that both boundary conditions and external actions may vary their rate of charge at these times. When those variations are exciting and unusual, convergence problems do appear. In this situation, the time step is reduced. At difficult time steps, several time step reductions may be required, which leads to important losses of CPU time. A method which is commonly used, is to limit the variations of the independent variables (h, or and θ) to pre-specified values within each time step. A method by Galarza et al (1999) is based on achieving acceptable mass balance in a time step, within a pre-specified number of iterations.

A combination of both methods is used here. The maximum allowable changes in the independent variables (pressure head, h, and moisture content, θ) in a time step (Δt) are

limited to acceptable values on the experience of other investigators with various flow models, and on the numerical experiments which are conducted in this work, such that:

$$\Delta\theta^{k} = \max.\left|\frac{\theta_i^{k} - \theta_i^{k-1}}{\theta_i^{k}}\right| \qquad 4.45$$

$\Delta\theta_{\max}^{k\pm1}$ are satisfied, if $\Delta\theta_{\max}^{k\pm1} = 10 * \delta$

Where:

δ is threshold value and equals 0.0001 cm^3/cm^3soil moisture content

The maximum time step in iteration (k+1) is computed according to:

$$\frac{\Delta t_{\max}^{k+1}}{\Delta t^{k}} = \left[\max\left(\frac{\Delta\theta^{k}}{\Delta\theta_{\max}^{k+1}}\right)\right]^{-1} \qquad 4.46$$

If the required convergence needs a very high degree of accuracy, the maximum number of iterations to be performed at any time step could be large. In order to reach optimum convergence criteria, if the accuracy of the solution is not achieved within a pre-specified number of iterations, the time step size is adjusted.

The modified time step ($\hat{\Delta}t$) can be computed by:

$$\hat{\Delta}t = \Delta t * \frac{k}{k_1} \qquad k_1 > k \qquad 4.47$$

Where:

k and k_1 are the number of iterations allowed and those which are actually performed to achieve the convergence criteria respectively.

4.5.2 Selection of space increment and grid size

The accuracy of the mass balance in the simulated soil volume is taken to be the main measure of suitability of the chosen space increment, for any particular application. For space increment, no comprehensive rules are available.

The rate of change in volumetric pressure head or moisture content in the soil volume is compared in each time step by:

$$\frac{\partial h}{\partial t} = \sum_{i=1}^{i=n} \left(h_i^{j+1} - h_i^j\right) \frac{v_i}{\Delta t^j} \qquad 4.48a$$

$$\frac{\partial v}{\partial t} = \sum_{i=1}^{i=n} \left(\theta^{j+1} - \theta^j\right) \frac{v_i}{\Delta t^j} \qquad 4.48b$$

Where:

$\frac{\partial v}{\partial t}$ is the rate of volumetric change of moisture content

$\frac{\partial h}{\partial t}$ is the rate of change pressure head content

i = n is the number of nodes in the soil profile

θ is the average moisture content in the soil profile which is computed by:

$$\overline{\theta} = \sum_{i=1}^{i=n} \frac{\theta_i}{n} \qquad 4.49$$

Where:

n is the number of nodes in the soil profile

$\overline{\theta}$ is the average moisture content in the soil profile

$\left[\frac{\partial v}{\partial t}\right]$ and $\left[\frac{\partial h}{\partial t}\right]$ are compared with actual rates of moisture and pressure head changes through the soil resulting from water entry, evaporation and root extraction during the time step. If either quantity is unacceptable, the space increments (Δz) are reduced, and the computations are repeated. A tolerance error equivalent to the convergence criterion multiplied by the total number of nodes (n) is allowed.

4.6 Water balance and computation results

Changes in moisture content in the root zone result from a number of interacting processes in the infiltration basin of a Micro-Catchment system, which should be analysed to obtain accurate estimates of such changes (Musters amd Bouten, 2000). The method used in the model computes the moisture volume of the entire soil in the root zone at the end of each time step.

$$W = \int_{i=n}^{i=1} \theta_i dz \qquad 4.50$$

Where:

W = the moisture volume in the entire simulated soil volume in the root zone

n = the total number of compartments (n, number of nodes in the soil profile) between the first and last node of the soil domain in the root zone

The water balance of the root zone in a time interval (Δt), is expressed as follows (Abraham and Tiwari, 1999; Srivastava, 2001; Everson, 2001)

$$\Delta W = W^{j+1} - W^j = [(q_{sur}) - (E + T + q_b)]\Delta t^j \qquad 4.51$$

Where:

ΔW is net change in water storage (cm)

q_{sur} is water added by rainfall and runoff (cm/day)

E is actual moisture depletion by evaporation (cm/day)

T is transpiration or total root extraction (cm/day)

q_b is flux through the bottom (or deep percolation, or drainage = +cm/day)

Transpiration (T) is computed by summing the water extracted by the root in the time step (Δt).

$$T = \int_{i=n}^{n} S_i dz = \sum_{i=1}^{n} S_i \Delta z_i \qquad 4.52$$

Where:

S_i is the sink term at node (i) at (Δt/2).

Flux through the bottom (q_b) is computed when it is assumed that the system is free draining. In this case the free drainage flux is:

$$q_b = q_n = -K(h_n^i) \qquad 4.53$$

ΔW is net change of moisture content in the soil surrounding the root zone within the defined region boundaries, and the quantity change in moisture content in the time interval (Δt^j) is calculated as:

$$\Delta W = \int_{i=n}^{i=1} \theta_i^{j+1} dz_i^{j+1} - \int_{i=n}^{i=1} \theta_i^j dz_i^j \qquad 4.54$$

q_{sur} is calculated as:

$$q_{sur} = \frac{\Delta W}{\Delta t^j} + E_{ac} + T_{ac} + q_b \qquad 4.55$$

Water balance simulation model and it's components are performed in section 8.2 8.2.3, 8.2.4, 8.3, 8.4, 8.4.3.

4.7. Discussion

As discussed in the previous chapter (chapter 3), by comparison of the analytical and numerical techniques, advantages and disadvantages it was argued that the numerical technique is the most suitable to treat the water balance model components proposed in this work. A systematic development of the numerical formulation was presented, and both the models for coupled rainfall and runoff, and soil moisture and root extraction were combined in a set of simultaneous equations, expressed in a matrix form suitable for a computer algorithm. A time centred finite difference scheme was integrated into the formulation to evaluate the time derivatives.

Comparing the merits of both finite element and finite difference techniques using Hills' (1989), Feddes' (1988) and Belmans et al's (1983) experiments illustrated that for the design of Micro-Catchment system problems, the finite difference is the most simple and efficient to use, except for high accuracy. The advantage of the finite difference method is its simplicity and efficiency in treating the time derivatives. On the other hand, the method is rather incapable of dealing with the complex geometries of flow regions. A slow convergence, a restriction to bilinear grids and difficulties in treating moving boundary conditions are other serious drawbacks of the method (Feddes et al, 1988, Nieber and

Feddes, 1999). It is also concluded that the method is the preferred technique for tracking the time evaluation of the complex surface infiltration, process evaporation, root extraction and possible runoff with bounded domains in the infiltration basin. In brief, the method is completely general with respect to geometry and material properties. Complex soil surface runoff generation and soil profiles of an isotropic characteristic are easily represented and vertical moisture flux boundary conditions may be specified at any point within the system. For these reasons, the finite difference method is selected to numerically interpret the model in this study.

The results of the coupled numerical model presented above and formulated in appendix C show that a mass conserving approximation based on the mixed form of Richard's equation, coupled with a lumped form of a time matrix, yields consistently reliable and robust numerical solutions for unsaturated flow problems in a water balance design (see chapter 6). As formulated in appendix C, I propose to use the mixed-form algorithm of the new convergence method of Huang et al (1996), because this new criterion seems more appropriate than the forms presented already, and because of physical considerations. The pressure head (h) based form of the equation, when used with a simple implicit (backward Eular) approximation in time gives consistently poor results, especially when a consistent finite deference approximation is used. Such approximations should be avoided. These observations are supported by other results as well. Van Dam and Feddes (2000) and Huang et al (1996) reported poor mass balance for standard pressure-head (h) based simulators. Celia et al. (1990 & 1987) reported similar mass balance problems when using a pressure-head based simulator. In addition, Celia et al. (1987) used the mixed form of the Richard's equation in conjunction with a collection approximation in space. Mass balance errors were consistently less than 1%. This indicates that the mixed formulation is robust with respect to mass balance (Huang et al, 1996). The numerical method performed very well for general unsaturated flow problems involving evaporation, infiltration and redistribution (Van Dam and Feddes, 2000), as well as in water balance design for a micro-catchment system. Thus the procedure is not restricted in any way to only monotonic infiltration problems.

Chapter 5: Computer model for micro-catchment system planning

5.1 Introduction

This chapter takes the numerical procedures developed in chapters 3 and 4 and describes how they can be brought together to form a computational model for micro-catchment design.

The numerical procedures are translated into computer algorithms and auxiliary algorithms are compiled to estimate rainfall runoff and crop evapotranspiration, and evaluate soil moisture flow and coefficients. When combined, these algorithms are shown to be capable of simulating most conditions of practical interest to aid the design of a micro-catchment system.

5.2 Model description

If the micro-catchment water balance model, which was formulated in chapter 4, is to be developed into a complex scheme consisting of a runoff area system and an infiltration basin, the runoff area and infiltration basin must satisfy certain constraints.

(a) It must guarantee the minimum discharge (rainfall and actual runoff) required for crop water requirements in the infiltration basin

(b) It must minimise the amount of water that cannot be stored in the infiltration basin from the runoff area, which is wasted to surface drainage from the infiltration basin.

The micro-catchment system design model was developed not only to analyse existing rainfall-runoff and water,supply and simulate soil moisture movement in the infiltration basin, but also to generate data to simulate future scenarios of these main input data.

The model to calculate optimum catchment size for a given environment is based on methodologies described in chapter 9.

The general description of the model is given in figure 5.1. It can be seen from this figure that the model is composed of a set of sub models. The input data section feeds data to all sub-models.

Sub model 1 calculates the potential evaporation and transpiration for a given set of climatic data.

Sub model 2 calculates the crop water requirements for different crops.

Sub model 3 calculates the potential and actual runoff from a given catchment.

The daily data from sub models 1, 2 and 3 are fed into sub model 4, which is at the heart of the programme. Sub model 4 calculates the daily water balance in an infiltration basin using a finite difference approach. The generated daily water balance data is used by sub model 5 to optimise micro-catchment design.

The model operates on a daily basis, and gives output information on actual evaporation, actual transpiration, infiltration and soil moisture variation in the infiltration basin. The soil water balance in a micro-catchment system also displays the micro-catchment size, together with operational details of available water in the infiltration basin and amount of flood water.

All model outputs taken from various daily simulations are saved to files for subsequent selection of optimum size of the micro-catchment system.

5.3 Data requirements and model sub programmes

5.3.1 Input data

The following information is required, as data input to the main model algorithm.

(a) Daily maximum and minimum temperature mean daily humidity maximum daily sunshine and mean daily wind speed are needed, together with latitude, longitude and altitude, in order to calculate reference evapotranspiration, and the fraction of it representing potential evaporation (see appendix A).

(b) Daily rainfall data: Although rainfall duration data is more valuable, this model can work with daily rainfall data and calculates daily potential and actual runoff (refer to chapter 7, 7.2.5 & 7.3).

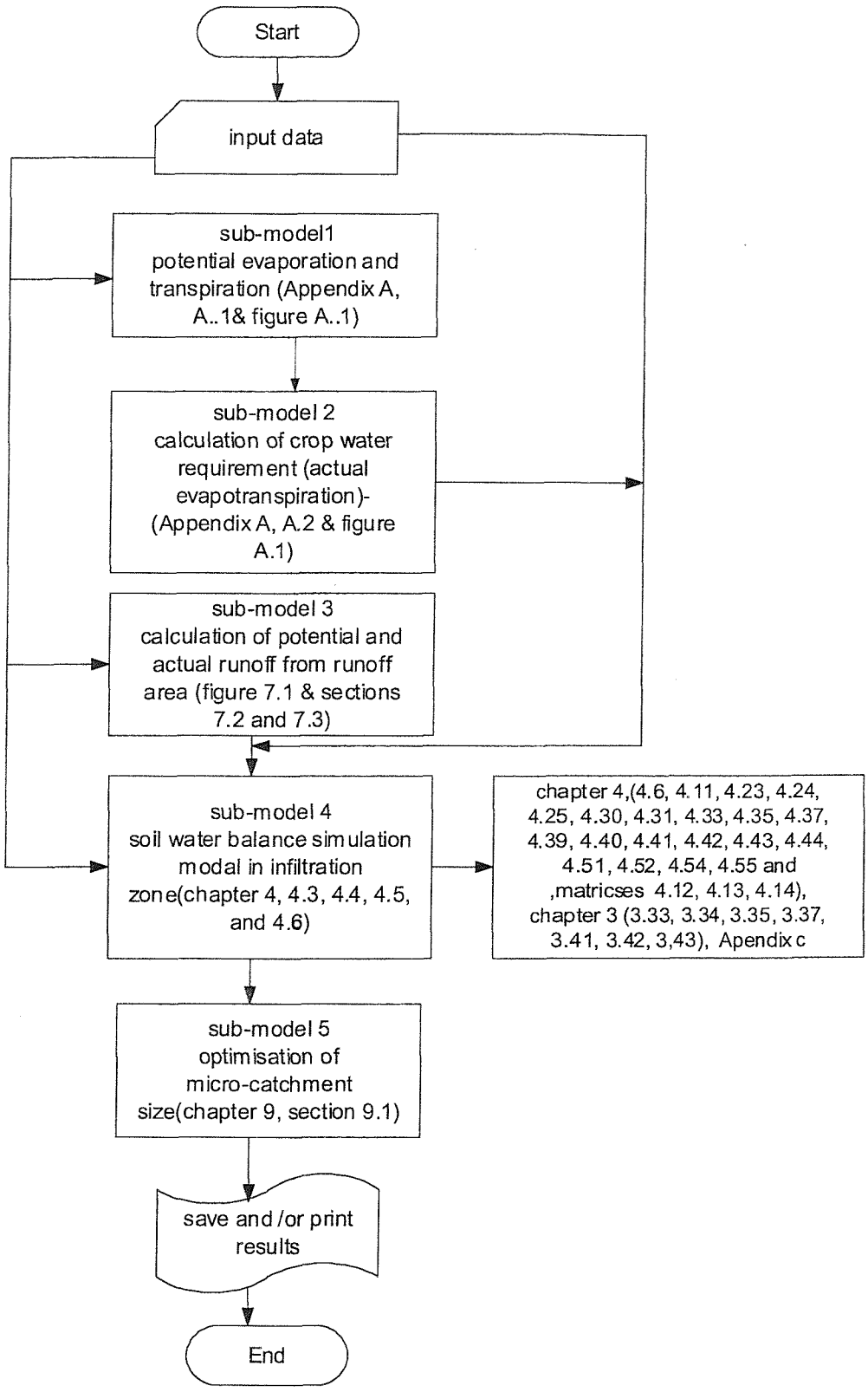

Figure 5.1: Flowchart of the main computer algorithm

(c) Physical soil properties expressed in physical soil composition, hydraulic conductivity (K) as a function of moisture content, saturated hydraulic conductivity (K_s), residual moisture content (θ_r), saturated moisture content (θ_s) and soil property coefficient data (such as α, n, m), which can be used in the formulation of the soil water retention curve, based on Van Genuchten (1980) equations.

(d) Soil profile depth, profile geometry, initial distribution of soil moisture (or soil pressure head).

(e) Maximum root depth: the root zone maximum possible limits as a time series and, if available, the root effectiveness function f(r,z) (See section 3.3.2.5).

Other input data for special applications are indicated where appropriate.

5.3.2 Model sub programmes

The model was written in visual basic language using spreadsheet and macros on Excel software. The simulation model has four main modules (See model flowchart in Figure 5.1).

In the first sub-model (Appendix A) the reference evapotranspiration and the fraction, that represents potential evaporation, were developed. The method selected here is Penman's (1948) method and the evaporation fraction is estimated using Ritchie's (1972, 1990) proposal. The modifications proposed by Montieth (1965) and by Kotsopoulos and Babajimopoulos (1997) were used to modify the Penman method. A flowchart of this algorithm indicating input requirements and details of the method used are given in Appendix A. The model calculates the irrigation water requirement and the method is described in detail in Appendix A.

The second sub-model (Figure 5.1) calculates the runoff from a given catchment using the methodologies described in chapter 3 and given in the flowchart in chapter 7 (figure 7.1). The model first calculates potential runoff from the rainfall characteristics and predicts actual runoff from the basin characteristics. See chapters 7 and 8 for its application.

The third sub-model (figure 5.1) generates a soil water balance calculation based on the water available in the infiltration basin, which is collected from the runoff area, and water losses consisting of evaporation, crop transpiration and deep percolation. The actual evaporation and root soil extraction are calculated in two components of the sub model from data provided from sub model 1, prediction of potential losses. The components for an integratal part of the transient infiltration model described in detail in chapter 4. The deep percolation that took place below the root zone is calculated. The performance of this model is illustrated and tested in chapters 6 and 8.

The forth sub-model, generates the optimum size of a micro-catchment system for providing the most favourable soil moisture conditions possible for a given crop. This model (see Figure 5.1) searches for the optimum value for the runoff area and the infiltration basin parameters entered in the model, which can only be achieved by a sensitivity analysis between maximum crop water requirement and the size of the runoff area and infiltration basin.

Through simulations, the computer user has the opportunity to request for the water balance model to present on screen various displays such as the graphics of the calibration, and the verification and validation phases of the model developed for design of a micro-catchment system. If desired, these graphics can also be printed and /or saved onto computer files.

5.4 Output data

5.4.1 Intermediate output

The main intermediate outputs are made up of:

(a) Actual evaporation
(b) Actual transpiration
(c) Total deep percolation
(d) Soil moisture variation in the infiltration basin and average moisture content in the root zone, in the surrounding plant root, and in the entire simulation soil volume.
(e) Moisture distribution in a vertical direction.

5.4.2 Final outputs

Final outputs include moisture flux between soil layers and root extraction distribution. It is also possible to obtain an output suitable for graphical presentation or a list of moisture transfer coefficients. In design mode, the irrigation periods, irrigation intervals and total duration of each cycle are also given as output.

The sub-models provide intermediate output, which is not only essential for operating the root zone water balance model, but can also be used to provide data about agroclimatic variables.

The coupled model provides a powerful tool for detailed studies of problems in moisture, rainfall-runoff, or coupled rainfall-runoff with moisture transfer and consumption by root extraction and soil surface evaporation. The results may be interpreted in a variety of forms, including graphical output, providing results, which are suitable for the designing of micro-catchment systems in arid climate projects.

Chapter 6: Model testing to design a micro-catchment system in arid climate and preliminary performances

6.1 Introduction

In this chapter the model is subjected to numerical tests to verify performance. It tests the accuracy of the numerical results and examines the reliability of its predictions. The approach adopted was to compare the model results with data that had been published and analysed in the literature.

The proposed model was tested in three component models as following:

a) Rainfall potential runoff sub-model

The proposed rainfall potential runoff sub-model was tested on one case. In this case, the sub-model was tested for consistency against the model of Diskin & Nazimov (1995).

The effectiveness of the proposed sub-model for prediction of potential runoff requires model procedures. A workable relationship between storm size and excess rainfall is demonstrated for two soil types.

b) Reference evapotranspiration model test

The reference evapotranspiration data estimated by the proposed daily evapotranspiration (ET) model formulated by modified Penman equations (See appendix A) were compared with the cropwat model values, which is a design based on Penman-Monteith (Hatfield and Allen, 1996).

c) Soil Water movement model test

The soil water movement model is tested in three stages. In the first stage, the results from the model were tested based on the basic assumption (Gottardi and Venuteli,1992) for a constant rate of infiltration in Berino loamy sand. In the next stage the model was tested for taking a constant pressure head at the top boundary, as

suggested by Celia et al (1990) in their simulation. The soil properties were taken from Van Genuchten (1980). In the third stage, the predictive capabilities of the model are then examined by comparing the model results with experimental observations, which have been published in recent literature. In this stage, the model is tested with the available data, which were made in developing the root extraction model.

6.2 Rainfall runoff sub-model test

A1 Potential runoff test

The performance of the proposed model was tested against the performance of the Diskin and Nazimov (1995) model, which is a linear reservoir model for the infiltration process. The same soil type as that of Diskin and Nazimov was selected and potential infiltration calculated using the Green & Ampt method first (Table 6.1). Comparisons of the output of the two models are given in figure 6.2. It is clear from the figure that the model predictions are in good agreement.

A2 Relationship between storm size and predicted potential runoff

Figure 6.3 & 6.4 show the relationship between storm size and predicted potential runoff for two given soil types in both cases, it can be seen that a linear regression line provides a good fit to the data account for over 95% of the variability (sig. 0.01).

Clearly the sub model procedure gives a good working relationship which will allow potential runoff to be predicted from storm size data, although there is some divergence from the line at low rainfall intensities inaccuracy in the estimate from this source is likely to be insignificant because of the small amount of rain infiltrated from the storms. The advantage of proposed model against Diskin model is that the proposed model with only soil profile infiltration data (f_p) and estimating two factor of A and B of Green and Ampt infiltration method can be run, however Diskin model needs to be available many factors.

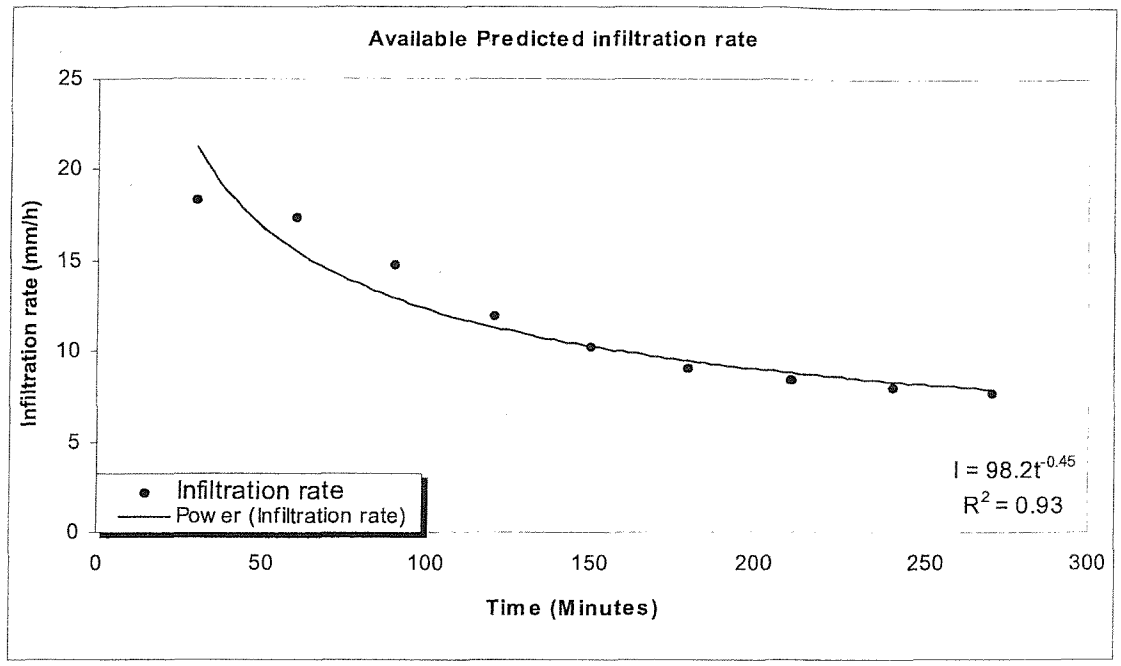

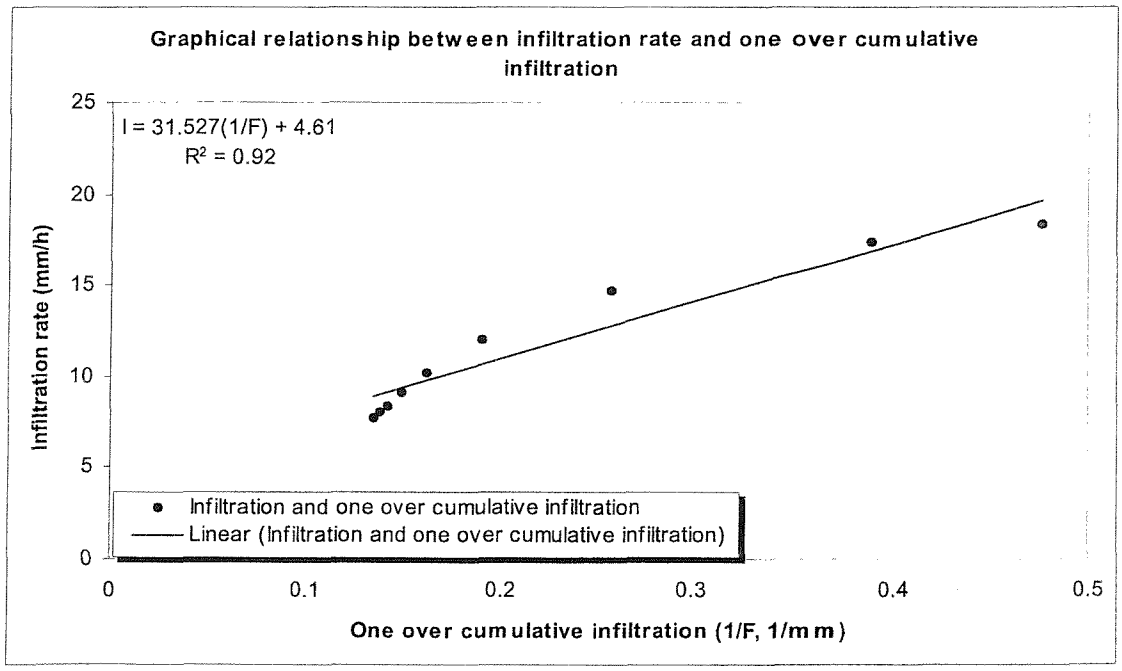

Fig 6.1: Potential infiltration curve and graphical relationship between infiltration and cumulative infiltration from available data in Diskin and Nazimov (1995).

Table 6.1: Comparison of rainfall excess calculated by Diskin & Nazimov model and proposed model

Time (minutes)	Estimated rainfall excess by proposed model	Cumulative rainfall Excess (mm),estimated by proposed model	Available rainfall excess (mm) Diskin et al	Available cumulative rainfall excess (mm) Diskin et al
0	0	0	0	0
30	0	0	0	0
60	0	0	0	0
90	0	0	0.05	0.05
120	2.12	2.12	2.14	2.19
150	1.43	3.54	1.41	3.61
180	1.06	4.60	1.16	4.77
210	0	4.60	0	4.77
240	0	4.60	0	4.77
270	0	4.60	0	4.77
300	2.60	7.20	2.19	6.96
330	4.30	11.50	4.11	11.07
360	3.07	14.57	2.37	13.44
390	1.35	15.91	1.42	14.85
420	0	15.91	0	14.85

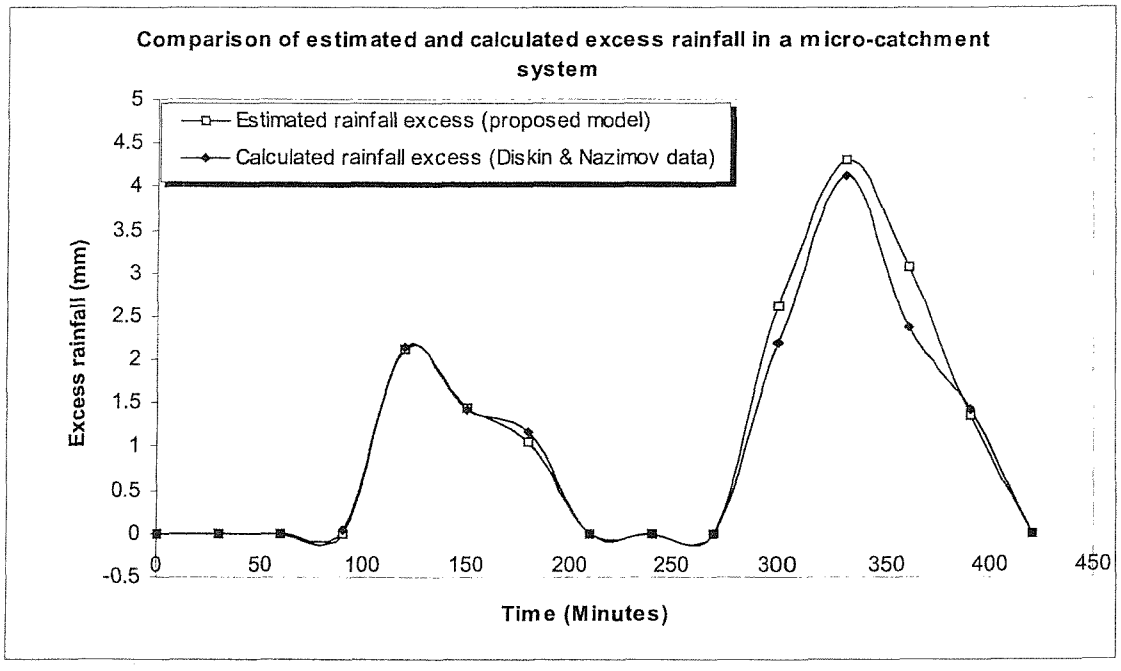

Fig 6.2: Comparison of proposed model results with those of Diskin and Nazimov's model.

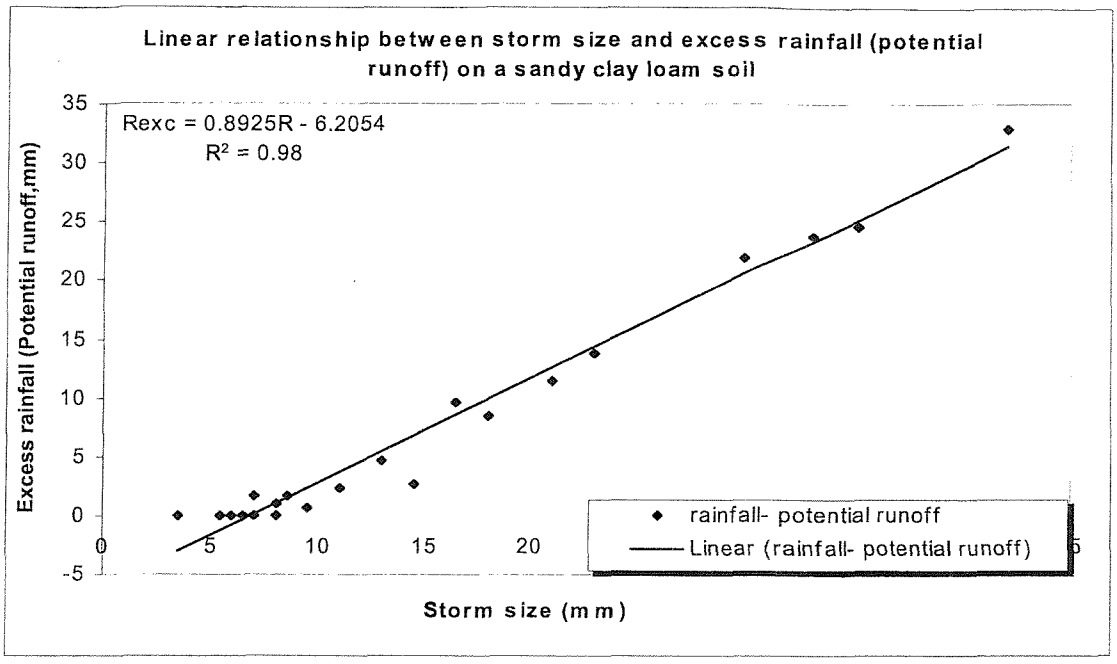

Fig: 6.3. Relationship between rainfall and rainfall excess (potential runoff) on a sandy clay soil in a micro-catchment system

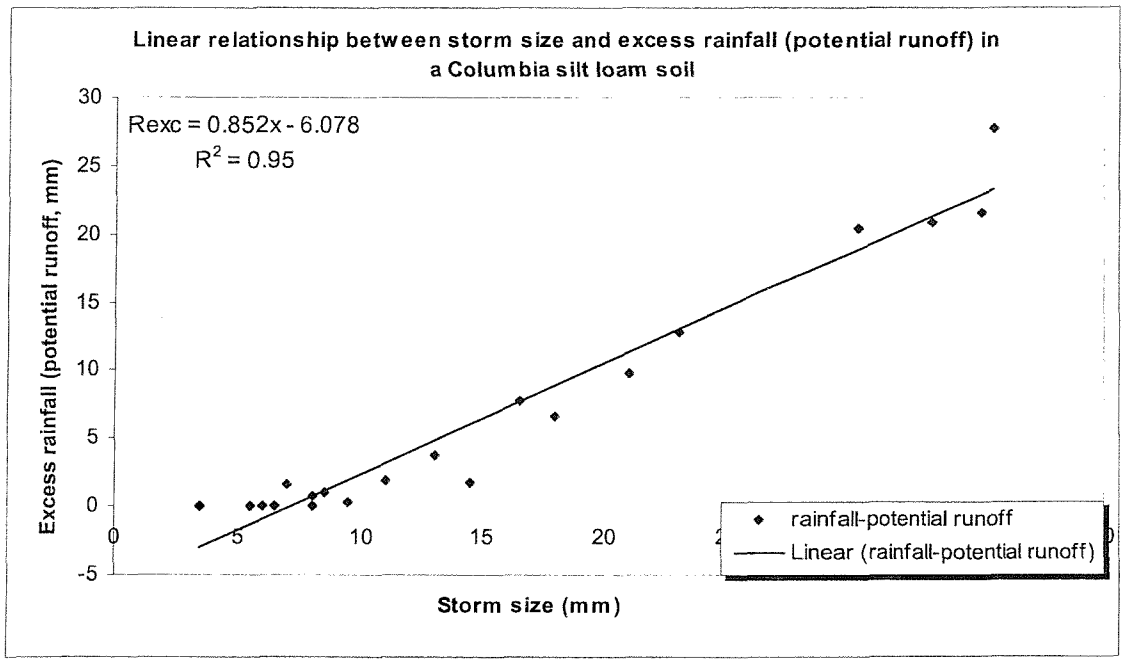

Fig: 6.4. Relationship between rainfall and rainfall excess (potential runoff) on a Columbia silt loam soil in a micro-catchment system

6.3 Estimation of the reliability of the sub-model calculating reference evapotranspiration

The estimation of evapotranspiration from the land surface is a basic requirement in a water balance model designed to estimate water availability and requirements in a micro-catchment system. Research in this area is abundant and has provided an extensive body of literature on the subject, with practical applications, mainly validated through adequate field measurements. The transfer of theoretical advances into field practice remains below potential, however, and practice is often based on local field observation, supported by experimentation. To provide for better use of theoretical findings and for faster application of up-to-date theory in design, it is interesting to examine the linkages between the different approaches currently adopted.

Evaluations and tests for almost all the available methods of calculating potential evapotranspiration show that they all perform better with local calibration (Jensen, 1980 and Rydzewski, 1987). Doorenbos and Pruitt (1977) and Raes (1988) reported an error of estimate in the range of plus or minus 10 to 20 percent for some climatic conditions. This shows that the use of one method of absolute accuracy is required but a universal method is very difficult to obtain. In a Penman equation (1948), two constants (*a, b*) are used in the calculation of a solar radiation term (see Appendix B). The values of those constants are subject to discussion. Many values for *a* and *b* were suggested for different regions in the world (Doorenbons and Pruitt, 1977). Penman used the values of 0.18 for *a* and 0.55 for *b* as suitable values for England. Doorenbos and Pruitt (1977) suggested values of 0.25 for *a* and 0.5 for *b* for practical purposes. Samir-El-Askari (1994) suggested values for a & b of 0.25 and 0.53 respectively. These figures were used both in the FAO Cropwat version of the Penman (1948) evapotranspiration model and were also used in the model described in this thesis.

Because of the widespread acceptance of the Cropwat model, it was used to make comparisons with the performance of the sub-model used in this work. Both models were run using data from Shiraz, Esphahan and Kashan in Iran. The results are given in figures 6.5, 6.6 and 6.7.

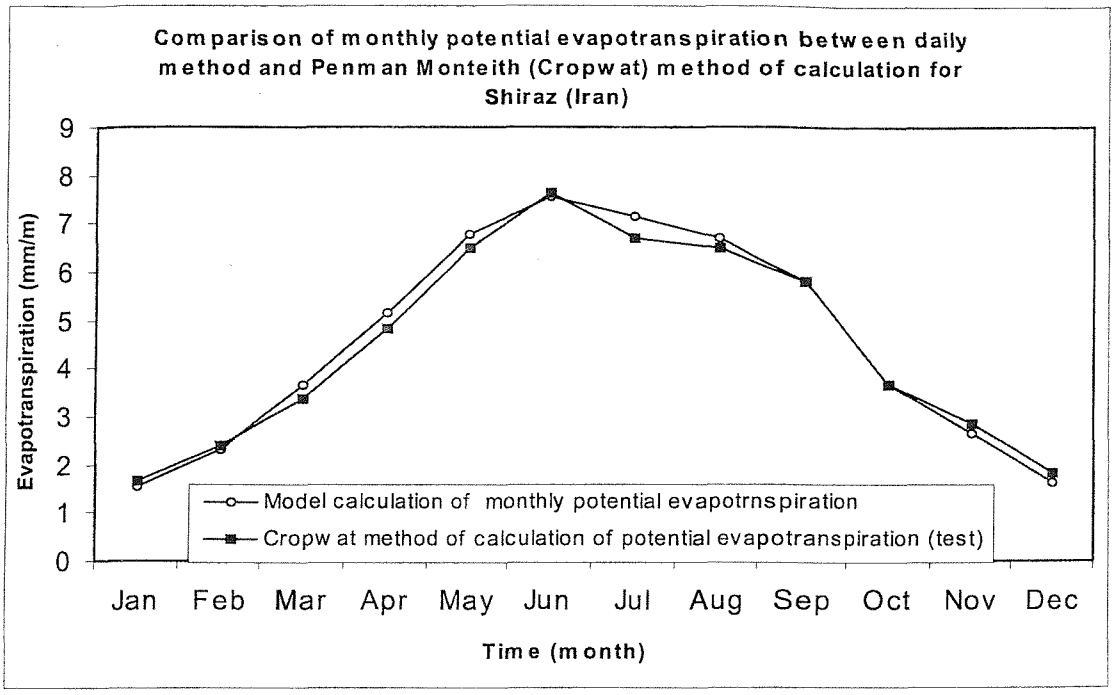

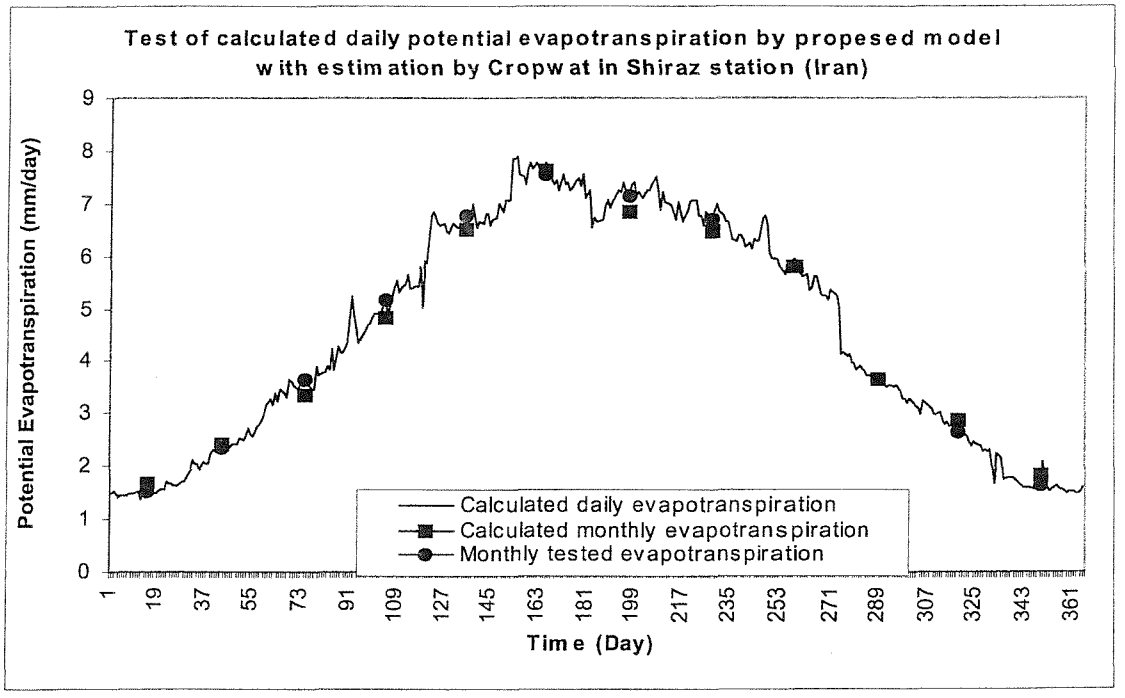

Figure 6.5: Daily and monthly comparison between the results of proposed model and Penman Monteith (Cropwat) when processing the same climatic data (at Shiraz station in Iran).

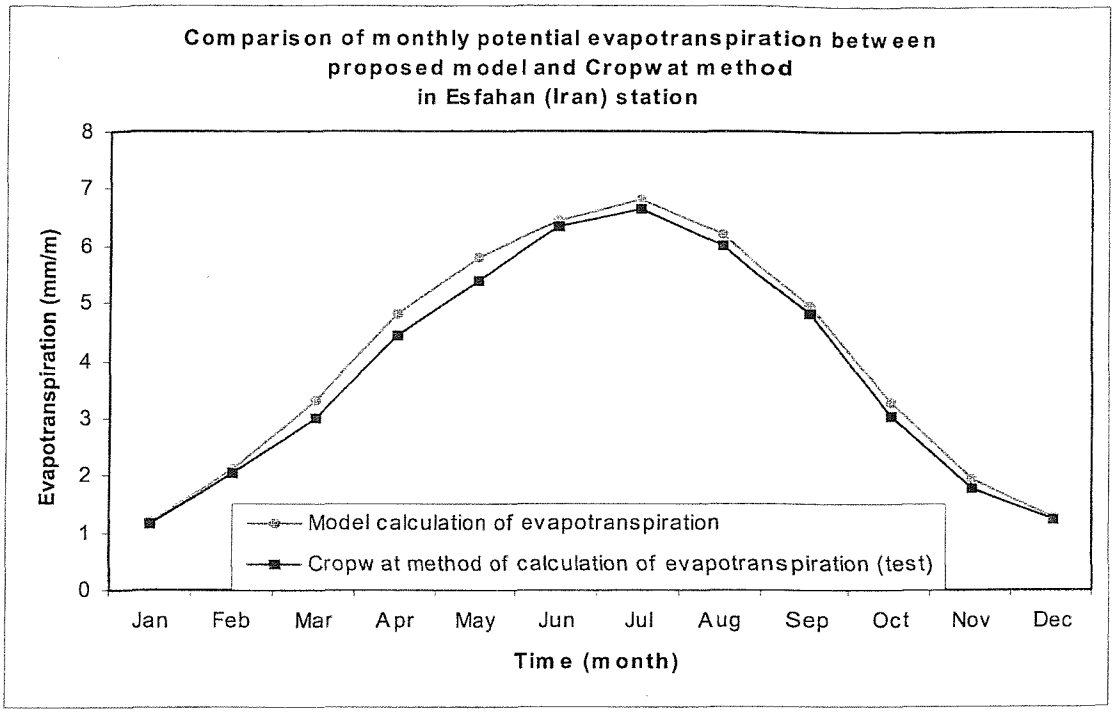

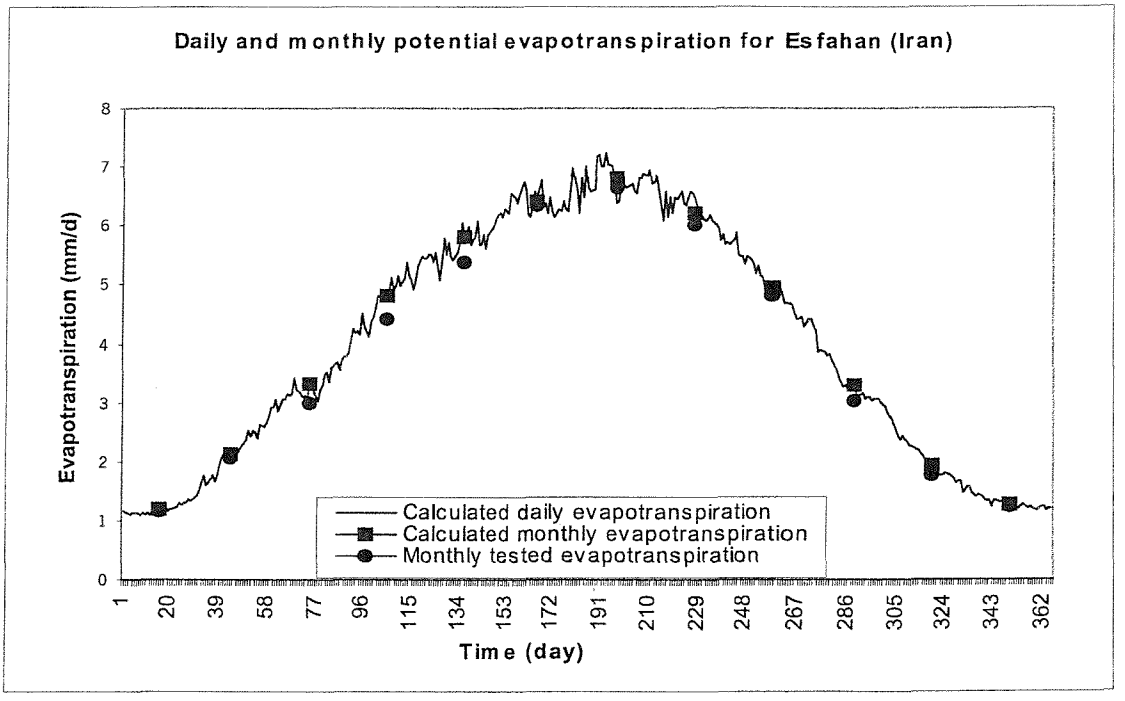

Figure 6.6: Daily and monthly comparison between the results of proposed model and Penman Monteith (Cropwat) when processing the same climatic data (at Esfahan station in Iran)

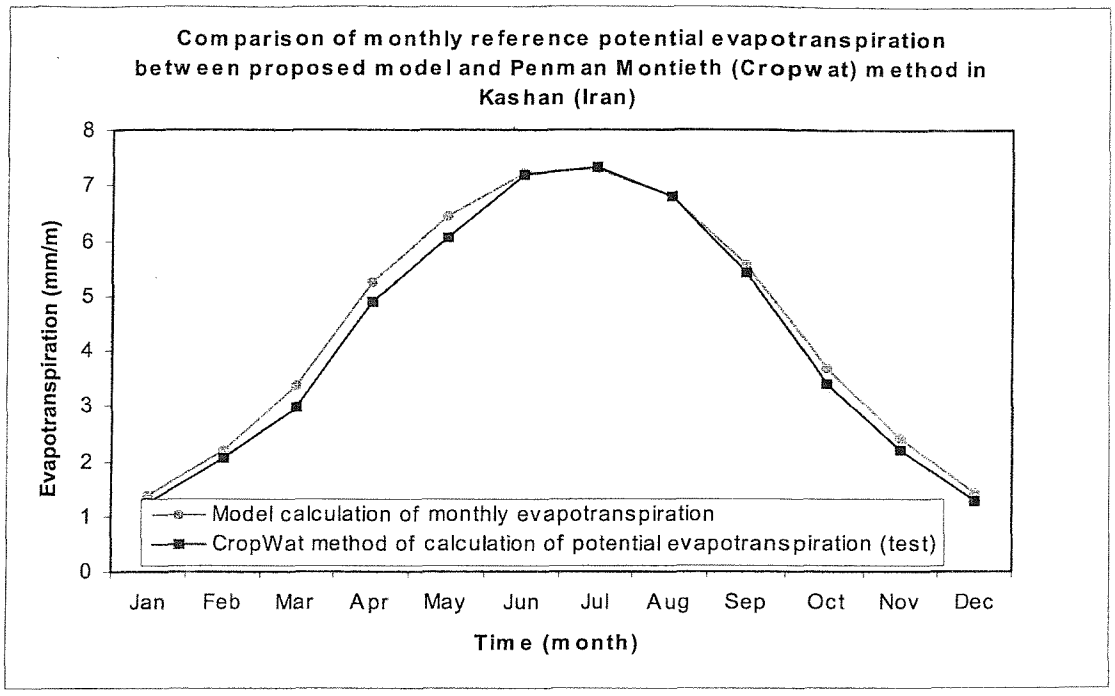

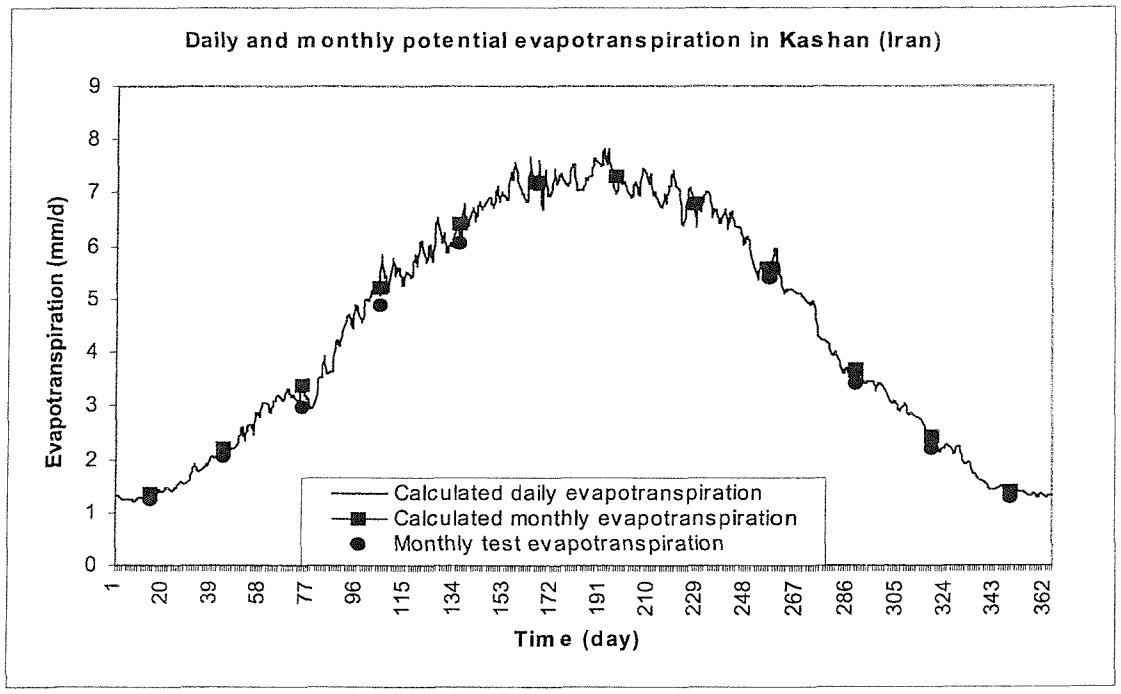

Figure 6.7: Daily and monthly comparison between the results of proposed model and Penman Monteith (Cropwat) when processing the same climatic data (at Kashan station in Iran).

6.4 Analysis of the performance of the proposed soil moisture balance sub-model

For the purpose of studying the performance of the soil water movement model, the soil properties were taken from Van Genuchten (1980), also used by Gottardi and Venutelli (1992) and Mathur and Rao (1999) as shown in table 5.2. Since the concept of the root extraction model is, in the main, based on published experimental results, a suitable test would be to compare the results of a simulation of an experiment with those that were experimentally measured. The experiment by Gottardi and Venutelli (1992), Celia et al (1990) and Mathur and Rao (1999) were chosen for this purpose.

The boundary conditions in the model were selected using the soil and experiments from the field (in chapter 4). The boundary conditions describe those in the object area, neglecting surface evaporation. The initial condition was taken to be a uniform moisture distribution at a specific soil moisture content and root zone fixed at a specific depth, as explained in table 6.2.

In addition to presenting water content versus depth curve for each test case, I considered the percent mass balance error.

The percent mass balance error is evaluated using the following formula:

$$\%Mass\ error = 100 * \left| \frac{true\ mass\ added\ to\ system}{true\ mass\ \text{model}\ to\ system} \right|$$

To obtain the calculated mass added to each finite difference volume, the mass from the nodal value of water content (assuming that the nodal value is the average value for the volume) was taken and the volume's initial water mass subtracted. The calculated mass added to the system is the sum of the masses that were added to each finite difference volume. The true mass added is simply the mass added as flux through the upper boundary minus the mass removed through the lower boundary. I emphasise that a perfect mass balance guarantees only that the mass entering the system is fully accounted for within the system.

The soil hydraulic functions $\theta(h)$ and $K(h)$ were described by Simunek, Wendroth and Van Genuchten (1998) and Van Genuchten (1980).

$$\theta(h) = \frac{\theta_s - \theta_r}{\left(1 + |\alpha h|^n\right)^m} + \theta_r \qquad \text{For } \theta_r \le \theta \le \theta_s \qquad 6.1$$

Where:

θ_r is residual water content (cm^3/cm^3)

θ_s is saturated water content (cm^3/cm^3)

α, m, and n are the empirical shape parameters estimated by fitting 6.1 to the experimental data.

α is the inverse of the pressure head at the inflection point;

n represents the steepness of the curve, which can be interpreted as a pore size distribution index; and

m is given by the expression m = 1- 1/n.

The unsaturated hydraulic conductivity, obtained by combining 6.1 with the pore size distribution of Mualem (1976), yields

$$K(h) = K_s \frac{\left[\left(1 + |ah|^n\right)^m - |\alpha h|^{n-1}\right]^2}{\left(1 + |ah|^n\right)^{m(l+2)}} \qquad 6.2$$

Where:

K_s = saturated hydraulic conductivity (cm/hr)

l = soil specific parameter, generally assumed as 0.5.

6.4.1 Test of simulation model against two available models (case 1)

The first case test was based on the study of Mathur and Rao (1999) and suitable experiments were reported by Gottardi and Venutelli (1992) for a constant rate of infiltration into a uniform soil column of Berino loamy sand. The soil hydraulic properties were assumed to follow Van Genuchten's (1980) curves, which also gave all the soil parameters required for a numerical simulation. The basic soil parameters used are shown in

table 6.3. The experiment was primarily for water entry into soil in the absence of root extraction.

Table 6.2: Test cases for comparison of soil water movement with available experimental data

Test Case No	Soil column depth (cm)	Initial conditions (cm)	Period of simulation (hour)	Top boundary (Infiltration rate, cm/hour)	Bottom boundary conditions
1	100	-80	0.28	10.69	Hydraulic conductivity
2	60	-1000	20	75	Hydraulic conductivity

Table 6.3. Basic data used to evaluate soil properties for three test cases of infiltration analysing water balance in a micro-catchment system

Soil kind	θr cm^3/cm^3	θs cm^3/cm^3	α	I	n	m	Ks (cm/h)	Reference
Berino loamy Sand	0.0286	0.366	0.028	0.5	2.239	0.553	22.54	Gottardi and Venutelli,1992
Clay loam	0.106	0.569	0.010	0.5	1.3954	0.2834	0.545	VanGenuchten, 1980
Loam	0.103	0.4	0.011	0.5	2.24	0.554	2.11	Zhang and Yang, 1996
Sandy loam	0.091	0.4	0.03	0.5	1.68	0.404	2.38	Kempt et al, 1997

This data was used for this simulation, but the initial pressure head was taken to be 80 cm (minus eighty) throughout the soil column, which is equivalent to a 0.143 cm^3/cm^3 of water content throughout. The depth of the simulation was 100 cm and the linear element size was taken as 1 cm. The total simulation period was 0.28 hours with time steps of 1.5 seconds. The top boundary was assumed to have a constant rate of infiltration equivalent to 10.69 cm/hour and initial moisture content of 0.143 cm^3/cm^3. The bottom boundary was

assumed as in Hills et al (1989). The magnitude of flux is given by the value of the hydraulic conductivity, evaluated at the initial head for lowest layer (Table 6.2).

The comparisons of simulated results with the experimental data and other models for constant discharge are shown in figure 6.8. It can be seen from this simulation that the model behaviour was excellent and a considerable improvement on Mathur & Rao's (1999) model. The total depth of water added to the system in a period of 0.28 hours was 2.9934 cm. The mass balance error in moisture content calculated at the end of the time period was about 0.007%, again showing excellent agreement. The mass balance errors and the performace times for the water content profiles shows that the CPU time for the proposed method is about one third of the Gottardi (1992) method and that the water balance errors of Mathur (1999) method (error = 0.124%) is greater than the proposed model (error = 0.007%).

6.4.2 Test of simulated pressure head against available models(case 2)

The second case was carried out taking a constant pressure head at the top boundary, as suggested by Celia et al. (1990) in their simulation. The soil properties were again taken from Van Genuchten (1980). The boundary conditions were taken as follows: the pressure head was assumed to be –1000 cm (h(z, 0) = -1000 cm suction head), which is equivalent to 0.034 cm^3/ cm^3 moisture content. The top boundary was assumed to have a constant head of 75 cm of water imposed; the bottom boundary was restricted to a constant pressure head the same as the initial amount. During the period of simulation the mass flux leaving the lower boundary is assumed to be due to gravity only. The magnitude of this flux based on gravity is given as equal to the value of the hydraulic conductivity calculated at the initial head for the lowest layer. The simulation was carried out on a column with a 60cm long profile and a 2.5cm sized linear element. The time period of simulation was 20 hours, taking time in steps of 120 seconds and the iteration convergence criterion was assumed to be 0.05 second. The simulated pressure head profiles are compared with those of Celia et al. (1990) and the results obtained by Mathur and Rao (1999) (figure 6.9). Again the model showed very good agreement with the data. In this performance comparison, time of iteration increased two times of the provided model and time of performance reduced about five times than other models.

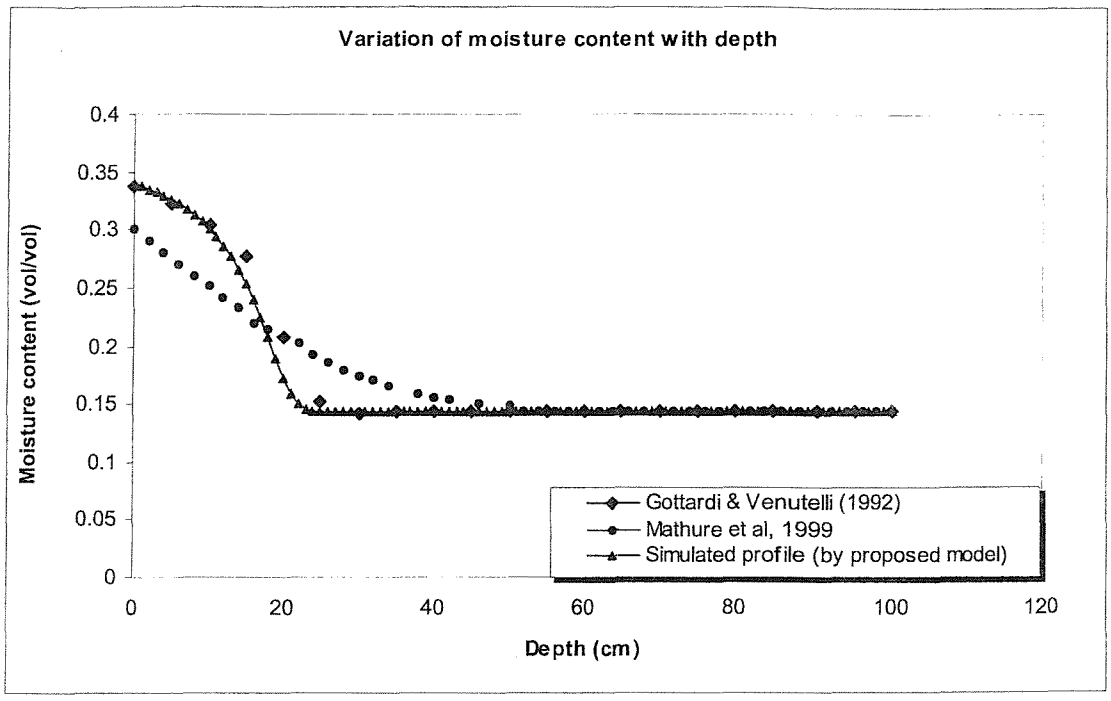

Figure 6.8: Finite difference variation of moisture content with depth

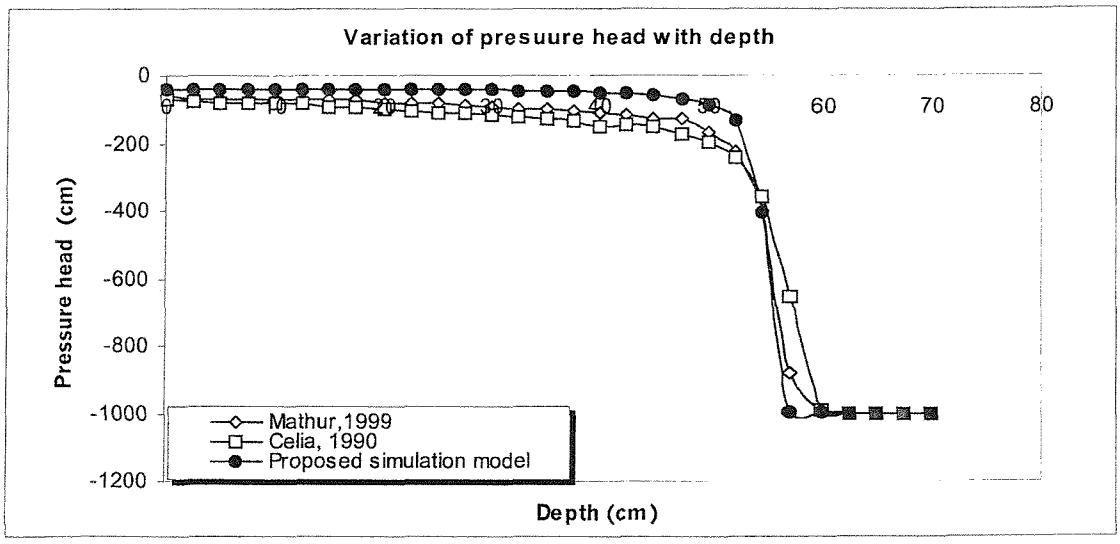

Figure 6.9: Comparison of pressure head variation with depth using finite difference solution method and available data.

6.4.3 Performance for the root water extraction term

After validating the model without using on extraction term, the model was further run with the extraction term detailed in section 4.3.3 (see chapter 4). The soil parameters for this case are again given in table 6.3, and the moisture content initially was assumed to be of 0.0527 cm^3/cm^3 throughout the column, which corresponds to a pressure head of –300 cm of water. The boundary condition at the top of the soil was assumed to be a zero flux boundary at the beginning of the simulation period, and the potential transpiration rate was assumed to be 0.025 cm/day. The soil profile, which was 100 cm in depth, was divided into 101 nodes with 100 elements each of one centimetre size. The root length at the start of the simulation was taken to be 13.66 cm; hence, the upper fourteen nodes contributed to the root water extraction in the model. The simulation was carried out for one day. The extraction of water with depth is shown after a 24-hour period in figure 6.10 and table 6.4. For the period of 24-hours, the sum of water taken up by the whole root system amounted to 0.02547 cm/day of the water (table 6.4). This value, when compared with the potential transpiration rate used in the root water extraction function, gives an error of less than 2%. Since the initial condition is the wet condition, the root water extraction will be at its potential rate, as stated earlier.

The root water uptake was about 44% in the top quarter, 28% and 21% in the next two quarters, and 7% in the bottom quarter. The model thus follows the traditional guidelines for the distribution for root water uptake with depth, namely, 40%, 30%, 20% and 10% in the four quarters, respectively (Withers and Vipond 1980, Teare and Peet, 1983).

6.4.4 Performance of water balance simulation model for different initial conditions in a micro-catchment system

After validating the model using the root water extraction term, but without using evaporation and micro-catchment system conditions, the model performance was further run with water balance performance, as detailed in section 4.6 (see chapter 4). The selected soil is a sandy loam soil, whose parameters for this case are again given in table 6.3, and the performance is described in the two following sections:

Table 6.4: Simulated pressures head moisture content and root extraction at the end of one day

Depth	Pressure head	Simulated-soil moist	Simulated-root-extraction	Root extraction	Root extraction	Ratio of Root extraction
Cm	Cm	v / v	v / v	Cm/day	in a quarter(Cm/day)	Percent
0	-355.986	0.05	0.05	0		
1	-343.196	0.05	0.05	0		
2	-335.696	0.05	0.05	0	0	44.52
3	-330.289	0.05	0.05	0		
4	-325.966	0.05	0.05	0		
5	-322.270	0.05	0.05	0	0.01	27.65
6	-318.957	0.05	0.05	0		
7	-315.896	0.05	0.05	0		
8	-313.026	0.05	0.05	0		
9	-310.337	0.05	0.05	0	0.01	21.31
10	-307.853	0.05	0.05	0		
11	-305.631	0.05	0.05	0		
12	-303.758	0.05	0.05	0	0	6.52
13	-302.348	0.05	0.05	0	0.03	
14	-301.430	0.05	0.05	0		
15	-300.845	0.05	0.05	0		
16	-300.483	0.05	0.05	0		
17	-300.266	0.05	0.05	0		
18	-300.141	0.05	0.05	0		
19	-300.072	0.05	0.05	0		
20	-300.035	0.05	0.05	0		
21	-300.017	0.05	0.05	0		
22	-300.008	0.05	0.05	0		
23	-300.003	0.05	0.05	0		
24	-300.001	0.05	0.05	0		
25	-300.001	0.05	0.05	0		
26	-300.00	0.05	0.05	0		
27	-300.000	0.05	0.05	0		
28	-300.000	0.05	0.05	0		
29	-300.000	0.05	0.05	0		
30	-300.000	0.05	0.05	0		
31	-300.000	0.05	0.05	0		
32	-300.000	0.05	0.05	0		
33	-300.000	0.05	0.05	0		
34	-300	0.05	0.05	0		
35	-300	0.05	0.05	0		
36	-300	0.05	0.05	0		
37	-300	0.05	0.05	0		
38	-300	0.05	0.05	0		
39	-300	0.05	0.05	0		
40	-300	0.05	0.05	0		
41	-300	0.05	0.05	0		
100	-300	0.05	0.05	0		

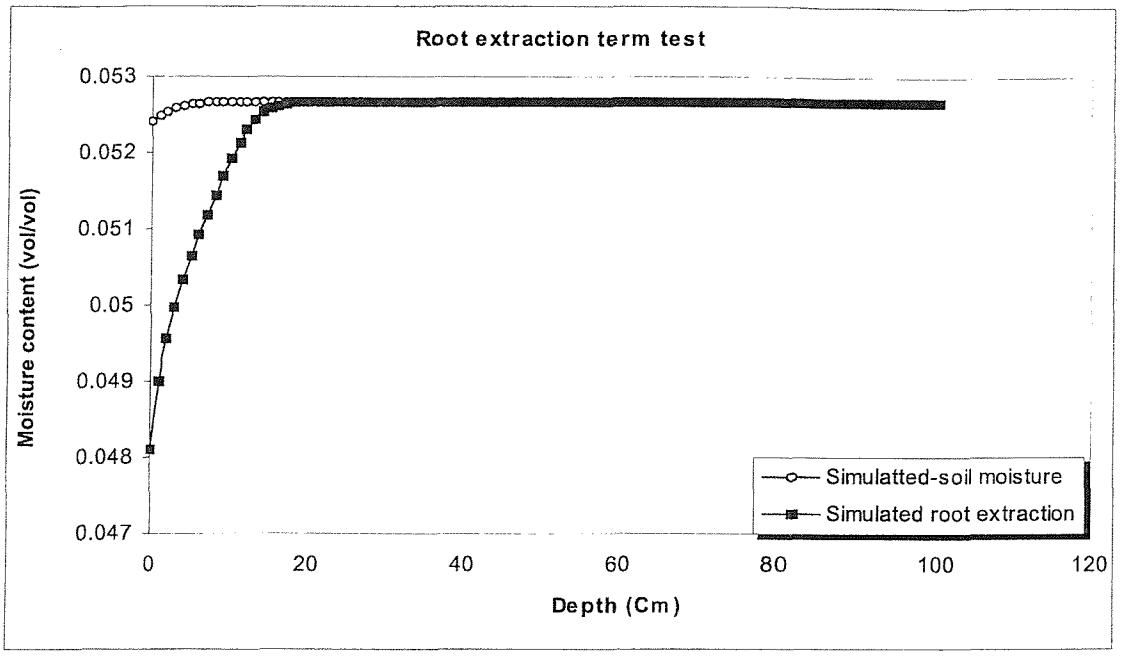

Figure 6.10: Moisture profile with root extraction term

I. First section:

In this section, as show in table 6.13, moisture content initially was assumed to be 0.0527 cm^3/cm^3 throughout the column, which corresponds to a pressure head of –300 cm of water. The boundary condition at the top of the soil was assumed to be a zero flux boundary at the beginning of the simulation period, and the potential transpiration rate was assumed to be 0.025 cm/day.

The soil profile, (100 cm in depth) was divided into 101 nodes with 100 elements each of one centimetre size. The root length in the period of each time interval was taken to be 100 cm. The simulation was carried out for one day. The extraction of water with depth is shown after a 24 hour period in figure 6.10 and table 6.4. For the period of 24 hours, the sum of water taken up by the whole root system amounted to 0.02547 cm/day of water (table 6.4). This value, when compared with the potential transpiration rate used in the root water extraction function, gives an error of less than 2%. Since the initial condition is the wet condition, the root water extraction will be at its potential rate as stated earlier.

Table 6.5: Water balance performance; initial information, results and percent of error in a micro-catchment system.

No	Time interval (hour)	Runoff area (cm^2)	Infiltration basin area (cm^2)	Soil kind in runoff area	Soil kind factor	Soil kind in infiltration basin	Slope in runoff area (S%)	Rainfall (mm/d)	Actual runoff (cm-depth)	Available water in infiltration basin (Z, cm-depth)
1	2	100	9	Sandy clay loam	1	Sandy loam	0.5	280	202.26	252.74
2	4	100	9	Sandy clay loam	1	Sandy loam	0.5	280	202.26	252.74
3	4	100	9	Sandy clay loam	1	Sandy loam	0.5	30	17.07	21.97
4	12	100	9	Sandy clay loam	1	Sandy loam	0.5	30	17.07	21.97
5	24	100	9	Sandy clay loam	1	Sandy loam	0.5	30	17.07	21.97
No	Time interval (hr)	Discharge per hour, Qin(cm/h)	Total discharge per time interval(qin ,T)	Actual evaporation (Eac, cm/time interval)	Root extraction (qroot, cm/time interval	Deep percolation (qdeep, cm/time interval)	Runoff from infiltration basin (qrun), cm	Δ W, cal	Δ W, est	Error. %
1	2	10.53	21.06	0.04	0.0009	2.8648E-06	17.75	3.27	3.25	-0.45
2	4	10.53	42.12	0.08	0.0008	5.73E-06	37.41	4.63	4.74	2.38
3	4	0.92	3.66	0.08	0.0009	5.7291E-06	0	3.58	3.56	-0.45
4	12	0.92	10.98	0.25	0.0007	1.719E-05	2.16	8.57	8.65	0.88
5	24	0.92	21.97	0.27	0.0005	3.4379E-05	7.47	14.22	14.19	-0.26

6.5 Discussion

Testing model results indicates performance as intended, with predictions of the root extraction pattern of the experimental data on which its concepts were based. By comparison with well-established analytical and numerical models for one-dimensional problems, it was demonstrated satisfactory numerical accuracy of the results. The predictive capabilities of the model were examined by simulating both laboratory experiments in two dimensions of time and space, and tests for coupled rainfall runoff and soil moisture, and uncoupled rainfall potential runoff flow in a micro-catchment system.

The rainfall runoff test provided in section 6.2.1 shows that the proposed model (in comparison with dada provided by Diskin (1995)) yields reliable and robust numerical solutions for rainfall excess flow problems in the runoff area of a micro-catchment system.

By comparing the results for moisture depletion from the root zone with various soil type and wetting patterns, it was shown that the concepts employed in the development of

the root extraction model are justified. The test cases also revealed that the numerical models give similar results, when the lower boundary of the root zone is assumed to be sealed or constant variation of soil moisture with depth variation. Since such a case resembles no real field condition, the proposed model showed it, that neglecting of moisture transfer across root zone boundary results in significant errors in depletion estimates. Using these results, the deficiencies in current methods of irrigation scheduling as based on this type of models were highlighted. In parallel, the merits of the proposed model in more accurately emulating actual field conditions were demonstrated. The role of moisture storage in the soil layers underlying the root zone was shown to be significant in controlling the moisture regime. This illustrated the possible errors that can be committed in water use calculations projections when simplistic models for moisture depletion are used.

Table 6.6: Simulated pressure head (cm), in water balance performance model for different initial conditions and 280-mm/day rainfall in a micro-catchment system (in figure 6.11).

Depth	initial, h=-80 cm	init, h= -80 cm	init, h= -80 cm	init, h= -80 cm	initi,h=-1000 cm	init-h=-1000 cm	init-h=-1000 cm
	initial moisture content	Simulated time, 0.28hr	Simulated time 0.5hr	Simulated time, 1hr	initial moisture content	Simulated time, 2hr	Simulated time,4hr
0	0.25	0.40	0.40	0.40	0.12	0.40	0.40
1	0.2	0.39	0.39	0.40	0.12	0.40	0.40
2	0.25	0.39	0.39	0.40	0.12	0.40	0.40
3	0.25	0.38	0.39	0.39	0.12	0.39	0.40
4	0.25	0.36	0.38	0.39	0.12	0.39	0.40
5	0.25	0.33	0.36	0.39	0.12	0.39	0.39
6	0.25	0.29	0.34	0.38	0.12	0.39	0.39
7	0.25	0.26	0.32	0.37	0.12	0.38	0.39
8	0.25	0.25	0.29	0.36	0.12	0.37	0.39
9	0.25	0.25	0.26	0.35	0.12	0.36	0.39
10	0.25	0.25	0.25	0.33	0.12	0.34	0.38
11	0.25	0.25	0.25	0.30	0.12	0.31	0.38
12	0.25	0.25	0.25	0.28	0.12	0.26	0.37
13	0.25	0.25	0.25	0.26	0.12	0.19	0.37
14	0.25	0.25	0.25	0.25	0.12	0.12	0.36
15	0.25	0.25	0.25	0.25	0.12	0.12	0.34
16	0.25	0.25	0.25	0.25	0.12	0.12	0.32
17	0.25	0.25	0.25	0.25	0.12	0.12	0.29
18	0.25	0.25	0.25	0.25	0.12	0.12	0.25
19	0.25	0.25	0.25	0.25	0.12	0.12	0.18
20	0.25	0.25	0.25	0.25	0.12	0.12	0.12
21	0.25	0.25	0.25	0.25	0.12	0.12	0.12
22	0.25	0.25	0.25	0.25	0.12	0.12	0.12
23	0.25	0.25	0.25	0.25	0.12	0.12	0.12
24	0.25	0.25	0.25	0.25	0.12	0.12	0.12
25	0.25	0.25	0.25	0.25	0.12	0.12	0.12
26	0.25	0.25	0.25	0.25	0.12	0.12	0.12
27	0.25	0.25	0.25	0.25	0.12	0.12	0.12
28	0.25	0.25	0.25	0.25	0.12	0.12	0.12
29	0.25	0.25	0.25	0.25	0.12	0.12	0.12
30	0.25	0.25	0.25	0.25	0.12	0.12	0.12
31	0.25	0.25	0.25	0.25	0.12	0.12	0.12
32	0.25	0.25	0.25	0.25	0.12	0.12	0.12
33	0.25	0.25	0.25	0.25	0.12	0.12	0.12
34	0.25	0.25	0.25	0.25	0.12	0.12	0.12
35	0.25	0.25	0.25	0.25	0.12	0.12	0.12
36	0.25	0.25	0.25	0.25	0.12	0.12	0.12
37	0.25	0.25	0.25	0.25	0.12	0.12	0.12
38	0.25	0.25	0.25	0.25	0.12	0.12	0.12
39	0.25	0.25	0.25	0.25	0.12	0.12	0.12
40	0.25	0.25	0.25	0.25	0.12	0.12	0.12
41	0.25	0.25	0.25	0.25	0.12	0.12	0.12
100	0.25	0.25	0.25	0.25	0.12	0.12	0.12

Table 6.7: Simulated pressure head (cm) in water balance performance model for different time interval and 30 mm rainfall in a micro-catchment system (in figure 6.12).

Depth	initial moisture	init-h=-1000 cm	init-h=-1000 cm	init-h=-1000 cm	Depth	initial moisture	init-h=-1000cm	init-h=-1000 cm	init-h=-1000 cm
		simulated, 4hr	simulated, 12hr	simulated, 24hr			smulated, 4hr	simulated, 12hr	simulated, 24hr
0	0.12	0.40	0.40	0.40	43	0.12	0.12	0.1216965	0.3729824
1	0.12	0.39	0.40	0.40	44	0.12	0.12	0.1216966	0.3696939
2	0.12	0.39	0.40	0.40	45	0.12	0.12	0.1216967	0.3658164
3	0.12	0.39	0.40	0.40	46	0.12	0.12	0.1216968	0.361206
4	0.12	0.39	0.40	0.40	47	0.12	0.12	0.1216969	0.3556693
5	0.12	0.39	0.40	0.40	48	0.12	0.12	0.121697	0.3489385
6	0.12	0.38	0.40	0.40	49	0.12	0.12	0.121697	0.3406295
7	0.12	0.38	0.40	0.40	50	0.12	0.12	0.1216971	0.3301664
8	0.12	0.37	0.39	0.40	51	0.12	0.12	0.1216972	0.3166324
9	0.12	0.36	0.39	0.40	52	0.12	0.12	0.1216973	0.2984559
10	0.12	0.35	0.39	0.40	53	0.12	0.12	0.1216974	0.2727291
11	0.12	0.34	0.39	0.40	54	0.12	0.12	0.1216975	0.2342821
12	0.12	0.32	0.39	0.40	55	0.12	0.12	0.1216976	0.179641
13	0.12	0.30	0.39	0.40	56	0.12	0.12	0.1216977	0.1260793
14	0.12	0.22	0.39	0.40	57	0.12	0.12	0.1216978	0.1217046
15	0.12	0.15	0.39	0.40	58	0.12	0.12	0.1216979	0.1216966
16	0.12	0.12	0.39	0.40	59	0.12	0.12	0.121698	0.1216967
17	0.12	0.12	0.39	0.39	60	0.12	0.12	0.1216981	0.1216968
18	0.12	0.12	0.39	0.39	61	0.12	0.12	0.1216982	0.1216969
19	0.12	0.12	0.39	0.39	62	0.12	0.12	0.1216982	0.1216971
20	0.12	0.12	0.38	0.39	63	0.12	0.12	0.1216983	0.1216972
21	0.12	0.12	0.38	0.39	64	0.12	0.12	0.1216984	0.1216973
22	0.12	0.12	0.38	0.39	65	0.12	0.12	0.1216985	0.1216974
23	0.12	0.12	0.38	0.39	66	0.12	0.12	0.1216986	0.1216976
24	0.12	0.12	0.37	0.39	67	0.12	0.12	0.1216987	0.1216977
25	0.12	0.12	0.37	0.39	68	0.12	0.12	0.1216988	0.1216978
26	0.12	0.12	0.36	0.39	69	0.12	0.12	0.1216989	0.1216979
27	0.12	0.12	0.36	0.39	70	0.12	0.12	0.121699	0.1216981
28	0.12	0.12	0.35	0.39	71	0.12	0.12	0.1216991	0.1216982
29	0.12	0.12	0.34	0.39	72	0.12	0.12	0.1216992	0.1216983
30	0.12	0.12	0.33	0.39	73	0.12	0.12	0.1216993	0.1216984
31	0.12	0.12	0.31	0.39	74	0.12	0.12	0.1216994	0.1216986
32	0.12	0.12	0.28	0.39	75	0.12	0.12	0.1216994	0.1216987
33	0.12	0.12	0.24	0.39	76	0.12	0.12	0.1216995	0.1216988
34	0.12	0.12	0.19	0.39	77	0.12	0.12	0.1216996	0.1216989
35	0.12	0.12	0.13	0.39	78	0.12	0.12	0.1216997	0.1216991
36	0.12	0.12	0.12	0.39	79	0.12	0.12	0.1216998	0.1216992
37	0.12	0.12	0.12	0.39	80	0.12	0.12	0.1216999	0.1216993
38	0.12	0.12	0.12	0.38	81	0.12	0.12	0.1217	0.1216994
39	0.12	0.12	0.12	0.38	82	0.12	0.12	0.1217001	0.1216996
40	0.12	0.12	0.12	0.38	83	0.12	0.12	0.1217002	0.1216997
41	0.12	0.12	0.12	0.38	84	0.12	0.12	0.1217003	0.1216998
42	0.12	0.12	0.12	0.38	100	0.12	0.12	0.1217017	0.1217017

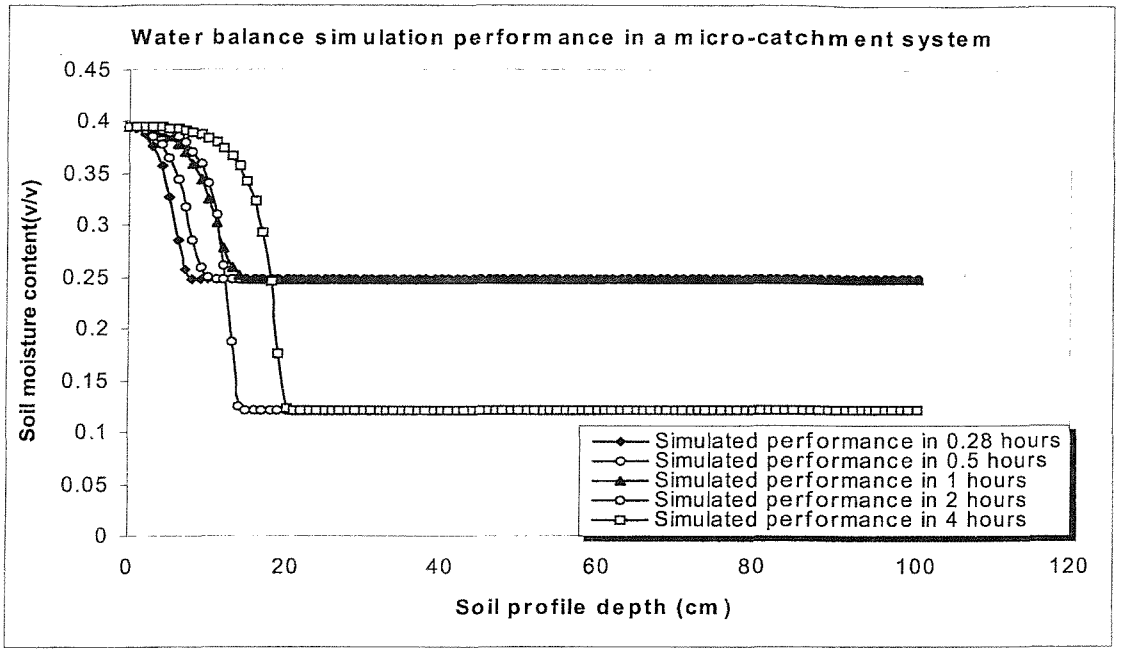

Figure 6.11: Predicted water content in different initial pressure head, different time interval with 280-mm daily rainfall in water balance performance and micro-catchment system conditions

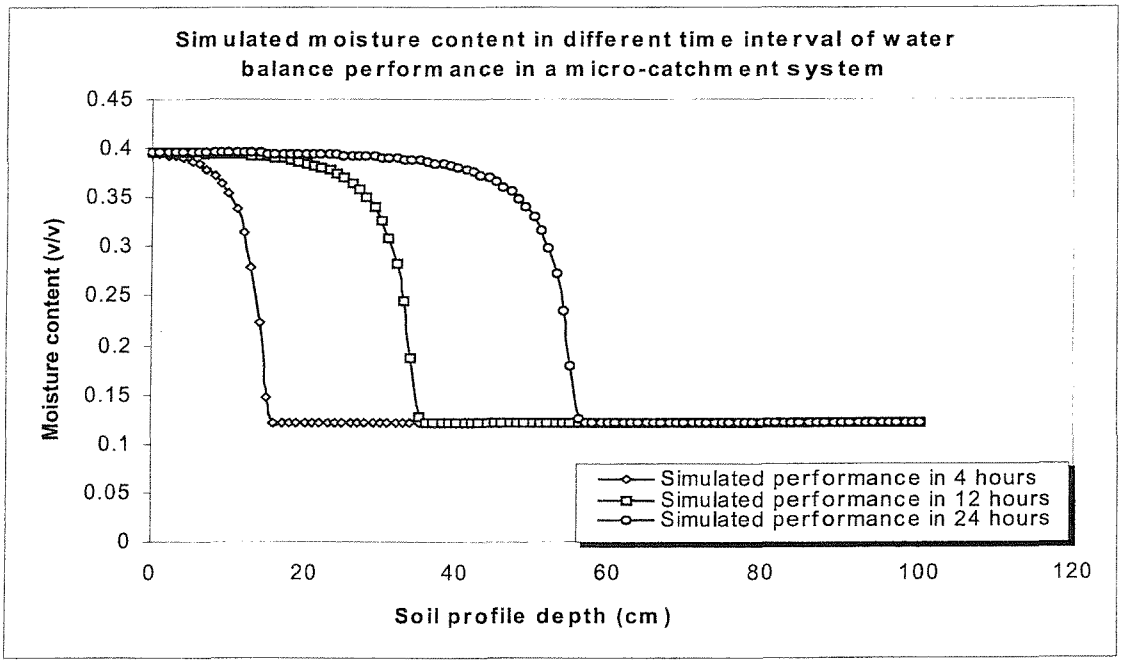

Figure 6.12: Simulated water content using proposed model in water balance performance in different time intervals, 30-mm rainfall, 100 square metres size of runoff area, slope 0.5% in a micro-catchment system.

Chapter 7 Analysis of the rainfall-runoff process in micro-catchment systems

7.1 Introduction

A model has been developed to estimate potential micro-catchment rainfall runoff. In this model, rainfall excess is considered as a function of rainstorm intensity and infiltration rate. The value of potential rainfall excess in a given time interval is equal to the rainfall value minus the predicted infiltration volume in that interval.

The effect on runoff of three different slopes (0.5, 5 and 10%) and five micro-catchment sizes (252, 324, 360, 396 and 432 m^2) was studied for 7 years in an area of India (Sharma, 1986). This data was used to establish a relationship between the effect of slope and catchment size on actual runoff.

7.2 Determination of excess rainfall and potential runoff

There is an initial period, for most rainfall events, during which all the rainfall infiltrates into the soil. During this period, the capacity of the soil to absorb water decreases until it becomes less than the rainfall intensity. At this point, the soil surface becomes ponded with water. As rainfall continues, the surface pondage exceeds the surface retention capacity and runoff begins. Under ponded conditions, the infiltration process is independent of the time distribution of rainfall. For an unsteady rainfall event in arid regions, there may be several periods during which the rainfall intensity exceeds the current infiltration rate and ponding may appear and disappear. The water balance equation for the runoff zone of a micro-catchment system, is described in section 3.3.1 (chapter 3) and the variables involved in an infiltration process are given as

$$R_C = R_C(t) = F(t) + G(t) + R_{exc,C}(t) = F + G + R_{exc,C} \qquad 7.1$$

Where:

R_C = cumulative rainfall in millimetres

F = cumulative infiltration in millimetres

G = surface pondage in millimetres

$R_{exc,C}$ = cumulative rainfall excess in millimetres, which is the source of runoff

The properties of the rainfall excess and the surface pondage are shown in the following equations. For a given ground surface condition there exists a maximum amount of water which can be retained on the surface without causing runoff (ie ponded water). This amount is also referred to as the retention capacity. The range of variation of the surface pondage is therefore limited by

$$0 \leq G \leq D \qquad 7.2$$

Where:

D is the maximum retention capacity in millimetres

G is surface pondage in millimetres

Consider the rate of change with respect to time, that is,

$$R_i = f + \frac{dG}{dt} + R_{exc} \qquad 7.3$$

Where:

R_i is the rainfall intensity in millimetres per hour

f is the infiltration rate in millimetres per hour,

R_{exc} is rainfall excess rate in millimetres per hour.

When the surface pondage reaches the maximum retention capacity and when rainfall intensity exceeds the infiltration rate, the rainfall excess becomes greater than zero, otherwise it equals zero. That is, (7.3),

$$R_{exc} = R_i - f_P \qquad \text{For } G = D \text{ and } R_i > f_P \qquad 7.4$$

$$R_{exc} = 0 \qquad \text{For } G < D \text{ and } R_i < f_P \qquad 7.5$$

Where:

R_i is rainfall intensity in a time step period in millimetre per hour

f_P is the potential infiltration capacity in millimetres per hour in the same time period of rainfall

The cumulative rainfall excess is by definition the time integral of the rainfall excess rate as follows:

$$R_{exc,C} = R_{exc,C}(t) = \int R_{exc}(t)dt \qquad 7.6$$

It follows from 7.4, 7.5, and 7.6 that

$$R_{exc,C}(t) > R_{exc,C}(t-1) \qquad \text{For } G = 0 \quad R_i > f_P \qquad 7.7$$

$$R_{exc,C}(t) = R_{exc,C}(t-1) \qquad \text{For } G < D \quad R_i < f_P \qquad 7.8$$

Where:

t-1 is a time prior to the time t in hours

7.2.1 Calculation of infiltration and excess rainfall in runoff basin

Runoff and infiltration estimates are often needed for ungaged catchments for the engineering design of micro-catchment systems. To meet this need, a model for estimating runoff volume based on measured daily storm rainfall and potential infiltration rate in a micro-catchment was developed. The model is based on the physical principles described in chapter 3. The model is simple to use and the following approach was adopted:

To enable runoff to be calculated it is first necessary to estimate the rate of infiltration during rainfall events. The conceptual model for calculating infiltration in the runoff zone takes precipitation falling in a given time interval and calculates the amount of potential runoff after subtracting the predicted infiltration for that period. Since infiltration rate is variable and depends on the level of saturation and type of soil, the model must

update the infiltration rate for successive time intervals taking into account the level of the saturation achieved by the preceding rainfall in different soil types.

Infiltration of water at the soil surface is a complex process, which is affected by soil factors such as hydraulic conductivity, initial water content, surface compacting, depth of profile, and water table depth. Plant factors such as extent of cover and depth of root zone and climatic factors such as intensity, duration also affect infiltration, as do time distribution of rainfall, temperature, and whether or not the soil is frozen. The preceding moisture content of the soil, however, is probably the main variable affecting the infiltration rate of a given soil type during a storm. The traditional Green and Ampt equation (1911) provides a practical and elegant solution to this problem by expressing infiltration rate against accumulative infiltration (see Chapter 3, section 3.3.1).

The equation as modified by Philips (1957) is:

$$f = A/F + B \qquad 7.9$$

Where:

f is infiltration rate, millimetres per hour

F is cumulative infiltration, millimetre

A and B are parameters of Green and Ampt equation

Figures 7.2, 7.3, and 7. 3 show the graphical relationship of this equation for three major soil types and are taken from Jensen (1980). The Green and Ampt linear approximations provide an ideal method for taking into account preceding soil moisture conditions when establishing the soil potential infiltration rate.

If the initial soil moisture condition is known, the actual infiltration rate of an initial time period (say 10-min) can be calculated from the Green and Ampt equation. If the rainfall rate exceeds the infiltration rate for a given time period the rainfall excesses can be calculated for that period. The infiltration rate of the second and subsequent time period is then calculated from the equation and the process repeated until precipitation excess occurs.

7.2.2 Model computation:

An important application of the model is for the calculation of the variations of the actual infiltration rate and its use in calculating the rainfall excess during and after a given rainstorm event. It is assumed that the potential infiltration curve for the area under consideration is known, and at that start of a storm the soil is dry (unsaturated).

The calculations of infiltration are carried out for successive intervals during a storm. The intervals are taken to be of equal size but this is not a required condition for the use of the model. In this study the time interval is divided in a short periods of time steps so that for each time period (time step), the rainfall intensity can be considered effectively constant. For each time step, the unknown value of the actual infiltration rate at the end of the time interval is calculated.

The variable input is the volume of rainfall in a given time step, $[R(t_{ste})]$ and constant parameters A, B, k, α are defined for a particular soil type in the Green and Ampt equation. A. B. k. and α, are model parameters. Assuming that the soils in arid regions are at unsaturated condition at the start of the storm, when rainfall intensity in the first time step is greater than the model parameter ($Ri(t_{ste}) > B$), then the soil infiltration rate is predicted as the maximum rate. Actual infiltration rate (f_{ac}) in time step is the amount of water that actually infiltrated into the soil. Runoff is the amount of collected rainfall excess in the infiltration basin of a micro-catchment system, considering slope and size of the system.

Computation begins with the conversion of the rainfall amount ($R(t_{ste})$) to a rainfall intensity ($Ri(t_{ste})$) for a given time step. Then a check is made for one of the necessary conditions of the model parameter, that is, rainfall intensity when it is greater than saturated hydraulic conductivity, K_S, ($K_S = B$, model parameter). If this condition is satisfied, then the predicted infiltration rate, (f_{pre}), is computed from the one over cumulative infiltration using the graphical relationship between infiltration and one over cumulative infiltration (Figure 7.2, 7.3, and 7.4). Predicted infiltration rate $[(f_{Pre}\ (t_{n-1})]$ calculated at the previous time step, and a check for the second necessary condition is made, that is, the rainfall intensity $[Ri(t_{ste})]$, which has to be greater than the predicted infiltration rate $[(f_P\ (t_{n-1})]$ at the previous

time step. If both conditions are satisfied, then the actual infiltration rate and runoff are computed as shown in computation of the model (Fig 7.1).

The model assumes that soils in arid regions are generally unsaturated at the start of a rainfall event. The model evaluates the amount of rainfall in the first and subsequent ten-minute time steps. The model takes ten minutes of rainfall data and assesses the amount of infiltration and potential ponding in each ten minutes period. However to improve the accuracy of the model in heavy rainfall, it is important to predict exactly when ponding begins. This is calculated by dividing the time steps for computational purpose along the following lines.

I. If rainfall intensity is less than saturated hydraulic conductivity in a ten-minute period, then all rainfall infiltrates and the time period is not subdivided.

II. If rainfall intensity is greater than saturated hydraulic conductivity and smaller than eighty percent of predicted potential infiltration rate at the end of the previous time step the ten-minute time step is divided into two equal parts of five minutes. (This is to help identify when ponding is likely to occur within a time period. The arbitrary level of eighty percent was selected in extension trial and error testing to establish an appropriate level of accuracy)

III. If in a ten minute period the intensity is greater than the saturated hydraulic conductivity but smaller than ninety five percent of predicted infiltration rate at the end of the previous time step, the time interval is divided into five equal parts of two minutes.

IV. Similarly if in a ten-minute period the rainfall intensity is less than ninety eight percent of predicted infiltration rate at the end of the last period but greater than saturated hydraulic conductivity the time step is divided into ten equal parts of minutes.

V. If the intensity is greater than ninety eight percent of the predicted infiltration rate, in a ten minute time period at the end of the previous time period the time period is split into half-minute time steps. The time of ponding is computed based on equation 7.30 in section 7.2.4.

The rainfall in each of the above time steps depends on the time step duration and is calculated as follows:

$$R(t_{ste}) = R(t_{int}) \qquad IF \quad R_i < B \qquad 7.10$$

$$R(t_{ste}) = \frac{t_{ste} * R(t_{\text{int}})}{t_{\text{int}}} \qquad IF \quad R_i > B \qquad 7.11$$

Where:

$R(t_{ste})$ is rainfall in a time step

$R(t_{int})$ is rainfall in a time interval

t_{int} is time interval, which in this study equals ten minutes

t_{ste} is time step (between 0.5-10 minutes)

As regards time step duration, attention should be given to a special case in which the duration of a rainfall event in a time interval is divided into many short periods (time steps) in such a way that within each period the rainfall intensity is essentially considered constant. For such a case the rainfall intensity is:

$$R_i(t_{ste}) = 60\left(\frac{R_C(t_n) - R_C(t_{n-1})}{t_n - t_{n-1}}\right) = R_i = Constant \qquad 7.12$$

Where:

$R_i(t_{ste})$ = rainfall intensity (mm per hour) at time step t,

t_n-t_{n-1} = nth time step duration (short period of divided time interval),

$R_C(t_n)$ = cumulative rainfall at the end of the nth time step, and

$R_C(t_{n-1})$ = cumulative rainfall in millimetres at the beginning of the nth time step.

The variable cumulative rainfall $R_C(t)$ within a short period of time step can be written as:

$$R_C(t_n) = R_C(t_{n-1}) + \int_{t_{n-1}}^{t} R_i(t)dt = R_C(t_{n-1}) + (t - t_{n-1})R_i \qquad 7.13$$

Where:

$R_C(t_n)$ is cumulative rainfall in time step n

$R_C(t_{n-1})$ is cumulative rainfall in time step n-1

$R_i(t)$ is rainfall intensity in time step

R_i is rainfall intensity

The infiltration rate is assumed initially to be equal to the rainfall in the selected short period of time step duration. Cumulative infiltration at the end of a time step (F) is computed from the sum of the infiltration depth of a selected time step and the cumulative infiltration of the previous time step. Predicted infiltration rate is expressed in millimetre per hour, and its value at any time step is denoted by $f_{\mathrm{Pre}}(t_{ste})$. The predicted infiltration rate is a function of rainfall intensity (R_i), and potential infiltration rate as predicted from the Green and Ampt linear relationship of infiltration rate against the reciprocal of cumulative infiltration for a given soil type. It is equal to potential infiltration rate at the time step calculated by the available potential infiltration equation (Fig 7.2, 7.3 and 7.4).

$$f_{pre}(t_{ste}) = A/F + B \qquad 7.14$$

Where:

A and B are the Green and Ampt parameters of graphical relationship between infiltration rate and cumulative infiltration (Fig, 7.3).

F is cumulative infiltration (mm)

$f_{\mathrm{Pre}}(t_{ste})$ is the predicted infiltration rate at the time step. The output is expressed in units of depth per unit time.

When the rainfall rate is less than the potential infiltration rate for a given time step, then the soil will be less saturated after that time step than it would be in the presence of an adequate water supply. If the potential infiltration rate at the end of a time step were to be established from a standard infiltration /time graph it is necessary to establish a concept effective that would correspond to the same level as the actual saturation achieved in the soil. This is achieved by the following.

In table 7.1, for computational purposes, the difference between the predicted time (t_{pre}) and the time step is calculated and the cumulative infiltration is given as time delay (t_{del}).

The predicted time (t_{pre}) of achieved predicted infiltration rate (f_{pre}) is a function of the infiltration rate (f) in a time step. ie.

$$t_{pre}^{-a} = \frac{f_{pre}}{k} \qquad \text{And} \qquad t_{pre} = (k / f_{pre})^{1/a} \qquad 7.15$$

Where:

t_{pre} is effective time of potential infiltration

k and α are two parameters of the available potential infiltration curve of a soil

f_{pre} is predicted infiltration (from Green and Ampt).

The predicted infiltration rate in each time is computed by the model. The actual infiltration rate, f_{ac}, at the end of the time step is defined by the actual time (t_{ac}) of infiltration from the infiltration - time curve, as shown in table 7.1.

The outputs of the soil surface rainfall runoff model in a micro-catchment system depend on the value of the predicted infiltration rate, $f_{pre}(t_{ste})$, and the value of rainfall input, $R(t_{ste})$, at the instant considered in each time step. Considering the definitions of the predicted infiltration, (f_{pre}), by Eq, 7.15, and denoting the rainfall intensity during the time step by $R_i(t)$, three cases are possible.

Case (A):

The rainfall intensity in a time interval is smaller than the saturated hydraulic conductivity ($K_s = B$) as a parameter of the model and predicted infiltration rate, $f_{Pre}(t_{n-1})$, at the end of previous time step, or the following relationship;

$$if \quad R_i(t_{ste}) < B$$

$$t_{ste} = t_{int} \qquad f_{ini}(t_{ste}) = R(t_{ste}) = R(t_{int}) \qquad 7.16$$

$$f_{ac} = f_{pre}(t_{ste}) \quad \text{and} \quad R_{exc} = 0$$

If the rainfall intensity in a given step is less than B (model parameter), then no runoff can be generated in the time step. All the rain in the time step is infiltrated into the soil and the actual infiltration rate is equal to rainfall volume. The computation of predicted infiltration rate,(f_{pre}) is updated to get the predicted infiltration rate($f_{pre}(t_{n+1})$) at the start of the next time step computation.

Case (B):

The rainfall intensity is larger than B (model parameter) and smaller than the potential infiltration rate at the previous time step [$f_{pre}(t_{n-1})$], (Table, 7.1, and Fig 7.1): or

$$If\ R_i(t_{ste}) > B \qquad f_{ac} = Kt_{ac}^{-\alpha} \quad \text{and}$$
$$If\ \ R_i(t_{ste}) < f_{Pre}(t_{n-1}) \qquad R_{exc} = 0 \qquad 7.17$$

In this case, rainfall intensity in the time step is compared with predicted infiltration rate for the time step duration being set as explained earlier (see equations 7.17).

$$f_{ini}(t_{ste}) = R(t_{ste}) \qquad and \qquad R_{exc} = 0. \qquad 7.18$$

Case (C):

The rainfall intensity is larger than the saturated hydraulic conductivity ($K_s = B$, Model parameter) and greater than the predicted infiltration calculated at time step ($f_{pre}(t_{ste})$.

$$R_i(t_{ste}) > B \qquad and \qquad R_i(t_{ste}) > f_{pre}(t_{ste}) \qquad 7.19$$

In this case;

$$f_{ini}(t_{ste}) = R_i(t_{ste}) \qquad 7.20$$

$$f_{a\,c}(t_{ste}) = f_{ac} = kt_{ac}^{-\alpha} \qquad 7.21$$

$$R_{exc} = \left(\frac{(R_i(t_{ste}) - f_{ac}(t_{ste})) * T_{ste}}{60} \right) \qquad 7.22$$

In the above three cases the calculations are summarised by the following equations

$$F = f_{ini}(t_n) + F(t_{n-1}) \qquad 7.23$$

$$\frac{1}{F} = \frac{1}{[f_{ini}(t_n) + F(t_{n-1})]} \qquad 7.24$$

$$f_{pre}(t_n) = A/F + B \qquad 7.25$$

$$t_{pre}^{-a} = \frac{f_{pre}}{k} \qquad and \qquad t_{pre} = (k / f_{pre})^{1/a} \qquad 7.26$$

Where:

$f_{a\,c}(t)$ is actual infiltration rate ,

$f_{ini}(t_{ste})$ in initial infiltration rate at a time step

$f_{pre}(t_n)$ in predicted infiltration rate at step n

$R_i(t_{ste})$ is rainfall intensity (mm/h),

$R(t_{ste})$ is total rainfall in a time step,

R_{exc} is rainfall excess

$f_{p\,re}(t_{ste})$ is predicted infiltration rate (mm/h) in a time step,

F is cumulative infiltration at time step

T_{ste} is time step duration (minute)

t_{pr} is predicted time of predicted infiltration (f_{pre}) at time step

A and B are Green and Ampt model parameters

a and k are parameters of model.

7.2.3 Evaluation and computation of ponding time

Ponding is defined, in infiltration studies, as the beginning of the formation of rainfall excess and runoff on the surface of the runoff area considered. At the start of the infiltration process and up to the time of ponding the rainfall intensity is smaller than the infiltration capacity (Ogden and Saghafian, 1997, Diskin and Nazimov. 1996). It follows that the actual infiltration rate in a time interval is equal to the rainfall intensity (Eqs. 7.16 and 7.17). The time of ponding marks the time at which the infiltration capacity changes from a rate larger than rainfall intensity to a rate equal or smaller to the intensity rate (Eqs. 3.10, and 7.19). Usually, the term's ponding and time of ponding (t_P) refer to events in which the upper soil layer has a zero initial storage volume. At the ponding time the rainfall intensity is of constant intensity (R_i), which is lower than the maximum infiltration capacity and higher than the minimum capacity or saturated hydraulic conductivity (Eq. 7.19).

For a very small time step (smaller than five minutes) rainfall intensity is considered to be effectively constant. The initial start of ponding is a function of cumulative infiltration, which in turn, is directly related to the cumulative precipitation. The cumulative infiltration at this time is a function of model parameters based on equation 3.12 and can be derived from the following.

$$F_P = \frac{K_s S_{av} M}{R_i(t_p) - K_s} \qquad 7.27$$

The ponding time, as explained in chapter three (section 3.3.1) can be obtained simply by combining equations 3.6 and 3.11 and letting $t = t_P$, as follow:

$$R_C(t_p) = R_C(t_{n-1}) + (t_p - t_{n-1}) * R_i, \qquad 7.28$$

And

$$t_p = \frac{R_C(t_P) - R_C(t_{n-1})}{R_i} + t_n \qquad 7.29$$

Combination of equations of 7.27, 7.28 and 7.29 yields:

$$t_p = \frac{\frac{K_s S_{av} M}{R_i(t_p) - K_s} + R_{exc}(t_{n-1}) - R_C(t_{n-1})}{R_i(t_p)} + t_n \qquad 7.30$$

Substituting to coefficient of: $A = K_s S_{av} M$, and B = K_s, the equation 7.30 becomes:

$$t_p = \frac{\frac{A}{R_i(t_p) - B} + R_{exc}(t_{n-1}) - R(t_{n-1})}{R_i(t_p)} + t_n \qquad 7.31$$

Where:

F_p in cumulative infiltration at time of ponding

$R_i(t_p)$ rainfall intensity at time of ponding

R_i rainfall intensity between two times steps

$R_c(t_p)$ cumulative rainfall at time of ponding

$R_{exc}(t_{n-1})$ rainfall excess at time of n-1

$R(t_{n-1})$ rainfall at time of n-1

A and B parameters of model

t_p time of ponding

S_{av} average soil suction

M initial soil water deficit

K_s saturated hydraulic conductivity

t_n time at nth time step

7.2.4 Estimating infiltration parameters for the model

There are two group parameters in the process of the rainfall runoff (rainfall-excess) model. The first relationship, is the relationship between infiltration rate and time under saturated conditions. This relationship should ideally be established experimentally for an area of interest, or, where that is not possible, it is necessary to establish the soil type and the approximate infiltration curve from the literature (ie Kostiakove, 1932.Lee, Jin et al, 1994 and Hartley, 1992). This relationship takes the form $F = Kt^{-a}$ (where t = time and K and a are coefficients)

The second relationship that is needed is the relationship between infiltration rate and one over cumulative infiltration. This curve can be derived from the above infiltration curve. A straight line approximates well to this relationship as described by Green and Ampt (1911) and takes the form

$$f = A/F + B$$

Where:

A and B are the Green and Ampt parameters of graphical relationship between infiltration rate and cumulative infiltration (see examples in figures 7.2, 7.3 and 7.4 for Colombia silt loam, sandy clay loam and light clay soils)

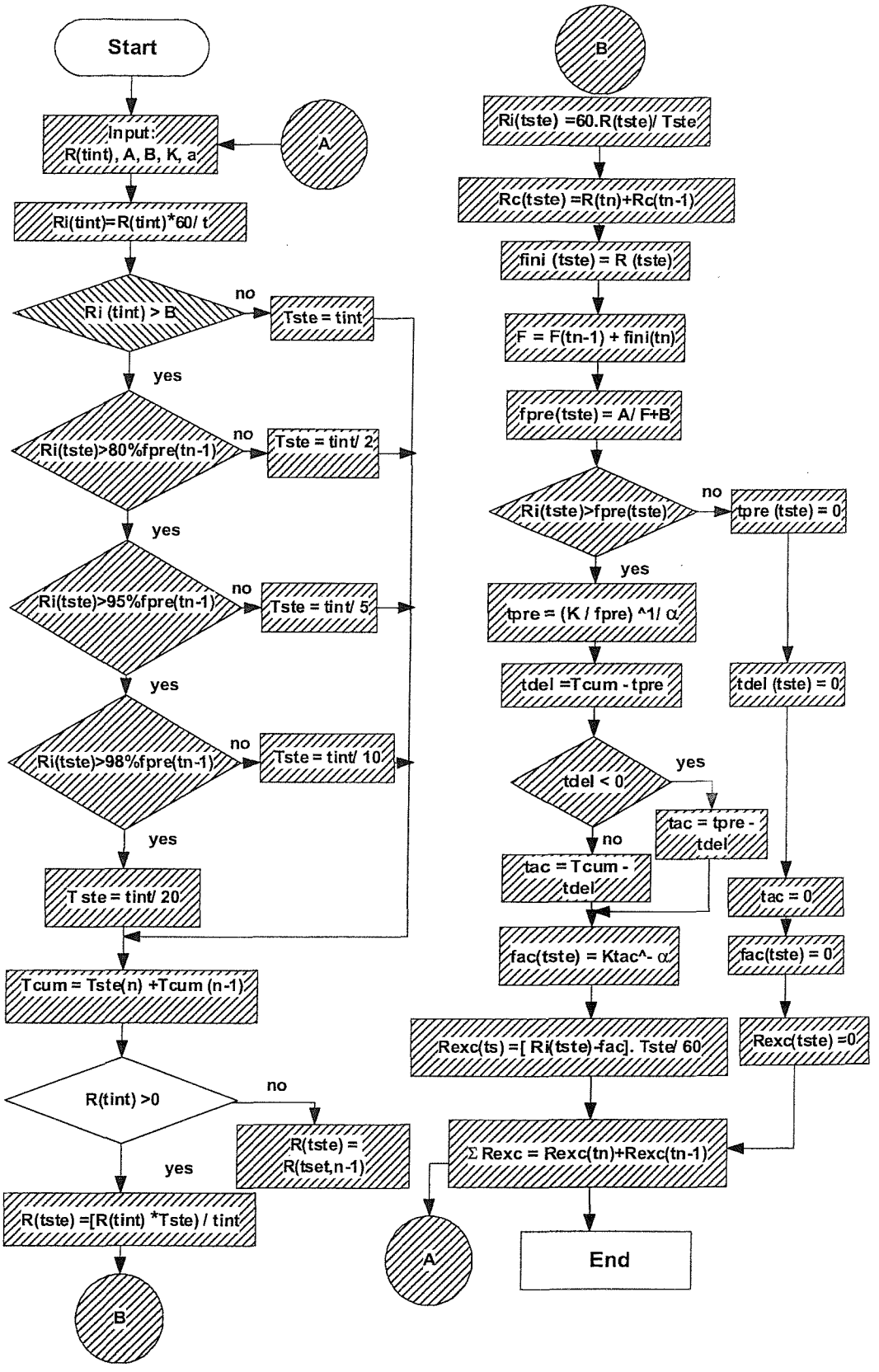

Fig. 7.1: Flowchart of computation infiltration & rainfall excess, computer model in a micro-catchment system.

NOTATION:

The following symbols are used in the flowchart of the designed rainfall runoff model in a micro-catchment system.

I. Rainfall and runoff symbols:

$R(t_{int})$ is rainfall in a time interval, which is ten minutes rainfall data

$R_i(t_{int})$ is rainfall intensity in a time interval

$R(t_{ste})$ is rainfall volume in each time step period

$R_i(t_{ste})$ is rainfall intensity (mm/h) in a time step

$R_c(t_{ste})$ is cumulative rainfall in a time step

R_{exc} is rainfall excess or potential runoff

II. Infiltration symbols:

$f_{ini}(t_{ste})$ is initial infiltration rate at time step period

$f_{pre}(t_{ste})$ is predicted infiltration rate at time step period

f_{ac} is actual infiltration rate at time step period

F is cumulative infiltration in a time step

III. Time symbols

t_{int} is time interval, which in this study is equal to ten minutes

t_{ste} is short period of time step long (sub divided of time interval)

T_{ste} is time step duration (e.g. 10, 5, 2, 1, 0.5 minutes duration)

t_{del} is time delay

t_n is time step at nth minutes

t_{n-1} is time of previous step

T_{cu} is cumulative time steps (minutes)

IV. Model coefficient symbols:

A and B are parameters of model and equals saturated hydraulic conductivity and

A is parameter of infiltration model

K is parameter of potential infiltration curve

α is parameter of infiltration curve

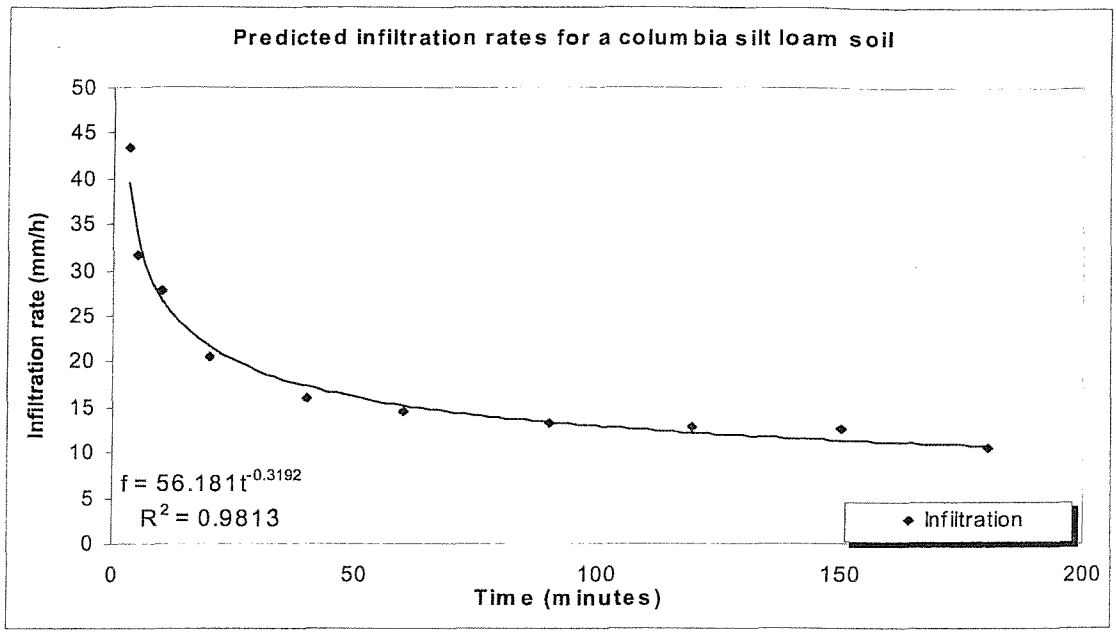

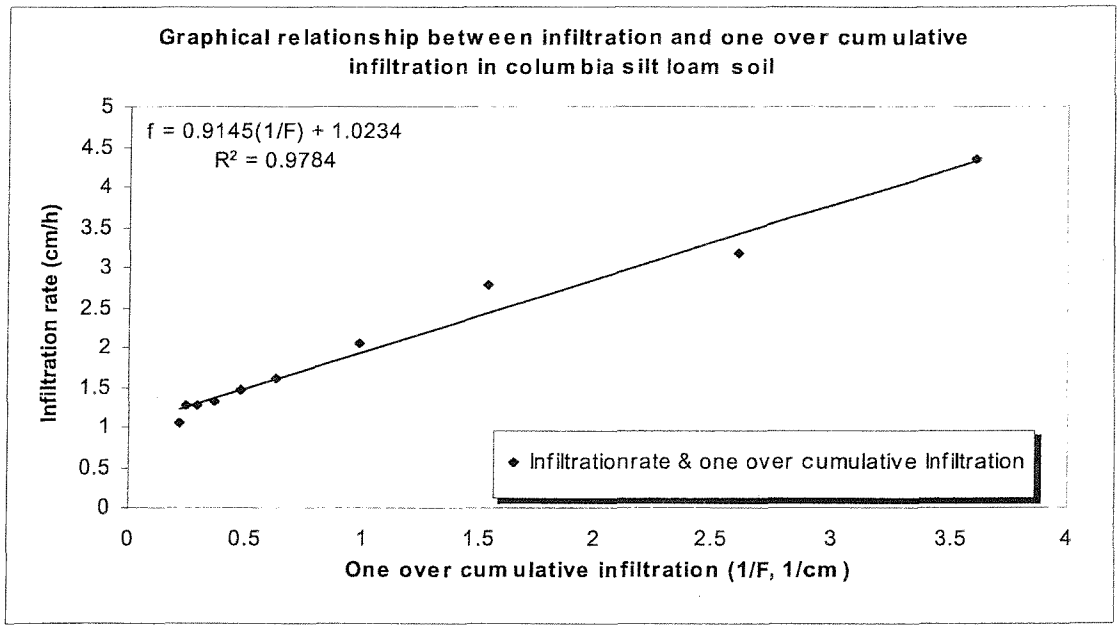

Fig. 7.2: Potential infiltration curve and graphical relationship between Infiltration and cumulative infiltration in Columbia silt loam soil

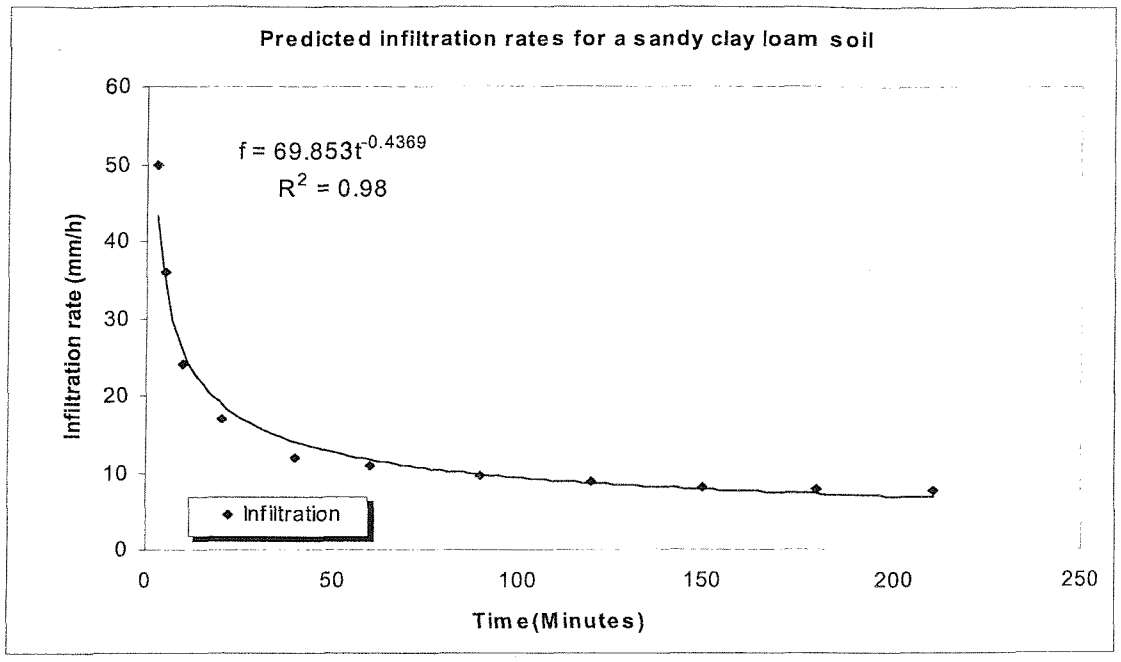

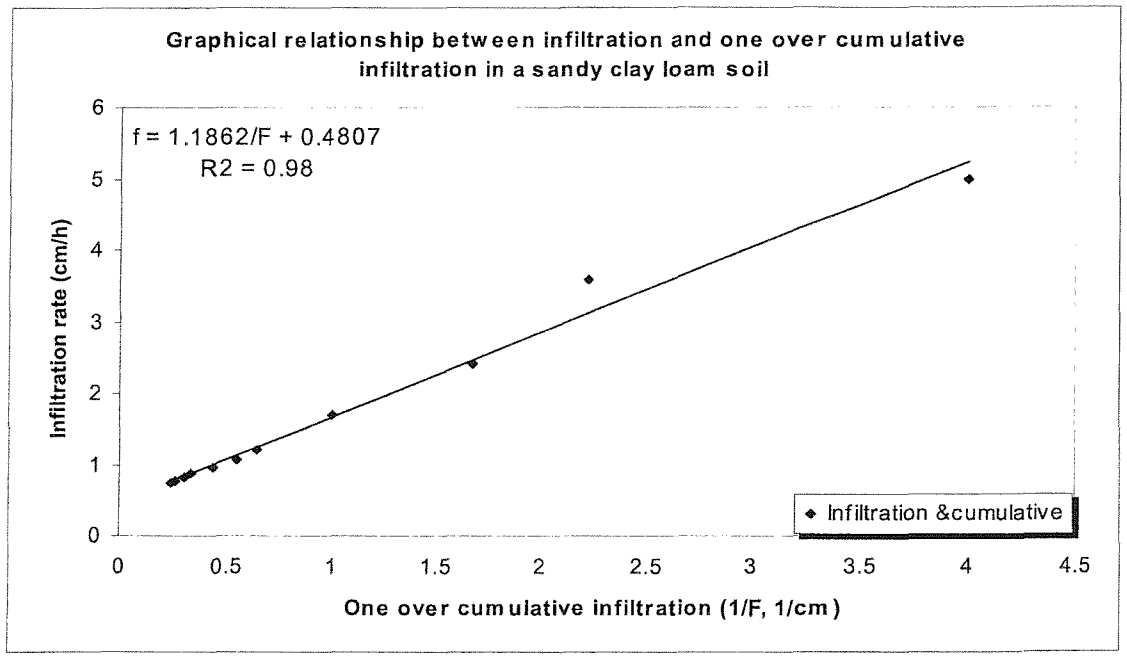

Fig. 7.3: Potential infiltration curve and graphical relationship between infiltration and cumulative infiltration in sandy clay loam soil

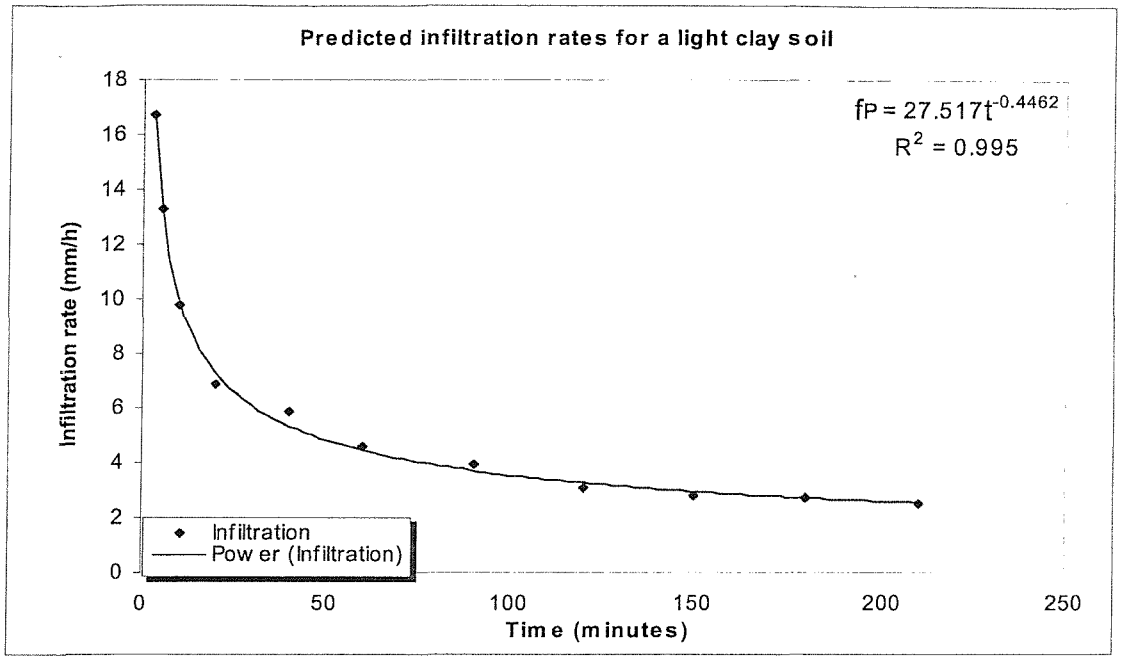

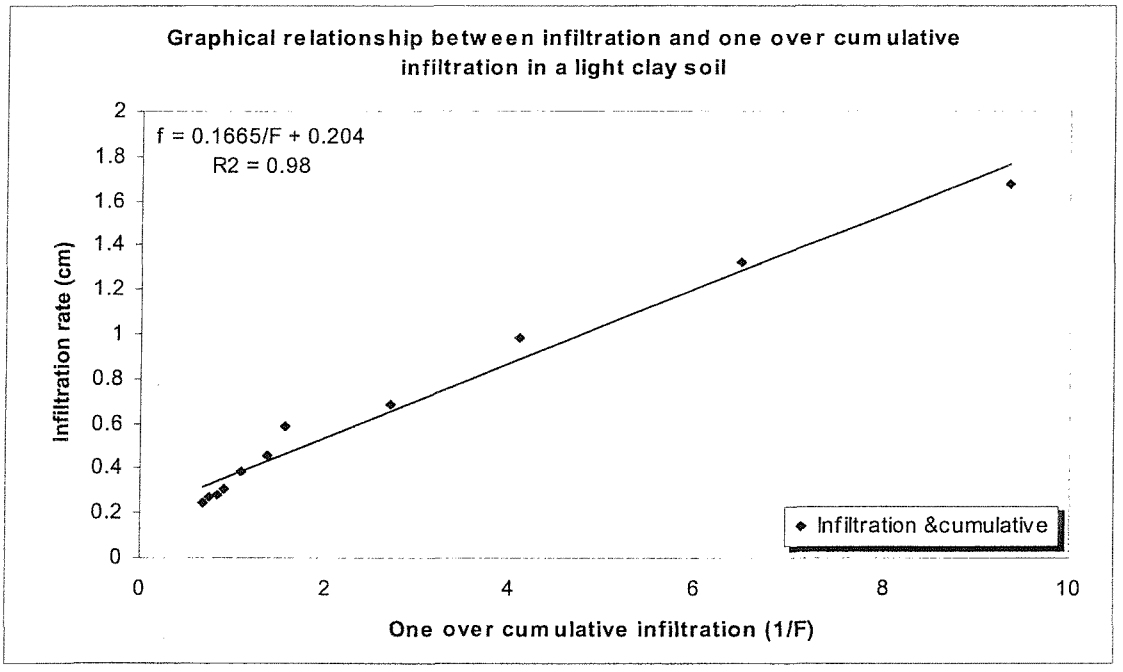

Fig 7.4: Potential infiltration curve and graphical relationship between infiltration and cumulative infiltration in light clay soil

Table 7.1: Experimental result of computation rainfall excess in Columbia silt loam and micro-catchment conditions

S1(2)	Computation of rainfall excess in a Columbia silt loam soil															
Time	R (t-int)	T-ste	T-cum	R (tste)	Ri (tste)	Rc (tste)	fini (t)	F	1/F	fpre (t)	tpre (t)	tdel	tact	fac(t)	Rexc	Σ Rexc
(min)	(mm)	(min)	(min)	(mm)	(mm/h)	(mm)	(mm)	(mm)	(1/mm)	(mm/h)	(min)	(min)	(min)	mm/h	mm	mm
1	2	3	4	5	6	7	8	9	10	11	12	13	14	15	16	17
0	0	0	0	0	0	0	0	0	0	0	0	0	0	0	0	0
10	1	10	10	1	6	1	1	1	1	102	0	0	0	0	0	0
11	5	5	15	2.5	30	3.5	2.5	3.5	0.29	36.4	0	0	0	0	0	0
	5	2	17	1	30	4.5	1	4.5	0.22	30.6	0	0	0	0	0	0
	5	0.5	17.5	0.25	30	4.75	0.25	4.75	0.21	29.5	0.86	16.6	0.86	29.5	0.004	0.004
	5	0.5	18	0.25	30	5	0.25	5	0.2	28.5	0.92	17.1	0.92	28.5	0.012	0.02
	5	0.5	18.5	0.25	30	5.25	0.25	5.25	0.19	27.7	0.99	17.5	0.99	27.7	0.02	0.04
	5	0.5	19	0.25	30	5.5	0.25	5.5	0.18	26.9	1.06	17.9	1.06	26.9	0.026	0.06
	5	0.5	19.5	0.25	30	5.75	0.25	5.75	0.17	26.1	1.12	18.4	1.12	26.1	0.032	0.09
	5	0.5	20	0.25	30	6	0.25	6	0.17	25.5	1.19	18.8	1.19	25.5	0.038	0.13
21	11.5	0.5	20.5	0.58	69	6.58	0.58	6.58	0.15	24.1	1.34	19.2	1.34	24.1	0.374	0.51
	11.5	0.5	21	0.58	69	7.15	0.58	7.15	0.14	23	1.49	19.5	1.49	23	0.383	0.89
	11.5	0.5	21.5	0.58	69	7.73	0.58	7.73	0.13	22.1	1.64	19.9	1.64	22.1	0.391	1.28
	11.5	0.5	22	0.58	69	8.3	0.58	8.3	0.12	21.3	1.78	20.2	1.78	21.3	0.398	1.68
	11.5	0.5	22.5	0.58	69	8.88	0.58	8.88	0.11	20.5	1.92	20.6	1.92	20.5	0.404	2.08
	11.5	0.5	23	0.58	69	9.45	0.58	9.45	0.11	19.9	2.06	20.9	2.06	19.9	0.409	2.49
	11.5	0.5	23.5	0.58	69	10	0.58	10	0.1	19.4	2.2	21.3	2.2	19.4	0.414	2.9
	11.5	0.5	24	0.58	69	10.6	0.58	10.6	0.09	18.9	2.33	21.7	2.33	18.9	0.418	3.32
	11.5	0.5	24.5	0.58	69	11.2	0.58	11.2	0.09	18.4	2.46	22	2.46	18.4	0.422	3.74
	11.5	0.5	25	0.58	69	11.8	0.58	11.8	0.09	18	2.58	22.4	2.58	18	0.425	4.17
	11.5	0.5	25.5	0.58	69	12.3	0.58	12.3	0.08	17.7	2.7	22.8	2.7	17.7	0.428	4.6
	11.5	0.5	26	0.58	69	12.9	0.58	12.9	0.08	17.3	2.82	23.2	2.82	17.3	0.431	5.03
	11.5	0.5	26.5	0.58	69	13.5	0.58	13.5	0.07	17	2.93	23.6	2.93	17	0.433	5.46
	11.5	0.5	27	0.58	69	14.1	0.58	14.1	0.07	16.7	3.04	24	3.04	16.7	0.435	5.9
	11.5	0.5	27.5	0.58	69	14.6	0.58	14.6	0.07	16.5	3.15	24.4	3.15	16.5	0.438	6.33
	11.5	0.5	28	0.58	69	15.2	0.58	15.2	0.07	16.3	3.25	24.7	3.25	16.3	0.44	6.77
	11.5	0.5	28.5	0.58	69	15.8	0.58	15.8	0.06	16	3.35	25.1	3.35	16	0.441	7.21
	11.5	0.5	29	0.58	69	16.4	0.58	16.4	0.06	15.8	3.45	25.6	3.45	15.8	0.443	7.66
	11.5	0.5	29.5	0.58	69	16.9	0.58	16.9	0.06	15.6	3.54	26	3.54	15.6	0.445	8.1
	11.5	0.5	30	0.58	69	17.5	0.58	17.5	0.06	15.5	3.63	26.4	3.63	15.5	0.446	8.55
31	11	0.5	30.5	0.55	66	18.1	0.55	18.1	0.06	15.3	3.72	26.8	3.72	15.3	0.422	8.97
	11	0.5	31	0.55	66	18.6	0.55	18.6	0.05	15.2	3.8	27.2	3.8	15.2	0.424	9.39
	11	0.5	31.5	0.55	66	19.2	0.55	19.2	0.05	15	3.88	27.6	3.88	15	0.425	9.82
	11	0.5	32	0.55	66	19.7	0.55	19.7	0.05	14.9	3.96	28	3.96	14.9	0.426	10.2
	11	0.5	32.5	0.55	66	20.3	0.55	20.3	0.05	14.8	4.04	28.5	4.04	14.8	0.427	10.7
	11	0.5	33	0.55	66	20.8	0.55	20.8	0.05	14.6	4.11	28.9	4.11	14.6	0.428	11.1
	11	0.5	33.5	0.55	66	21.4	0.55	21.4	0.05	14.5	4.18	29.3	4.18	14.5	0.429	11.5
	11	0.5	34	0.55	66	21.9	0.55	21.9	0.05	14.4	4.25	29.7	4.25	14.4	0.43	12
	11	0.5	34.5	0.55	66	22.5	0.55	22.5	0.04	14.3	4.32	30.2	4.32	14.3	0.431	12.4
	11	0.5	35	0.55	66	23	0.55	23	0.04	14.2	4.39	30.6	4.39	14.2	0.432	12.8
	11	0.5	35.5	0.55	66	23.6	0.55	23.6	0.04	14.1	4.45	31	4.45	14.1	0.432	13.3

	11	0.5	36	0.55	66	24.1	0.55	24.1	0.04	14	4.52	31.5	4.52	14	0.433	13.7
	11	0.5	36.5	0.55	66	24.7	0.55	24.7	0.04	13.9	4.58	31.9	4.58	13.9	0.434	14.1
	11	0.5	37	0.55	66	25.2	0.55	25.2	0.04	13.9	4.64	32.4	4.64	13.9	0.434	14.6
	11	0.5	37.5	0.55	66	25.8	0.55	25.8	0.04	13.8	4.7	32.8	4.7	13.8	0.435	15
	11	0.5	38	0.55	66	26.3	0.55	26.3	0.04	13.7	4.75	33.2	4.75	13.7	0.436	15.4
	11	0.5	38.5	0.55	66	26.9	0.55	26.9	0.04	13.6	4.81	33.7	4.81	13.6	0.436	15.9
	11	0.5	39	0.55	66	27.4	0.55	27.4	0.04	13.6	4.86	34.1	4.86	13.6	0.437	16.3
	11	0.5	39.5	0.55	66	28	0.55	28	0.04	13.5	4.92	34.6	4.92	13.5	0.437	16.7
	11	0.5	40	0.55	66	28.5	0.55	28.5	0.04	13.4	4.97	35	4.97	13.4	0.438	17.2
41	6.5	0.5	40.5	0.33	39	28.8	0.33	28.8	0.03	13.4	5	35.5	5	13.4	0.213	17.4
	6.5	0.5	41	0.33	39	29.2	0.33	29.2	0.03	13.4	5.03	36	5.03	13.4	0.214	17.6
	6.5	0.5	41.5	0.33	39	29.5	0.33	29.5	0.03	13.3	5.06	36.4	5.06	13.3	0.214	17.8
	6.5	0.5	42	0.33	39	29.8	0.33	29.8	0.03	13.3	5.09	36.9	5.09	13.3	0.214	18
	6.5	0.5	42.5	0.33	39	30.1	0.33	30.1	0.03	13.3	5.12	37.4	5.12	13.3	0.214	18.2
	6.5	0.5	43	0.33	39	30.5	0.33	30.5	0.03	13.2	5.14	37.9	5.14	13.2	0.215	18.5
	6.5	0.5	43.5	0.33	39	30.8	0.33	30.8	0.03	13.2	5.17	38.3	5.17	13.2	0.215	18.7
	6.5	0.5	44	0.33	39	31.1	0.33	31.1	0.03	13.2	5.2	38.8	5.2	13.2	0.215	18.9
	6.5	0.5	44.5	0.33	39	31.4	0.33	31.4	0.03	13.1	5.23	39.3	5.23	13.1	0.215	19.1
	6.5	0.5	45	0.33	39	31.8	0.33	31.8	0.03	13.1	5.25	39.7	5.25	13.1	0.216	19.3
	6.5	0.5	45.5	0.33	39	32.1	0.33	32.1	0.03	13.1	5.28	40.2	5.28	13.1	0.216	19.5
	6.5	0.5	46	0.33	39	32.4	0.33	32.4	0.03	13.1	5.3	40.7	5.3	13.1	0.216	19.8
	6.5	0.5	46.5	0.33	39	32.7	0.33	32.7	0.03	13	5.33	41.2	5.33	13	0.216	20
	6.5	0.5	47	0.33	39	33.1	0.33	33.1	0.03	13	5.36	41.6	5.36	13	0.217	20.2
	6.5	0.5	47.5	0.33	39	33.4	0.33	33.4	0.03	13	5.38	42.1	5.38	13	0.217	20.4
	6.5	0.5	48	0.33	39	33.7	0.33	33.7	0.03	12.9	5.4	42.6	5.4	12.9	0.217	20.6
	6.5	0.5	48.5	0.33	39	34	0.33	34	0.03	12.9	5.43	43.1	5.43	12.9	0.217	20.8
	6.5	0.5	49	0.33	39	34.4	0.33	34.4	0.03	12.9	5.45	43.5	5.45	12.9	0.218	21.1
	6.5	0.5	49.5	0.33	39	34.7	0.33	34.7	0.03	12.9	5.48	44	5.48	12.9	0.218	21.3
	6.5	0.5	50	0.33	39	35	0.33	35	0.03	12.8	5.5	44.5	5.5	12.8	0.218	21.5
51	1	10	60	1	6	36	1	36	0.03	12.8	0	0	0	0	0	21.5

7.2.5 Rainfall runoff regression relationship in a micro-catchment system

The procedure for calculating potential excess runoff developed in section 7.2 was applied to rainfall intensity data gathered from a dry area of the north of Nigeria. The data gave rainfall every ten minutes for 22 storms. The potential runoff curve calculated for sandy clay loam, Columbia silt loam and light clay assigned data from graphs 7.5, 7.6 and 7.7. An example of the calculation of intermediate output for Columbia silt loam is given in Appendix B. The output data of predicted excess rainfall for every one of the 22 storms are summarised graphically for every soil type in figures 7.5, 7.6 and 7.7.

It can be seen from this data that a linear relationship exists between storm size and potential runoff and that statistical analysis of this relationship shows not only that the linear

relations are a significant fit but they are also a very good fit to the soil in a micro-catchment system.

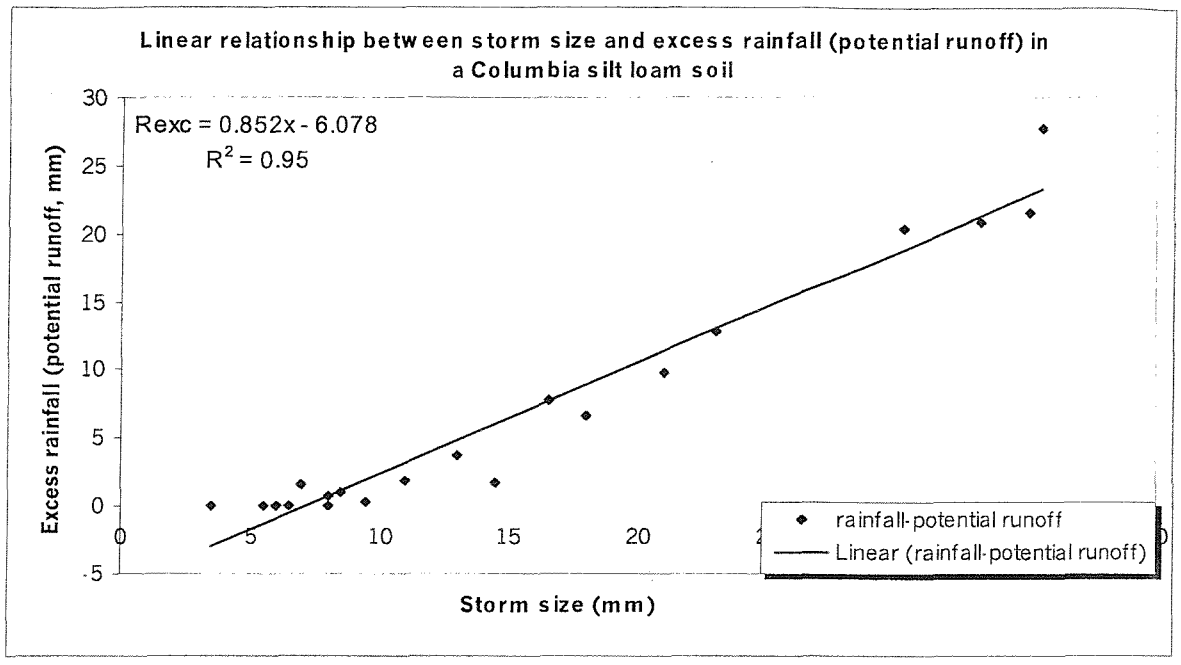

Fig: 7.5. Relationship between storm size and rainfall excess (Potential runoff) on a Columbia silt loam soil in a micro-catchment system

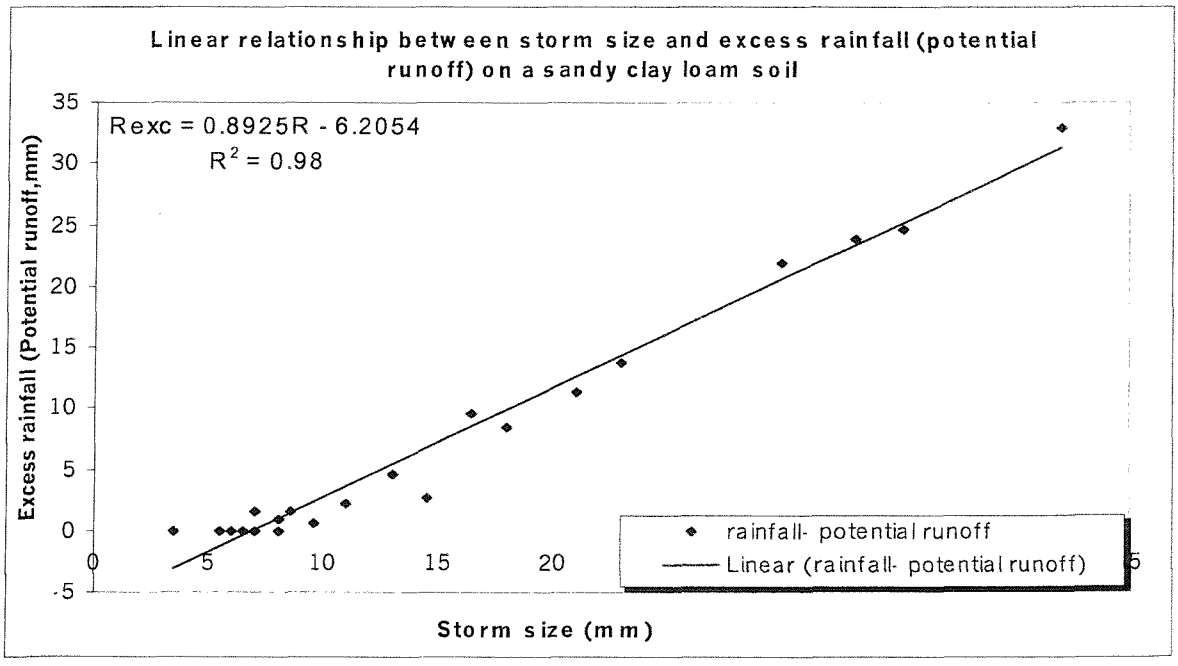

Fig: 7.6. Relationship between storm size and rainfall excess (Potential runoff) on a sandy clay soil in a micro-catchment system

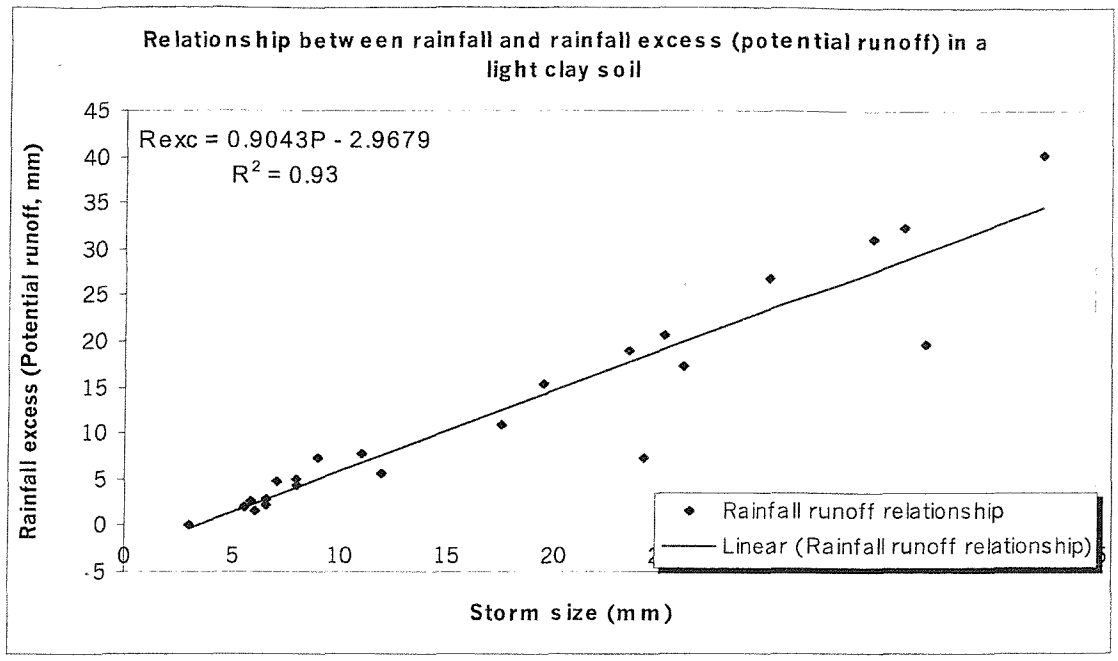

Fig: 7.7. Relationship between storm size and rainfall excess (Potential runoff) on a light clay soil in a micro-catchment system

7.3 Effect of size and slope of catchment on runoff generation in a micro-catchment system

To calculate actual micro-catchment runoff from potential runoff it is essential to consider the effect of catchment size and catchment slope. The relationship between potential runoff and catchment slope and size has been developed using experimental data collected by Sharma (1986) and Sharma et al (1982), in the arid Northwest of India on the sandy loam soils of the central arid zone Research Institute, Jodhpur for a period of seven years from 1975 to 1981. The data was obtained from catchments having suitable combinations of catchment slope 0.5%, 5% and 10% and catchment slope length, which is a function of micro-catchment size. The relationship of catchment size to infiltration basin size for a particular slope is

$$h.A_b = e.P.A_R$$

Where:

e is runoff coefficient (function of slope and micro-catchment size)

P is rainfall (mm)

A_R is runoff area (m^2)

h is depth of runoff collected in infiltration basin (cm), and

A_b is infiltration basin area (m^2)

7.3.1 Description of numerical results of analysing slope and size of a micro-catchment

The two general relationships between runoff over 7 years of a micro-catchment for different catchment slopes and slope lengths are given in figures 7.8 and 7.9. As can be seen, during the first years, the generated runoff was smaller than in the latter years; this was the result of the formation of a soil crust, which formed over time in the runoff area. Over the first seven years, the increases were approximately linear, but clearly they must level off over time. The value of the correlation coefficient in all micro-catchment sizes, slopes and lengths of slopes approached between 0.97-0.99 for 0.5 percent of slope and 0.78-0.98 for 5 percent slope of runoff area in the period of 7 years.

These relationships are summarised in table 7.2. The mean runoff efficiency as a percentage of rainfall increased from the minimum of 13.6 to 37%, 37.1 to 45.4% and 25.2 to 46.6% at 0.5, 5 and 10% slopes, respectively. It can also be seen from table 7.2 that the % runoff increases from 34.3 to 55 percent (with average 40.5%) for 5.12 metres length, 26.1 to 49.9 percent (average 38.4%) for 7 metres length, 25.6 to 38.7 percent average for 8.5 meter length.

In table 7.3, an investigation was carried out to establish the relationship between potential runoff and actual runoff to establish the runoff efficiency from the relationship between potential runoff and micro-catchment size in a specific slope of runoff area. As can be seen from figure 7.12 three general regression relationships between runoff efficiency and micro-catchment size for three slopes can be established (table 7.3).

In order to estimate runoff efficiency from potential runoff the linear regressions of figure 7.12 are moved to a parallel line of figure 7.13 for a range of 0.5-10 % slope conditions. The estimated runoff is experienced as a fraction of hundred percent to given a coefficient, b.

Table 7.2: Mean annual runoff-rainfall ratio (%) at different slopes and different micro-catchment lengths.

year	Slope: 0.5%	Slope: 5%	Slope: 10%		Length 5.12 M	Length 7 M	Length 8.5 M	Length,10.7 5 M	Length 14.5 M
1	13.6	35.3	25.2		34.3	26.1	25.6	22.6	15
2	19.2	36.8	34.9		35.1	34.4	28.2	26.5	25.3
3	20.2	37.8	35.2		35.2	35.1	28.7	27.8	25.8
4	23.3	39.8	38.3		37.8	37.1	31.8	28.8	28.1
5	25.7	40.7	38.5		41.7	39.9	35.5	32.9	32.3
6	29.6	41.2	45.2		46.5	46.1	35.6	34.9	34.7
7	37.1	45.4	46.6		55	49.9	38.7	36.5	35
Mean	24.1	39.57143	37.7		40.8	38.4	32	30	28

Table 7.3: Relationship between micro-catchment size and runoff efficiency (% of rainfall) and runoff efficiency as a percent of potential runoff

micro-catchment size (m^2)	Runoff (%of rainfall)	Runoff (%of rainfall)	Runoff (%of rainfall)	Average Runoff efficiency (between range 0.5-10%)	
	0.50%	5%	10%	Runoff (%of rainfall)	Runoff (% of Potential runoff)
252	32.1	46.9	45.1	41.37	61.77
324	31.6	40.9	43.7	38.73	57.84
360	26.6	37.6	42.1	35.43	52.91
396	20.6	36	34	30.2	45.09
432	13.3	34.9	25.1	24.43	36.48

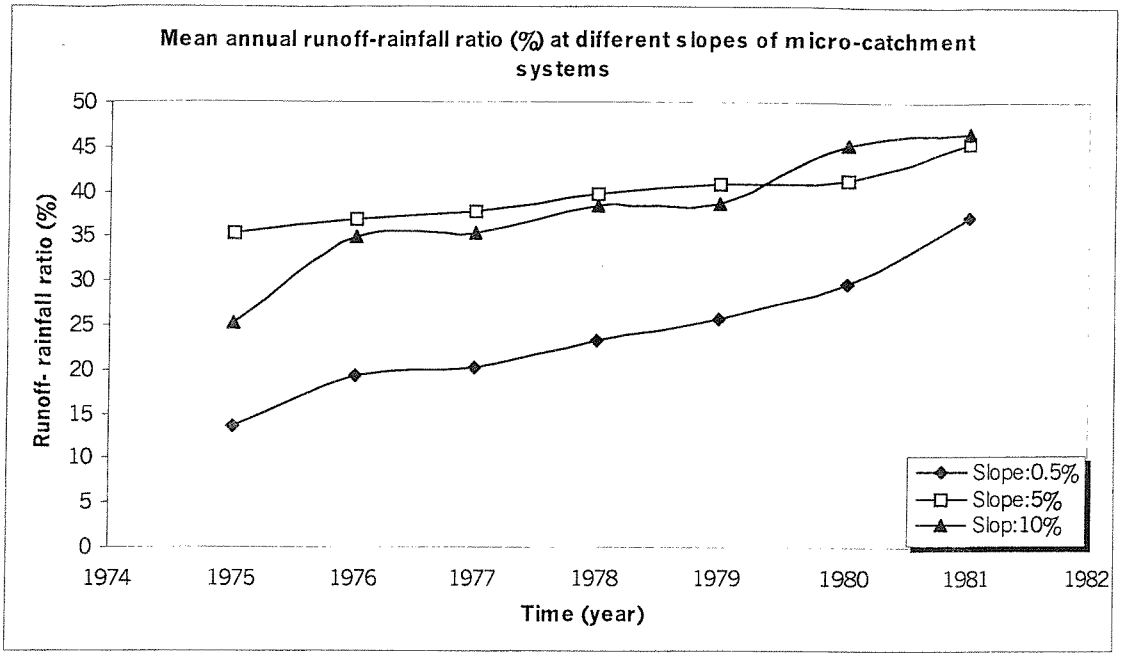

Figure 7.8: A general relationship between time and mean annual runoff-rainfall ratio (%) at different slopes in runoff areas of a micro-catchment system.

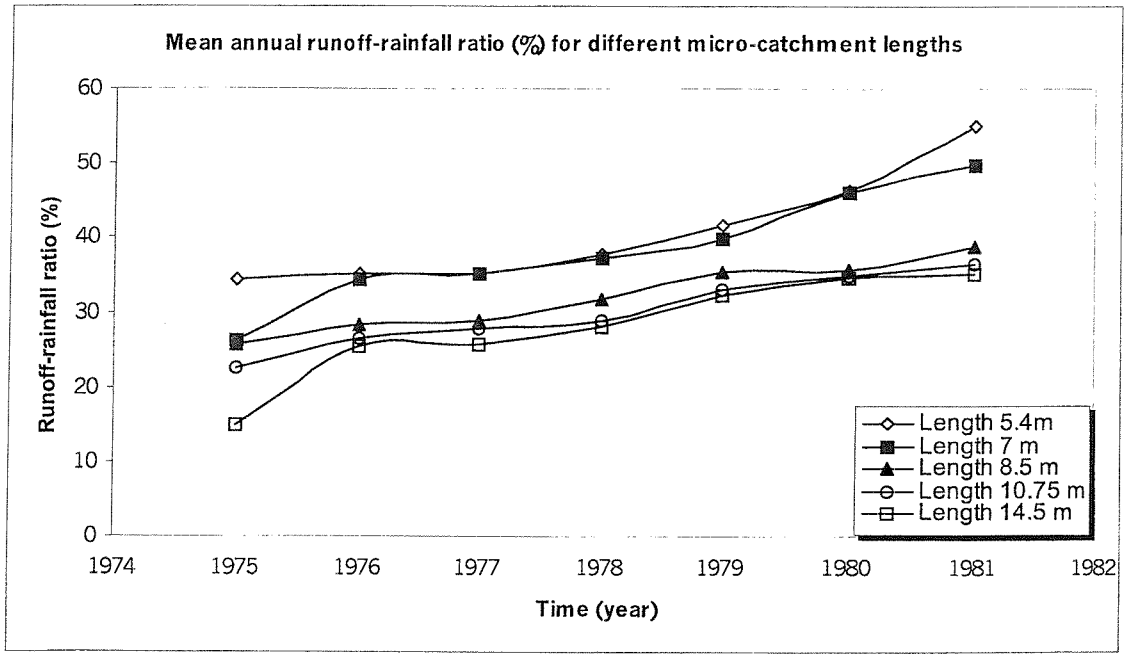

Figure 7.9: A general relationship between time and mean annual runoff-rainfall ratio (%) at different micro-catchment lengths.

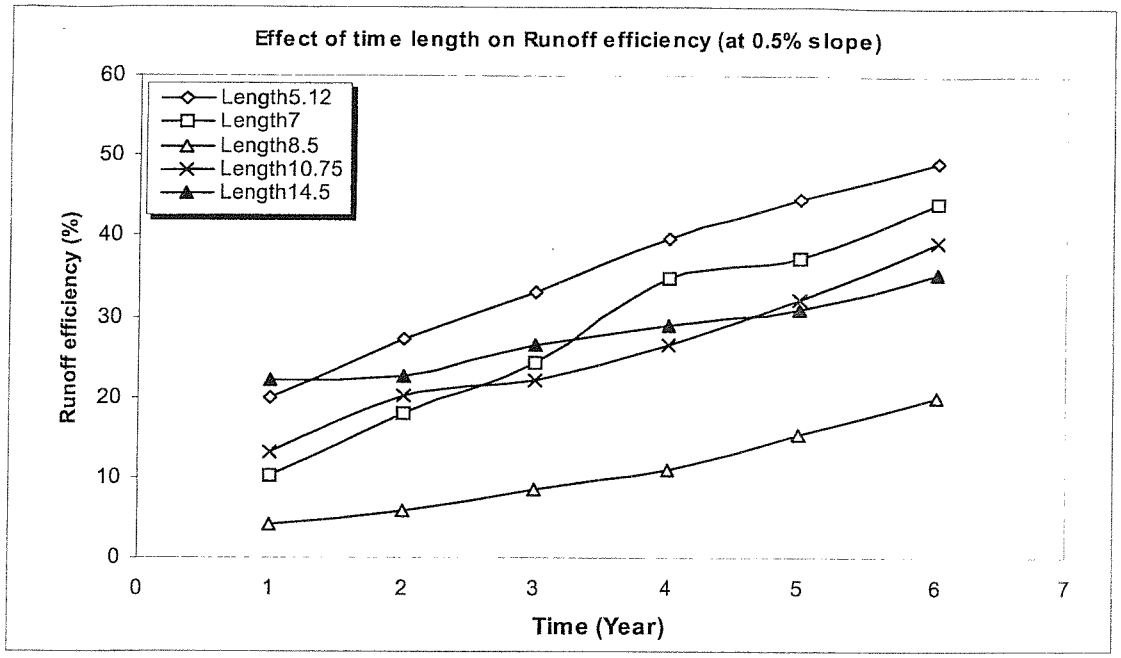

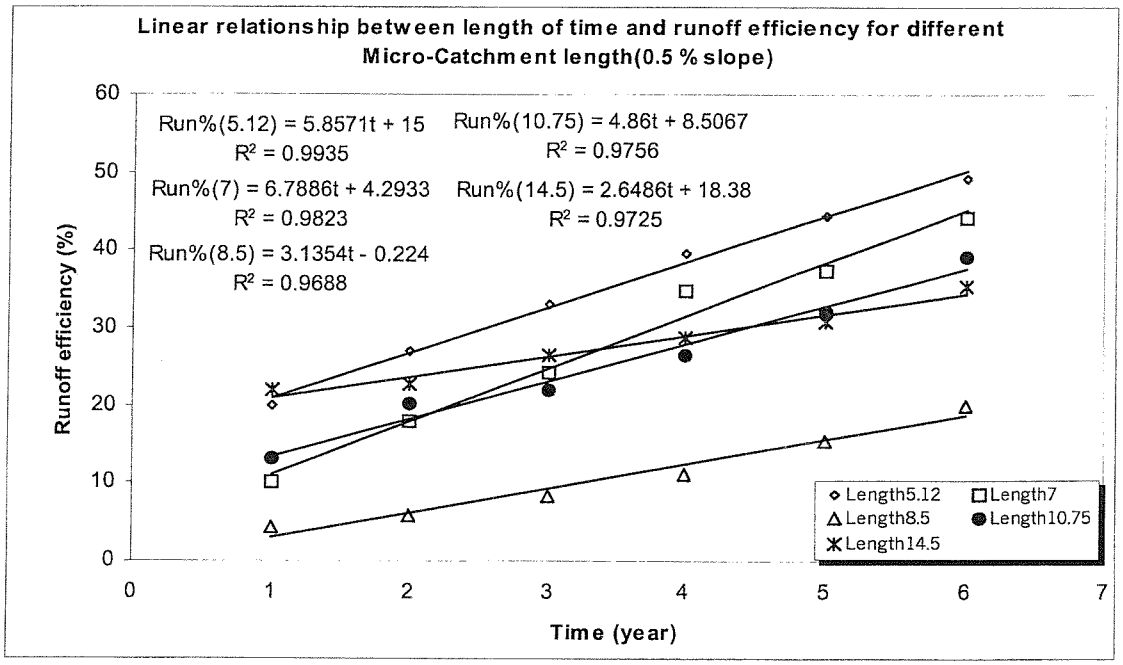

Figure 7.10: Effect of time length on runoff efficiency and linear relationship between time length and runoff efficiency in 0.5 % slope and different lengths of micro-catchment system.

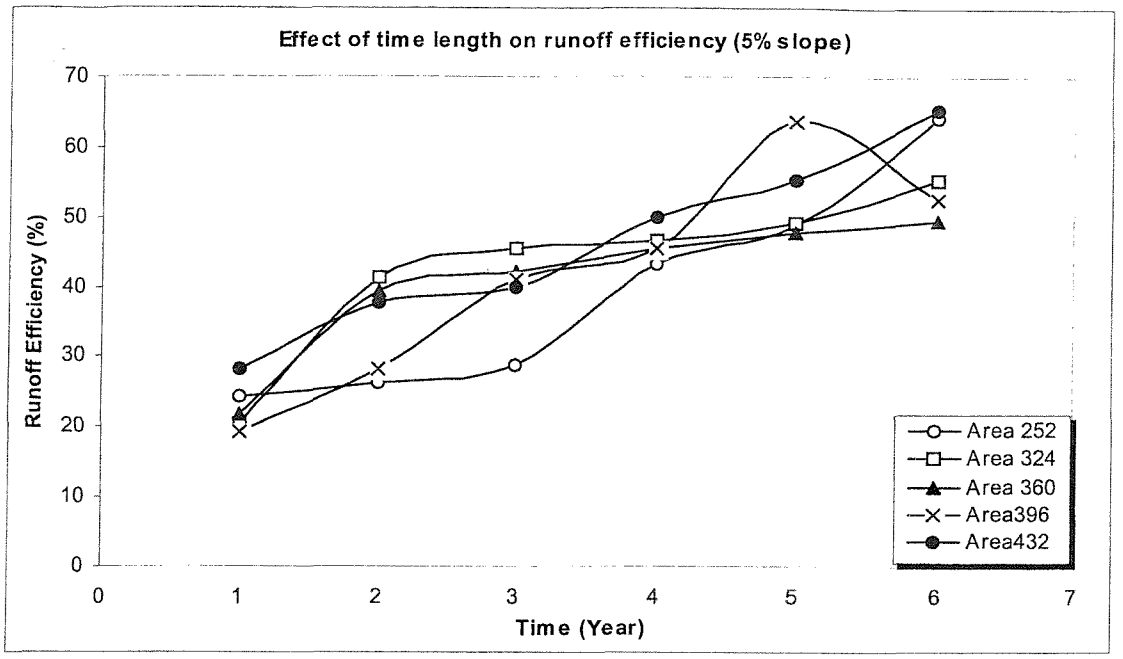

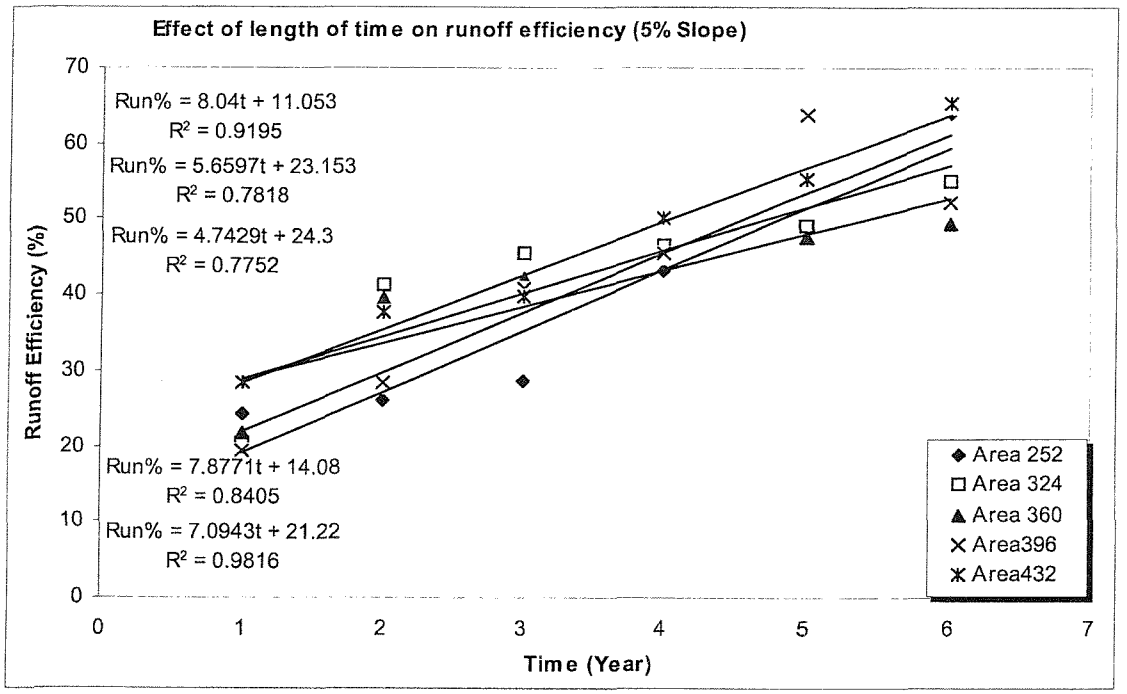

Figure 7.11: Effect of time length on runoff efficiency and linear relationship between time length and runoff efficiency in 5 % slope and different micro-catchment areas.

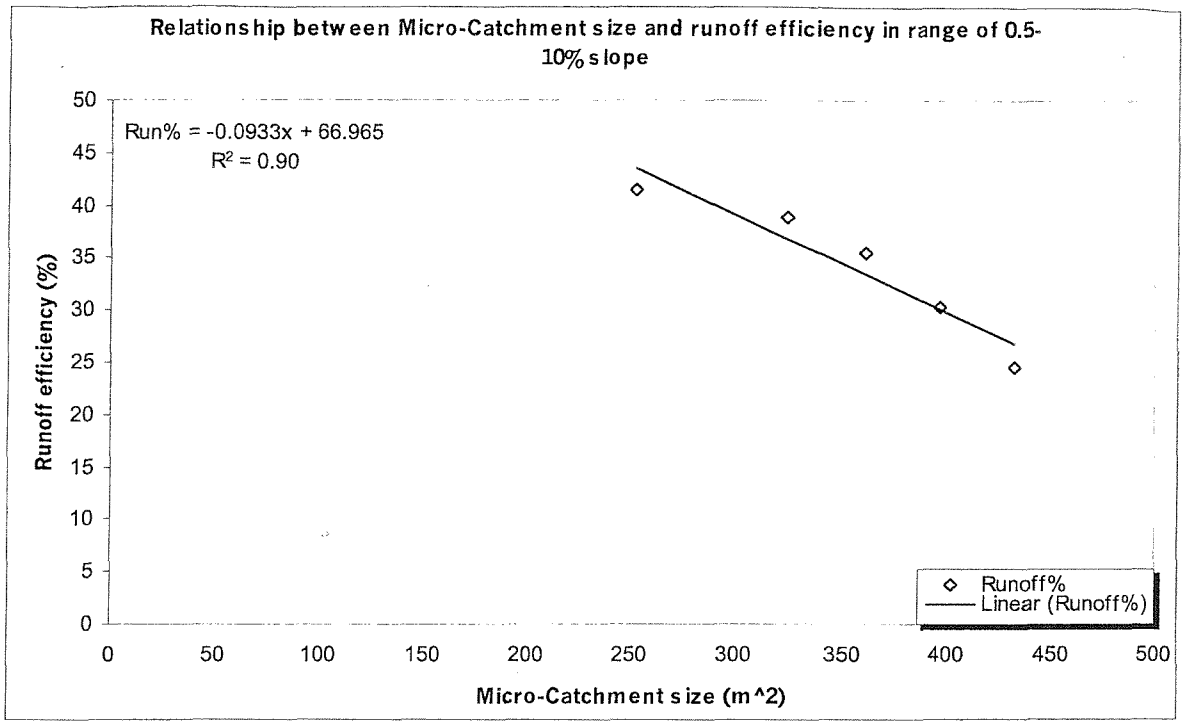

Figure 7.12: Relationship between runoff efficiency (% of rainfall) and micro-catchment size in a specific range of 0.5-10% slope

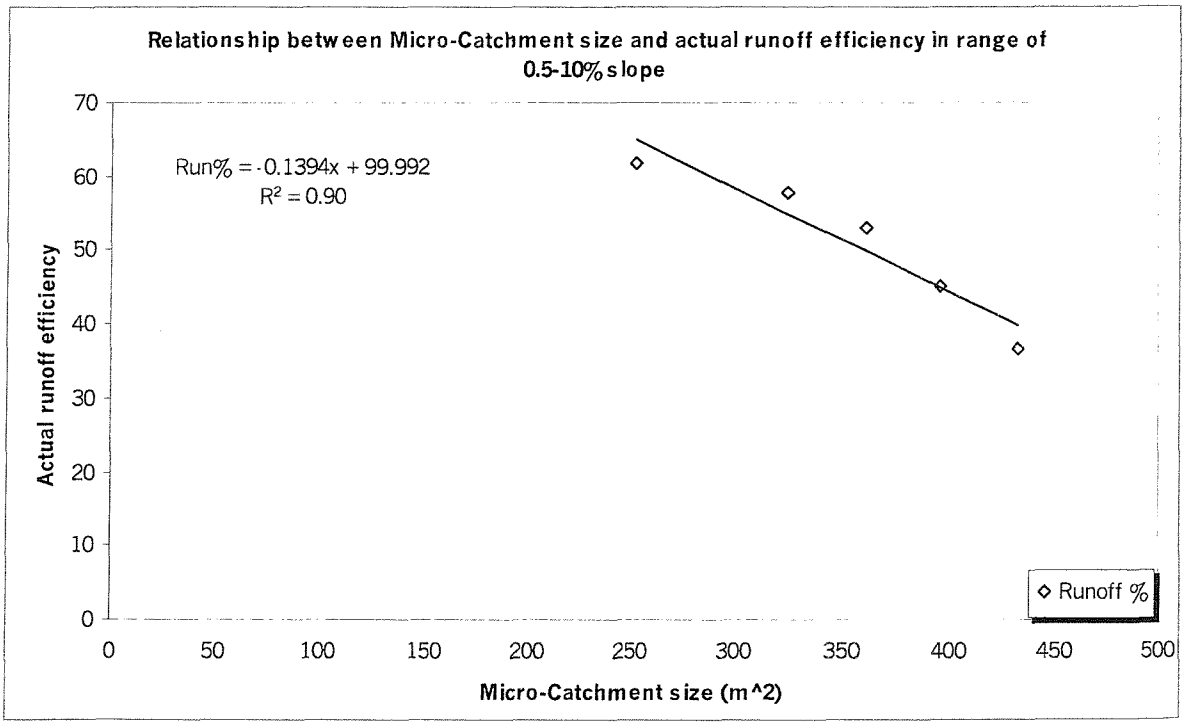

Fig 7.13: Relationship between micro-catchment size and runoff efficiency (% of potential runoff) in a specific range of 0.5-10% slope

7.4 Discussion

A hydrological rainfall runoff sub model was developed to estimate potential runoff in Micro-Catchment systems conditions. With the values of the infiltration parameters obtained graphically, the excess rainfall can be computed for each event. The cumulative runoff is computed for each storm size, using rainfall excess in each time interval for multiple events during a storm period (see appendix B). The cumulative rainfall and cumulative potential runoff obtained from 22 storms were used to establish a regression relationship between rainfall and potential runoff. The actual runoff was derived from field data from India.

An important feature of the model is the demonstration that reasonable results are obtained (Figure 7.5, 7.6 and 7.7) when it is assumed that the calculation of soil water infiltrated and the excess rainfall process depend on the actual infiltration rate in the upper soil layer. The second particular important feature of the model is to show the relationship between rainfall intensity, infiltration and excess rainfall based on the actual infiltration rate, instead of representing the infiltration capacity as a function of time.

The model has the following advantages and limitations:

(1) With the estimated initial values of A and B (two main parameters of the model, estimated from figures 7.2, 7.3 and 7.4), the excess rainfall hyetograph can be estimated easily for any event, using soil surface infiltration data and the regression relationship between infiltration and one over cumulative infiltration. The soil infiltration can be estimated, based on laboratory or field observations.

(2) Model parameters (A and B) depend on the soil properties and can be taken as constant for a fixed runoff area of a micro-catchment system. B is the saturated hydraulic conductivity of the soil and A depends on capillary potential and antecedent soil moisture, which can be estimated easily by soil infiltration data. The cumulative infiltration and one over cumulative infiltration depend on the soil properties and can be taken as constant for a fixed micro-catchment for a specific soil.

(3) Threshold values of storm rainfall for generation of runoff is the most important limitations of model that depends on soil type and storm size. Testing of 22 storm size on

three soil type shows that minimum storm size needed to generate runoff are between 3 mm for light clay and 6 mm for sandy clay loam and coulomb silt loam soil.

Chapter 8: Analysis of water balance in a micro-catchment system

8.1 Introduction

Soil type, meteorological conditions and system operation characteristics of a micro-catchment affect the design of a micro-catchment system. This chapter examines how these factors can be taken into account by a developed micro-catchment design.

The stochastic modelling of daily rainfall may be considered in two components, namely the temporal distribution of rainfall during a day and the number of rainy days. Ideally long sequences of historic data are needed for modelling of most semi-arid and arid areas, unfortunately, long sequences of data are scarce and short sequences are the norm. To allow these short sequence of say 10 years to be extended, it has been found that sequences of wet and dry days can be extended using a synthetic transition matrix of the Moarkov chain (Jimoh and Webster, 1996., Bogardi., et al. 1988).

This chapter uses extended sets of Iranian data and investigates, using the model, the availability of water resources for cropping within micro-catchments within the agroclimatic zones of the data sets.

8.2 Water balance evaluation

The water balance components considered in the model are given in section 4.6 (of chapter 4). The inflow to the infiltration basin of a micro-catchment system consists of the total water originating from precipitation in the infiltration basin and generated runoff from runoff area. The losses consist of water leaving the infiltration basin through evaporation, transpiration (root extraction), surface runoff, and deep percolation below the root zone as given in equation 4.51(chapter 4). The potential evapotranspiration model, (ET_p), given in appendix A, was used to calculate evapotranspiration (ET_p) using data from three Iranian meteorological stations. These calculations are given in Appendix A. The total amount of water available is the same as the depth of water available at the surface of the infiltration basin.

In a micro-catchment irrigation system, water is supplied from two major sources. The water resource can be considered as uncontrolled direct precipitation in the infiltration basin plus water from runoff collected from a runoff area and temporarily stored on the surface of the infiltration basin. This runoff supply is a vital source in meeting crop demand in arid regions. Thus the objective of designing a micro-catchment system is to ensure that the crop water requirement can be met throughout the growing season from water stored within the soil of the infiltration basin. To achieve this there is clearly an optimum size of runoff area to the infiltration area for any given set of environmental variables (soil and crop types).

8.2.1 Methodology for daily rainfall pattern generation

Using limited historical data for any given location, the daily pattern of rainfall values at different probability levels can be generated. For this purpose, a two stage, first order Markov chain model is used to determine whether it will be wet or dry on a given day (Buishand 1978, Stern, 1980, and Sen Zekai, 1980). Two transitional probabilities are needed for this model. The first is the probability that tomorrow will be wet if today is dry and the second is the probability that tomorrow will be wet if today is wet.

Let a day with rainfall depth equal to or more than a threshold value be designated as a wet day (with binary code one) and one with no rainfall or less than a threshold value be designated as a dry day (with binary code zero). A wet (dry) event refers to a sequence of consecutive wet (or dry) dates. A sequence of wet and dry days Q, is obtained from the daily rainfall record;

$$Q = X_1, X_2, X_3, \ldots\ldots X_{n-1}, X_n \qquad (8.1)$$

Where:

X_1 , X_2 , X_3 , *or* X_n is either zero or one and the

Suffixes 1, 2, ….n denote the days when the records are taken.

The sequence is said to fit a Markov Chain model if the variable X_1 depends on the previous values, X_{t-1} , X_{t-2}, ...The order of the Chain is the smallest positive integer that satisfies equation 8.1 for all n values (Jimoh and Webster, 1996).

The transition probability P_{ab}(t), is estimated as

$$P_{ab}(t) = \Pr ob.(X_t = b / X_{t-1} = a) = \frac{number.of, years, X_t = b, and, X_{t-1} = a}{number.of.years, X_{t-1} = a} \qquad (8.2)$$

Where: P_{ab} is the probability of a day :

Being wet (b=1) given that the previous day was wet (a = 1)

Being dry (b=0) given that the previous day was wet (a = 1)

Being wet (b=1) given that the previous day was dry (a = 0)

Being dry (b=0) given that the previous day was dry (a = 0)

X_t equals number of years that today has the condition of b (b = 0, 1), X_{t-1} equals number of years that previous day has got the condition of a (a = 0, 1)

There is general agreement that the first-order Markov model is easy to apply (e.g. Buishand 1978, Stern and Coe 1984, Woolhider et al, 1993, Sharma, 1996, Zhan-Qian and Berliner, 1999). In the first order Markov model the probability of rainfall on any day depends only on whether the previous day is wet or dry. In this model, based on daily rainfall records, a sequence of 0's and it's depending on the days with no rain and rain respectively is obtained. The transition probabilities of P_{11} and P_{00} for each day of the year are defined as

$$P_{11}(t) = \frac{number.of.years.that.today.and.the.previous.day.is.wet}{number.of.years.that.previous.day.is.wet} \qquad 8.3$$

$$P_{oo}(t) = \frac{number.of.years.that.today.and.previous.day.is.dry}{number.of.years.that.previous.day.is.dry} \qquad 8.4$$

Where t is equal to 1,.....365. The transitional probability is then used to generate a sequence of wet and dry days as described by Jimoh and Webster (1996). During the generation procedure, the state of the first day (for a first order) and first two Julian days (for a second order) of the year are assumed to be 0. That is, y_1=0 for a first order, representing a

dry day (assumed). This assumption is not far from the reality at the stations considered. The state of the remaining days is obtained by generating a uniformly distributed random number, $R_u(t)$ in the interval 0 to 1 using the RAND() command in Excel 7 (Excel 1997) spreadsheet and considering the conditions in equations 8.5. In this way a sequence of 0's and 1's is obtained. The sequence is then used to generate rainfall amount. Clearly, whenever a zero occurs, the corresponding rainfall amount is zero, but when a 1 occurs, a way of introducing a value, which represents a rainfall amount, is needed. This is discussed in the next section.

To simulate the rainfall amount in three rain gage stations in Iran (Shiraz, Esfahan and Kashan) The probability distribution function (pdf) of the exponential distribution is written as follows by a general variable X, or daily rainfall event (the numerical result is shown in appendix D),

$$f_x(x) = \lambda e^{-\lambda x} \qquad \text{For } x \geq 0, \lambda > 0 \qquad (8.5)$$
$$= 0 \text{ otherwise.}$$

For the same conditions, the cumulative distribution function (cdf) based on Kottegoda et al (1998) is

$$F_x(x) = P(x_1 \leq x) = 1 - e^{-\lambda x} \qquad (8.6)$$

Where:

λ is a parameter = inverse of daily rainfall

The relative frequencies are computed by dividing the number of occurrences in each class of rainfall by the total number of rain occurrences (See appendix D, Tables D.1, D.2, D.3 and figures D.1, D.2 and D.3). The expected relative frequency in each class is then calculated from the equation:

$$Fx_i = \Delta x_i * p_A(x_i) \qquad (8.7)$$

Where:

x_i is the midpoint of class interval, Δx = rain amount in interval, and

$p_A(x_i)$ is the exponential distribution of rainfall given by equation 8.3 (Haan, 1979).

In order to check the quality of precipitation, the cumulative probability of the observed and theoretical rainfall expected for the three stations in Iran is plotted in Appendix D4, D5 and D6.

Random observations may be generated from probability distributions by making use of the fact that the cumulative probability function for any continuous variable is uniformly distributed over the interval 0 to1 (Zali. A., et al. 1994. Kottegoda, 1980). Thus for any variable Y with probability density function $P_Y(y)$, in equation 8.8 is a uniform distributed over 0 and 1.

$$P_Y(y) = \int_{-\infty}^{y} P_Y(x)dx \qquad (8.8)$$

A procedure for generation of a random number with value y from $P_Y(y)$ is

1. Select a random number R_u from a uniform distribution in interval (0,1).
2. Set $P_Y(y) = R_u$ in equation 8.8
3. Solve for y.

In this study, in order to obtain a rainfall amount for a wet day for the three climatic stations in Iran, having exponential distribution with mean and standard deviation equal to the historic rainfall, the following steps were followed.

A uniformly distributed random number R_u in the interval of 0 to 1 is generated.

B parameter of the exponential distribution (λ) is obtained using the mean of wet days in the historical data.

C by having R_u, λ and using the following relationship between rainfall (x) and probability (or R_u, as a randomly number between 0 and 1), the value of rainfall generated is shown below.

$$P = 1 - e^{-\lambda x} \qquad 0<P<1 \tag{8.9}$$

$$e^{\lambda x} = 1 - P, \ldots\ldots\ldots\ldots\ldots\ldots \lambda x = LN(1-P) \tag{8.10}$$

$$x = -\frac{1}{\lambda} LN(1-P) \tag{8.10.a}$$

Where:

P as described in steps 2 equals to R_u (between 0 and 1).

8.2.2 Generation of data

To generate daily rainfall series requires both the occurrence and the magnitude of the historic rainfall at each station. In this study, 10 years of data has been used to generate the parameters as outlined above as well as generating daily rainfall values. Then 100 sets of Z year's data generated using the methods discussed above, where Z is the length (in years) of the historical record used to determine the transition probabilities. The characteristics of the sequence that is monthly number of wet days and monthly values of rainfall were determined. This procedure was repeated Z times, where Z was the length (in years) of the historical data (in this study Z = 10 years). The average monthly values of 100 sets of Z year's data were obtained both for occurrence and magnitudes, as suggested by Jimoh and Webster (1996). The generated data are compared with historic data, whose results are presented in Figures 8.1 and 8.2 in appendix D7 and D8. To show the degree of divergence of generated data from the historical values objective function, X (Error, %) was calculated. Equation 8.11 defines the objective function. It can clearly be seen from appendix D, tables 7 and 8, that the data clearly shows good agreement between the model & relative results.

$$X = 100 * \frac{\sum_{i=1}^{k} \sqrt{(O_i - E_i)^2}}{\sum_{i=1}^{k} O_i} \tag{8.11}$$

Where:

O_i is monthly average of historic records (Observed value)

E_i is monthly average of generated data (Expected value)

i is an indicator, varies from 1 to k

k is maximum number of years, (100 years in this study).

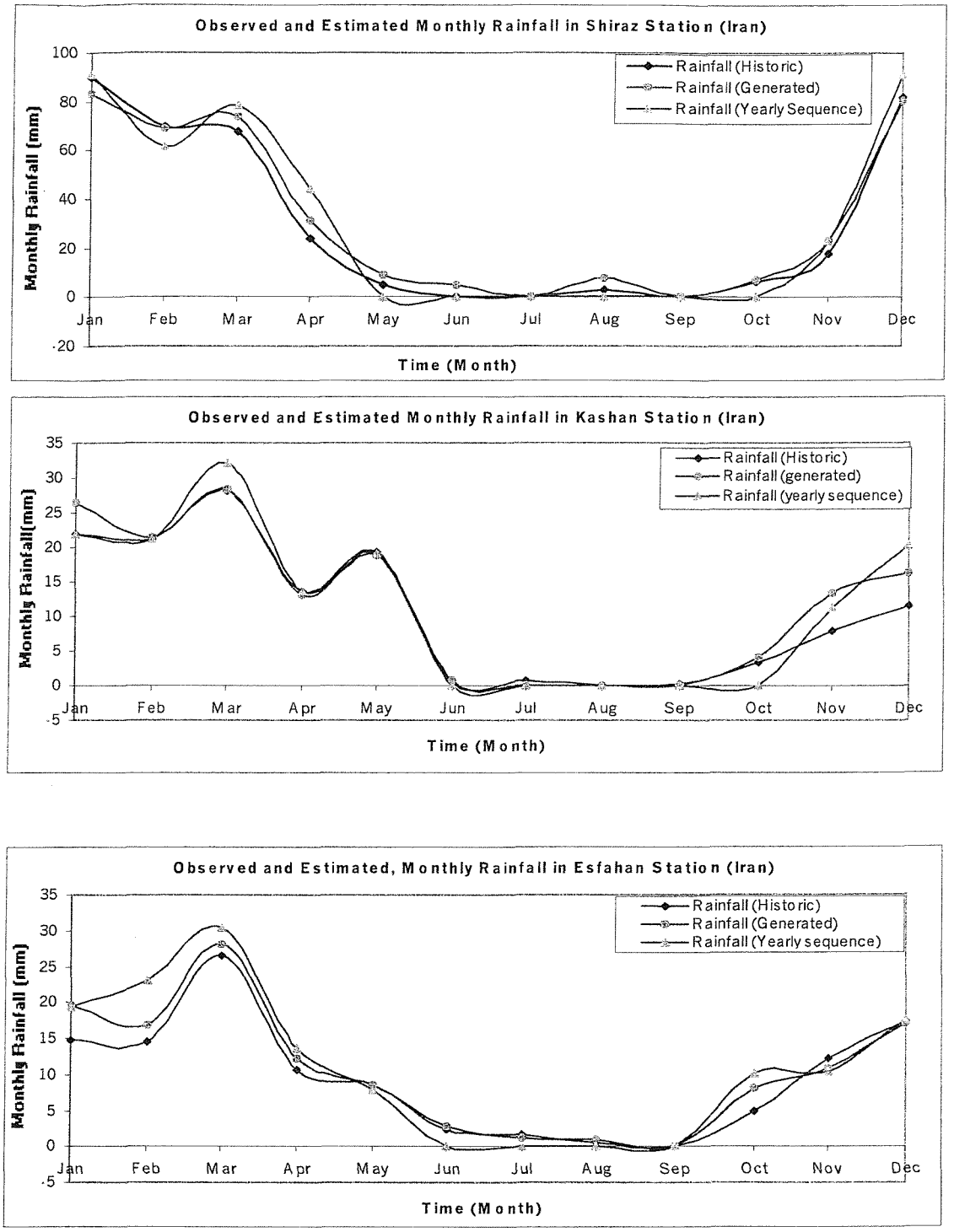

Figure 8.1: Comparison of monthly average historic rainfall with monthly average of 100 years generated data in three stations in Iran (Shiraz, Esfahan and Kashan)

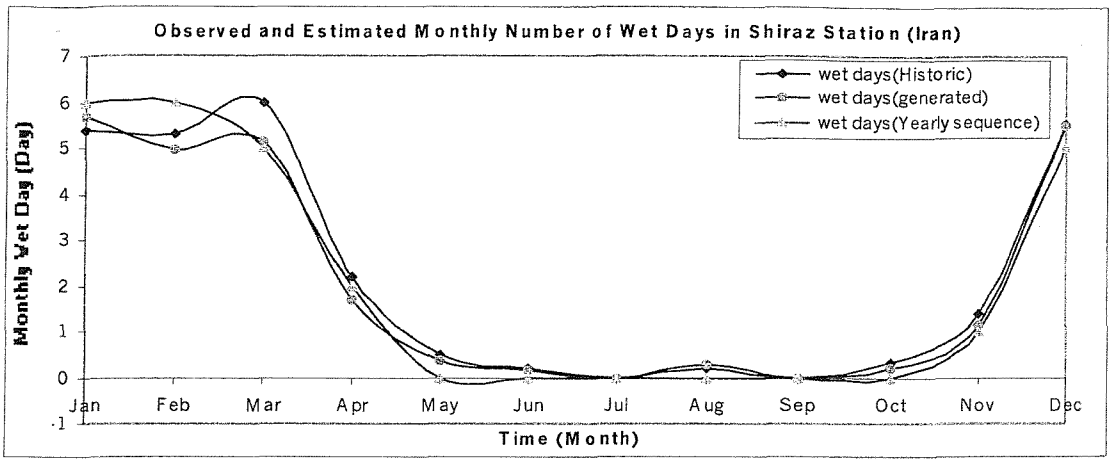

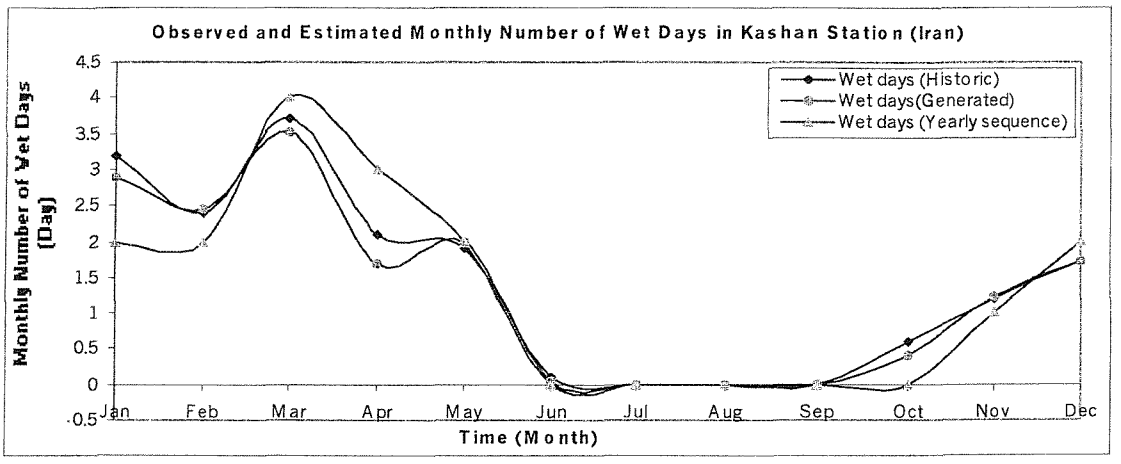

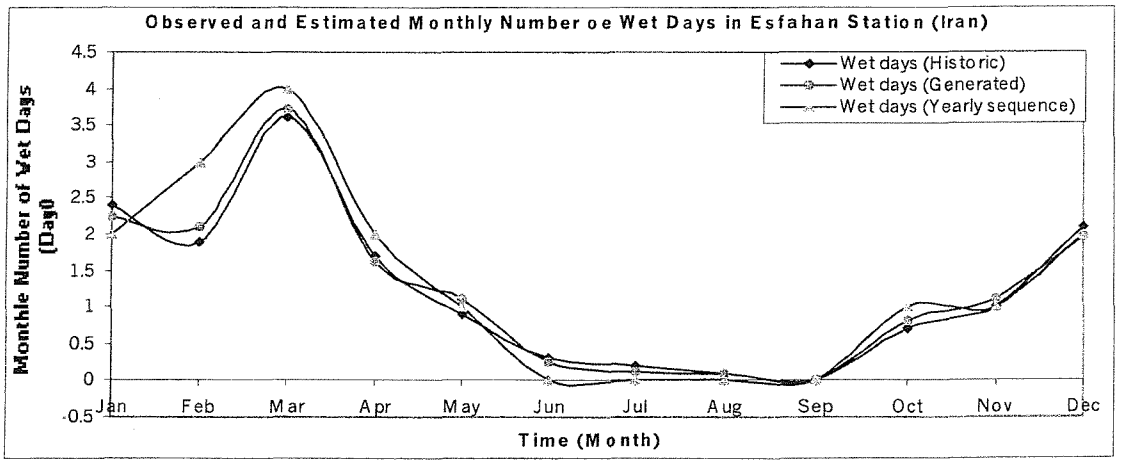

Figure 8.2: Comparison of monthly average historic number of wet days with monthly average of 100 years generated wet days data in three stations in Iran (Shiraz, Esfahan and Kashan)

The data from the synthetic model was used to calculate the daily rainfall for three stations in Iran (Kashan, Esfahan and Shiras), see appendix D, table 9. The generated data were used for Micro-Catchment system design.

8.2.3 Calculation of potential crop evapotranspiration

A model was developed to calculate daily reference evapotranspiration (ET_o), based on modified Penman equations (Kotsopoulos and Babajimpoulos, 1997), see appendix A for detailed output calculation. The model was used to calculate the potential daily water requirements for a Pistachio crop. Ten years data was taken from calculated local meteorological stations in Iran (Shiraz, Esfahan, and Kashan stations) (see appendix A for data). Evapotranspiration and potential soil evaporation for this crop at these sites is given in Figure 8.3, and appendix A (Table A1).

8.2.4 Performance of the model for modelling soil moisture infiltration in infiltration basins

The model is used in this section to study the evaluation of soil water potential during water entry, in a catchment system sited on a sandy loam soil with given properties (Fig. 8.1).

Three micro-catchment sizes with three different runoff areas (100, 150 and 200 square metres) and four different infiltration basins (of 9, 16, 25 and 36 square metres) were used, and the simulation time was set for 24 hours with 20 millimetres of rainfall, and potential surface evaporation of 0.5 cm/day. Potential transpiration was set at 7.2-mm/ day. The maximum soil profile depth was taken as 220 cm and the maximum root depth for pistachio taken as 150 centimetres (Spiegel-Roy et al, 1977). In this example, the initial moisture distribution was assumed to be uniform at wilting point, representing conditions at the start of the growing season after the field had been left fallow for a long period. The soil moisture distribution was studied at a simulated a 24-hour period. Figure 8.4 shows the cumulative infiltration (storage) in the soil. The general pattern of storage is consistent, because all runs with stored moisture showed predictable performance. The greater efficiency of a smaller catchment is clearly evident, with the amount of stored water per unit area of catchment increasing. Figure 8.5 shows the predicted moisture distribution in the soil profile for 12 catchment configurations.

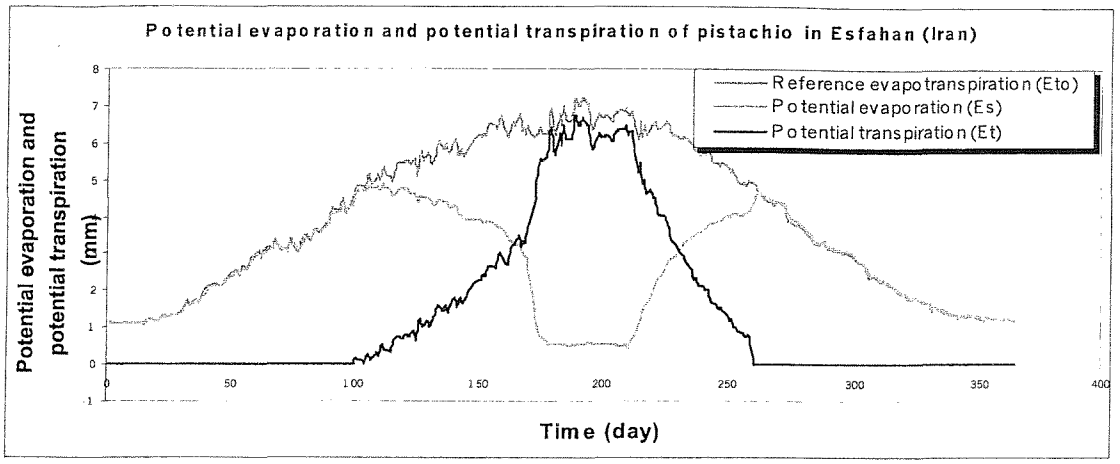

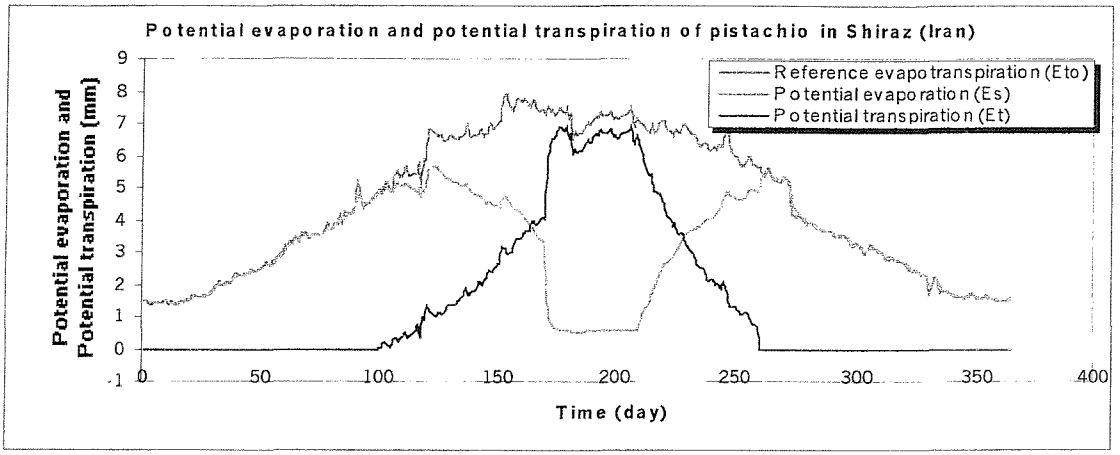

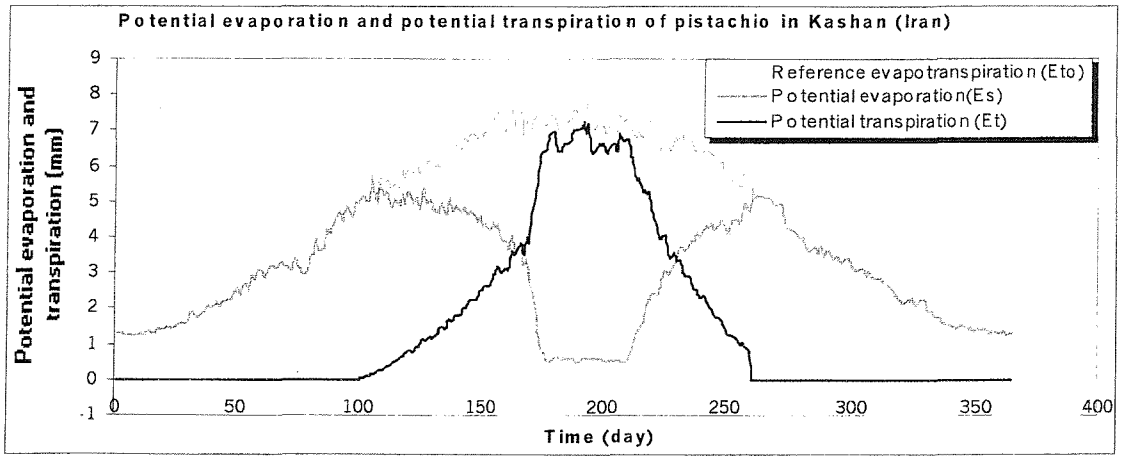

Figure 8.3: Reference evapotranspiration, potential evaporation and potential transpiration (for pistachio) in three climatic stations in Iran (Esfahan, Shiraz and Kashan).

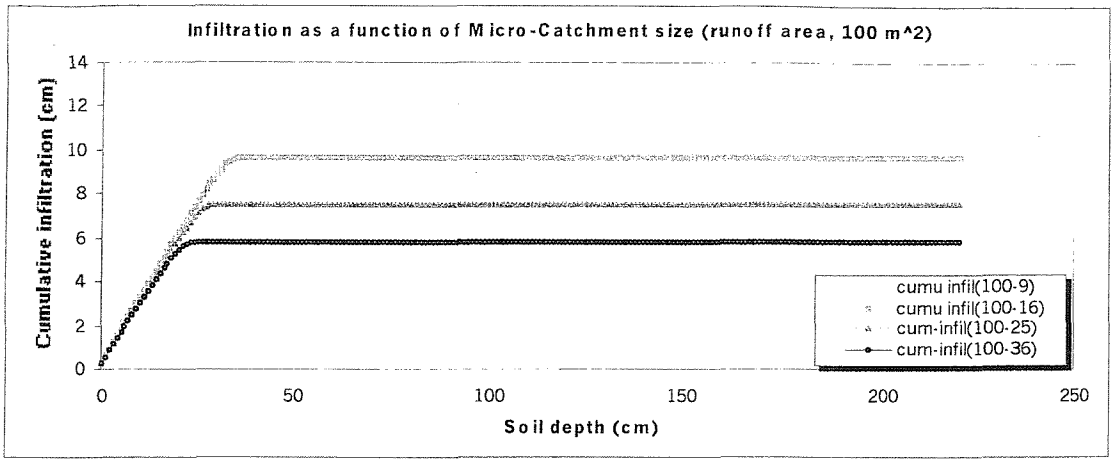

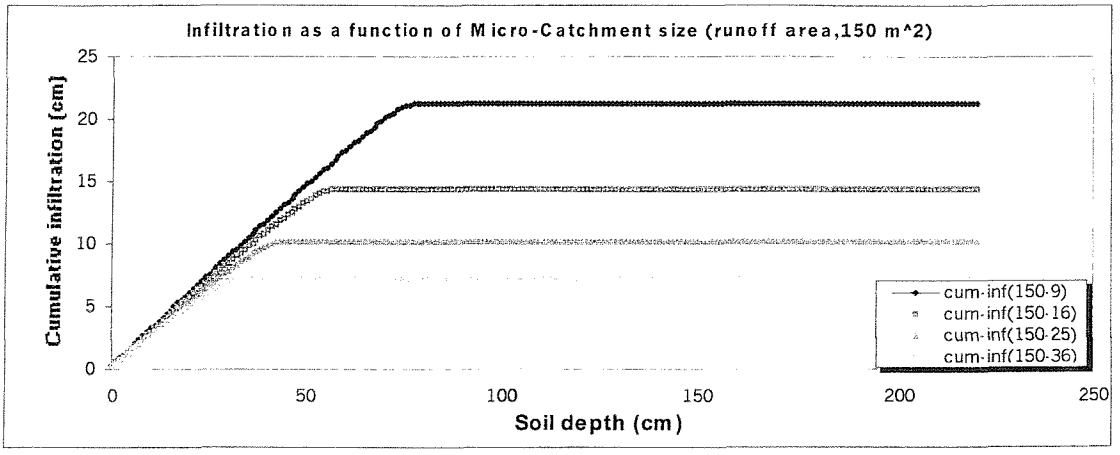

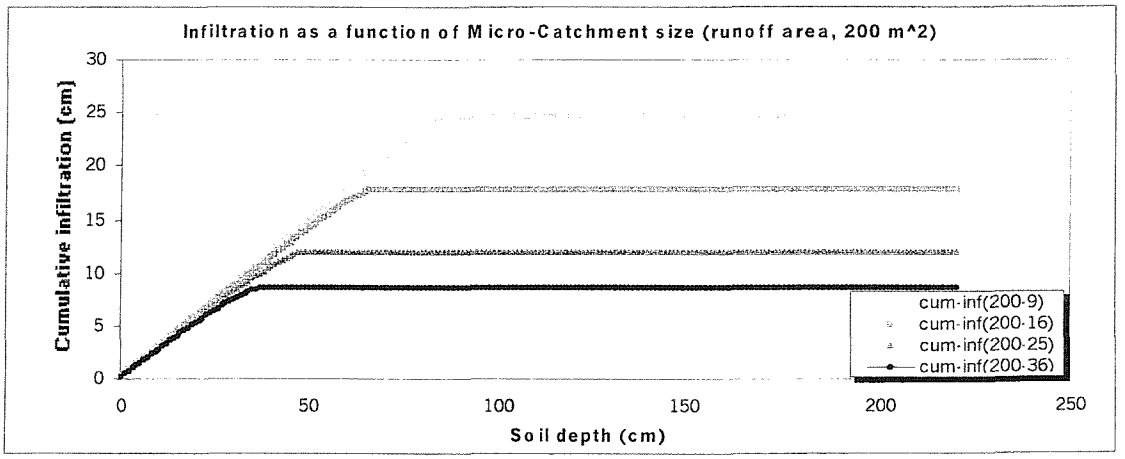

Figure 8.4: Computed cumulative infiltration and distance to the wetting front in a micro-catchment system.

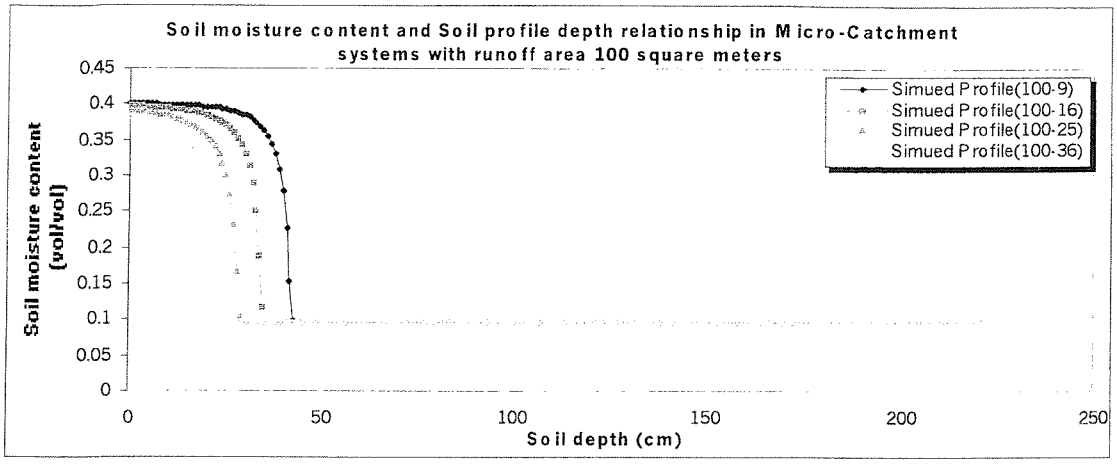

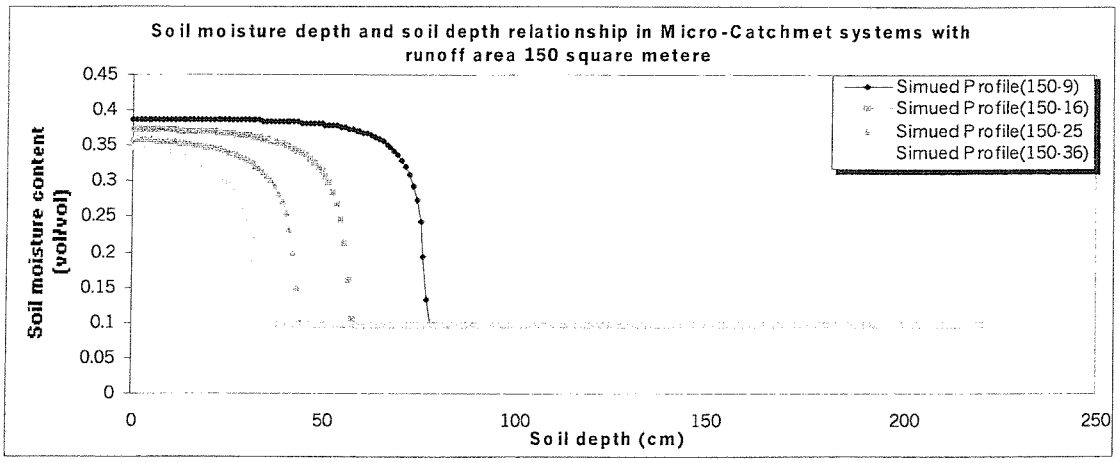

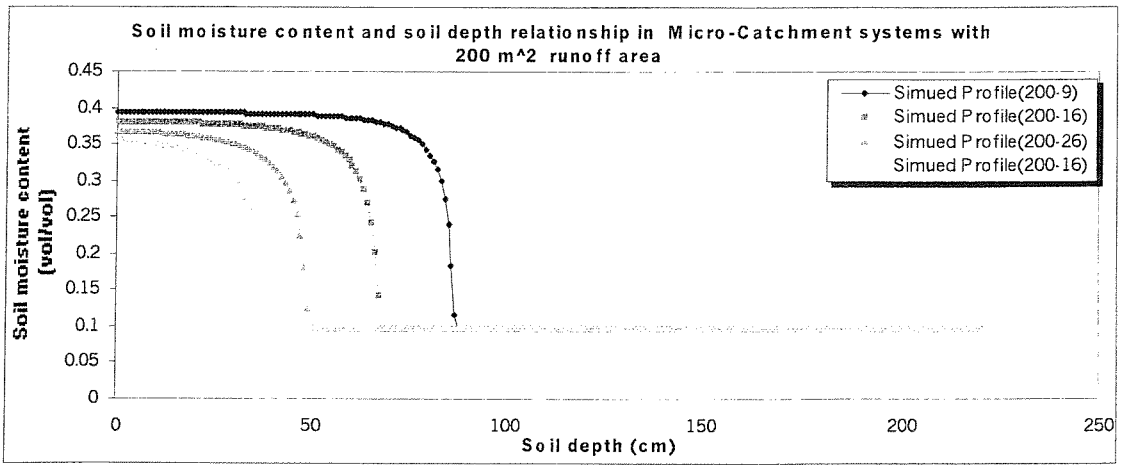

Figure 8.5: Computed soil moisture profiles at three different micro-catchments size and four infiltration basin sizes.

The shape of the soil moisture curves and their rate of advance are of importance in irrigation timing and control of the moisture regime in the root zone. With the proposed model, it is possible to predict the relative position of the wetting front and moisture content in a vertical direction in relation to the geometry of the root zone. This facilitates the selection of the most appropriate rate of water application, and the total amount of water to be applied. The model enables moisture gradients to be made at any location, thus permitting control of the moisture regime in the root zone.

8.3 Analysis of soil-water conditions during rainfall-runoff and cycles of depletion in micro-catchment systems throughout the year

The model is used in this section to demonstrate how to model soil moisture conditions throughout the year to show the level of soil moisture deficit at any time.

8.3.1 An introductory example of using the proposed model in relation to storage and depletion period of moisture in a micro-catchment system

The physical characteristics of the micro-catchment system being considered are given below.

1. The micro-catchment has a runoff area of 120 m^2. The simulation is started at a point in the start of the rainy season when the soil conditions were equivalent to wilting point. The soil in the runoff area is sandy clay loam and loam in the infiltration basin. The crop is pistachio and available soil water for this crop is considered to be moisture between field capacity and wilting point (0.107 cm^3/cm^3) in the root zone.

2. The average daily value of evaporative demand (reference evapotranspiration) is estimated daily, using the proposed model in appendix A and ten years available data for Kashan station (in Iran, see appendix A). Based on predicted evaporation demand the potential evapotranspiration is separated into potential soil evaporation and potential transpiration (see appendix A and section 8.2.3.). For simplicity, it is assumed that during the night evaporation, is 10 percent of the day value. The only

water supply to the root zone in the infiltration basin is the irregular rainfall and runoff water received from the runoff area of the micro-catchment.

3. The infiltration basin, is approximately 36 square metres. Average rooting depth is 150 cm for pistachio (Spiegel-Roy et al, 1977), and root distribution is considered to be uniform down to 220 cm soil profile depth.

4. The length of growing stages of pistachio is based on FAO Irrigation and drainage paper (Allen. Richard G, et al, 1998). It provides four distinct growth stages and a total growing period for various types and locations. The main growing season is typically from the 21st of March until 21st September. During the rainy season, out of the growing season, runoff is available, but the trees are dormant, have no leaves and thus transpiration is negligible compared to soil evaporation. During the growing season, evaporation is minimum and transpiration maximum, depending on soil moisture content and root extraction eligibility.

8.3.2 Soil moisture storage and depletion

Simulations were run throughout a year and the monthly summary output of soil moisture storage characteristics are given in figure 8.7a for the rainy winter season and in figure 8.7b for the hot summer growing season. Figures 8.7a and b show the changes in soil moisture storage that takes place during the year. The figures clearly demonstrate the importance of saturating the root zone prior to the start of the rainy season and demonstrate the crop is progressive depletion in the summer, with severe water shortages after July.

Figures 8.6a and 8.7a clearly demonstrate the model is capable of modelling the progressive redistribution of the accommodative rainfall into the deep layers of the soil profile as winter progresses. Figures 8.6b and 8.7b on the other hand show the drying of the soil in the summer, with the roots progressively extracting water from the deep layers as the upper layers becomes depleted. The later summer months show severe water stress. In particular the hot months of June and July rapidly deplete the stored water.

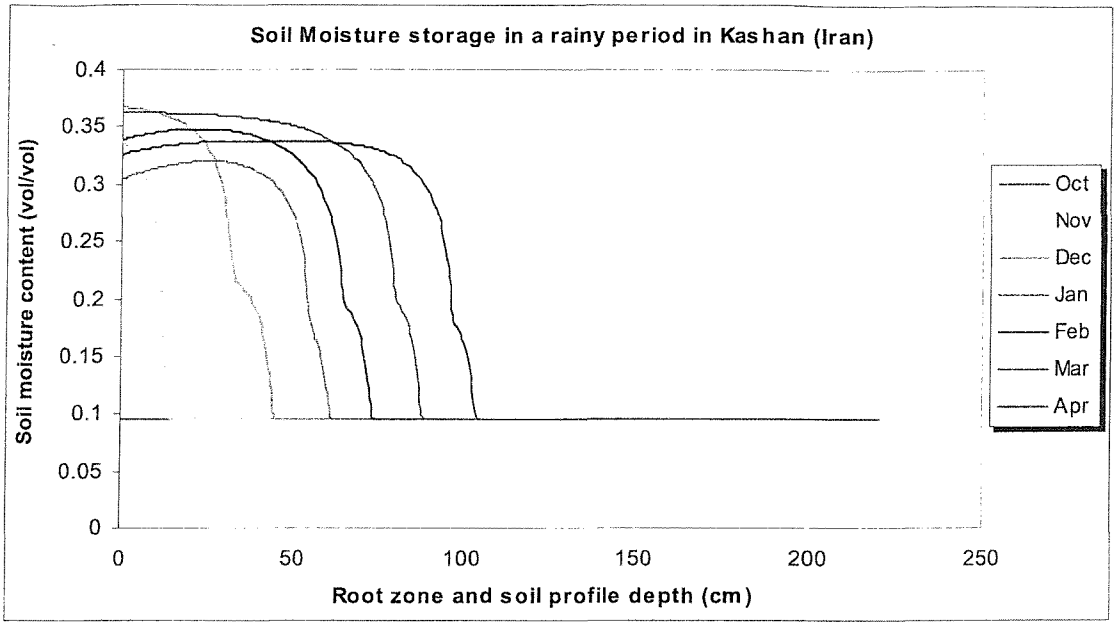

8.6a: Soil moisture states in winter rainy season and in micro-catchment systems conditions

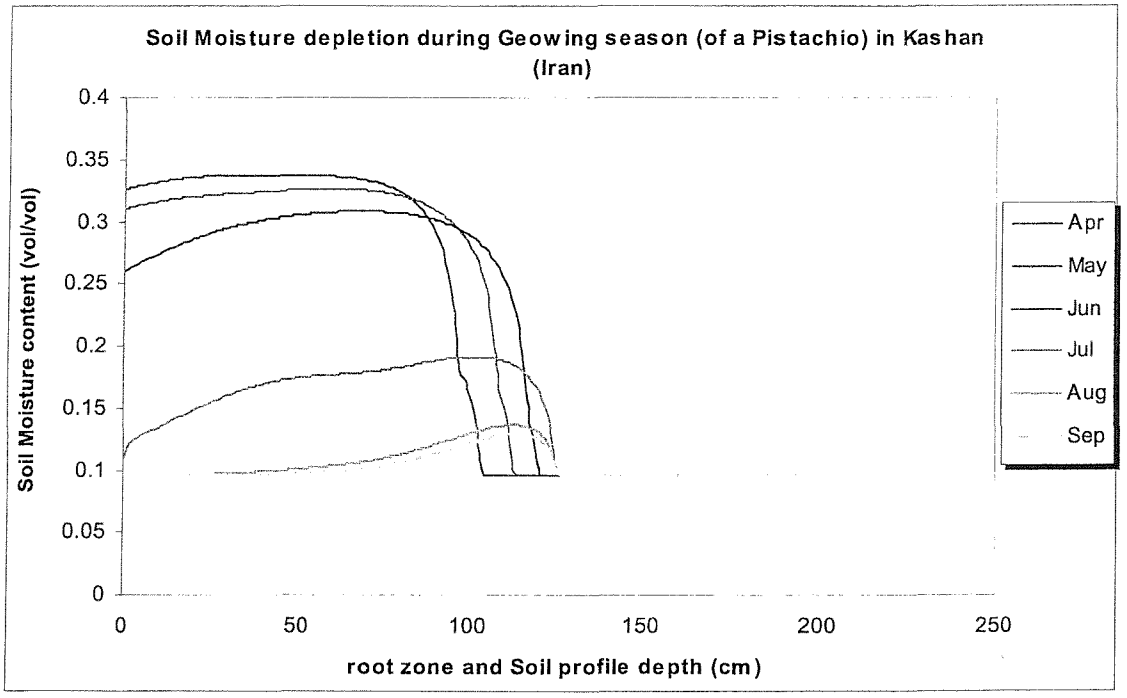

Figure 8.6b: Soil moisture states in the root zone during growing season and in micro-catchment system conditions.

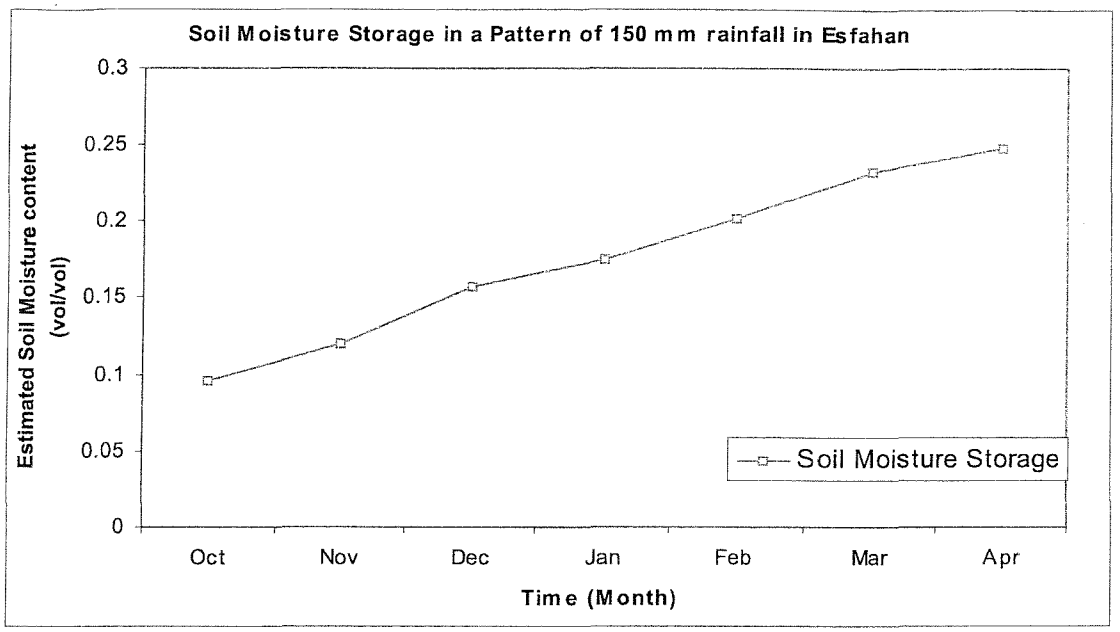

Figure 8.7a: Monthly simulated values of soil water storage a pattern of 150-mm rainfall in Kashan (Iran).

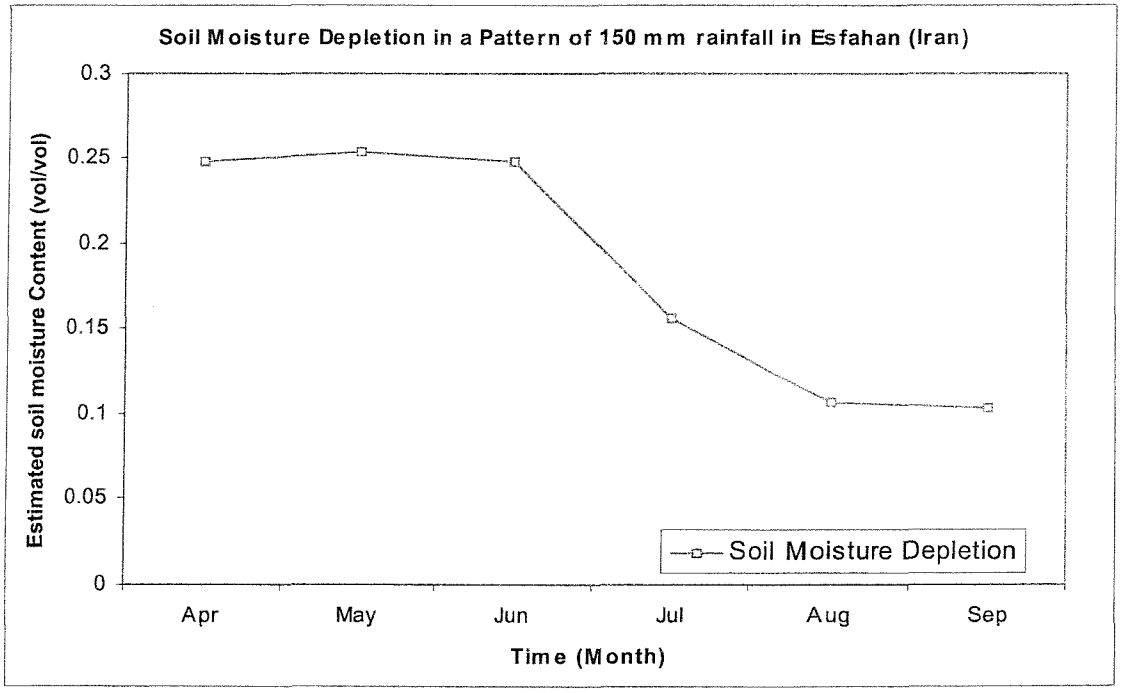

Figure 8.7b: Monthly simulated values of soil water depletion in a pattern of 150-mm rainfall in Kashan (Iran).

The above section shows two important features of moisture conditions between winter and summer periods. It shows the importance of ensuring that the root zone is at field capacity at the end of the rainy season. The rapid depletion in summer also shows the importance of catching as much of the late rains as possible to top up the soil profile in spring to help reduce the moisture stress in the late summer.

Ideally the model would be tested and calibrated against micro-catchment instruments with climate data and soil moisture tensiometer arrays. Unfortunately, this is beyond the scope of this work. The model resulting in the two graphs, however, is the behaviour that one would expect and indicates that the model appears to perform well.

8.4 Investigation of runoff generation, and its influence on controlling the moisture regime in the root zone of a micro-catchment system

8.4.1 Description of numerical experiments

The following data was used to demonstrate the capability of the model to predict runoff from storm data.

a. Soil properties: A sandy clay loam soil lies in the runoff area and loam soil in the infiltration basin, (the physical properties of this soil are shown in table 6.3). A light clay soil was also used on a runoff area to observe the effect of different soil hydraulic properties on the generation of water runoff. The initial moisture content was taken to be uniform and at wilting point.

b. Evaporative demand: The values of potential evapotranspiration were calculated from average daily climatic data from three climatic stations in Iran, using the evaporation and model given in appendix A. The generated potential evapotranspiration data was used to generate potential evaporation and potential transpiration (Appendix A, Table A.1).

c. Crop characteristics: The maximum root zone extension limits of pistachio was taken to be 1.5 m deep (the maximum soil depth is 220 cm) in a selected infiltration basin area.

The trees (pistachio) planted at the centre of the infiltration basin, was situated on the lower side of the micro-catchment.

d. Water resources available: the only water resource available was taken as rainfall

e. Micro-catchment characteristics: the micro-catchments were all taken as being square and prepared to uniform slopes between 0.5-10%. The micro-catchment sizes of the runoff area and infiltration basin selected for the test are given in table 8.1 and 8.2.

8.4.2 Investigation of generated runoff

In order to evaluate runoff generation from the runoff area of a micro-catchment system, three series of numerical experiments were carried out using rainfall data from Esfahan, Kashan, Shiraz with mean average rainfall of 156, 226 and 230 mm respectively. and two soil types sandy clay loam and light clay in the runoff areas, giving six experimental micro-catchments in all. Five micro-catchment sizes were taken for each experiment series. The experimental combinations together with their estimated runoff are given in table 8.1.

Table 8.1 and figure 8.8 show the calculated potential runoff from the experiment catchments. The results shows that the major part of rainfall is lost as infiltration from the runoff area and evaporation during dry spells and that runoff efficiency remains low. This loss is caused by the distribution of rainfall, soil kind and micro-catchment system characteristics in the runoff area. For example, at Esfahan, Kashan and Shiraz 19.4%, 14% and 21.4% of storms respectively were too small or had too little rainfall intensity to produce runoff in the experiments carried out on sandy clay loam.

The performance of the micro-catchment systems in producing runoff can be expressed as runoff efficiency. One way to do this is to apply the linear regression model (Diskin, 1972), to describe the relation between rainfall and runoff. This relationship was discussed in the previous chapter (see 7.3).

Table 8.1. Runoff efficiency estimated from generated runoff in six series Micro-Catchment systems in three climatic stations of Esfahan Kashan and Shiraz (Iran)

Mean annual precipitation mm	Total generated water in runoff area (m3)	Soil Type	Exp, No	Given infiltration area (m2)	Runoff area (m2)	Calculated Runoff (m3)	Runoff efficiency %
156	6.88	Scl	1	36	44	1.97	0.29
Esfahan	10.01	Scl	2	36	64	2.86	0.29
	13.14	Scl	3	36	84	3.74	0.28
	17.83	Scl	4	36	114	5.05	0.28
	22.52	Scl	5	36	144	6.35	0.28
Average	14.1					3.99	0.28
156	6.88	Lc	1	36	44	4.11	0.60
	10.01	Lc	2	36	64	5.95	0.60
Esfahan	13.14	Lc	3	36	84	7.79	0.59
	17.83	Lc	4	36	114	10.59	0.59
	22.52	Lc	5	36	144	13.25	0.59
Average	14.1					8.34	0.59
226	9.86	Scl	1	36	44	3.34	0.34
Kashan	14.34	Scl	2	36	64	4.83	0.34
	18.82	Scl	3	36	84	6.32	0.34
	25.54	Scl	4	36	114	8.55	0.33
	32.26	Scl	5	36	144	10.74	0.33
Average	20.16					6.76	0.34
226	9.86	Lc	1	36	44	6.16	0.63
Kashan	14.34	Lc	2	36	64	8.96	0.63
	18.82	Lc	3	36	84	11.68	0.62
	25.54	Lc	4	36	114	15.85	0.62
	32.26	Lc	5	36	144	19.87	0.62
Average	20.16					12.5	0.62
230	10.12	Scl	1	36	44	5.68	0.56
Shiraz	14.72	Scl	2	36	64	8.26	0.56
	19.32	Scl	3	36	84	10.84	0.56
	26.22	Scl	4	36	114	14.59	0.56
	33.12	Scl	5	36	144	18.43	0.56
Average	20.7					11.56	0.56
230	10.12	Lc	1	36	44	7.44	0.73
Shiraz	14.72	Lc	2	36	64	10.82	0.73
	19.32	Lc	3	36	84	14.11	0.73
	26.22	Lc	4	36	114	19.04	0.73
	33.12	Lc	5	36	144	24.05	0.73
Average	20.7					15.09	0.73

Explanation of table:

Soil Type: Scl = sandy clay Loam

Lc = light clay

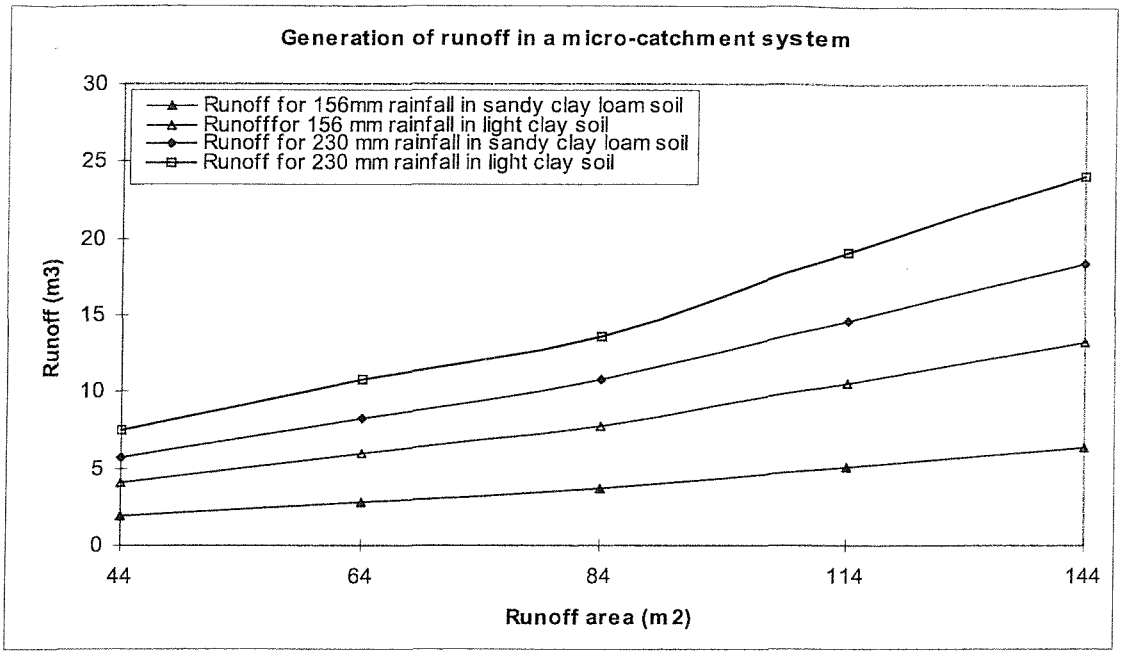

Figure 8.8: Relationship between rainfall and size of runoff area, soil type and generated runoff in a micro-catchment system

The following definition can be used to express runoff efficiency for the whole season in a single number.

$$e_r = \frac{Run}{P} \qquad 8.15$$

Where:

e_r is the runoff efficiency and

P is rainfall for the entire rainy season

For the six series micro-catchments subjected in table 8.2, the runoff efficiency for each experiment number and average of each series is calculated as 0.28, 0.59, 0.34, 0.62, 0.59, and 0.73 respectively. These values, as might be expected, are considerably higher than the value of 0.03-0.05 (Boers et al. 1986) often found for large catchment areas. These numbers illustrate the advantage of micro-catchment systems for water harvesting.

8.4.3 The catchment infiltration model and its operation

The first two sections of this chapter show how the model calculates runoff from climatic data and its relationship with size of runoff area. Chapter 4 (see 4.6) described the finite difference water balance model for an infiltration basin to calculate crop transpiration, soil surface evaporation, deep percolation and soil moisture storage between two time steps. This section combines to give a whole catchment water balance model and gives an example of its operation.

The results of numerical water balance experiments for the two series of Micro-Catchment system are shown in figures 8.10a and 8.10b. In the first series, the infiltration basin size is constant and equals 36 m^2, but the runoff area is different. In the second series micro-catchment size is constant and equals 120 m^2. However the infiltration basin size is changed (9, 16, 25, 36 m^2) and the corresponding runoff area is also changed to (111, 104, 95 and 84 m^2). The model is used to simulate a water balance in cycles of rainy and growing seasons. The results of these experiments are discussed below:

Figures 8.10A & 8.10B have shown the water balance of an infiltration basin with 230mm and 270mm rainfall. Clearly most of the water entering the infiltration basin generated in winter, with summer rains during the growing season contributing little to the overall water balance. At the end of the rainy season, after evaporation and deep percolation losses a portion of the soil moisture is available for trees at the beginning of the growing season.

The efficiency of the process of soil water storage in the infiltration basin can be defined as:

$$e_s = \frac{\Delta W}{Ap} \qquad 8.16$$

Where:

e_s is the soil storage efficiency

ΔW is soil moisture storage and

Ap = sum of rainfall and runoff collected water in infiltration basin that infiltrated into the soil

The effect of catchment size on the amount of water stored in a $36m^2$ infiltration basin is shown in figures 8.9 and 8.10A. Clearly, increasing the runoff area from 44 m^2 to 144 m^2 only made a small change to the total amount of stored water available. This is because of deep percolation losses. Therefore increasing the catchment size made a significant change to the amount of water stored at the end of the rainy and growing seasons, increasing from 0% to 25% at the end of growing season.

The effect of changing the infiltration basin size for a given runoff area of 120 m^2 is shown in figures 8.10 B. Clearly, increasing the infiltration basin size above 25 m^2 does not increase the amount of stored water in the root zone in this agro climatic zone. It is also clear that a 25 m^2 infiltration basin and $95m^2$ runoff area (in 120 m^2 micro-catchment size) are capable of supporting a pistachio crop in this agro climatic zone, with 270 mm rainfall with 20 m^3 of generated water (available water in the infiltration basin) being stored in the root zone soil. The reason for the flat response to larger catchment infiltration basins is not just that beyond a certain size the runoff area becomes restricting but also as the infiltration basin area increases so does the soil surface areas for evaporation.

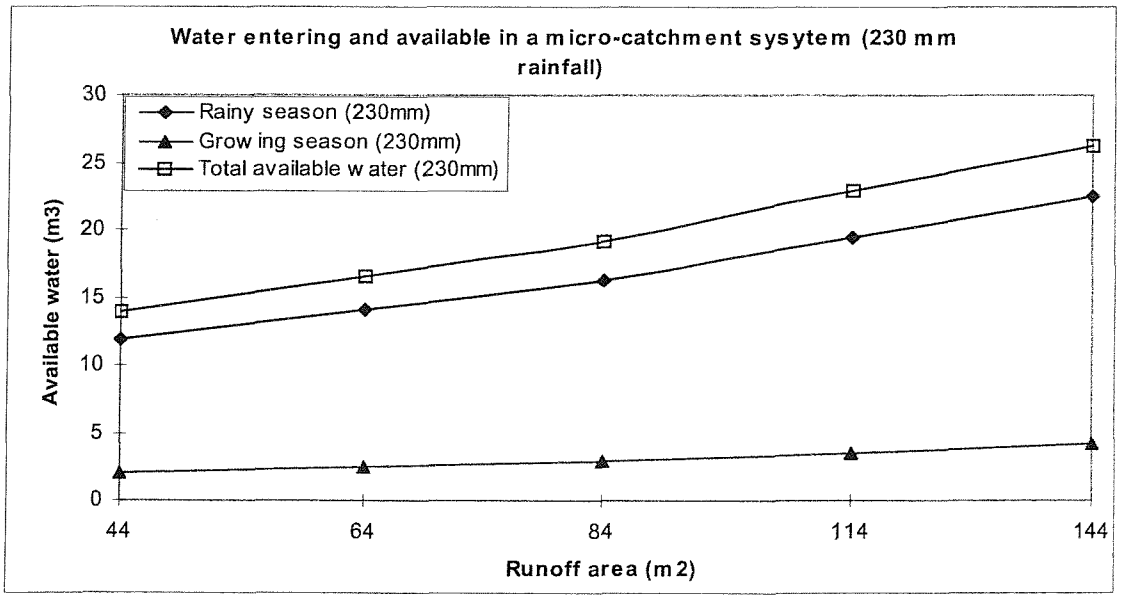

Figure 8.9: Relationship between runoff area and the water entering the infiltration basin (230-mm rainfall)

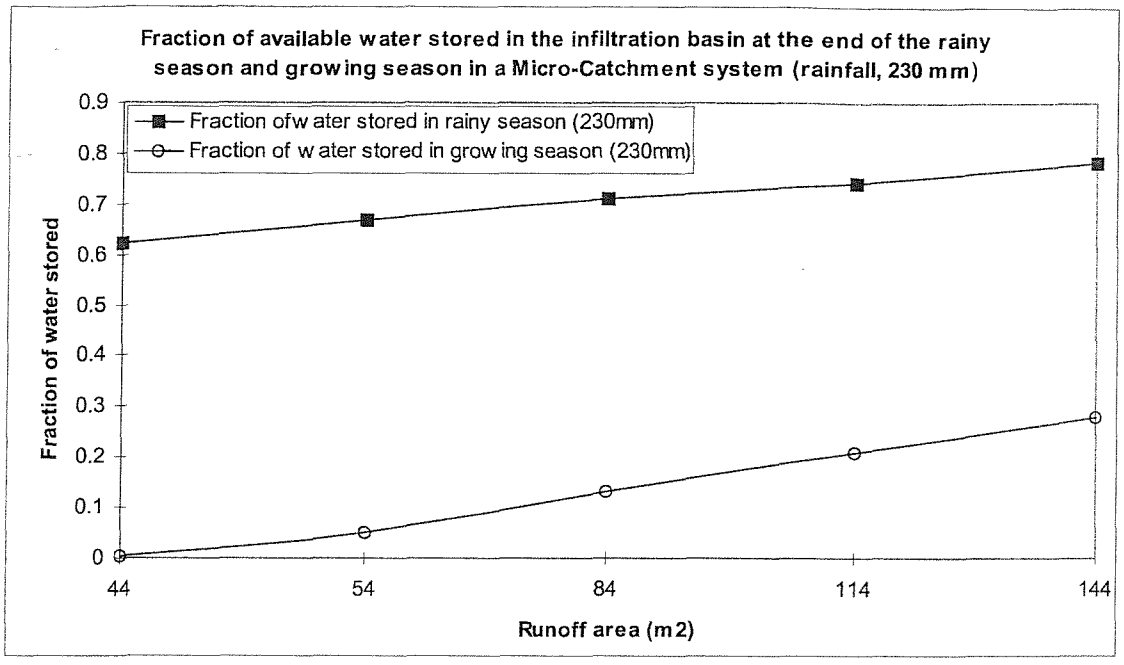

Figure 8.10 (A): Relationship between runoff area and storage efficiency in 230-mm rainfall

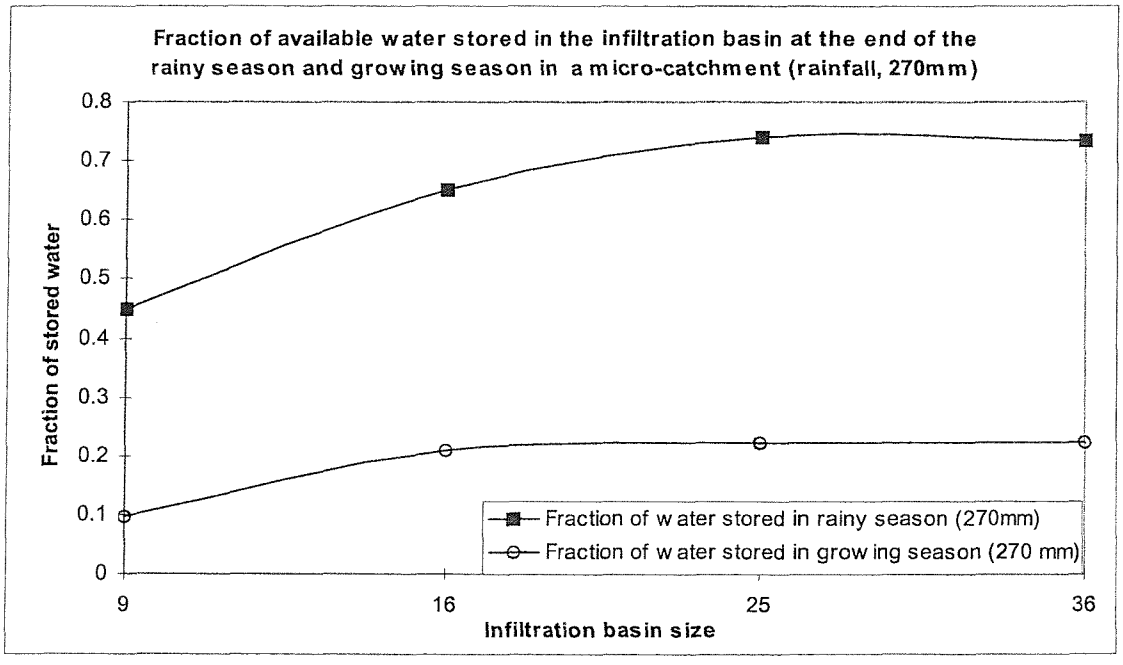

Figure 8.10 (B): Relationship between infiltration basin size and storage efficiency in 270-mm rainfall for a 120-m2 Micro-Catchment size.

8.5. Discussion

In this chapter climatic and soil data are fed into the model to examine its performance at modelling the water supply within the root zone. The model appears to behave consistently and to produce output for the pistachio crop that appears very realistic in terms of the amount of water being made available to the crop in the root zone.

The performance of all the components of the model have also been examined for reliability therefore feel that the model is suitable for the optimisation of micro-catchment design, which is conducted in the next chapter.

Chapter 9. Estimating optimum size of micro-catchment systems using the model

9.1 Introduction

The proposed model can be used to establish the optimum size of runoff area and infiltration basin for a Micro-Catchment in a given location and for a specific cropping pattern. Optimisation is achieved when the collected rainfall and runoff from the infiltration basin provides the most favourable moisture regime for root extraction and plant growth.

9.2 Optimisation of catchment size

I General methodology

The optimisation of a catchment for a given environment is performed in three stages.

a) The potential runoff for a range of runoff catchment sizes is calculated for a given location from daily rainfall data, soil type and slope using the methodology described in chapter 7.
b) The seasonal water balance for the infiltration basin of a given area is calculated for a runoff basin of a given size using the local climatic data and daily rainfall data, soil type, and runoff catchment area using the methodology described in chapter 8.
c) The above approach is used to develop an output data matrix for different combinations of runoff areas and catchment sizes showing the annual available water resources (evaporation $E_t + E_s$) for a crop.
d) Comparison of a theoretical annual crop water demand with that provided by the catchments allows the optimum system to be selected. The micro-catchment system that meets the annual crop water demand and which has the smallest footprint is selected for further study. The seasonal water supply is checked to ensure that the crop water demand can be met throughout the year.

Example of the use of the methodology

Three sites were selected in Iran for testing the methodology. Shiraz, with a mean annual rainfall of 270mm/y and loam soils, Esfahan with a mean annual pattern rainfall of

200 mm/y and loam soils and Kashan with a mean annual rainfall pattern of 100mm/y and loam soils. The daily rainfall data for these planted sites are given in appendix D and detailed soil data is given in chapter 6 (table 6.3). These are very dry climates and a drought tolerant crop that is already grown in the area is essential to ensure reliable crop production. The crop selected for this study was pistachio, the agronomic characteristics of which were given in chapter 8 (8.4). The area of the rooting zone of a pistachio tree is said to be $36m^2$ (Boers et al, 1986). The size of the infiltration basin must therefore be in multiples of 36 m^2.

The above approach was used to establish the amount of water available for the Kashan site which is a 36 m^2 planted micro-catchment runoff catchment of 44/ 64/ 84/114 /144 m^2. The water balance for the infiltration basin and the different catchment sizes is shown in table 9.1 and figure 9.1(A).

Table 9.1: Total water resource entering a 36 m^2 infiltration basin in Kashan (100-mm rainfall) with catchments of different sizes and showing the amount of water available for transpiration

Runoff area (m^2)	Total water entry in Micro-Catchment (m^3) (figure 9.1A)	Available water for transpiration (m^3) (figure 9.1A)
44	5.3	2.1 (58.3 mm)
64	6.1	2.4 (66.7 mm)
84	6.4	2.7 (75 mm)
114	8.0	3.1 (86 mm)
144	9.1	3.6 (100 mm)

The pistachio tree is said to require between 7 and 12 m^3 of water for transpiration to produce a crop of nuts (Oron et al, 1987). Over a root area of 36 m^2 this equals to the equivalent crop water E_t of 195 -333 mm. Clearly, the micro-catchment is incapable of meeting crop water demand in Kashan with 100-mm rainfall.

Figure 9.2 (B) shows the water balance for a similar 36m^2 catchment for Esfahan in a year in which the mean annual precipitation was 200 mm. Unfortunately, despite the fact that increasing the catchment size from 44 to 144 m^2 increased the amount of water entering the infiltration basin from 10-16 m^3, the amount that was available to the crop in the growing season only rose from 6-8 m^3. Beyond 64 m^2, increasing the catchment size did not increase the availability of water. As can be seen from the graph, the additional water was either lost to deep percolation or evaporation during the cool non-growing season, when most of the precipitation occurs. The crop is said to require between 7-12 m^3 of water for crop production (Oron, et al 1987), with yields increasing with greater water supply. It is therefore clear that the optimum catchment size for this amount of precipitation is likely to be 64 m^2, but even then, the water supply will be severely limited as the test data was taken from a wet year. If the programme were run for a dry year it would show that the micro-catchment could not be designed to provide sufficient water for crop production in Esfahan.

Figure 9.1 (C) shows similar data but for a dry year in Shiraz when mean annual precipitation was 230 mm. In this year it is clear that there is no increase in available moisture for the crop beyond a runoff area of 44 m^2 (see figure 9.1C), when 10 m^3 of water is available to the crop in the cropping season. The reason that this pattern occurs is that precipitation mainly falls in winter when the crop is not in leaf. Therefore any additional water that fills the soil profile to rooting depth is wasted.

The above data shows that micro-catchments can be efficient at increasing the availability of water in the soil profile but unfortunately pistachio is poorly suited to utilise the additional water because of the fact that precipitation falls in the winters while the crop grows in spring and summer. The moisture holding capacity of the soil therefore limits the efficiency of the micro-catchment system. This is clearly shown when comparing water use efficiency

$$e_{use} = \frac{E_t}{Ap} \qquad 9.1$$

Where: e_{use} is the water use efficiency in a micro-catchment system

E_t is actual transpiration, and Ap is applied water, which is collected in the infiltration basin and infiltrated through the soil

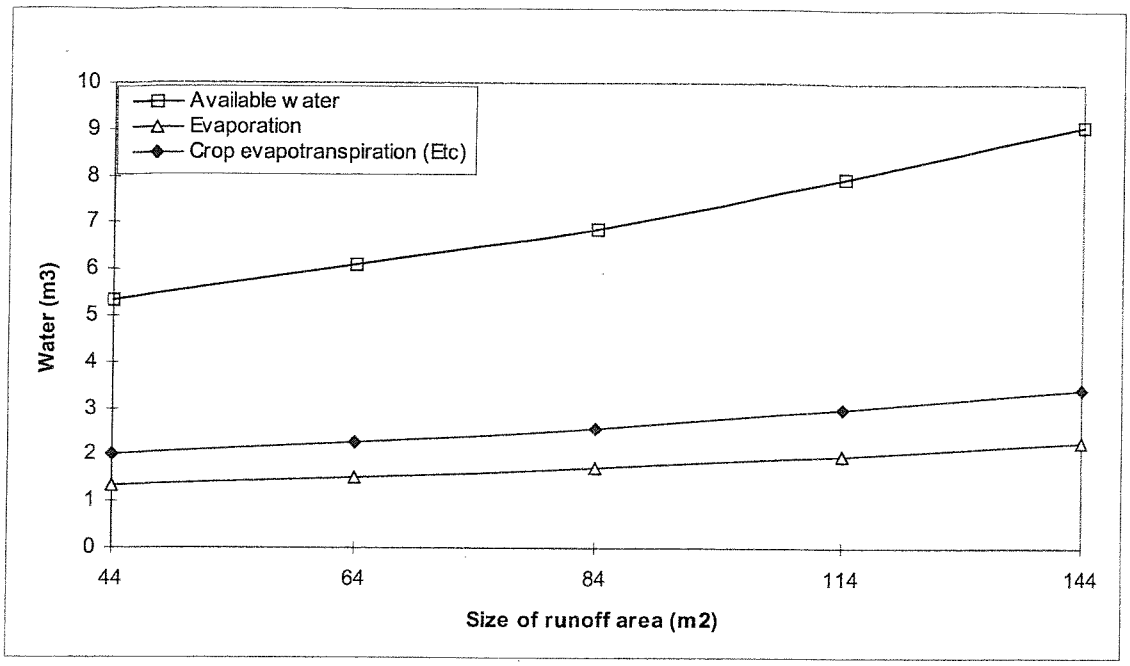

Figure 9.1(A): Relationship between runoff area and the water resources for a 36 m^2 infiltration basin planted with pistachio in Kashan, with 100 mm annual precipitation

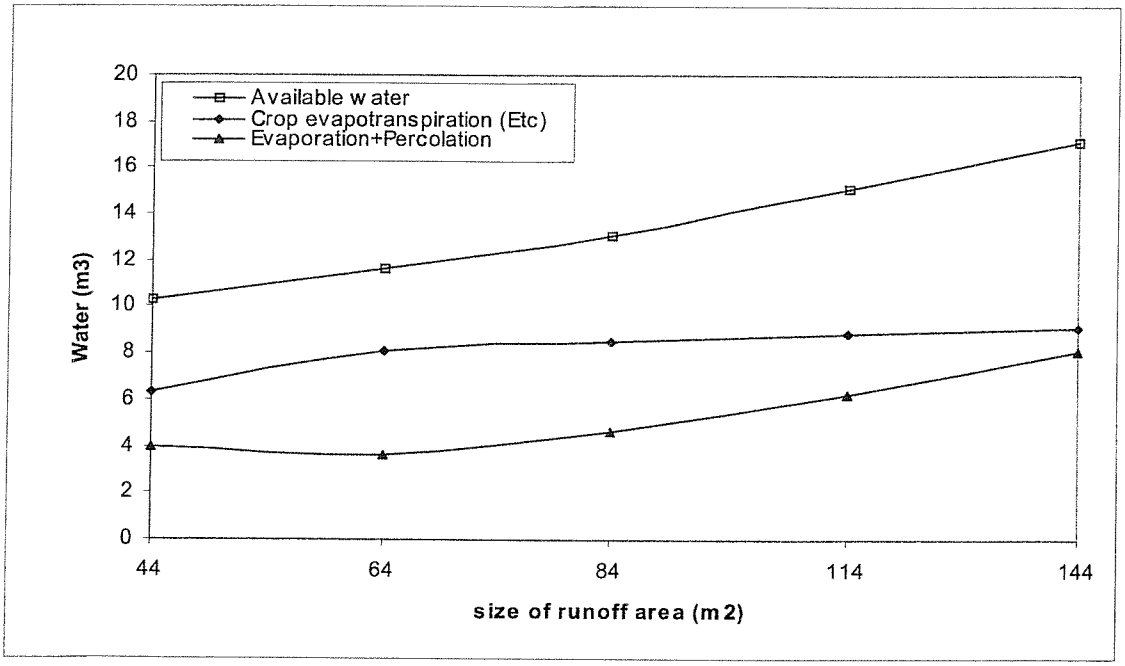

Figure 9.1(B): Relationship between runoff area and the water resources for a 36 m^2 infiltration basin planted with pistachio in Esfahan, with 200 mm annual precipitation

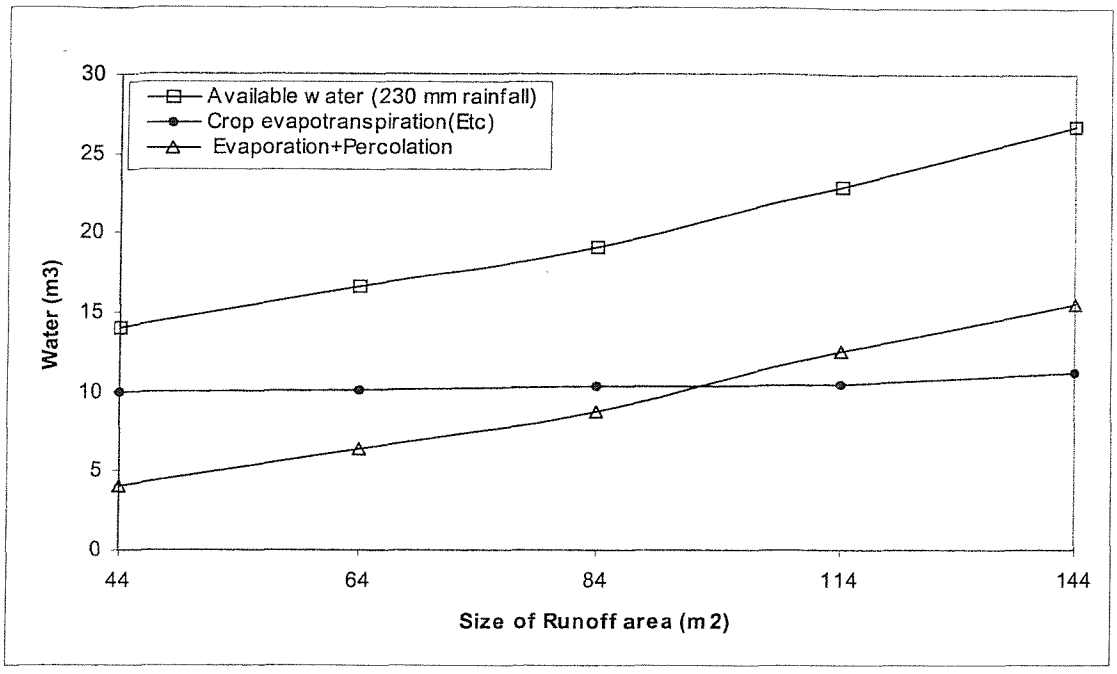

Figure 9.1(C): Relationship between runoff area and the water resources for a 36 m^2 infiltration basin planted with pistachio in Shiraz, with 230 mm annual precipitation

Figure 9.2 shows the water use efficiency for two rainfall patterns with annual precipitation of 200 and 230 mm as a function of runoff area. As can be seen in this general picture, as rainfall becomes smaller or drier the water use is more efficient.

9.3 Relationship between micro-catchment size and yield prediction

In a micro-catchment the annual yield function for pistachio tree can be written in the form:

$$\frac{y_{ac}}{y_{\max}} = \frac{W_{av}}{W_{av} + k} \qquad W_{av} \geq W_{\min} \qquad 9.2a$$

$$y_{ac} = 0 \qquad W_{av} < W_{min} \qquad 9.2b$$

Where:

y_{ac} is the actual yield of nuts per tree (in kilograms)

y_{max} is the maximum yield per tree (in kilograms),

k is a constant characterising each plant,

W_{min} is the minimum amount of water required per year tree (in cubic meters), and W_{av} is the volume of water available per tree in each Micro-Catchment (in cubic mets) (Oron and Enthoven., 1987).

This general functional relationship is based on analytical analysis and not on systematic field experiments of the yield as a function of the water applied (Reca et al. 2001-I & II, Montesinos, et al, 2001. and Oron and Enthoven, 1987). Further analysis and calculations with reported data show that for pistachio nuts (unpeeled) the yield function for W_{av} =2m^3 is given by (Figure 9.4):

$$y_{ac} = 12\frac{W_{av}}{(W_{av}+4)} \qquad \text{For } W_{av} \geq 2 \qquad 9.3$$

Where:

Y_{ac} is actual yield per tree

W_{av} is average water requirement per tree

Figure 9.3 shows a relationship between predicted yield in pistachio and available water per tree. In the case of Esfahan, a micro-catchment runoff area of 64m^2 and infiltration basin of 36 m^2 would be an acceptable size of micro-catchment to give a yield of about 8-kg/ tree.

For a given location, soil type, slope and crop the above procedure can be applied to the dry average, and wet years to establish the optimum size of runoff area that will ensure acceptable crop in dry and an economic crop in average years.

Once the optimum size of an infiltration basin has been established using the above procedure it is essential to ensure that dry periods do not occur within a cropping season that can result in crop failure. The programme can achieve this, by displaying the soil moisture balance for a selected catchment for the whole cropping season. Clearly, if soil moisture falls bellow permanent wilting point for any significant length of time it is essential to look at increasing the size of the runoff area. Section 8.4.2 (see chapter 8) shows this balance for Shiraz with its 230 mm annual rainfall, a 36 m^2 infiltration basin and for a given catchment runoff area.

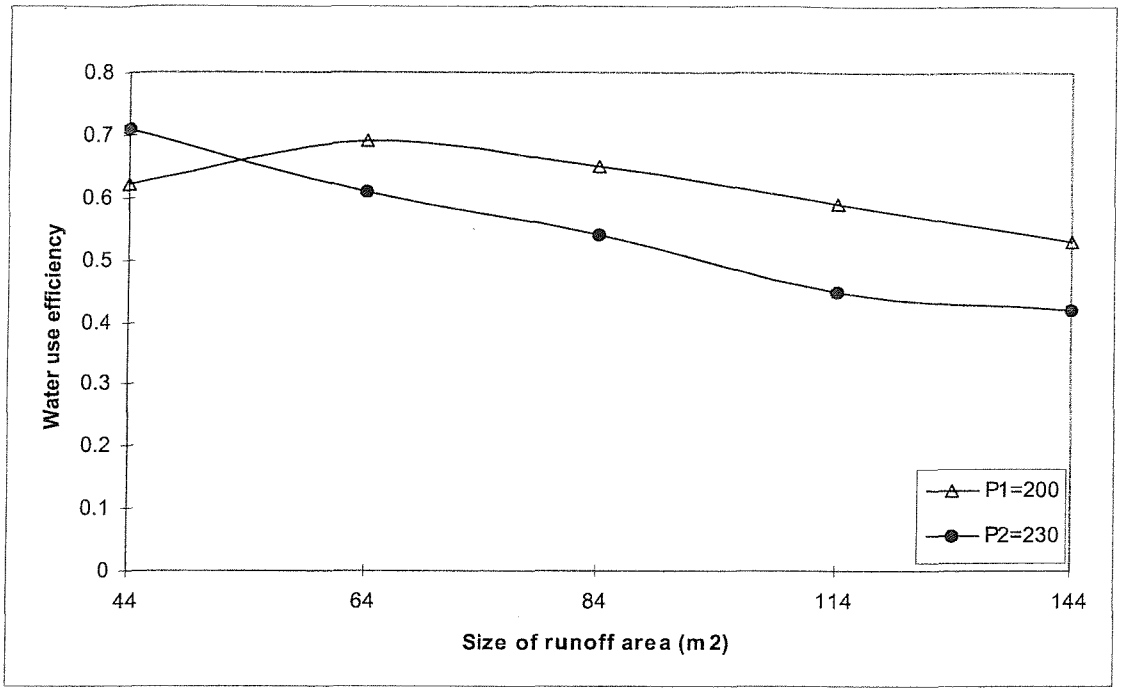

Figure 9.2: Water use efficiency for pistachio as a function of runoff area in 200mm, and 230mm annual rainfall regions.

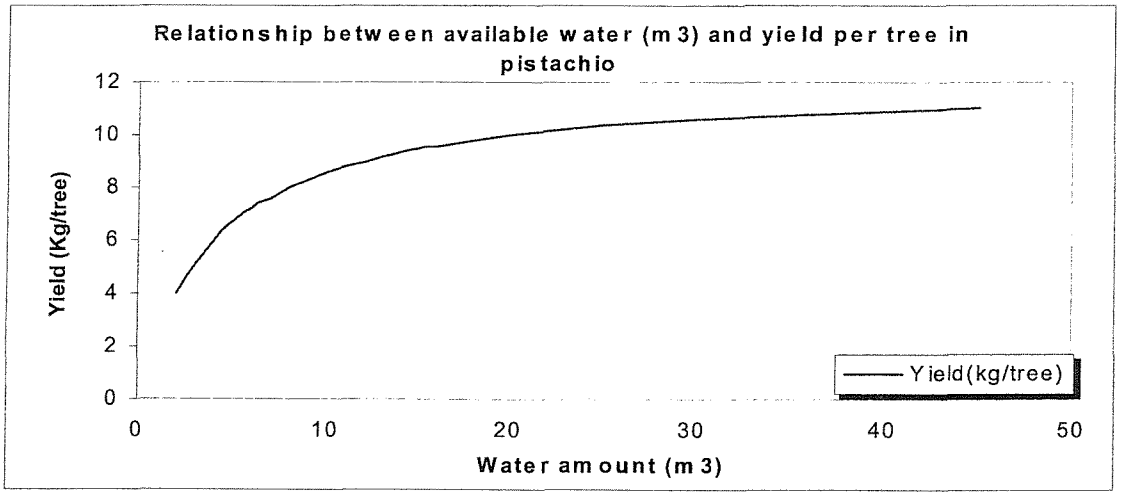

Figure 9.3: Water amount and yield (per tree) relationship in pistachio (Oron and Enthoven, 1987).

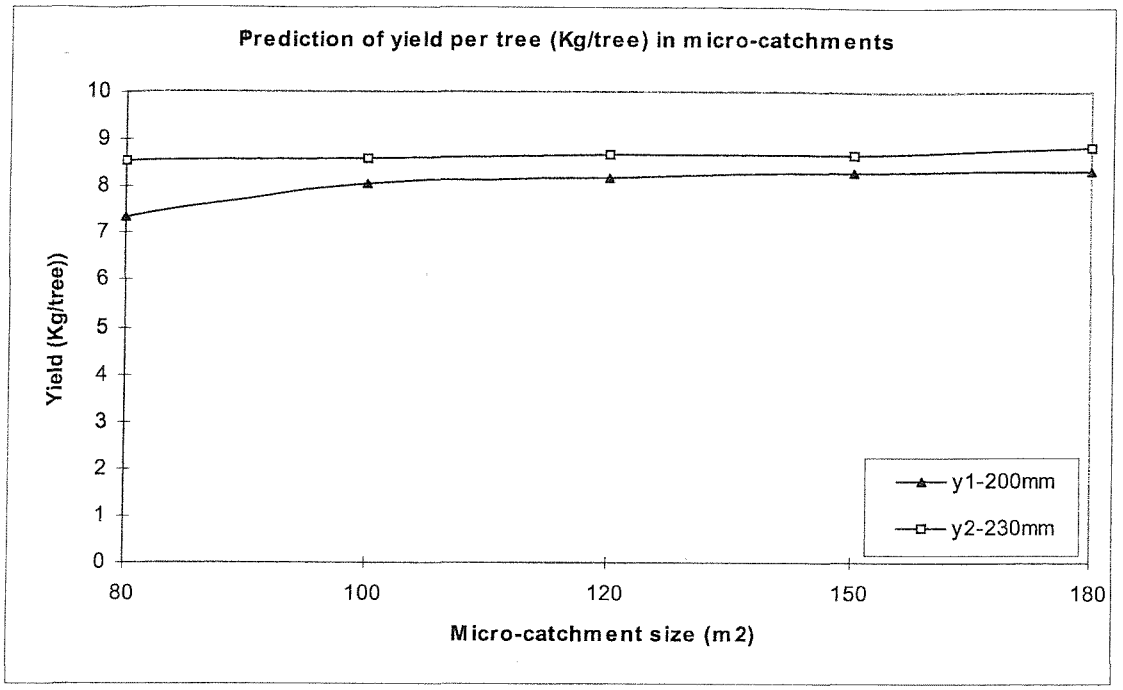

Figure 9.4: Predicted pistachio yield (kg/tree), as a function runoff area size in a micro-catchment (with constant 36 m^2 infiltration basin size) for 200 and 230 mm rainfall in the arid region.

10 Discussion, and conclusions

10.1. General discussion

Unlike irrigation and drainage practices, which are capable of supplying a perfect water balance in the root zones, micro-catchment farming is largely under the control of the elements. Rainfall patterns and evapotranspiration drive the system and all that the engineer can hope to do is drive the balance in favour of ensuring that the soil can meet crop water demand.

The correct design of a micro-catchment irrigation system based on water harvesting needs to be robust to take account of the spatial and temporal variability of rainfall, water requirement of the crops, and in addition catchment characteristics in arid regions. micro-catchment design in this thesis tackled this problem in three distinct stages: firstly, the development of a technique for rainfall analysis to predict generated water from runoff areas of a micro-catchment, secondly, the development of a technique to analyse the water balance in the root zone of the infiltration basin of a micro-catchment and finally the development of methods to optimise micro-catchment sizes.

It was concluded from the literature in chapter 2 that a multi-criterion methodology for analysing rainfall runoff relations, moisture movement in the soil, root extraction, crop waters requirement and planning of water management system was required. The methodology needed to be capable of overcoming the shortcomings of subjective methods, which are currently used for design of micro-catchment systems. In this respect, the research has shown that the proposed modelling approach is a better alternative for establishing and designing a micro-catchemt system in arid regions. In particular, the research has shown that:

The numerical procedures can be translated into effective computer algorithms (chapter 5). A set of auxiliary algorithms was also compiled to estimate the runoff in runoff areas, soil surface evaporation, and transpiration, and to evaluate moisture transport coefficients. Combining these algorithms produced a model, which was shown to be capable of simulating most conditions of practical interest in the field. This model also provides a powerful tool for detailed studies of problems in moisture transfer and storage in infiltration

basin, aid design of micro-catchment systems, and making it possible to optimise runoff areas.

The model was subjected to numerous tests in chapter 6, to verify its performance and the accuracy of the numerical results, and examine the reliability of its predictions. Comparison of the model results with analytical and numerical solutions of rainfall runoff, reference evapotranspiration and soil water flow, which have been published in the recent literature, showed that the results are sufficiently accurate, and the agreement with the reported data is good. In addition, this model responded well to show the differences in water consumption and water balance between different amounts of rainfall.

The runoff model, which was developed in chapter 7, allowed potential runoff from individual storms to be calculated from daily precipitation data, soil infiltration characteristics and slope. The potential infiltration was calculated from the rainfall duration intensity relationship, infiltration rate curves and soil slope. The relationship proved to be quite robust when tested on experimental data (see figure 6.2). The advantage of this approach is that it allowed potential runoff to be calculated for a range of agroclimatic areas. This calculation can be performed from long-term rainfall data and from basic soil characteristics, which can easily be measured in the field, or if this is not possible they can be estimated from standard graphs of soil infiltration characteristics that are given for different soil types in the textbooks. When a sufficient amount of rainfall data is not available for a realistic simulation over time, say 20 years; a Markov chain type model can be effectively used to extend the number of years data for modelling purposes.

Various procedures were investigated for assessing the availability of water in the infiltration basin for plant growth. The amount and frequency of water available for entering the soil of infiltration zones was calculated from the runoff model described in chapter 7 and from precipitation falling directly on the surface of the infiltration basin. However because of the infrequent nature of the precipitation, with much of it falling out of the growing season, a significant amount of water is lost to deep percolation below the root zone for the pistachio crop and from surface evaporation. The convential irrigation mass balance approach for calculating crop water requirements for irrigation would not have been adequate for estimating available soil moisture under these conditions. Although potential

evapotranspiration can be estimated with reasonable accuracy, evaporation and transpiration cannot be estimated with any certainty because of the poor relationship between water stress, moisture content and evapotranspiration. The procedure used in the present study could be much more reliably to evaluate soil moisture storage in the rainy season and depletion in the growth season, as well as storage efficiency and use efficiency, if this relationship were better understood.

The numerical approach suggested by Milly (1985), Celia et al (1990), and Huang et al (1996), was used to study the moisture changes that take place over time. The advantage of this approach is that it allowed deep percolation, evaporation and transpiration losses all to be identified, as well as changes to moisture content at different levels. The finite difference model that was developed appears to be able to realistically assess the water and soil moisture balance as shown in section 8.4.2. The strength of this model is that it allows the user to take account of actual rooting depth over time and incorporate the redistribution of water that always takes place by capillary action in a drying soil. It also treats transpiration and evaporation separately, an issue that is particularly important when considering tree crops. The model needed to identity the water balance under a pistachio crop in three-agroclimatic zones in Iran, where it appeared to give meaningful results.

Detailed repeated cycles of the simulation model in different sizes of micro-catchment system in chapter 8 showed that: with different rainfall and micro-catchment sizes, the loss of moisture from the root zone by deep percolation can be a very significant mechanism in depleting moisture from this zone. The moisture depletion by percolation was shown to increase with an increase in runoff area, reduction in infiltration basin size, and increase in evaporative demand. It also depended on the rate of rainfall and available water in the infiltration basin, and its timing in relation to rainy season and growth season, and soil moisture conditions. Finally, it was shown that more inflow results in more deep percolation.

A detailed study on the effect of various micro-catchment sizes on the moisture storage efficiency in the infiltration basin and total losses during the growth season from the root zone clearly indicated that the design of micro-catchment systems needs to take account of all factors in selecting the size of the runoff area in a particular rainfall, soil type and crops. In doing so, it is important to monitor the behaviour of the micro-catchment, not only

in a typical year of rainfall and single size of runoff area, but also over many years with different rainfall patterns and different possible micro-catchment configurations, changes in size of both runoff area or infiltration basin size.

In chapter 9, an optimisation procedure was proposed in order to carry out micro-catchment system planning in relationship to micro-catchment size, water use efficiency and yield. The approach allowed optimal water harvesting and the closest practical match to the crop water requirements to be achieved. Optimal size of runoff area functions for a crop are generated, considering the crop's water stress sensibility during its phenological stages, evapotranspiration and effective precipitation, growth season irrigation and natural distribution of rainfall.

A number of methods to optimise runoff area in micro-catchment systems were examined in chapter 9, using the proposed model. It was possible to demonstrate for each soil and crop types a relationship between runoff area and the ratio between potential crop evapotranspiration to total available water (water use efficiency). It was also possible to demonstrate a relationship between runoff area and yield per tree, using the proposed model and yield relationship with crop evapotranspiration. Such a relationship allows the selection of optimum size of runoff area to be selected to provide the most favourable moisture regime for root extraction to compete with other mechanisms of moisture depletion. For a selected textured soil, it was concluded that a runoff area could be selected which provides a commensurate water supply to plant needs, as dictated by evaporative demand.

The model was tested in conjunction with the runoff model to help predict the micro-catchment size in three-agroclimatic zones in Iran. Pistachio was selected as an appropriate crop as it grows in all three areas. The size of the infiltration zone was set at $36m^2$, as this is the rooting area of a typical tree. The model was capable of identifying the optimum size of runoff area although the use of pistachio as a crop on which to test the model was a little unfortunate, as it limited the scope of the micro-catchment to achieve high water use efficiencies. This was become most of the precipitation is in the cool winter period when the crop is not in leaf. The result in that increasing the catchment above a certain size just results in more water being lost to deep percolation, as the crop is unable to utilise it at this time of

year. Nevertheless the model results appear logical and predict realistic amounts of water for crop use.

10.2 Further work

This study was limited by lack of soil, crop and hydrological data in arid regions. In order to improve the reliability of the micro-catchment system design computer model developed in this study the following recommendations for future work should be carried out.

1. Laboratory analysis of physical properties of soil samples in typical arid regions where rain water harvesting takes place in order to find out a range of soil texture or the soil water retention curve and limited range of Green and Ampt parameters (A & B).
2. Determination of runoff coefficient and threshold value of runoff in the field for a range of physical soil properties and range of slopes in the typical arid regions, in order to find out a specific range runoff efficiency.
3. To construct a field site micro-catchment for growing other typical crops example alfalfa and test the model values in the field against a set of experimental results. This is seen as a priority area for continuing the work and would allow the model to be fine-turned against results.
4. Carry out a sensitivity analysis for specific crops and a range of rainfall at different probability to assess the effect of changes in rainfall and probability in micro-catchment size.

Appendix A: Estimating of Reference Evapotranspiration (Eto) and Crop evaporative Demand

A.1 Reference Evapotranspiration (Eto)

Penman's (1948) equation which is modified by Kotsopoulos and Babajimopoulos (1997), states that the daily evaporative demand can be computed for a reference crop by:

$$ET_o = C * \left[\frac{\Delta}{\Delta + \gamma} .* R_n + \frac{\gamma}{\Delta + \gamma} * Ea \right] \quad \text{(A.1)}$$

Where:

ET_o = reference crop evapotranspiration (mm/d)

C = adjustment factor

Δ = Slope of the saturation vapor pressure curve at mean air temperature (Millibars /°C)

γ= Psychrometric constant (millibars/°C)

Rn = net solar radiation in evaporation units (mm/d)

$Ea.$ = Aerodynamic term (mm/day)

A.1.1 The adjustment factor (C)

$$C = c_1 + c_2 + c_3 + c_4 + c_5 + c_6 + c_7 + c_8 \quad \text{(A.2)}$$

$$C_1 = 1.5033 - 1.5904(RH_{\max})^{-0.125} + 0.3216(R_s)^{0.2} \quad \text{(A.2-1)}$$

$$C_2 = -0.2454(U_d)^{2/3} + 0.03985(U_r)(U_d)^{0.4} \quad \text{(A.2-2)}$$

$$C_3 = +0.02215(U_d)^{0.55}(RH_{\max})^{0.45} + 0.002548(R_s)^{1.45}(U_d)^{2/3} \quad \text{(A.2-3)}$$

$$C_4 = -2.3464 * 10^{-6}(RH_{\max})^{1..5}(R_s)^{1..5}(U_r) \quad \text{(A.2-4)}$$

$$C_5 = -1.01086 * 10^{-7}(RH_{\max})^{1..5}(R_s)^{1..5}(U_r) \quad \text{(A.2-5)}$$

$$C_6 = -8.15849 * 10^{-6}(RH_{\max})^{1..5}(U_d)^{0.4}(U_r) \quad \text{(A.2-6)}$$

$$C_7 = -0.000496(R_s)^{1..5}(U_d)^{0.4}(U_r) \quad \text{(A.2-7)}$$

$$C_8 = +1.19257 * 10^{-6}(RH_{\max})^{1..5}(R_s)^{1..5}(U_d)^{0.4}(U_r) \quad \text{(A.2-8)}$$

Where:

RH_{max} = maximum relative humidity (%)

R_s = solar radiation (mm/d)

U_d = mean wind velocity (m/s), and

U_r = expresses the ratio between daytime (7:00 a.m.- 7.00 p.m.) and night time (7.00 PM.- 7.00 Am.) wind speed.

A.1.2 The aerodynamic term (E_a)

The aerodynamic term has been described in several different forms in which most commons is

$$E_a = f(u)(e_s - e_d) \qquad \text{(A.3)}$$

Which f *(u)* denoted as:

$$f(u) = 0.27\left(1 + \frac{U}{100}\right) \qquad \text{(A.3-1)}$$

Where:

Ea = aerodynamic term (mm/day)

e_s = Saturation atmospheric vapour pressure (millibars)

e_d = Actual vapor pressure (millibars)

U = Wind speed (Km/day) at some reference height h generally 2 meters. The units on wind speed are dependent on the time base of (1); for example if Rn is expressed in mm/d then wind speed is in m/d or km/d.

A.1.3 Saturation vapor pressure

Several equations have been developed to describe the saturation vapor pressure, e_s, as a function of air temperature (T). The proposed equation here has the form of Svehlik's (1987) and Kotsopoulos et al (1997) equations and is the following:

$$e_s = (6.1051.e^x) \text{ (Millibar)} \qquad \text{(A.4)}$$

Where:

e = Base of natural logarithms ($e = 2.71828283$) and

$$x = \frac{18.0788.T - 0.00254.T^2}{T + 248.57} \qquad \text{(A.4-1)}$$

Vapor pressure of the air (e_d) can be calculated as a function of relative humidity (*Rh*), (Allen, 1996).

$$e_d = (e_s * RH_{mea})/100 \text{ (Millibar)} \quad \text{(A.5)}$$

Where:

RH_{mea} = mean air humidity (%)

A.1.4 Slope of saturation vapor pressure (Δ)

The slope of saturation vapor pressure (Δ) with respect to air temperature, T, may be calculated from (5) and has the following form:

$$\Delta = e_s \cdot \left[\frac{4650.79}{(T + 248.57)^2} - 0.00254 \right] \quad \text{(A.6)}$$

A.1.5 The psychrometric constant (γ)

$$\gamma = 0.38585 * \frac{P}{597.3 - 0.566 * T_c} \quad \text{(A.7)}$$

Where:

P = Atmospheric pressure (mm Hg) and may be calculated as follows:

$$P = 0.75\left(1013.2 - \frac{Alt}{9.3}\right) \quad \text{(A.7-1)}$$

Where: Alt = altitude of the location in meters above mean see level

A.1.6 The net solar radiation (Rn)

The net solar radiation, *Rn*, is estimated as a function of the extraterrestrial radiation, *Ra*, and the maximum sunshine hours, *N* (Doorenbos and Pruitt 1977). To calculate *Rn* the different steps involved are:

$$R_n = E_i - E_o \quad \text{(A.8)}$$

Where:

E_i = incoming radiation (energy)

E_o = outgoing radiation (energy)

A.1.7 The incoming radiation (E_i)

$$E_i = R_a(a + b * \frac{n}{N})(1 - r) \quad \text{(A.9)}$$

The incoming radiation is a function of daily values of extraterrestrial radiation (Ra) and can be estimated by the equation:

$$Rs = (a+b*n/N)\ Ra \qquad \text{(A.10)}$$

Where:

N = maximum daily sunshine duration and n is actual daily sunshine hours.

a, b = constants to be determined experimentally (defult values used in the program are a = 0.25, and b = 0.53)

r = reflection coefficient (crop albedo) = 0.25 for grass

A.1.8 The extraterrestrial radiation (R_a)

Daily values of extraterrestrial radiation can be estimated analytically from the latitude of location (La) and the calendar day (l) by improved equation of Duffie and Beckman (1980); Evapotranspiration (1990) derived by Kotsopoulos and Babajimopoulos (1997).

$$Ra = \left[M + c_1.\cos\left(\frac{2\pi l}{365} + c_2\right) + c_3.\cos\left(\frac{4\pi l}{365} + c_4\right)\right] \qquad \text{(A.11)}$$

Where:

$$M = 14.6008 + 3.6467.10^{-3}.La - 2.5243.10^{-3}.La^2 + 1.12618.10^{-5}.La^{-3} \qquad \text{(A.11-1)}$$

$$c_1 = -0.5033 + 0.167828.La - 1.0012.10^{-5}.La^2 - 7.3082.10^{-6}.La^3 \qquad \text{(A.11-2)}$$

$$c_2 = 3.1304 + 0.02034.La - 0.000641.La^2 + 6.1547.10^{-6}.La^3 \qquad \text{(A.11-3)}$$

$$c_3 = 0.6228 + 4.1487.10^{-3}.La - 1.94428.10^{-4}.La^2 - 2.7384.10^{-6}.La^3 \qquad \text{(A.11-4)}$$

$$c_4 = 3.4721 - 0.000647.La - 0.000047.La^2 \qquad \text{(A.11-5)}$$

A.1.9 Maximum Sunshine Duration (N)

The required daily maximum sunshine value, N, can be estimated analytically from the latitude of the location, La, and the calendar day, l, Kotsopoulos and Babajimopoulos (1997) suggest the following equation for the estimation of N:

$$N = \omega_s.\left(\frac{24}{\pi}\right) + M \qquad \text{(A.12)}$$

Where:

$$M = 0.1172 + 0.0008936.La + 7.4152.La^3. \qquad \text{(A.12-1)}$$

The calculation of ωs based on δ computed by equation:

$$\omega_s = \arccos\left[-\tan\left(\frac{2\pi.La}{360}\right).\tan(\delta)\right]. \quad \text{(rad)} \qquad \text{(A.13)}$$

Where:

ω_s = sunset hour angle (in rad); La = latitude in degrees; and δ = solar declination (rad).

$$\delta = 0.4093\sin\left[\frac{2\pi.(283+l}{365}\right] \qquad \text{(rad)} \qquad \text{(A.14)}$$

Where:

l = the number of the day in the year.

A.1.10 The out going energy (E_o)

The out going radiation or net long wave radiation (Eo) can be determined from available temperature (T), vapor pressure (e_d) and ratio n/N data.

$$Rn = \sigma T_k^4 (0.56 - 0.092\sqrt{ed}) * (0.1 + 0.9n/N) \qquad \text{(A.15)}$$

Where:

σT_k^4 is black body radiation at mean air temperature.

$\sigma = 2.018 * 10^{-9}$ (Stefan Boltzmann's constant $mmd^{-1}*K^{-4}$),

T_k = absolute temperature (= Tc+273.15).

A. 2 Crop evaporative demand

The calculation procedure for crop evaporative demand, consist of:

1. identify the length of crop growth stages, and selecting the basal crop coefficients;
2. adjusting the selected basal crop coefficients for climatic conditions during stage;
3. determining basal crop coefficient values for any period during the growing season
4. estimating leaf area index
5. calculating crop transpiration and soil evaporation

The basal crop coefficient for periods of growth stages is calculated as following:

$$K_{cb,mid,end} = K_{cb,mid,end}(Tab) + [0.04(u_2 - 2) - 0.004(RH_{mea} - 45)]\left(\frac{h}{3}\right)^{0.3} \quad \text{A.16}$$

Where:

$K_{cb,mid,end}$ is value for basal crop coefficient (K_{cb}) in mid or end of crop growing season,

U_2 is mean value for daily wind speed at 2-meter height over grass during the mid or late season growth stage [ms^{-1}],

RH_{mea} is mean value for daily relative humidity during the mid or late season stage (%),

h is mean plant height during the mid or late season stage [m].

The basal crop coefficient during, (K_{cb}) between the end of the previous stage ($K_{cb,prev}$) and at the beginning of the next stage ($K_{cb,next}$), is estimated as:

$$K_{cbi} = K_{cbi,prev} + \left[\frac{d_i - \sum(L_{prv})}{L_{stage}}\right](K_{cb,next} - K_{cb,prev}) \quad \text{A.17}$$

Where:

d_i is day number within the growing season [1...length of the growing season]

K_{cbi} is basal crop coefficient on day I,

L stage length of the stage under consideration (days)

Σ(Lstage) is sum of the lengths of all previous stages (days)

Basal crop coefficient full ($K_{cb\ full}$) can be estimated from the following equation:

$$K_{cb,full} = K_{cb,h} + [0.04(u_2 - 2) - 0.004(RH_{mea} - 45)]\left(\frac{h}{3}\right)^{0.3} \quad \text{A.18}$$

Where:

$K_{cb,h}$ is estimated as: $K_{cb,h}$ = 1+0.1 for h ≤ 2 m. where $K_{cb,h}$ is limited to ≤ 1.2 when h> 2 m.

The leaf area index values of the individual plantings are estimated by equation:

$$Lai = -1.4\ln\left[1 - \frac{K_{cb} - K_{c,\min}}{K_{cb,full} - K_{c,\min}}\right] \quad \text{A.19}$$

Where:

$K_{c,min}$ is the minimum basal crop coefficient for bare soil (= 0.15-0.2),

$K_{cb,full}$ is the maximum mid season K_c expected for the crop,

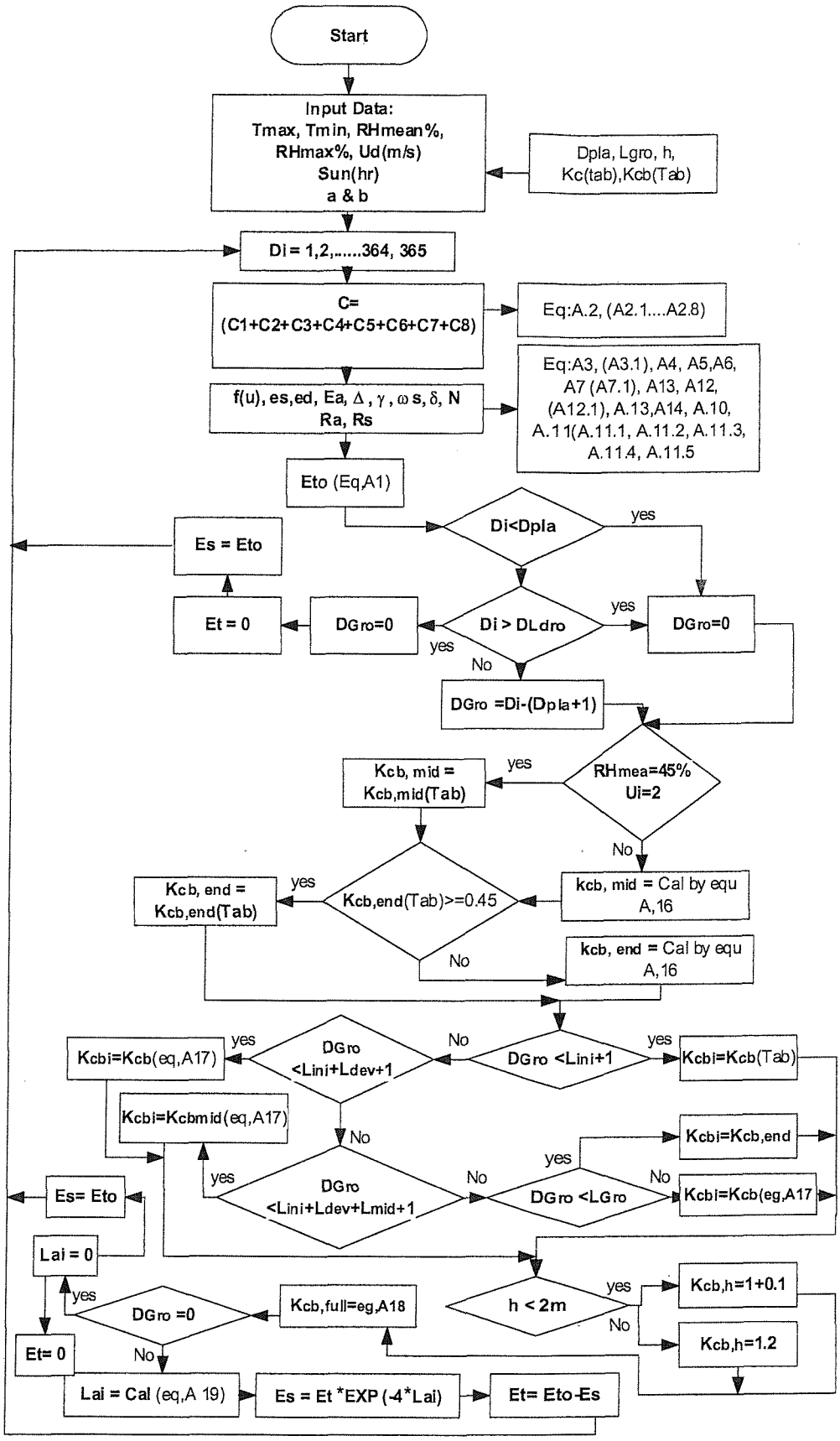

Figure A.1 Flowchart of Auxiliary Algorithm for computation of Reference evapotranspiration and Crop evaporative Demand

Table A1: Calculation of Reference evapotranspiration, Potential evaporation and Potential transpiration (for Pistachio) in three climatic stations of Iran (Shiraz, Esfahan and Kashan)

	Shiraz	Shiraz	Shiraz	Kashan	Kashan	Kashan	Esfahan	Esfahan	Esfahan
Day	Refe eva(Eto)	Pot eva(Ep)	Pot T(Et)	Ref eva(Eto)	Pot,eva(Es)	Pot T (Et)	Ref eva(Eto)	Pot eva(Ep)	Pot T(Et)
1	1.47	1.47	0	1.31	1.31	0	1.16	1.16	0
2	1.50	1.49	0	1.32	1.32	0	1.11	1.139	0
3	1.46	1.47	0	1.29	1.29	0	1.13	1.136	0
4	1.39	1.43	0	1.24	1.24	0	1.11	1.12	0
5	1.43	1.43	0	1.24	1.24	0	1.14	1.13	0
10	1.46	1.45	0	1.24	1.24	0	1.10	1.11	0
15	1.39	1.40	0	1.35	1.35	0	1.09	1.10	0
20	1.53	1.50	0	1.41	1.41	0	1.19	1.19	0
25	1.60	1.61	0	1.47	1.47	0	1.29	1.27	0
30	1.77	1.72	0	1.63	1.63	0	1.44	1.40	0
35	1.94	1.99	0	1.83	1.83	0	1.69	1.66	0
40	2.31	2.22	0	2.01	2.01	0	2.06	1.94	0
45	2.32	2.31	0	2.17	2.17	0	2.10	2.12	0
50	2.54	2.47	0	2.46	2.46	0	2.51	2.40	0
55	2.57	2.59	0	2.47	2.47	0	2.63	2.54	0
60	3.16	3.00	0	3.06	3.06	0	2.92	2.86	0
65	3.46	3.36	0	3.20	3.20	0	3.17	3.09	0
70	3.52	3.53	0	3.15	3.15	0	3.14	3.19	0
75	3.56	3.55	0	3.32	3.32	0	3.39	3.30	0
80	3.75	3.73	0	3.39	3.39	0	3.49	3.36	0
85	3.82	3.93	0	3.65	3.65	0	3.67	3.63	0
90	4.37	4.28	0	4.31	4.31	0	3.86	3.81	0
95	4.44	4.49	0	4.87	4.87	0	4.53	4.34	0
100	4.89	4.82	0	4.96	4.96	0	4.62	4.50	0
101	4.92	4.86	0.06	5.06	5.06	0.01	4.83	4.66	0.17
102	4.88	4.85	0.03	5.17	5.15	0.03	4.81	4.71	0.10
103	5.14	4.96	0.18	5.17	5.12	0.05	4.84	4.74	0.10
104	5.16	5.00	0.16	5.08	5.00	0.08	4.71	4.68	0.03
105	4.88	4.87	0.01	5.83	5.71	0.12	4.91	4.73	0.18
107	5.43	5.08	0.34	5.43	5.25	0.18	4.90	4.77	0.13
108	5.53	5.17	0.36	5.16	4.95	0.20	4.97	4.76	0.21
110	5.39	5.07	0.32	5.43	5.14	0.29	4.97	4.74	0.23
113	5.38	5.03	0.35	5.33	4.93	0.39	5.15	4.79	0.36
114	5.41	4.97	0.44	5.26	4.83	0.43	5.09	4.71	0.37
116	5.45	4.89	0.56	5.38	4.86	0.52	5.08	4.56	0.53
118	5.03	4.71	0.32	5.85	5.20	0.65	5.47	4.73	0.74
120	5.88	5.00	0.87	5.98	5.23	0.75	5.45	4.74	0.71
122	6.83	5.63	1.20	5.70	4.92	0.78	5.50	4.72	0.78
124	6.63	5.61	1.01	6.04	5.12	0.92	5.54	4.64	0.90
126	6.61	5.50	1.11	6.14	5.10	1.04	5.42	4.41	1.02
128	6.45	5.31	1.14	6.06	4.95	1.11	5.50	4.49	1.01
130	6.63	5.27	1.37	5.96	4.80	1.16	5.47	4.44	1.03
132	6.55	5.15	1.39	6.06	4.79	1.28	5.53	4.32	1.22
134	6.58	5.07	1.51	6.48	5.01	1.47	6.04	4.46	1.58

136	6.73	5.03	1.69	6.28	4.76	1.52	5.84	4.38	1.46
138	6.76	5.02	1.73	6.37	4.75	1.62	5.66	4.27	1.40
140	6.65	4.83	1.82	6.72	4.90	1.82	6.08	4.27	1.81
142	6.80	4.76	2.04	6.67	4.76	1.90	5.68	4.06	1.63
144	6.60	4.61	1.99	6.70	4.66	2.03	5.61	3.94	1.67
146	6.73	4.51	2.21	6.91	4.69	2.22	5.95	3.94	2.01
148	6.91	4.52	2.39	6.71	4.46	2.26	6.09	3.93	2.17
150	7.06	4.44	2.63	7.12	4.58	2.53	6.20	3.91	2.30
152	7.85	4.64	3.20	7.02	4.39	2.63	6.27	3.84	2.44
154	7.89	4.75	3.14	6.92	4.23	2.69	6.53	3.87	2.66
156	7.50	4.51	2.99	7.23	4.28	2.95	6.47	3.82	2.64
158	7.66	4.36	3.29	7.30	4.19	3.11	6.54	3.70	2.84
160	7.66	4.23	3.43	7.00	3.89	3.11	6.59	3.66	2.93
161	7.79	4.17	3.62	6.82	3.73	3.09	6.19	3.51	2.67
162	7.64	4.05	3.59	6.84	3.68	3.16	6.14	3.38	2.76
163	7.63	3.95	3.67	7.66	4.03	3.64	6.35	3.33	3.02
164	7.50	3.84	3.66	7.21	3.71	3.50	6.56	3.31	3.25
165	7.76	3.79	3.96	7.12	3.59	3.53	6.47	3.24	3.23
166	7.68	3.71	3.96	7.59	3.74	3.85	6.78	3.25	3.53
167	7.44	3.57	3.87	7.06	3.41	3.65	6.29	3.13	3.16
168	7.38	3.44	3.94	6.69	3.17	3.52	6.39	3.04	3.34
170	7.27	3.22	4.05	6.93	3.12	3.81	6.47	2.87	3.60
172	7.38	1.24	6.14	7.44	2.11	5.34	6.15	1.88	4.27
174	7.26	0.74	6.53	7.24	1.18	6.06	6.25	1.09	5.16
176	7.43	0.62	6.81	7.23	0.79	6.44	6.26	0.72	5.54
178	7.32	0.58	6.73	7.31	0.47	6.84	6.64	0.53	6.11
180	7.10	0.57	6.53	7.54	0.63	6.91	6.61	0.54	6.06
182	6.54	0.54	6.00	7.04	0.63	6.41	6.79	0.56	6.23
183	6.74	0.54	6.20	7.04	0.61	6.43	6.48	0.54	5.94
184	6.65	0.53	6.11	7.26	0.62	6.64	7.00	0.54	6.46
186	6.68	0.53	6.15	7.30	0.58	6.72	6.59	0.52	6.07
187	6.96	0.54	6.42	7.32	0.58	6.74	6.60	0.51	6.09
188	7.08	0.55	6.53	7.62	0.59	7.02	7.17	0.52	6.66
190	7.04	0.55	6.48	7.51	0.49	7.02	7.01	0.52	6.50
191	7.17	0.56	6.61	7.63	0.54	7.09	7.00	0.53	6.47
192	7.24	0.57	6.67	7.83	0.59	7.24	7.23	0.54	6.68
194	7.38	0.58	6.80	7.81	0.60	7.21	7.00	0.57	6.42
196	7.26	0.58	6.68	6.98	0.60	6.38	6.37	0.56	5.81
198	7.39	0.59	6.81	7.25	0.60	6.65	6.77	0.54	6.23
200	7.20	0.57	6.63	7.21	0.57	6.65	6.65	0.53	6.12
202	7.17	0.57	6.60	6.91	0.56	6.36	6.72	0.54	6.18
204	7.25	0.58	6.68	7.20	0.56	6.64	6.55	0.52	6.03
205	7.35	0.58	6.77	7.11	0.56	6.55	6.82	0.51	6.31
206	7.52	0.59	6.93	6.96	0.54	6.42	6.81	0.51	6.29
208	6.88	0.57	6.32	7.32	0.55	6.77	6.85	0.48	6.36
210	7.02	0.56	6.45	7.33	0.57	6.77	6.72	0.52	6.20
212	6.97	0.96	6.01	7.03	0.80	6.23	6.85	0.57	6.28
213	6.82	1.17	5.66	6.87	0.95	5.91	6.57	0.70	5.87
214	6.71	1.35	5.36	6.73	1.12	5.61	6.09	0.88	5.21

215	7.02	1.58	5.45	6.98	1.36	5.62	6.57	1.10	5.47
216	6.67	1.73	4.95	6.80	1.51	5.29	6.15	1.28	4.87
217	6.77	1.89	4.88	7.09	1.76	5.33	6.46	1.50	4.96
218	6.86	2.06	4.80	7.13	1.93	5.20	6.22	1.59	4.63
219	7.04	2.24	4.80	7.41	2.18	5.24	6.47	1.77	4.70
220	7.07	2.41	4.66	7.14	2.25	4.88	6.45	1.92	4.53
221	7.08	2.56	4.52	7.06	2.38	4.67	6.57	2.09	4.48
222	6.78	2.64	4.14	6.48	2.33	4.15	6.36	2.21	4.15
224	6.58	2.80	3.78	6.54	2.61	3.93	6.48	2.46	4.02
226	6.74	3.05	3.69	7.11	3.07	4.04	6.52	2.71	3.81
228	6.88	3.29	3.59	6.37	2.97	3.40	6.20	2.87	3.33
230	6.85	3.52	3.33	6.66	3.30	3.36	6.12	3.01	3.11
232	6.64	3.64	3.00	7.00	3.67	3.33	6.11	3.16	2.95
234	6.52	3.75	2.76	6.54	3.63	2.91	6.07	3.33	2.74
237	6.41	3.89	2.52	6.52	3.88	2.64	5.76	3.46	2.30
240	6.16	4.04	2.12	6.31	3.99	2.31	5.70	3.60	2.10
242	6.12	4.15	1.97	6.63	4.34	2.29	5.75	3.73	2.02
245	6.29	4.43	1.86	6.32	4.37	1.96	5.48	3.83	1.64
246	6.75	4.67	2.08	6.02	4.23	1.79	5.47	3.87	1.61
248	6.59	4.88	1.70	6.18	4.47	1.70	5.48	3.95	1.53
250	5.96	4.68	1.29	5.76	4.30	1.46	5.36	4.03	1.33
253	5.74	4.62	1.12	5.67	4.42	1.26	5.14	4.07	1.08
254	5.67	4.62	1.05	5.69	4.49	1.20	5.10	4.08	1.02
257	5.95	4.92	1.04	5.45	4.47	0.98	4.95	4.07	0.87
258	5.80	4.93	0.87	5.94	4.92	1.01	4.83	4.07	0.76
260	5.60	4.90	0.70	5.55	4.72	0.83	4.95	4.20	0.75
265	5.61	5.54	0	5.16	5.08	0	4.52	4.58	0
270	5.34	5.28	0	4.94	4.93	0	4.42	4.40	0
275	4.15	4.39	0	4.26	4.26	0	3.89	3.98	0
280	3.83	3.92	0	3.93	3.93	0	3.66	3.72	0
285	3.71	3.75	0	3.72	3.72	0	3.23	3.29	0
290	3.59	3.63	0	3.60	3.60	0	3.13	3.17	0
295	3.52	3.52	0	3.46	3.46	0	3.03	3.06	0
300	3.28	3.27	0	3.30	3.30	0	2.93	2.96	0
305	3.24	3.14	0	3.00	3.00	0	2.43	2.54	0
310	2.98	3.02	0	2.85	2.85	0	2.25	2.30	0
315	2.75	2.80	0	2.62	2.62	0	2.11	2.14	0
320	2.65	2.67	0	2.21	2.21	0	1.93	1.93	0
325	2.40	2.44	0	2.21	2.21	0	1.76	1.77	0
330	2.30	2.30	0	2.05	2.05	0	1.65	1.66	0
335	1.76	1.95	0	1.73	1.73	0	1.44	1.47	0
340	1.70	1.74	0	1.52	1.52	0	1.32	1.35	0
345	1.60	1.60	0	1.52	1.52	0	1.30	1.31	0
350	1.55	1.61	0	1.39	1.39	0	1.24	1.27	0
355	1.64	1.61	0	1.36	1.36	0	1.22	1.23	0
360	1.51	1.52	0	1.30	1.30	0	1.19	1.19	0
365	1.58	1.54	0	1.31	1.31	0	1.19	1.19	0

Appendix B: Rainfall-Runoff tables and Figures

This appendix consists of some tables and some figures of rainfall runoff sub model, relationships, which was analysed in chapter 7.

Table B1: Computation of Potential Runoff in storm (S1) and Sandy Clay loam soil

S1	Computation of rainfall excess in a Sandy Clay loam soil															
Time	R(ts)	T-step	T-cum	R(ts)	Ri(ts)	Rc(ts)	f(t)	F	1/F	fpr(t)	tpr(t)	tdel	tact	fac(t)	Rexc	Σ Rexc
(min)	(mm)	(min)	(min)	(mm)	(mm/h)	(mm)	(mm)	(mm)	(1/mm)	(mm/h)	(min)	(min)	(min)	mm/h	mm	mm
1	2	3	4	5	6	7	8	9	10	11	12	13	14	15	16	17
0	0	0	0	0	0	0	0	0	0	70	0	0	0	0	0	0
	1	5	5	0.5	6	0.5	0.5	0.5	2	242	0	0	0	0	0	0
	1	5	10	0.5	6	1	0.5	1	1	123.4	0	0	0	0	0	0
10	5	5	15	2.5	30	3.5	2.5	3.5	0.29	38.7	0	0	0	0	0	0
	5	5	20	2.5	30	6	2.5	6	0.17	24.6	10.9	9.08	10.9	24.6	0.45	0.45
20-30	11.5	0.5	20.5	0.58	69	6.58	0.58	6.58	0.15	22.6	12.9	7.59	12.9	22.8	0.38	0.84
	11.5	0.5	21	0.58	69	7.15	0.58	7.15	0.14	21.4	15	6	15	21.4	0.4	1.23
	11.5	0.5	21.5	0.58	69	7.73	0.58	7.73	0.13	20.2	17.2	4.31	17.2	20.2	0.41	1.64
	11.5	0.5	22	0.58	69	8.3	0.58	8.3	0.12	19.1	19.5	2.54	19.5	19.1	0.42	2.06
	11.5	0.5	22.5	0.58	69	8.88	0.58	8.88	0.11	18.2	21.8	0.7	21.8	18.2	0.42	2.48
	11.5	0.5	23	0.58	69	9.45	0.58	9.45	0.11	17.4	24.2	-1.2	25.4	17	0.43	2.91
	11.5	0.5	23.5	0.58	69	10	0.58	10	0.1	16.6	26.7	-3.2	29.8	15.8	0.44	3.36
	11.5	0.5	24	0.58	69	10.6	0.58	10.6	0.10	16	29.2	-5.2	34.4	14.9	0.45	3.81
	11.5	0.5	24.5	0.58	69	11.2	0.58	11.2	0.09	15.4	31.7	-7.2	39	14.1	0.46	4.26
	11.5	0.5	25	0.58	69	11.8	0.58	11.8	0.09	14.9	34.3	-9.3	43.7	13.4	0.46	4.73
	11.5	0.5	25.5	0.58	69	12.3	0.58	12.3	0.08	14.4	36.9	-11	48.4	12.8	0.47	5.20
	11.5	0.5	26	0.58	69	12.9	0.58	12.9	0.08	14	39.6	-14	53.2	12.3	0.47	5.67
	11.5	0.5	26.5	0.58	69	13.5	0.58	13.5	0.07	13.6	42.3	-16	58	11.9	0.48	6.14
	11.5	0.5	27	0.58	69	14.1	0.58	14.1	0.07	13.3	44.9	-18	62.9	11.4	0.48	6.62
	11.5	0.5	27.5	0.58	69	14.6	0.58	14.6	0.07	12.9	47.6	-20	67.7	11.1	0.48	7.11
	11.5	0.5	28	0.58	69	15.2	0.58	15.2	0.07	12.6	50.3	-22	72.6	10.7	0.49	7.53
	11.5	0.5	28.5	0.58	69	15.8	0.58	15.8	0.06	12.3	53	-25	77.5	10.4	0.49	8.08
	11.5	0.5	29	0.58	69	16.4	0.58	16.4	0.06	12.1	55.7	-27	82.4	10.2	0.49	8.57
	11.5	0.5	29.5	0.58	69	16.9	0.58	16.9	0.06	11.8	58.4	-29	87.3	9.91	0.49	9.06
	11.5	0.5	30	0.58	69	17.5	0.58	17.5	0.06	11.6	61.1	-31	92.2	9.68	0.49	9.56
30-40	11	0.5	30.5	0.55	66	18.1	0.55	18.1	0.06	11.4	63.7	-33	96.8	9.47	0.47	10.0
	11	0.5	31	0.55	66	18.6	0.55	18.6	0.05	11.2	66.2	-35	101	9.28	0.47	10.5
	11	0.5	31.5	0.55	66	19.2	0.55	19.2	0.05	11	68.8	-37	106	9.1	0.47	11.0
	11	0.5	32	0.55	66	19.7	0.55	19.7	0.05	10.8	71.3	-39	111	8.94	0.48	11.4
	11	0.5	32.5	0.55	66	20.3	0.55	20.3	0.05	10.7	73.8	-41	115	8.78	0.48	11.9
	11	0.5	33	0.55	66	20.8	0.55	20.8	0.05	10.5	76.3	-43	120	8.64	0.48	12.4
	11	0.5	33.5	0.55	66	21.4	0.55	21.4	0.05	10.4	78.8	-45	124	8.5	0.48	12.9
	11	0.5	34	0.55	66	21.9	0.55	21.9	0.05	10.2	81.3	-47	129	8.37	0.48	13.4
	11	0.5	34.5	0.55	66	22.5	0.55	22.5	0.05	10.1	83.8	-49	133	8.24	0.48	13.9
	11	0.5	35	0.55	66	23	0.55	23	0.04	9.96	86.3	-51	138	8.13	0.48	14.3
	11	0.5	35.5	0.55	66	23.6	0.55	23.6	0.04	9.84	88.7	-53	142	8.02	0.48	14.8
	11	0.5	36	0.55	66	24.1	0.55	24.1	0.04	9.73	91.1	-55	146	7.91	0.48	15.3

	11	0.5	36.5	0.55	66	24.7	0.55	24.7	0.04	9.62	93.5	-57	150	7.81	0.48	15.8
	11	0.5	37	0.55	66	25.2	0.55	25.2	0.04	9.51	95.9	-59	155	7.72	0.49	16.3
	11	0.5	37.5	0.55	66	25.8	0.55	25.8	0.04	9.41	98.2	-61	159	7.63	0.49	16.8
	11	0.5	38	0.55	66	26.3	0.55	26.3	0.04	9.32	101	-63	163	7.54	0.49	17.2
	11	0.5	38.5	0.55	66	26.9	0.55	26.9	0.04	9.23	103	-64	167	7.46	0.49	17.7
	11	0.5	39	0.55	66	27.4	0.55	27.4	0.04	9.14	105	-66	171	7.38	0.49	18.2
	11	0.5	39.5	0.55	66	28	0.55	28	0.04	9.05	107	-68	175	7.31	0.49	18.7
	11	0.5	40	0.55	66	28.5	0.55	28.5	0.04	8.97	110	-70	179	7.23	0.49	19.2
40-50	6.5	0.5	40.5	0.33	39	28.8	0.33	28.8	0.04	8.92	111	-71	182	7.2	0.27	19.5
	6.5	0.5	41	0.33	39	29.2	0.33	29.2	0.04	8.88	112	-71	184	7.16	0.27	19.7
	6.5	0.5	41.5	0.33	39	29.5	0.33	29.5	0.04	8.83	114	-72	186	7.12	0.27	20.0
	6.5	0.5	42	0.33	39	29.8	0.33	29.8	0.04	8.79	115	-73	188	7.09	0.27	20.3
	6.5	0.5	42.5	0.33	39	30.1	0.33	30.1	0.03	8.75	116	-74	190	7.06	0.27	20.5
	6.5	0.5	43	0.33	39	30.5	0.33	30.5	0.03	8.70	118	-75	192	7.02	0.27	20.8
	6.5	0.5	43.5	0.33	39	30.8	0.33	30.8	0.03	8.66	119	-75	194	6.99	0.27	21.1
	6.5	0.5	44	0.33	39	31.1	0.33	31.1	0.03	8.62	120	-76	196	6.96	0.27	21.3
	6.5	0.5	44.5	0.33	39	31.4	0.33	31.4	0.03	8.58	121	-77	198	6.93	0.27	21.6
	6.5	0.5	45	0.33	39	31.8	0.33	31.8	0.03	8.54	123	-78	200	6.9	0.27	21.9
	6.5	0.5	45.5	0.33	39	32.1	0.33	32.1	0.03	8.51	124	-78	202	6.87	0.27	22.1
	6.5	0.5	46	0.33	39	32.4	0.33	32.4	0.03	8.47	125	-79	204	6.84	0.27	22.4
	6.5	0.5	46.5	0.33	39	32.7	0.33	32.7	0.03	8.43	126	-80	206	6.81	0.27	22.7
	6.5	0.5	47	0.33	39	33.1	0.33	33.1	0.03	8.40	128	-81	208	6.78	0.27	22.9
	6.5	0.5	47.5	0.33	39	33.4	0.33	33.4	0.03	8.36	129	-81	210	6.75	0.27	23.2
	6.5	0.5	48	0.33	39	33.7	0.33	33.7	0.03	8.33	130	-82	212	6.72	0.27	23.5
	6.5	0.5	48.5	0.33	39	34	0.33	34	0.03	8.29	131	-83	214	6.7	0.27	23.8
	6.5	0.5	49	0.33	39	34.4	0.33	34.4	0.03	8.26	132	-83	216	6.67	0.27	24.0
	6.5	0.5	49.5	0.33	39	34.7	0.33	34.7	0.03	8.23	134	-84	218	6.65	0.27	24.3
	6.5	0.5	50	0.33	39	35	0.33	35	0.03	8.20	135	-85	220	6.62	0.27	24.6
50-60	1	5	55	0.5	6	35.5	0.5	35.5	0.03	8.15	0	0	0	0	0	24.6
	1	5	60	0.5	6	36	0.5	36	0.03	8.10	0	0	0	0	0	24.6

Table B2: Computation of Potential runoff in storm (S2) and in Sandy Clay Loam soil

S2	**Computation of rainfall excess in a Sandy Clay loam soil**															
Time	R(ts)	T-step	T-cum	R(ts)	Ri(ts)	Rc(ts)	f(t)	F	1/F	fpr(t)	tpr(t)	tdel	tact	fac(t)	Rexc	Σ Rexc
(min)	(mm)	(min)	(min)	(mm)	(mm/h)	(mm)	(mm)	(mm)	(1/mm)	(mm/h)	(min)	(min)	(min)	mm/h	mm	mm
1	2	3	4	5	6	7	8	9	10	11	12	13	14	15	16	17
0	0	0	0	0	0	0	0	0	0	70	0	0	0	0	0	0
0-10	0.5	10	10	0.5	3	0.5	0.5	0.5	2	242	0	0	0	0	0	0
10.-20	0.5	10	20	0.5	3	1	0.5	1	1	123.4	0	0	0	0	0	0
20-30	0.5	10	30	0.5	3	1.5	0.5	1.5	0.67	83.89	0	0	0	0	0	0
30-40	0.5	10	40	0.5	3	2	0.5	2	0.5	64.12	0	0	0	0	0	0
40-50	0.5	10	50	0.5	3	2.5	0.5	2.5	0.4	52.26	0	0	0	0	0	0
50-60	3	5	55	1.5	18	4	1.5	4	0.25	34.46	0	0	0	0	0	0
	3	5	60	1.5	18	5.5	1.5	5.5	0.18	26.37	0	0	0	0	0	0

Table B3: Computation of Potential runoff in Storm (S3) and in Sandy Clay Loam soil

S3	Computation of rainfall excess in a Sandy Clay loam soil															
Time	R(ts)	T-step	T-cum	R(ts)	Ri(ts)	Rc(ts)	f(t)	F	1/F	fpr(t)	tpr(t)	tdel	tact	fac(t)	Rexc	Σ Rexc
(min)	(mm)	(min)	(min)	(mm)	(mm/h)	(mm)	(mm)	(mm)	(1/mm)	(mm/h)	(min)	(min)	(min)	mm/h	mm	mm
1	2	3	4	5	6	7	8	9	10	11	12	13	14	15	16	17
0	0	0	0	0	0	0	0	0	0	0	0	0	0	0	0	0
0-10	0.5	10	10	0.5	3	0.5	0.5	0.5	2	242	0	0	0	0	0	0
10.-20	3.5	5	15	1.75	21	2.25	1.75	2.25	0.44	57.53	0	0	0	0	0	0
	3.5	5	20	1.75	21	4	1.75	4	0.25	34.46	0	0	0	0	0	0
20-30	1.5	5	25	0.75	9	4.75	0.75	4.75	0.21	29.78	0	0	0	0	0	0
	1.5	5	30	0.75	9	5.5	0.75	5.5	0.18	26.37	0	0	0	0	0	0
30-40	5.5	0.5	30.5	0.28	33	5.78	0.28	5.78	0.17	25.35	10.2	20.3	10.2	25.3	0.06	0.06
	5.5	0.5	31	0.28	33	6.05	0.28	6.05	0.17	24.41	11.1	19.9	11.1	24.4	0.07	0.14
	5.5	0.5	31.5	0.28	33	6.33	0.28	6.33	0.16	23.56	12	19.5	12	23.6	0.08	0.21
	5.5	0.5	32	0.28	33	6.6	0.28	6.6	0.15	22.78	13	19	13	22.8	0.09	0.30
	5.5	0.5	32.5	0.28	33	6.88	0.28	6.88	0.15	22.06	14	18.5	14	22.1	0.09	0.39
	5.5	0.5	33	0.28	33	7.15	0.28	7.15	0.14	21.4	15	18	15	21.4	0.1	0.49
	5.5	0.5	33.5	0.28	33	7.43	0.28	7.43	0.14	20.78	16	17.5	16	20.8	0.1	0.59
	5.5	0.5	34	0.28	33	7.7	0.28	7.7	0.13	20.21	17.1	16.9	17.1	20.2	0.11	0.70
	5.5	0.5	34.5	0.28	33	7.98	0.28	7.98	0.13	19.68	18.2	16.3	18.2	19.7	0.11	0.81
	5.5	0.5	35	0.28	33	8.25	0.28	8.25	0.12	19.19	19.3	15.7	19.3	19.2	0.12	0.92
	5.5	0.5	35.5	0.28	33	8.53	0.28	8.53	0.12	18.72	20.4	15.1	20.4	18.7	0.12	1.04
	5.5	0.5	36	0.28	33	8.8	0.28	8.8	0.11	18.29	21.5	14.5	21.5	18.3	0.12	1.16
	5.5	0.5	36.5	0.28	33	9.08	0.28	9.08	0.11	17.88	22.6	13.9	22.6	17.9	0.13	1.29
	5.5	0.5	37	0.28	33	9.35	0.28	9.35	0.11	17.49	23.8	13.2	23.8	17.5	0.13	1.42
	5.5	0.5	37.5	0.28	33	9.63	0.28	9.63	0.10	17.13	25	12.5	25	17.1	0.13	1.55
	5.5	0.5	38	0.28	33	9.9	0.28	9.9	0.10	16.79	26.1	11.9	26.1	16.8	0.14	1.69
	5.5	0.5	38.5	0.28	33	10.2	0.28	10.2	0.10	16.46	27.3	11.2	27.3	16.5	0.14	1.82
	5.5	0.5	39	0.28	33	10.5	0.28	10.5	0.10	16.16	28.5	10.5	28.5	16.2	0.14	1.96
	5.5	0.5	39.5	0.28	33	10.7	0.28	10.7	0.09	15.87	29.7	9.76	29.7	15.9	0.14	2.11
	5.5	0.5	40	0.28	33	11	0.28	11	0.09	15.59	31	9.04	31	15.6	0.15	2.25
40-50	0.5	10	50	0.5	3	11.5	0.5	11.5	0.09	15.12	0	0	0	0	0	2.25
50-60	0.5	10	60	0.5	3	12	0.5	12	0.08	14.69	0	0	0	0	0	2.25
60-70	0.5	10	70	0.5	3	12.5	0.5	12.5	0.08	14.3	0	0	0	0	0	2.25

Table B4: Computation of Potential runoff in storm (S4) and in Sandy Clay Loam soil

S4	Computation of rainfall excess in a Sandy Clay loam soil															
Time	R(ts)	T-step	T-cum	R(ts)	Ri(ts)	Rc(ts)	f(t)	F	1/F	fpr(t)	tpr(t)	tdel	tact	fac(t)	Rexc	Σ Rexc
(min)	(mm)	(min)	(min)	(mm)	(mm/h)	(mm)	(mm)	(mm)	(1/mm)	(mm/h)	(min)	(min)	(min)	mm/h	mm	mm
1	2	3	4	5	6	7	8	9	10	11	12	13	14	15	16	17
0	0	0	0	0	0	0	0	0	0	0	0	0	0	0	0	0
0-10	0.5	10	10	0.5	3	0.5	0.5	0.5	2	242	0	0	0	0	0	0
10.-20	0.5	10	20	0.5	3	1	0.5	1	1	123.4	0	0	0	0	0	0
20-30	2	5	25	1	12	2	1	2	0.5	64.12	0	0	0	0	0	0
	2	5	30	1	12	3	1	3	0.33	44.35	0	0	0	0	0	0
30-40	5.5	5	35	2.75	33	5.75	2.75	5.75	0.17	25.44	10.1	24.9	10.1	25.4	0.63	0.63

	5.5	0.5	35.5	0.28	33	6.03	0.28	6.03	0.17	24.49	11	24.5	11	24.5	0.07	0.70
	5.5	0.5	36	0.28	33	6.3	0.28	6.3	0.16	23.64	11.9	24.1	11.9	23.6	0.08	0.78
	5.5	0.5	36.5	0.28	33	6.58	0.28	6.58	0.15	22.85	12.9	23.6	12.9	22.8	0.08	0.86
	5.5	0.5	37	0.28	33	6.85	0.28	6.85	0.15	22.12	13.9	23.1	13.9	22.1	0.09	0.95
	5.5	0.5	37.5	0.28	33	7.13	0.28	7.13	0.14	21.46	14.9	22.6	14.9	21.5	0.1	1.05
	5.5	0.5	38	0.28	33	7.4	0.28	7.4	0.14	20.84	15.9	22.1	15.9	20.8	0.1	1.15
	5.5	0.5	38.5	0.28	33	7.68	0.28	7.68	0.13	20.26	17	21.5	17	20.3	0.11	1.26
	5.5	0.5	39	0.28	33	7.95	0.28	7.95	0.13	19.73	18.1	20.9	18.1	19.7	0.11	1.37
	5.5	0.5	39.5	0.28	33	8.23	0.28	8.23	0.12	19.23	19.2	20.3	19.2	19.2	0.11	1.48
	5.5	0.5	40	0.28	33	8.5	0.28	8.5	0.12	18.76	20.3	19.7	20.3	18.8	0.12	1.60
40-50	0.5	10	50	0.5	3	9	0.5	9	0.11	17.99	0	0	0	0	0	1.60
50-60	0.5	10	60	0.5	3	9.5	0.5	9.5	0.11	17.29	0	0	0	0	0	1.60

Table B5: Computation of Potential runoff in storm (S8) and in Sandy Clay Loam soil

S8	**Computation of rainfall excess in a Sandy Clay loam soil**															
Time	R(ts)	T-step	T-cum	R(ts)	Ri(ts)	Rc(ts)	f(t)	F	1/F	fpr(t)	tpr(t)	tdel	tact	fac(t)	Rexc	Σ Rexc
(min)	(mm)	(min)	(min)	(mm)	(mm/h)	(mm)	(mm)	(mm)	(1/mm)	(mm/h)	(min)	(min)	(min)	mm/h	mm	mm
1	2	3	4	5	6	7	8	9	10	11	12	13	14	15	16	17
0	0	0	0	0	0	0	0	0	0	70	0	0	0	0	0	0
0-10	2	5	5	1	12	1	1	1	1	123.4	0	0	0	0	0	0
	2	5	10	1	12	2	1	2	0.5	64.12	0	0	0	0	0	0
10.-20	10	2	12	2	60	4	2	4	0.25	34.46	5.04	6.96	5.04	34.5	0.85	0.85
	10	0.5	12.5	0.5	60	4.5	0.5	4.5	0.22	31.17	6.34	6.16	6.34	31.2	0.24	1.09
	10	0.5	13	0.5	60	5	0.5	5	0.2	28.53	7.76	5.24	7.76	28.5	0.26	1.35
	10	0.5	13.5	0.5	60	5.5	0.5	5.5	0.18	26.37	9.29	4.21	9.29	26.4	0.28	1.63
	10	0.5	14	0.5	60	6	0.5	6	0.17	24.58	10.9	3.08	10.9	24.6	0.3	1.93
	10	0.5	14.5	0.5	60	6.5	0.5	6.5	0.15	23.06	12.6	1.86	12.6	23.1	0.31	2.24
	10	0.5	15	0.5	60	7	0.5	7	0.14	21.75	14.4	0.56	14.4	21.8	0.32	2.56
	10	0.5	15.5	0.5	60	7.5	0.5	7.5	0.13	20.62	16.3	-0.8	17.1	20.2	0.33	2.89
	10	0.5	16	0.5	60	8	0.5	8	0.13	19.63	18.3	-2.3	20.5	18.7	0.34	3.23
	10	0.5	16.5	0.5	60	8.5	0.5	8.5	0.12	18.76	20.3	-3.8	24	17.4	0.35	3.59
	10	0.5	17	0.5	60	9	0.5	9	0.11	17.99	22.3	-5.3	27.6	16.4	0.36	3.95
	10	0.5	17.5	0.5	60	9.5	0.5	9.5	0.11	17.29	24.4	-6.9	31.3	15.5	0.37	4.32
	10	0.5	18	0.5	60	10	0.5	10	0.1	16.67	26.6	-8.6	35.1	14.8	0.38	4.70
	10	0.5	18.5	0.5	60	10.5	0.5	10.5	0.10	16.1	28.7	-10	39	14.1	0.38	5.08
	10	0.5	19	0.5	60	11	0.5	11	0.10	15.59	31	-12	42.9	13.5	0.39	5.47
	10	0.5	19.5	0.5	60	11.5	0.5	11.5	0.09	15.12	33.2	-14	46.9	13	0.39	5.86
	10	0.5	20	0.5	60	12	0.5	12	0.08	14.69	35.5	-15	50.9	12.5	0.4	6.26
20-30	2.5	0.5	20.5	0.13	15	12.1	0.13	12.1	0.08	14.59	36	-16	51.6	12.5	0.02	6.28
	2.5	0.5	21	0.13	15	12.3	0.13	12.3	0.08	14.49	36.6	-16	52.2	12.4	0.02	6.30
	2.5	0.5	21.5	0.13	15	12.4	0.13	12.4	0.08	14.39	37.2	-16	52.9	12.3	0.02	6.32
	2.5	0.5	22	0.13	15	12.5	0.13	12.5	0.08	14.3	37.7	-16	53.5	12.3	0.02	6.34
	2.5	0.5	22.5	0.13	15	12.6	0.13	12.6	0.08	14.2	38.3	-16	54.1	12.2	0.02	6.37
	2.5	0.5	23	0.13	15	12.8	0.13	12.8	0.08	14.11	38.9	-16	54.8	12.1	0.02	6.39
	2.5	0.5	23.5	0.13	15	12.9	0.13	12.9	0.08	14.02	39.5	-16	55.4	12.1	0.02	6.41
	2.5	0.5	24	0.13	15	13	0.13	13	0.08	13.93	40.1	-16	56.1	12	0.02	6.44
	2.5	0.5	24.5	0.13	15	13.1	0.13	13.1	0.08	13.84	40.6	-16	56.8	12	0.03	6.46

	2.5	0.5	25	0.13	15	13.3	0.13	13.3	0.08	13.76	41.2	-16	57.4	11.9	0.03	6.49
	2.5	0.5	25.5	0.13	15	13.4	0.13	13.4	0.08	13.68	41.8	-16	58.1	11.8	0.03	6.52
	2.5	0.5	26	0.13	15	13.5	0.13	13.5	0.07	13.59	42.4	-16	58.7	11.8	0.03	6.54
	2.5	0.5	26.5	0.13	15	13.6	0.13	13.6	0.07	13.51	42.9	-16	59.4	11.7	0.03	6.57
	2.5	0.5	27	0.13	15	13.8	0.13	13.8	0.07	13.43	43.5	-17	60.1	11.7	0.03	6.60
	2.5	0.5	27.5	0.13	15	13.9	0.13	13.9	0.07	13.36	44.1	-17	60.7	11.6	0.03	6.63
	2.5	0.5	28	0.13	15	14	0.13	14	0.07	13.28	44.7	-17	61.4	11.6	0.03	6.66
	2.5	0.5	28.5	0.13	15	14.1	0.13	14.1	0.07	13.2	45.3	-17	62.1	11.5	0.03	6.68
	2.5	0.5	29	0.13	15	14.3	0.13	14.3	0.07	13.13	45.9	-17	62.7	11.5	0.03	6.71
	2.5	0.5	29.5	0.13	15	14.4	0.13	14.4	0.07	13.06	46.4	-17	63.4	11.4	0.03	6.74
	2.5	0.5	30	0.13	15	14.5	0.13	14.5	0.07	12.99	47	-17	64.1	11.3	0.03	6.77
30-40	3.5	0.5	30.5	0.18	21	14.7	0.18	14.7	0.07	12.89	47.8	-17	65.2	11.3	0.08	6.86
	3.5	0.5	31	0.18	21	14.9	0.18	14.9	0.07	12.79	48.7	-18	66.3	11.2	0.08	6.94
	3.5	0.5	31.5	0.18	21	15	0.18	15	0.07	12.7	49.5	-18	67.5	11.1	0.08	7.02
	3.5	0.5	32	0.18	21	15.2	0.18	15.2	0.07	12.61	50.3	-18	68.6	11	0.08	7.10
	3.5	0.5	32.5	0.18	21	15.4	0.18	15.4	0.07	12.52	51.1	-19	69.8	10.9	0.08	7.19
	3.5	0.5	33	0.18	21	15.6	0.18	15.6	0.06	12.44	51.9	-19	70.9	10.9	0.08	7.27
	3.5	0.5	33.5	0.18	21	15.7	0.18	15.7	0.06	12.35	52.8	-19	72	10.8	0.09	7.36
	3.5	0.5	34	0.18	21	15.9	0.18	15.9	0.06	12.27	53.6	-20	73.2	10.7	0.09	7.44
	3.5	0.5	34.5	0.18	21	16.1	0.18	16.1	0.06	12.19	54.4	-20	74.3	10.6	0.09	7.53
	3.5	0.5	35	0.18	21	16.3	0.18	16.3	0.06	12.11	55.2	-20	75.5	10.6	0.09	7.62
	3.5	0.5	35.5	0.18	21	16.4	0.18	16.4	0.06	12.03	56.1	-21	76.6	10.5	0.09	7.70
	3.5	0.5	36	0.18	21	16.6	0.18	16.6	0.06	11.95	56.9	-21	77.7	10.4	0.09	7.79
	3.5	0.5	36.5	0.18	21	16.8	0.18	16.8	0.06	11.88	57.7	-21	78.9	10.4	0.09	7.88
	3.5	0.5	37	0.18	21	17	0.18	17	0.06	11.81	58.5	-22	80	10.3	0.09	7.97
	3.5	0.5	37.5	0.18	21	17.1	0.18	17.1	0.06	11.73	59.3	-22	81.2	10.2	0.09	8.06
	3.5	0.5	38	0.18	21	17.3	0.18	17.3	0.06	11.66	60.2	-22	82.3	10.2	0.09	8.15
	3.5	0.5	38.5	0.18	21	17.5	0.18	17.5	0.06	11.59	61	-22	83.4	10.1	0.09	8.24
	3.5	0.5	39	0.18	21	17.7	0.18	17.7	0.06	11.53	61.8	-23	84.6	10.1	0.09	8.33
	3.5	0.5	39.5	0.18	21	17.8	0.18	17.8	0.06	11.46	62.6	-23	85.7	9.99	0.09	8.42
	3.5	0.5	40	0.18	21	18	0.18	18	0.06	11.4	63.4	-23	86.8	9.93	0.09	8.52
40-50	1	5	45	0.5	6	18.5	0.5	18.5	0.05	11.22	0	0	0	0	0	8.52
50-60	0.5	10	55	0.5	3	19	0.5	19	0.05	11.05	0	0	0	0	0	8.52
60-70	0.5	10	65	0.5	3	19.5	0.5	19.5	0.05	10.89	0	0	0	0	0	8.52
70-80	0	10	75	0.5	3	20	0.5	20	0.05	10.74	0	0	0	0	0	8.52
80-90	0	10	85	0.5	3	20.5	0.5	20.5	0.05	10.59	0	0	0	0	0	8.52
90-100	0.5	10	95	0.5	3	21	0.5	21	0.05	10.46	0	0	0	0	0	8.52

Table B6: Computation of Potential Runoff in storm (T1) and Sandy Clay loam soil

T1	**Computation of rainfall excess in a Sandy Clay loam soil**															
Time	R(ts)	T-step	T-cum	R(ts)	Ri(ts)	Rc(ts)	f(t)	F	1/F	fpr(t)	tpr(t)	tdel	tact	fac(t)	Rexc	Σ Rexc
(min)	(mm)	(min)	(min)	(mm)	(mm/h)	(mm)	(mm)	(mm)	(1/mm)	(mm/h)	(min)	(min)	(min)	mm/h	mm	Mm
1	2	3	4	5	6	7	8	9	10	11	12	13	14	15	16	17
0	0	0	0	0	0	0	0	0	0	70	0	0	0	0	0	0
0-10	7	5	5	3.5	42	3.5	3.5	3.5	0.29	38.7	3.86	1.14	3.86	38.7	0.28	0.28
	7	0.5	5.5	0.35	42	3.85	0.35	3.85	0.26	35.62	4.67	0.83	4.67	35.6	0.05	0.33
	7	0.5	6	0.35	42	4.2	0.35	4.2	0.24	33.05	5.55	0.45	5.55	33	0.07	0.40

	7	0.5	6.5	0.35	42	4.55	0.35	4.55	0.22	30.88	6.48	0.02	6.48	30.9	0.09	0.50
	7	0.5	7	0.35	42	4.9	0.35	4.9	0.20	29.02	7.47	-0.5	7.94	28.3	0.11	0.61
	7	0.5	7.5	0.35	42	5.25	0.35	5.25	0.19	27.4	8.52	-1	9.53	26.1	0.13	0.74
	7	0.5	8	0.35	42	5.6	0.35	5.6	0.18	25.99	9.61	-1.6	11.2	24.3	0.15	0.89
	7	0.5	8.5	0.35	42	5.95	0.35	5.95	0.17	24.74	10.8	-2.3	13	22.8	0.16	1.05
	7	0.5	9	0.35	42	6.3	0.35	6.3	0.16	23.64	11.9	-2.9	14.9	21.5	0.17	1.22
	7	0.5	9.5	0.35	42	6.65	0.35	6.65	0.15	22.64	13.2	-3.7	16.9	20.3	0.18	1.40
	7	0.5	10	0.35	42	7	0.35	7	0.14	21.75	14.4	-4.4	18.9	19.3	0.19	1.59
10.-20	2	5	15	1	12	8	1	8	0.13	19.63	0	0	0	0	0	1.59
	2	5	20	1	12	9	1	9	0.11	17.99	0	0	0	0	0	1.59
20-30	0.5	10	30	0.5	3	9.5	0.5	9.5	0.11	17.29	0	0	0	0	0	1.59
30-40	0.5	10	40	0.5	3	10	0.5	10	0.1	16.67	0	0	0	0	0	1.59
40-50	0.5	10	50	0.5	3	10.5	0.5	10.5	0.10	16.1	0	0	0	0	0	1.59
50-60	0.5	10	60	0.5	3	11	0.5	11	0.10	15.59	0	0	0	0	0	1.59
60-70	0.5	10	70	0.5	3	11.5	0.5	11.5	0.09	15.12	0	0	0	0	0	1.59
70-80	0.5	10	80	0.5	3	12	0.5	12	0.09	14.69	0	0	0	0	0	1.59
80-90	0.5	10	90	0.5	3	12.5	0.5	12.5	0.08	14.3	0	0	0	0	0	1.59
90-100	0.5	10	100	0.5	3	13	0.5	13	0.08	13.93	0	0	0	0	0	1.59

Table B7: Computation of Potential Runoff in storm (T3) and Sandy Clay loam soil

T3	**Computation of rainfall excess in a Sandy Clay loam soil**															
Time	R(ts)	T-step	T-cum	R(ts)	Ri(ts)	Rc(ts)	f(t)	F	1/F	fpr(t)	tpr(t)	tdel	tact	fac(t)	Rexc	Σ Rexc
(min)	(mm)	(min)	(min)	(mm)	(mm/h)	(mm)	(mm)	(mm)	(1/mm)	(mm/h)	(min)	(min)	(min)	mm/h	mm	mm
1	2	3	4	5	6	7	8	9	10	11	12	13	14	15	16	17
0	0	0	0	0	0	0	0	0	0	70	0	0	0	0	0	0
0-10	1	5	5	0.5	6	0.5	0.5	0.5	2	242	0	0	0	0	0	0
	1	5	10	0.5	6	1	0.5	1	1	123.4	0	0	0	0	0	0
10.-20	1.5	5	15	0.75	9	1.75	0.75	1.75	0.57	72.59	0	0	0	0	0	0
	1.5	5	20	0.75	9	2.5	0.75	2.5	0.4	52.26	0	0	0	0	0	0
20-30	0.5	10	30	0.5	3	3	0.5	3	0.33	44.35	0	0	0	0	0	0
30-40	2.5	5	35	1.25	15	4.25	1.25	4.25	0.24	32.72	0	0	0	0	0	0
	2.5	5	40	1.25	15	5.5	1.25	5.5	0.18	26.37	0	0	0	0	0	0
40-50	4	2	42	0.8	24	6.3	0.8	6.3	0.16	23.64	11.9	30.1	11.9	23.6	0.01	0.01
	4	0.5	42.5	0.2	24	6.5	0.2	6.5	0.15	23.06	12.6	29.9	12.6	23.1	0.01	0.02
	4	0.5	43	0.2	24	6.7	0.2	6.7	0.15	22.51	13.4	29.6	13.4	22.5	0.01	0.03
	4	0.5	43.5	0.2	24	6.9	0.2	6.9	0.15	22	14.1	29.4	14.1	22	0.02	0.05
	4	0.5	44	0.2	24	7.1	0.2	7.1	0.14	21.51	14.8	29.2	14.8	21.5	0.02	0.07
	4	0.5	44.5	0.2	24	7.3	0.2	7.3	0.14	21.06	15.6	28.9	15.6	21.1	0.02	0.09
	4	0.5	45	0.2	24	7.5	0.2	7.5	0.13	20.62	16.3	28.7	16.3	20.6	0.03	0.12
	4	0.5	45.5	0.2	24	7.7	0.2	7.7	0.13	20.21	17.1	28.4	17.1	20.2	0.03	0.15
	4	0.5	46	0.2	24	7.9	0.2	7.9	0.13	19.82	17.9	28.1	17.9	19.8	0.03	0.19
	4	0.5	46.5	0.2	24	8.1	0.2	8.1	0.12	19.45	18.7	27.8	18.7	19.5	0.04	0.23
	4	0.5	47	0.2	24	8.3	0.2	8.3	0.12	19.1	19.5	27.5	19.5	19.1	0.04	0.27
	4	0.5	47.5	0.2	24	8.5	0.2	8.5	0.12	18.76	20.3	27.2	20.3	18.8	0.04	0.31
	4	0.5	48	0.2	24	8.7	0.2	8.7	0.12	18.44	21.1	26.9	21.1	18.4	0.05	0.36
	4	0.5	48.5	0.2	24	8.9	0.2	8.9	0.11	18.14	21.9	26.6	21.9	18.1	0.05	0.41
	4	0.5	49	0.2	24	9.1	0.2	9.1	0.11	17.84	22.7	26.3	22.7	17.8	0.05	0.46
	4	0.5	49.5	0.2	24	9.3	0.2	9.3	0.11	17.56	23.6	25.9	23.6	17.6	0.05	0.51

	4	0.5	50	0.2	24	9.5	0.2	9.5	0.11	17.29	24.4	25.6	24.4	17.3	0.06	0.57
50-60	0.5	10	60	0.5	3	10	0.5	10	0.1	16.67	0	0	0	0	0	0.57
60-70	0.5	10	70	0.5	3	10.5	0.5	10.5	0.10	16.1	0	0	0	0	0	0.57
70-80	0.5	10	80	0.5	3	11	0.5	11	0.09	15.59	0	0	0	0	0	0.57
80-90	1	5	85	0.5	6	11.5	0.5	11.5	0.09	15.12	0	0	0	0	0	0.57
	1	5	90	0.5	6	12	0.5	12	0.08	14.69	0	0	0	0	0	0.57
90-100	0.5	10	100	0.5	3	12.5	0.5	12.5	0.08	14.3	0	0	0	0	0	0.57
100-110	0.5	10	110	0.5	3	13	0.5	13	0.08	13.93	0	0	0	0	0	0.57

Table B8: Computation of Potential Runoff in storm (T4) and Sandy Clay loam soil

T4	Computation of rainfall excess in a Sandy Clay loam soil															
Time	R(ts)	T-step	T-cum	R(ts)	Ri(ts)	Rc(ts)	f(t)	F	1/F	fpr(t)	tpr(t)	tdel	tact	fac(t)	Rexc	Σ Rexc
(min)	(mm)	(min)	(min)	(mm)	(mm/h)	(mm)	(mm)	(mm)	(1/mm)	(mm/h)	(min)	(min)	(min)	mm/h	mm	mm
1	2	3	4	5	6	7	8	9	10	11	12	13	14	15	16	17
0	0	0	0	0	0	0	0	0	0	0	0	0	0	0	0	0
0-10	0.5	10	10	0.5	3	0.5	0.5	0.5	2	242	0	0	0	0	0	0
10.-20	0.5	10	20	0.5	3	1	0.5	1	1	123.4	0	0	0	0	0	0
20-30	1	5	25	0.5	6	1.5	0.5	1.5	0.67	83.89	0	0	0	0	0	0
	1	5	30	0.5	6	2	0.5	2	0.5	64.12	0	0	0	0	0	0
30-40	0.5	10	40	0.5	3	2.5	0.5	2.5	0.4	52.26	0	0	0	0	0	0
40-50	0.5	10	50	0.5	3	3	0.5	3	0.33	44.35	0	0	0	0	0	0
50-60	2.5	5	55	1.25	15	4.25	1.25	4.25	0.24	32.72	0	0	0	0	0	0
	2.5	5	60	1.25	15	5.5	1.25	5.5	0.18	26.37	0	0	0	0	0	0
60-70	2.5	5	65	1.25	15	6.75	1.25	6.75	0.15	22.38	0	0	0	0	0	0
	2.5	5	70	1.25	15	8	1.25	8	0.12	19.63	0	0	0	0	0	0

Table B9: Computation of Potential Runoff in storm (T6) and Sandy Clay loam soil

T6	Computation of rainfall excess in a Sandy Clay loam soil															
Time	R(ts)	T-step	T-cum	R(ts)	Ri(ts)	Rc(ts)	f(t)	F	1/F	fpr(t)	tpr(t)	tdel	tact	fac(t)	Rexc	Σ Rexc
(min)	(mm)	(min)	(min)	(mm)	(mm/h)	(mm)	(mm)	(mm)	(1/mm)	(mm/h)	(min)	(min)	(min)	mm/h	mm	mm
1	2	3	4	5	6	7	8	9	10	11	12	13	14	15	16	17
0	0	0	0	0	0	0	0	0	0	70	0	0	0	0	0	0
0-10	2	5	5	1	12	1	1	1	1	123.4	0	0	0	0	0	0
	2	5	10	1	12	2	1	2	0.5	64.12	0	0	0	0	0	0
10.-20	3.5	5	15	1.75	21	3.75	1.75	3.75	0.27	36.44	0	0	0	0	0	0
	3.5	5	20	1.75	21	5.5	1.75	5.5	0.18	26.37	0	0	0	0	0	0
20-30	11	0.5	20.5	0.55	66	6.05	0.55	6.05	0.17	24.41	11.1	9.41	11.1	24.4	0.35	0.35
	11	0.5	21	0.55	66	6.6	0.55	6.6	0.15	22.78	13	8	13	22.8	0.36	0.71
	11	0.5	21.5	0.55	66	7.15	0.55	7.15	0.14	21.4	15	6.5	15	21.4	0.37	1.08
	11	0.5	22	0.55	66	7.7	0.55	7.7	0.13	20.21	17.1	4.91	17.1	20.2	0.38	1.46
	11	0.5	22.5	0.55	66	8.25	0.55	8.25	0.12	19.19	19.3	3.24	19.3	19.2	0.39	1.85
	11	0.5	23	0.55	66	8.8	0.55	8.8	0.11	18.29	21.5	1.51	21.5	18.3	0.4	2.25
	11	0.5	23.5	0.55	66	9.35	0.55	9.35	0.11	17.49	23.8	-0.3	24.1	17.4	0.4	2.65
	11	0.5	24	0.55	66	9.9	0.55	9.9	0.10	16.79	26.1	-2.1	28.3	16.2	0.41	3.07

	11	0.5	24.5	0.55	66	10.5	0.55	10.5	0.10	16.16	28.5	-4	32.6	15.3	0.42	3.49
	11	0.5	25	0.55	66	11	0.55	11	0.09	15.59	31	-6	36.9	14.4	0.43	3.92
	11	0.5	25.5	0.55	66	11.6	0.55	11.6	0.09	15.08	33.4	-7.9	41.3	13.7	0.44	4.36
	11	0.5	26	0.55	66	12.1	0.55	12.1	0.08	14.61	35.9	-9.9	45.8	13.1	0.44	4.78
	11	0.5	26.5	0.55	66	12.7	0.55	12.7	0.08	14.18	38.4	-12	50.4	12.6	0.44	5.24
	11	0.5	27	0.55	66	13.2	0.55	13.2	0.08	13.79	41	-14	55	12.1	0.45	5.69
	11	0.5	27.5	0.55	66	13.8	0.55	13.8	0.07	13.43	43.5	-16	59.6	11.7	0.45	6.14
	11	0.5	28	0.55	66	14.3	0.55	14.3	0.07	13.1	46.1	-18	64.2	11.3	0.46	6.60
	11	0.5	28.5	0.55	66	14.9	0.55	14.9	0.07	12.79	48.7	-20	68.8	11	0.46	7.06
	11	0.5	29	0.55	66	15.4	0.55	15.4	0.07	12.51	51.2	-22	73.5	10.7	0.46	7.52
	11	0.5	29.5	0.55	66	16	0.55	16	0.07	12.24	53.8	-24	78.1	10.4	0.46	7.98
	11	0.5	30	0.55	66	16.5	0.55	16.5	0.06	12	56.4	-26	82.8	10.1	0.47	8.45
30-40	4.5	0.5	30.5	0.23	27	16.7	0.23	16.7	0.06	11.9	57.5	-27	84.4	10.1	0.14	8.59
	4.5	0.5	31	0.23	27	17	0.23	17	0.06	11.81	58.5	-28	86	9.98	0.14	8.73
	4.5	0.5	31.5	0.23	27	17.2	0.23	17.2	0.06	11.71	59.6	-28	87.6	9.9	0.14	8.87
	4.5	0.5	32	0.23	27	17.4	0.23	17.4	0.06	11.62	60.6	-29	89.2	9.82	0.14	9.02
	4.5	0.5	32.5	0.23	27	17.6	0.23	17.6	0.06	11.54	61.7	-29	90.8	9.74	0.14	9.16
	4.5	0.5	33	0.23	27	17.9	0.23	17.9	0.06	11.45	62.7	-30	92.4	9.67	0.14	9.30
	4.5	0.5	33.5	0.23	27	18.1	0.23	18.1	0.06	11.37	63.8	-30	94	9.59	0.15	9.45
	4.5	0.5	34	0.23	27	18.3	0.23	18.3	0.06	11.29	64.8	-31	95.6	9.52	0.15	9.59
	4.5	0.5	34.5	0.23	27	18.5	0.23	18.5	0.05	11.21	65.9	-31	97.2	9.46	0.15	9.74
	4.5	0.5	35	0.23	27	18.8	0.23	18.8	0.05	11.13	66.9	-32	98.8	9.39	0.15	9.89
	4.5	0.5	35.5	0.23	27	19	0.23	19	0.05	11.06	68	-32	100	9.32	0.15	10.03
	4.5	0.5	36	0.23	27	19.2	0.23	19.2	0.05	10.99	69	-33	102	9.26	0.15	10.18
	4.5	0.5	36.5	0.23	27	19.4	0.23	19.4	0.05	10.91	70	-34	104	9.2	0.15	10.33
	4.5	0.5	37	0.23	27	19.7	0.23	19.7	0.05	10.84	71.1	-34	105	9.14	0.15	10.48
	4.5	0.5	37.5	0.23	27	19.9	0.23	19.9	0.05	10.78	72.1	-35	107	9.08	0.15	10.63
	4.5	0.5	38	0.23	27	20.1	0.23	20.1	0.05	10.71	73.1	-35	108	9.02	0.15	10.78
	4.5	0.5	38.5	0.23	27	20.3	0.23	20.3	0.05	10.64	74.2	-36	110	8.97	0.15	10.93
	4.5	0.5	39	0.23	27	20.6	0.23	20.6	0.05	10.58	75.2	-36	111	8.91	0.15	11.08
	4.5	0.5	39.5	0.23	27	20.8	0.23	20.8	0.05	10.52	76.2	-37	113	8.86	0.15	11.23
	4.5	0.5	40	0.23	27	21	0.23	21	0.05	10.46	77.3	-37	115	8.8	0.15	11.38
40-50	1.5	2	42	0.3	9	21.3	0.3	21.3	0.05	10.38	0	0	0	0	0	11.38
	1.5	2	44	0.3	9	21.6	0.3	21.6	0.05	10.3	0	0	0	0	0	11.38
	1.5	2	46	0.3	9	21.9	0.3	21.9	0.05	10.22	0	0	0	0	0	11.38
	1.5	2	48	0.3	9	22.2	0.3	22.2	0.05	10.15	0	0	0	0	0	11.38
	1.5	2	50	0.3	9	22.5	0.3	22.5	0.04	10.08	0	0	0	0	0	11.38
50-60	0.5	10	60	0.5	3	23	0.5	23	0.04	9.96	0	0	0	0	0	11.38
60-70	0.5	10	70	0.5	3	23.5	0.5	23.5	0.04	9.86	0	0	0	0	0	11.38

Table B10: Computation of Potential Runoff in storm (M3) and Sandy Clay loam soil

M3	**Computation of rainfall excess in a Sandy Clay loam soil**															
Time	R(ts)	T-step	T-cum	R(ts)	Ri(ts)	Rc(ts)	f(t)	F	1/F	fpr(t)	tpr(t)	tdel	tact	fac(t)	Rexc	Σ Rexc
(min)	(mm)	(min)	(min)	(mm)	(mm/h)	(mm)	(mm)	(mm)	(1/mm)	(mm/h)	(min)	(min)	(min)	mm/h	mm	Mm
1	2	3	4	5	6	7	8	9	10	11	12	13	14	15	16	17
0	0	0	0	0	0	0	0	0	0	0	0	0	0	0	0	0
0-10	0.5	10	10	0.5	3	0.5	0.5	0.5	2	242	0	0	0	0	0	0

10.-20	0.5	10	20	0.5	3	1	0.5	1	1	123.4	0	0	0	0	0	0
20-30	0.5	10	30	0.5	3	1.5	0.5	1.5	0.67	83.89	0	0	0	0	0	0
30-40	0.5	10	40	0.5	3	2	0.5	2	0.5	64.12	0	0	0	0	0	0
40-50	0.5	10	50	0.5	3	2.5	0.5	2.5	0.4	52.26	0	0	0	0	0	0
50-60	0.5	10	60	0.5	3	3	0.5	3	0.33	44.35	0	0	0	0	0	0
60-70	5	5	65	2.5	30	5.5	2.5	5.5	0.18	26.37	9.29	55.7	9.29	26.4	0.3	0.30
	5	0.5	65.5	0.25	30	5.75	0.25	5.75	0.17	25.44	10.1	55.4	10.1	25.4	0.04	0.34
	5	0.5	66	0.25	30	6	0.25	6	0.17	24.58	10.9	55.1	10.9	24.6	0.05	0.39
	5	0.5	66.5	0.25	30	6.25	0.25	6.25	0.16	23.79	11.8	54.7	11.8	23.8	0.05	0.44
	5	0.5	67	0.25	30	6.5	0.25	6.5	0.15	23.06	12.6	54.4	12.6	23.1	0.06	0.50
	5	0.5	67.5	0.25	30	6.75	0.25	6.75	0.15	22.38	13.5	54	13.5	22.4	0.06	0.56
	5	0.5	68	0.25	30	7	0.25	7	0.14	21.75	14.4	53.6	14.4	21.8	0.07	0.63
	5	0.5	68.5	0.25	30	7.25	0.25	7.25	0.14	21.17	15.4	53.1	15.4	21.2	0.07	0.70
	5	0.5	69	0.25	30	7.5	0.25	7.5	0.13	20.62	16.3	52.7	16.3	20.6	0.08	0.78
	5	0.5	69.5	0.25	30	7.75	0.25	7.75	0.13	20.11	17.3	52.2	17.3	20.1	0.08	0.86
	5	0.5	70	0.25	30	8	0.25	8	0.13	19.63	18.3	51.7	18.3	19.6	0.09	0.95

Table B11: Computation of Potential Runoff in storm (M4) and Sandy Clay loam soil

M4	**Computation of rainfall excess in a Sandy Clay loam soil**															
Time	R(ts)	T-step	T-cum	R(ts)	Ri(ts)	Rc(ts)	f(t)	F	1/F	fpr(t)	tpr(t)	tdel	tact	fac(t)	Rexc	Σ Rexc
(min)	(mm)	(min)	(min)	(mm)	(mm/h)	(mm)	(mm)	(mm)	(1/mm)	(mm/h)	(min)	(min)	(min)	mm/h	mm	mm
1	2	3	4	5	6	7	8	9	10	11	12	13	14	15	16	17
0	0	0	0	0	0	0	0	0	0	70	0	0	0	0	0	0
0-10	1	5	5	0.5	6	0.5	0.5	0.5	2	242	0	0	0	0	0	0
	1	5	10	0.5	6	1	0.5	1	1	123.4	0	0	0	0	0	0
10.-20	2	5	15	1	12	2	1	2	0.5	64.12	0	0	0	0	0	0
	2	5	20	1	12	3	1	3	0.33	44.35	0	0	0	0	0	0
20-30	3	5	25	1.5	18	4.5	1.5	4.5	0.22	31.17	0	0	0	0	0	0
	3	5	30	1.5	18	6	1.5	6	0.17	24.58	0	0	0	0	0	0

Table B12: Computation of Potential Runoff in storm (M5) and Sandy Clay loam soil

M5	**Computation of rainfall excess in a Sandy Clay loam soil**															
Time	R(ts)	T-step	T-cum	R(ts)	Ri(ts)	Rc(ts)	f(t)	F	1/F	fpr(t)	tpr(t)	tdel	tact	fac(t)	Rexc	Σ Rexc
(min)	(mm)	(min)	(min)	(mm)	(mm/h)	(mm)	(mm)	(mm)	(1/mm)	(mm/h)	(min)	(min)	(min)	mm/h	mm	mm
1	2	3	4	5	6	7	8	9	10	11	12	13	14	15	16	17
0	0	0	0	0	0	0	0	0	0	70	0	0	0	0	0	0
0-10	1	5	5	0.5	6	0.5	0.5	0.5	2	242	0	0	0	0	0	0
	1	5	10	0.5	6	1	0.5	1	1	123.4	0	0	0	0	0	0
10.-20	3	5	15	1.5	18	2.5	1.5	2.5	0.4	52.26	0	0	0	0	0	0
	3	5	20	1.5	18	4	1.5	4	0.25	34.46	0	0	0	0	0	0
20-30	13.5	0.5	20.5	0.68	81	4.68	0.68	4.68	0.21	30.18	6.83	13.7	6.83	30.2	0.42	0.42
	13.5	0.5	21	0.68	81	5.35	0.68	5.35	0.19	26.98	8.82	12.2	8.82	27	0.45	0.87
	13.5	0.5	21.5	0.68	81	6.03	0.68	6.03	0.17	24.49	11	10.5	11	24.5	0.47	1.35
	13.5	0.5	22	0.68	81	6.7	0.68	6.7	0.15	22.51	13.4	8.65	13.4	22.5	0.49	1.83
	13.5	0.5	22.5	0.68	81	7.38	0.68	7.38	0.14	20.89	15.8	6.66	15.8	20.9	0.5	2.33
	13.5	0.5	23	0.68	81	8.05	0.68	8.05	0.12	19.54	18.5	4.54	18.5	19.5	0.51	2.85
	13.5	0.5	23.5	0.68	81	8.73	0.68	8.73	0.12	18.4	21.2	2.32	21.2	18.4	0.52	3.37

	13.5	0.5	24	0.68	81	9.4	0.68	9.4	0.11	17.43	24	0	24	17.4	0.53	3.90
	13.5	0.5	24.5	0.68	81	10.1	0.68	10.1	0.10	16.58	26.9	-2.4	29.3	16	0.54	4.44
	13.5	0.5	25	0.68	81	10.8	0.68	10.8	0.09	15.84	29.8	-4.8	34.7	14.8	0.55	4.99
	13.5	0.5	25.5	0.68	81	11.4	0.68	11.4	0.09	15.19	32.9	-7.4	40.2	13.9	0.56	5.55
	13.5	0.5	26	0.68	81	12.1	0.68	12.1	0.08	14.61	35.9	-9.9	45.8	13.1	0.57	6.11
	13.5	0.5	26.5	0.68	81	12.8	0.68	12.8	0.08	14.09	39	-13	51.5	12.5	0.57	6.69
	13.5	0.5	27	0.68	81	13.5	0.68	13.5	0.07	13.63	42.1	-15	57.3	11.9	0.58	7.26
	13.5	0.5	27.5	0.68	81	14.1	0.68	14.1	0.07	13.2	45.3	-18	63.1	11.4	0.58	7.84
	13.5	0.5	28	0.68	81	14.8	0.68	14.8	0.07	12.82	48.4	-20	68.9	11	0.58	8.42
	13.5	0.5	28.5	0.68	81	15.5	0.68	15.5	0.07	12.47	51.6	-23	74.7	10.6	0.59	9.01
	13.5	0.5	29	0.68	81	16.2	0.68	16.2	0.06	12.15	54.8	-26	80.5	10.3	0.59	9.6
	13.5	0.5	29.5	0.68	81	16.8	0.68	16.8	0.06	11.86	57.9	-28	86.4	9.96	0.59	10.19
	13.5	0.5	30	0.68	81	17.5	0.68	17.5	0.06	11.59	61.1	-31	92.2	9.68	0.59	10.79
30-40	12.5	0.5	30.5	0.63	75	18.1	0.63	18.1	0.06	11.35	64	-34	97.5	9.44	0.55	11.33
	12.5	0.5	31	0.63	75	18.8	0.63	18.8	0.05	11.13	66.9	-36	103	9.23	0.55	11.88
	12.5	0.5	31.5	0.63	75	19.4	0.63	19.4	0.05	10.93	69.8	-38	108	9.03	0.55	12.43
	12.5	0.5	32	0.63	75	20	0.63	20	0.05	10.74	72.7	-41	113	8.84	0.55	12.98
	12.5	0.5	32.5	0.63	75	20.6	0.63	20.6	0.05	10.56	75.5	-43	119	8.67	0.55	13.53
	12.5	0.5	33	0.63	75	21.3	0.63	21.3	0.05	10.39	78.4	-45	124	8.51	0.55	14.09
	12.5	0.5	33.5	0.63	75	21.9	0.63	21.9	0.05	10.23	81.2	-48	129	8.36	0.56	14.64
	12.5	0.5	34	0.63	75	22.5	0.63	22.5	0.04	10.08	84	-50	134	8.22	0.56	15.2
	12.5	0.5	34.5	0.63	75	23.1	0.63	23.1	0.04	9.94	86.8	-52	139	8.09	0.56	15.76
	12.5	0.5	35	0.63	75	23.8	0.63	23.8	0.04	9.80	89.6	-55	144	7.96	0.56	16.32
	12.5	0.5	35.5	0.63	75	24.4	0.63	24.4	0.04	9.67	92.3	-57	149	7.84	0.56	16.88
	12.5	0.5	36	0.63	75	25	0.63	25	0.04	9.55	95	-59	154	7.73	0.56	17.44
	12.5	0.5	36.5	0.63	75	25.6	0.63	25.6	0.04	9.44	97.7	-61	159	7.63	0.56	18
	12.5	0.5	37	0.63	75	26.3	0.63	26.3	0.04	9.33	100	-63	164	7.53	0.56	18.56
	12.5	0.5	37.5	0.63	75	26.9	0.63	26.9	0.04	9.22	103	-66	169	7.44	0.56	19.12
	12.5	0.5	38	0.63	75	27.5	0.63	27.5	0.04	9.12	106	-68	173	7.35	0.56	19.69
	12.5	0.5	38.5	0.63	75	28.1	0.63	28.1	0.04	9.03	108	-70	178	7.26	0.56	20.25
	12.5	0.5	39	0.63	75	28.8	0.63	28.8	0.04	8.93	111	-72	183	7.18	0.57	20.82
	12.5	0.5	39.5	0.63	75	29.4	0.63	29.4	0.03	8.85	113	-74	187	7.1	0.57	21.38
	12.5	0.5	40	0.63	75	30	0.63	30	0.03	8.76	116	-76	192	7.03	0.57	21.95

Table B13: Computation of Potential Runoff in storm (M8) and Sandy Clay loam soil

M8	**Computation of rainfall excess in a Sandy Clay loam soil**															
Time	R(ts)	T-step	T-cum	R(ts)	Ri(ts)	Rc(ts)	f(t)	F	1/F	fpr(t)	tpr(t)	tdel	tact	fac(t)	Rexc	Σ Rexc
(min)	(mm)	(min)	(min)	(mm)	(mm/h)	(mm)	(mm)	(mm)	(1/mm)	(mm/h)	(min)	(min)	(min)	mm/h	mm	Mm
1	2	3	4	5	6	7	8	9	10	11	12	13	14	15	16	17
0	0	0	0	0	0	0	0	0	0	0	0	0	0	0	0	0
0-10	0.5	10	10	0.5	3	0.5	0.5	0.5	2	242	0	0	0	0	0	0
10.-20	0.5	10	20	0.5	3	1	0.5	1	1	123.4	0	0	0	0	0	0
20-30	0.5	10	30	0.5	3	1.5	0.5	1.5	0.67	83.89	0	0	0	0	0	0
30-40	3	5	35	1.5	18	3	1.5	3	0.33	44.35	0	0	0	0	0	0
	3	5	40	1.5	18	4.5	1.5	4.5	0.22	31.17	0	0	0	0	0	0
40-50	2	5	45	1	12	5.5	1	5.5	0.18	26.37	0	0	0	0	0	0
	2	5	50	1	12	6.5	1	6.5	0.15	23.06	0	0	0	0	0	0

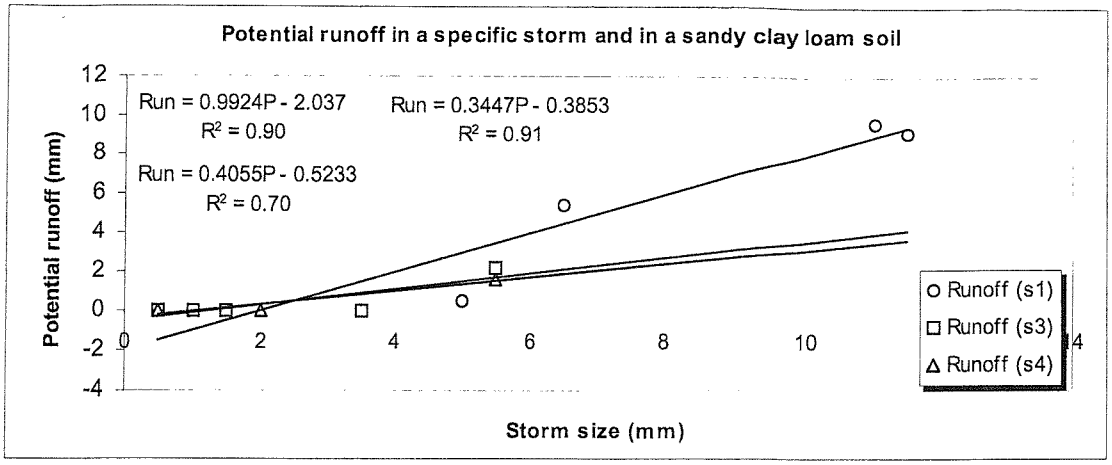

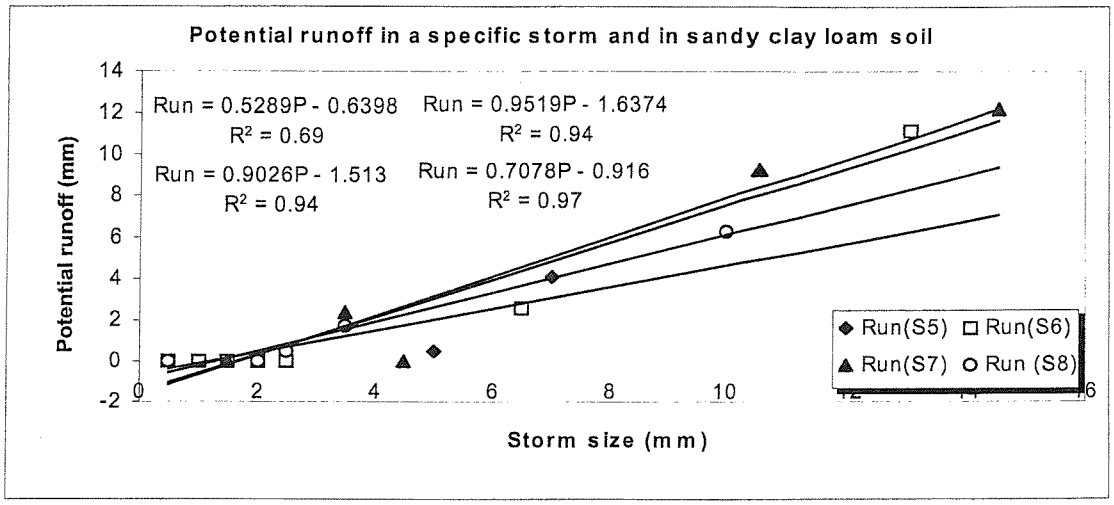

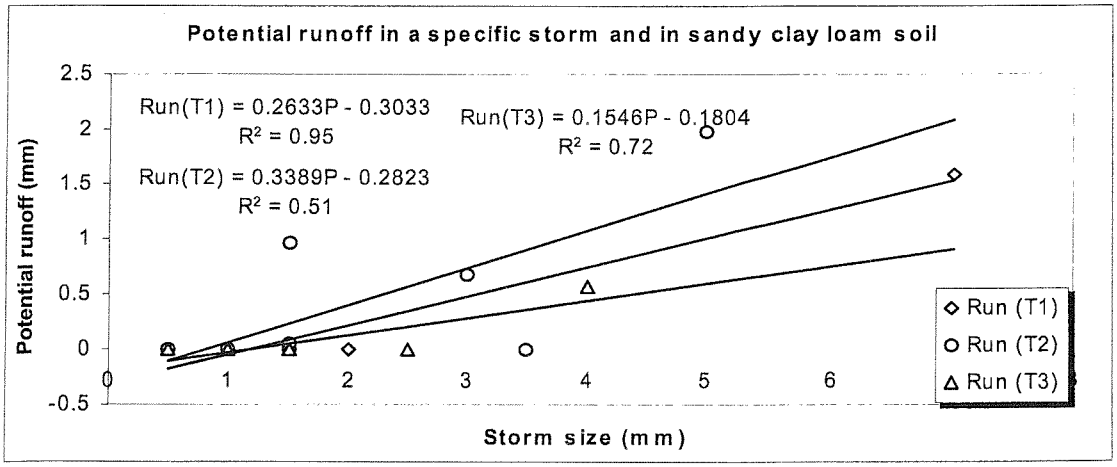

Figure B.1: Storm size and Potential Runoff relationship in sandy clay loam soil (storms S1, S3, S4, S5, S6, S7, S8 T1, T2, and T3)

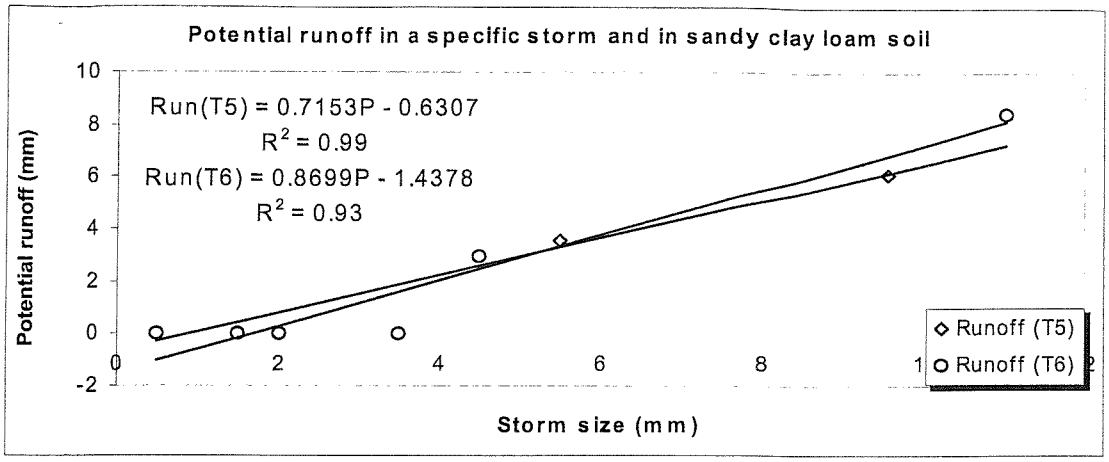

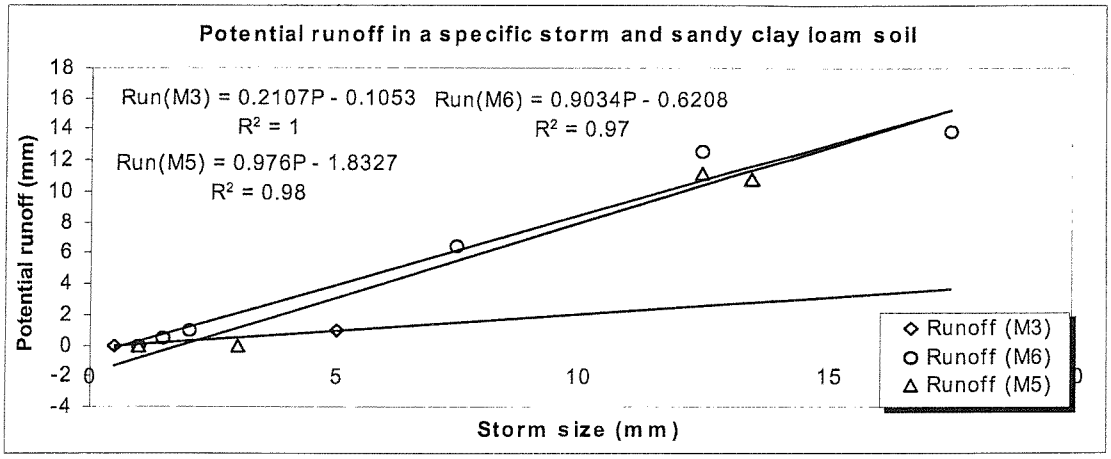

Figure B.2: Storm size and Potential Runoff relationship in sandy clay loam soil (storms T5, T6, M3, M5 and M6)

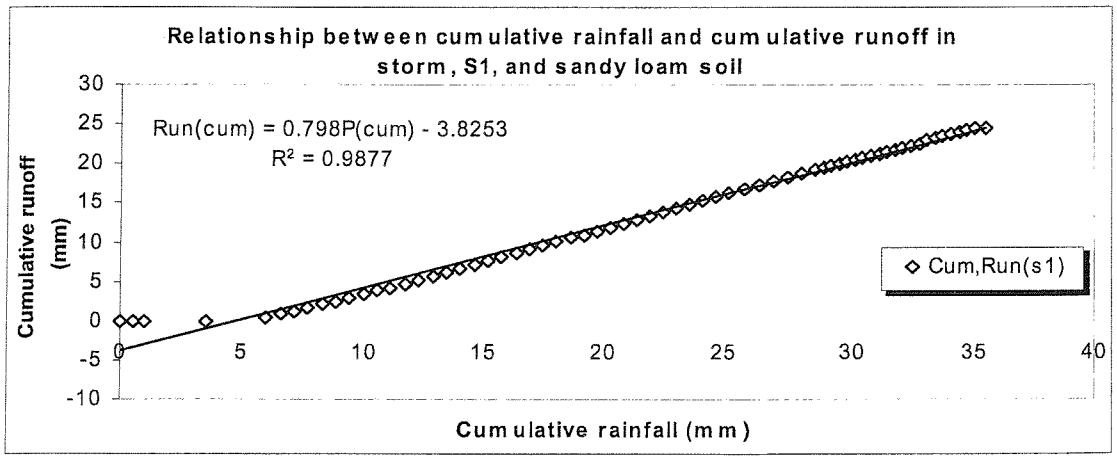

Figure B3: Cumulative Rainfall and cumulative runoff relationship in sandy clay loam soil (Storm S1)

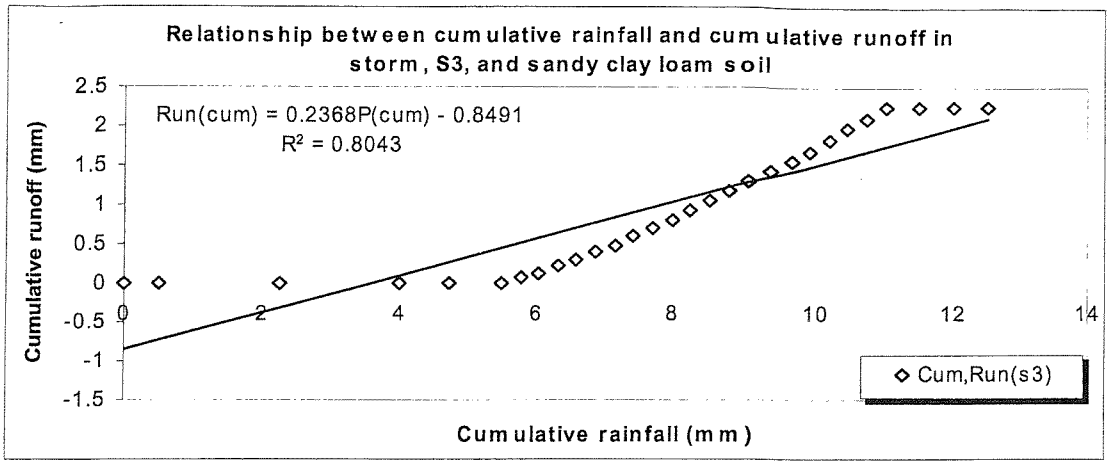

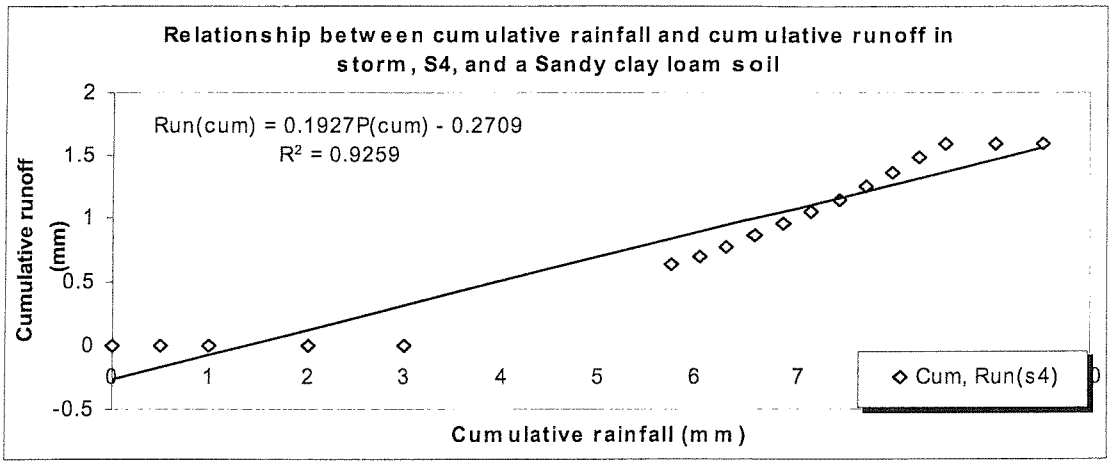

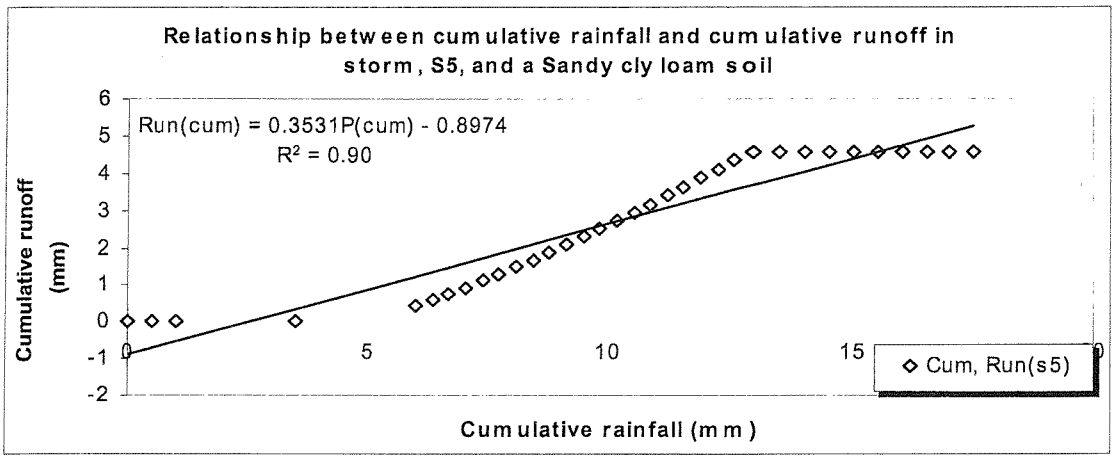

Figure B4: Cumulative Rainfall and cumulative runoff relationship in sandy clay loam soil (Storm S3, S4 and S5)

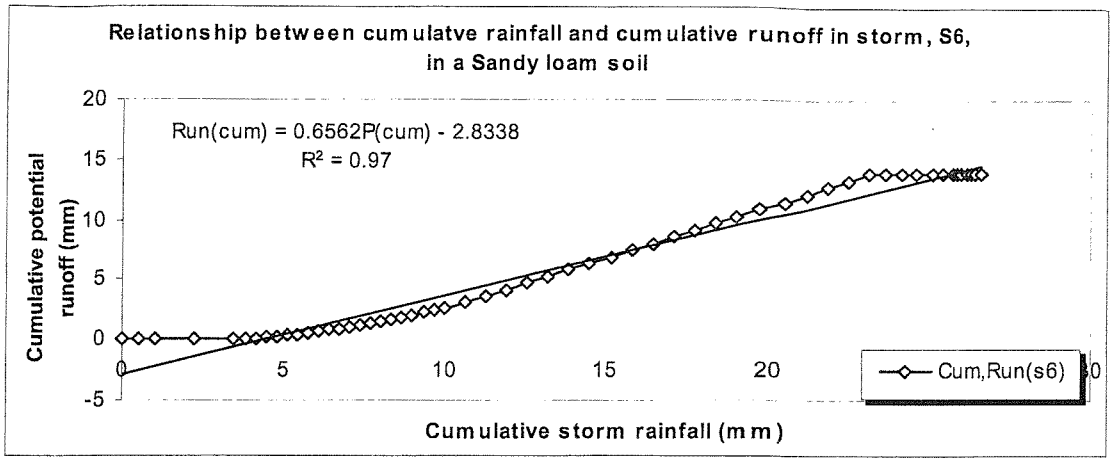

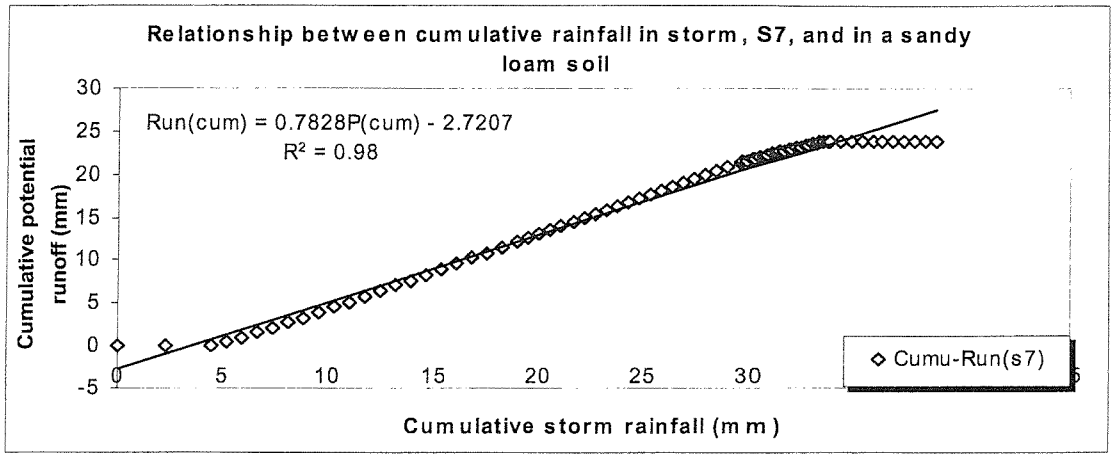

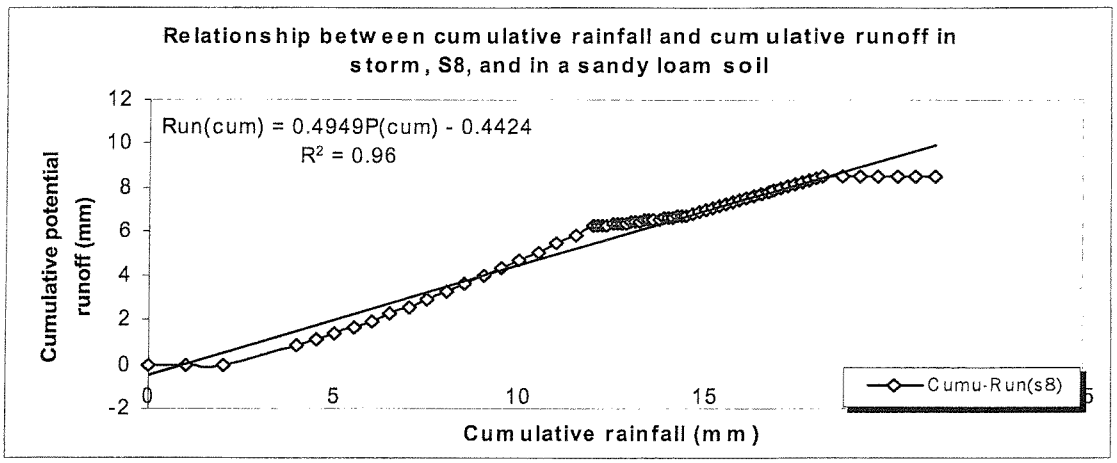

Figure B5: Cumulative Rainfall and cumulative runoff relationship in sandy clay loam soil (Storm S6, S7 and S8)

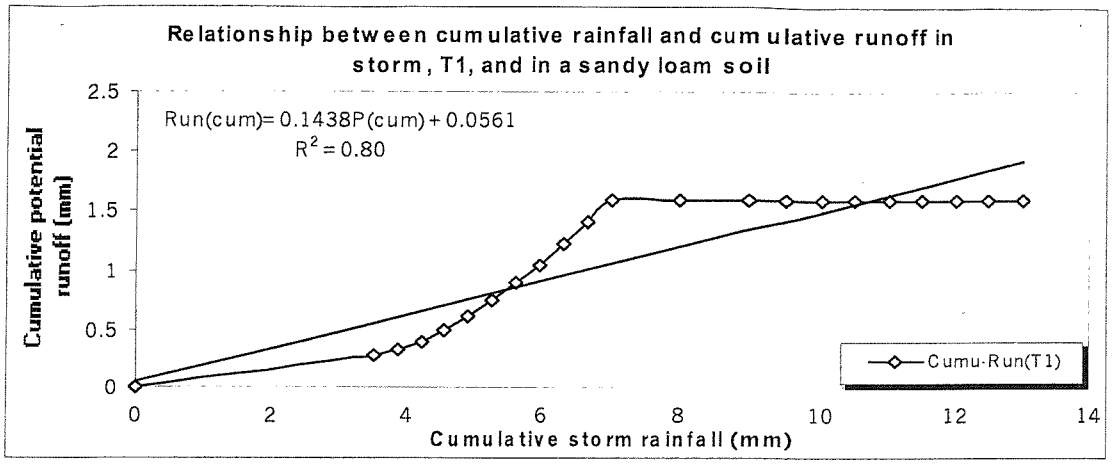

Figure B6: Cumulative Rainfall and cumulative runoff relationship in sandy clay loam soil (Storm T1)

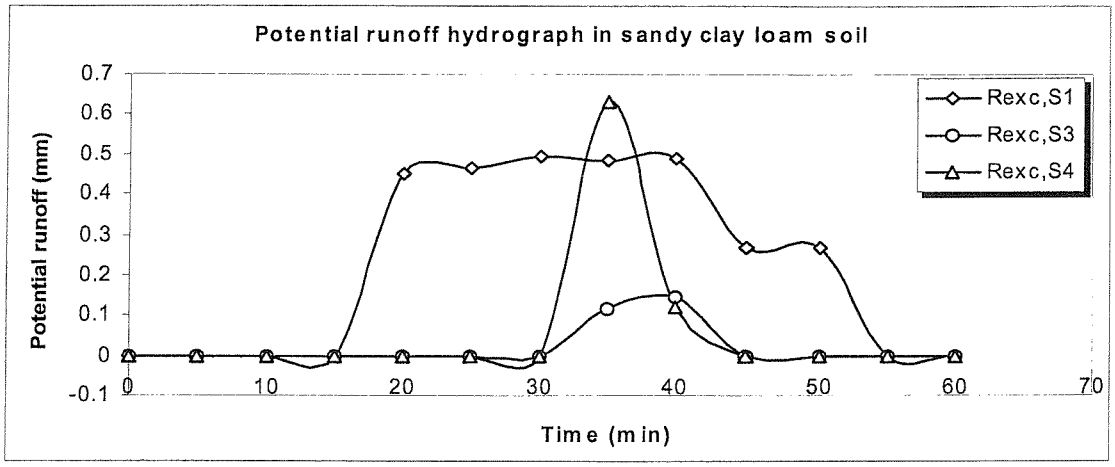

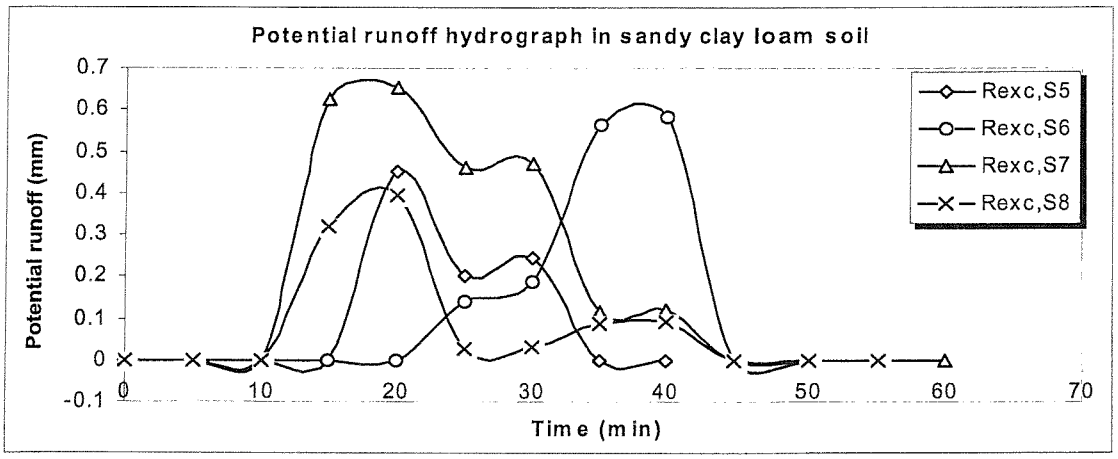

Figure B7: Potential runoff Hydrograph in sandy clay loam soil (For storms S1, S3, S4, S5, S6, S7 and S8)

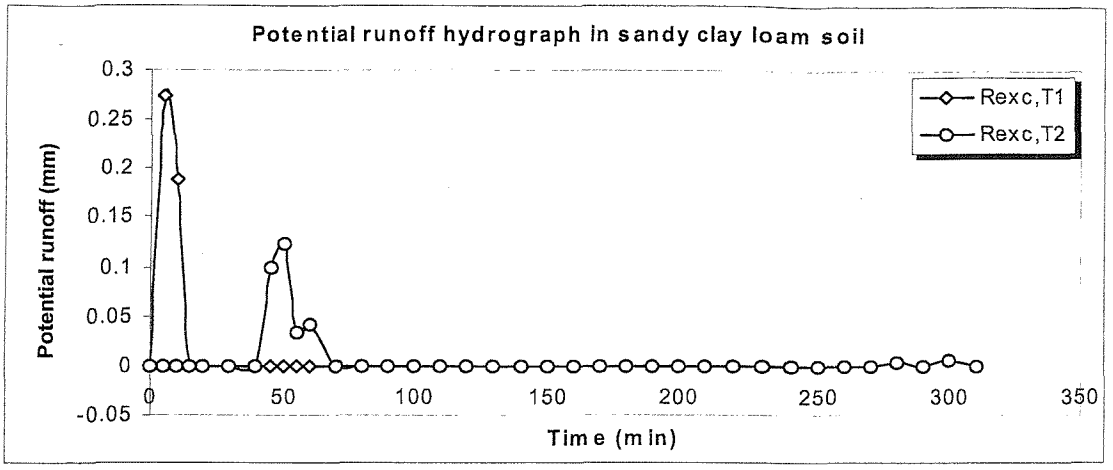

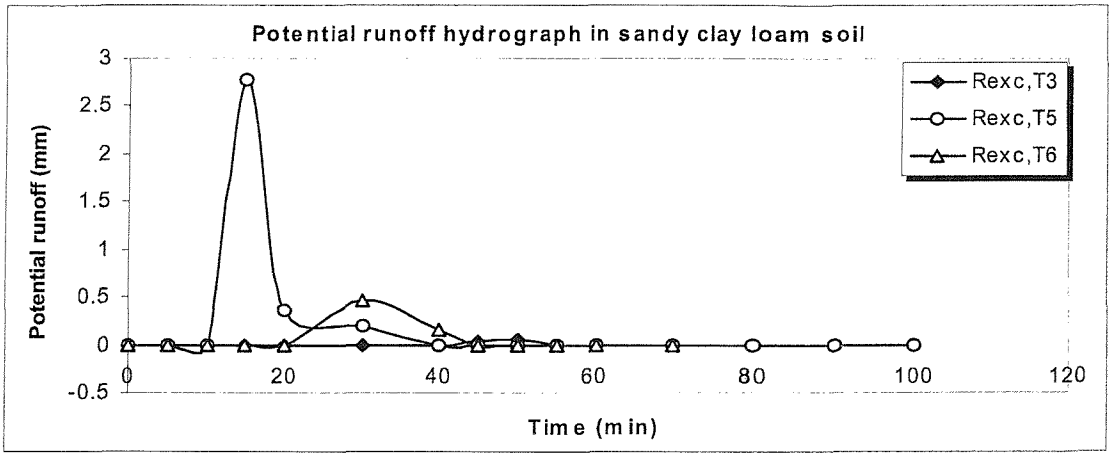

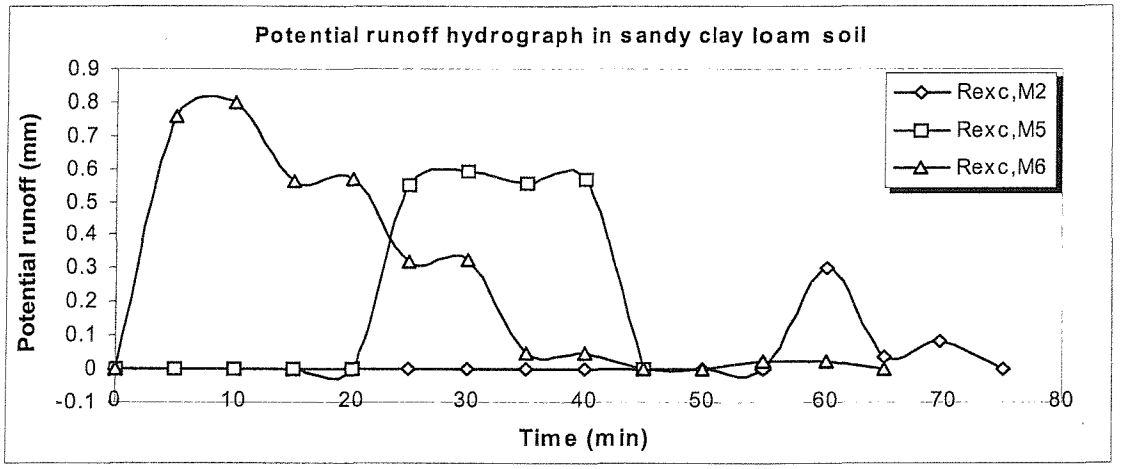

Figure B8: Potential runoff Hydrograph in sandy clay loam soil (For storms T1, T2, T5, T6, M2, M5 and M6)

Table B14: Computation of Potential Runoff in storm (S1) and Light Clay soil

S1	Computation of rainfall excess in a Light Clay soil															
Time	R(ts)	T-step	T-cum	R(ts)	Ri(ts)	Rc(ts)	f(t)	F	1/F	Fpr(t)	tpr(t)	tdel	tact	fac(t)	Rexc	Σ Rexc
(min)	(mm)	(min)	(min)	(mm)	(mm/h)	(mm)	(mm)	(mm)	(1/mm)	(mm/h)	(min)	(min)	(min)	mm/h	mm	mm
1	2	3	4	5	6	7	8	9	10	11	12	13	14	15	16	17
0	0	0	0	0	0	0	0	0	0	37.5	0	0	0	0	0	0
	1	5	5	0.5	6	0.5	0.5	0.5	2	35.34	0	0	0	0	0	0
	1	5	10	0.5	6	1	0.5	1	1	18.69	0	0	0	0	0	0
10	5	0.5	10.5	0.25	30	1.25	0.25	1.25	0.8	15.36	3.69	6.81	3.69	15.4	0.12	0.12
	5	0.5	11	0.25	30	1.5	0.25	1.5	0.67	13.14	5.23	5.77	5.23	13.1	0.14	0.26
	5	0.5	11.5	0.25	30	1.75	0.25	1.75	0.57	11.55	6.97	4.53	6.97	11.6	0.15	0.42
	5	0.5	12	0.25	30	2	0.25	2	0.5	10.37	8.89	3.11	8.89	10.4	0.16	0.58
	5	0.5	12.5	0.25	30	2.25	0.25	2.25	0.44	9.44	11	1.54	11	9.44	0.17	0.75
	5	0.5	13	0.25	30	2.5	0.25	2.5	0.4	8.7	13.2	-0.2	13.3	8.65	0.18	0.93
	5	0.5	13.5	0.25	30	2.75	0.25	2.75	0.36	8.10	15.5	-2	17.4	7.67	0.19	1.12
	5	0.5	14	0.25	30	3	0.25	3	0.33	7.59	17.9	-3.9	21.7	6.95	0.19	1.31
	5	0.5	14.5	0.25	30	3.25	0.25	3.25	0.31	7.16	20.3	-5.8	26.2	6.4	0.2	1.50
	5	0.5	15	0.25	30	3.5	0.25	3.5	0.29	6.80	22.9	-7.9	30.7	5.96	0.2	1.70
	5	0.5	15.5	0.25	30	3.75	0.25	3.75	0.27	6.48	25.4	-9.9	35.4	5.59	0.2	1.91
	5	0.5	16	0.25	30	4	0.25	4	0.25	6.20	28.1	-12	40.1	5.29	0.21	2.11
	5	0.5	16.5	0.25	30	4.25	0.25	4.25	0.24	5.96	30.7	-14	44.9	5.03	0.21	2.32
	5	0.5	17	0.25	30	4.5	0.25	4.5	0.22	5.74	33.4	-16	49.8	4.8	0.21	2.53
	5	0.5	17.5	0.25	30	4.75	0.25	4.75	0.21	5.55	36.1	-19	54.6	4.61	0.21	2.74
	5	0.5	18	0.25	30	5	0.25	5	0.2	5.37	38.7	-21	59.5	4.43	0.21	2.96
	5	0.5	18.5	0.25	30	5.25	0.25	5.25	0.19	5.21	41.4	-23	64.4	4.28	0.21	3.17
	5	0.5	19	0.25	30	5.5	0.25	5.5	0.18	5.07	44.1	-25	69.2	4.14	0.22	3.39
	5	0.5	19.5	0.25	30	5.75	0.25	5.75	0.17	4.94	46.8	-27	74.1	4.02	0.22	3.60
	5	0.5	20	0.25	30	6	0.25	6	0.17	4.82	49.5	-29	78.9	3.91	0.22	3.82
20-30	11.5	0.5	20.5	0.58	69	6.58	0.58	6.58	0.15	4.57	55.5	-35	90.6	3.67	0.54	4.36
	11.5	0.5	21	0.58	69	7.15	0.58	7.15	0.14	4.37	61.5	-40	102	3.48	0.55	4.91
	11.5	0.5	21.5	0.58	69	7.73	0.58	7.73	0.13	4.20	67.3	-46	113	3.33	0.55	5.46
	11.5	0.5	22	0.58	69	8.3	0.58	8.3	0.12	4.05	73	-51	124	3.19	0.55	6.01
	11.5	0.5	22.5	0.58	69	8.88	0.58	8.88	0.11	3.92	78.6	-56	135	3.08	0.55	6.56
	11.5	0.5	23	0.58	69	9.45	0.58	9.45	0.11	3.80	83.9	-61	145	2.98	0.55	7.11
	11.5	0.5	23.5	0.58	69	10	0.58	10	0.1	3.70	89.1	-66	155	2.89	0.55	7.66
	11.5	0.5	24	0.58	69	10.6	0.58	10.6	0.09	3.61	94.2	-70	164	2.82	0.55	8.21
	11.5	0.5	24.5	0.58	69	11.2	0.58	11.2	0.09	3.53	99.1	-75	174	2.75	0.55	8.76
	11.5	0.5	25	0.58	69	11.8	0.58	11.8	0.09	3.46	104	-79	183	2.69	0.55	9.31
	11.5	0.5	25.5	0.58	69	12.3	0.58	12.3	0.08	3.39	108	-83	191	2.63	0.55	9.87
	11.5	0.5	26	0.58	69	12.9	0.58	12.9	0.08	3.33	113	-87	200	2.58	0.55	10.42
	11.5	0.5	26.5	0.58	69	13.5	0.58	13.5	0.07	3.28	117	-91	208	2.54	0.55	10.97
	11.5	0.5	27	0.58	69	14.1	0.58	14.1	0.07	3.23	121	-94	216	2.49	0.55	11.53
	11.5	0.5	27.5	0.58	69	14.6	0.58	14.6	0.07	3.18	125	-98	223	2.46	0.55	12.08
	11.5	0.5	28	0.58	69	15.2	0.58	15.2	0.07	3.14	129	-101	230	2.42	0.55	12.64
	11.5	0.5	28.5	0.58	69	15.8	0.58	15.8	0.06	3.10	133	-104	237	2.39	0.56	13.19
	11.5	0.5	29	0.58	69	16.4	0.58	16.4	0.06	3.06	137	-108	244	2.36	0.56	13.75
	11.5	0.5	29.5	0.58	69	16.9	0.58	16.9	0.06	3.02	140	-111	251	2.33	0.56	14.3
	11.5	0.5	30	0.58	69	17.5	0.58	17.5	0.06	2.99	144	-114	257	2.31	0.56	14.86

30-40	11	0.5	30.5	0.55	66	18.1	0.55	18.1	0.06	2.96	147	-116	263	2.28	0.53	15.39
	11	0.5	31	0.55	66	18.6	0.55	18.6	0.05	2.94	150	-119	269	2.26	0.53	15.92
	11	0.5	31.5	0.55	66	19.2	0.55	19.2	0.05	2.91	153	-121	274	2.24	0.53	16.45
	11	0.5	32	0.55	66	19.7	0.55	19.7	0.05	2.89	156	-124	279	2.22	0.53	16.98
	11	0.5	32.5	0.55	66	20.3	0.55	20.3	0.05	2.87	158	-126	284	2.2	0.53	17.52
	11	0.5	33	0.55	66	20.8	0.55	20.8	0.05	2.84	161	-128	289	2.19	0.53	18.05
	11	0.5	33.5	0.55	66	21.4	0.55	21.4	0.05	2.82	164	-130	294	2.17	0.53	18.58
	11	0.5	34	0.55	66	21.9	0.55	21.9	0.05	2.8	166	-132	299	2.16	0.53	19.11
	11	0.5	34.5	0.55	66	22.5	0.55	22.5	0.05	2.78	169	-134	303	2.14	0.53	19.64
	11	0.5	35	0.55	66	23	0.55	23	0.04	2.76	171	-136	308	2.13	0.53	20.18
	11	0.5	35.5	0.55	66	23.6	0.55	23.6	0.04	2.75	174	-138	312	2.11	0.53	20.71
	11	0.5	36	0.55	66	24.1	0.55	24.1	0.04	2.73	176	-140	316	2.1	0.53	21.24
	11	0.5	36.5	0.55	66	24.7	0.55	24.7	0.04	2.72	178	-142	320	2.09	0.53	21.77
	11	0.5	37	0.55	66	25.2	0.55	25.2	0.04	2.70	180	-143	324	2.08	0.53	22.31
	11	0.5	37.5	0.55	66	25.8	0.55	25.8	0.04	2.69	183	-145	328	2.07	0.53	22.84
	11	0.5	38	0.55	66	26.3	0.55	26.3	0.04	2.67	185	-147	331	2.06	0.53	23.37
	11	0.5	38.5	0.55	66	26.9	0.55	26.9	0.04	2.66	187	-148	335	2.05	0.53	23.9
	11	0.5	39	0.55	66	27.4	0.55	27.4	0.04	2.65	189	-150	338	2.04	0.53	24.44
	11	0.5	39.5	0.55	66	28	0.55	28	0.04	2.64	191	-151	342	2.03	0.53	24.97
	11	0.5	40	0.55	66	28.5	0.55	28.5	0.04	2.62	192	-152	345	2.02	0.53	25.5
40-50	6.5	0.5	40.5	0.33	39	28.8	0.33	28.8	0.04	2.62	194	-153	347	2.02	0.31	25.81
	6.5	0.5	41	0.33	39	29.2	0.33	29.2	0.03	2.61	195	-154	348	2.01	0.31	26.12
	6.5	0.5	41.5	0.33	39	29.5	0.33	29.5	0.03	2.61	196	-154	350	2.01	0.31	26.43
	6.5	0.5	42	0.33	39	29.8	0.33	29.8	0.03	2.60	197	-155	351	2.01	0.31	26.74
	6.5	0.5	42.5	0.33	39	30.1	0.33	30.1	0.03	2.59	198	-155	353	2	0.31	27.04
	6.5	0.5	43	0.33	39	30.5	0.33	30.5	0.03	2.59	199	-156	354	2	0.31	27.35
	6.5	0.5	43.5	0.33	39	30.8	0.33	30.8	0.03	2.58	200	-156	356	1.99	0.31	27.66
	6.5	0.5	44	0.33	39	31.1	0.33	31.1	0.03	2.58	201	-157	357	1.99	0.31	27.97
	6.5	0.5	44.5	0.33	39	31.4	0.33	31.4	0.03	2.57	202	-157	359	1.99	0.31	28.28
	6.5	0.5	45	0.33	39	31.8	0.33	31.8	0.03	2.56	203	-158	360	1.98	0.31	28.59
	6.5	0.5	45.5	0.33	39	32.1	0.33	32.1	0.03	2.56	204	-158	362	1.98	0.31	28.89
	6.5	0.5	46	0.33	39	32.4	0.33	32.4	0.03	2.55	204	-158	363	1.98	0.31	29.2
	6.5	0.5	46.5	0.33	39	32.7	0.33	32.7	0.03	2.55	205	-159	364	1.97	0.31	29.51
	6.5	0.5	47	0.33	39	33.1	0.33	33.1	0.03	2.54	206	-159	366	1.97	0.31	29.82
	6.5	0.5	47.5	0.33	39	33.4	0.33	33.4	0.03	2.54	207	-160	367	1.97	0.31	30.13
	6.5	0.5	48	0.33	39	33.7	0.33	33.7	0.03	2.53	208	-160	368	1.96	0.31	30.44
	6.5	0.5	48.5	0.33	39	34	0.33	34	0.03	2.53	209	-160	369	1.96	0.31	30.75
	6.5	0.5	49	0.33	39	34.4	0.33	34.4	0.03	2.52	210	-161	371	1.96	0.31	31.06
	6.5	0.5	49.5	0.33	39	34.7	0.33	34.7	0.03	2.52	211	-161	372	1.96	0.31	31.36
	6.5	0.5	50	0.33	39	35	0.33	35	0.03	2.52	211	-161	373	1.95	0.31	31.67
50-60	1	0.5	50.5	0.05	6	35.1	0.05	35.1	0.03	2.52	212	-161	373	1.95	0.03	31.71
	1	0.5	51	0.05	6	35.1	0.05	35.1	0.03	2.51	212	-161	372	1.95	0.03	31.74
	1	0.5	51.5	0.05	6	35.2	0.05	35.2	0.03	2.51	212	-160	372	1.95	0.03	31.77
	1	0.5	52	0.05	6	35.2	0.05	35.2	0.03	2.51	212	-160	372	1.95	0.03	31.81
	1	0.5	52.5	0.05	6	35.3	0.05	35.3	0.03	2.51	212	-160	372	1.96	0.03	31.84
	1	0.5	53	0.05	6	35.3	0.05	35.3	0.03	2.51	212	-159	372	1.96	0.03	31.87
	1	0.5	53.5	0.05	6	35.4	0.05	35.4	0.03	2.51	212	-159	371	1.96	0.03	31.91
	1	0.5	54	0.05	6	35.4	0.05	35.4	0.03	2.51	213	-159	371	1.96	0.03	31.94
	1	0.5	54.5	0.05	6	35.5	0.05	35.5	0.03	2.51	213	-158	371	1.96	0.03	31.98

	1	0.5	55	0.05	6	35.5	0.05	35.5	0.03	2.51	213	-158	371	1.96	0.03	32.01
	1	0.5	55.5	0.05	6	35.6	0.05	35.6	0.03	2.51	213	-157	370	1.96	0.03	32.04
	1	0.5	56	0.05	6	35.6	0.05	35.6	0.03	2.51	213	-157	370	1.96	0.03	32.08
	1	0.5	56.5	0.05	6	35.7	0.05	35.7	0.03	2.51	213	-157	370	1.96	0.03	32.11
	1	0.5	57	0.05	6	35.7	0.05	35.7	0.03	2.51	213	-156	370	1.96	0.03	32.14
	1	0.5	57.5	0.05	6	35.8	0.05	35.8	0.03	2.51	213	-156	369	1.96	0.03	32.18
	1	0.5	58	0.05	6	35.8	0.05	35.8	0.03	2.51	214	-156	369	1.96	0.03	32.21
	1	0.5	58.5	0.05	6	35.9	0.05	35.9	0.03	2.50	214	-155	369	1.96	0.03	32.25
	1	0.5	59	0.05	6	35.9	0.05	35.9	0.03	2.50	214	-155	369	1.96	0.03	32.28
	1	0.5	59.5	0.05	6	36	0.05	36	0.03	2.50	214	-154	368	1.96	0.03	32.31
	1	0.5	60	0.05	6	36	0.05	36	0.03	2.50	214	-154	368	1.96	0.03	32.35

Table B15: Computation of Potential Runoff in storm (S2) and Light Clay soil

S2	**Computation of rainfall excess in a Light Clay soil**															
Time	R(ts)	T-step	T-cum	R(ts)	Ri(ts)	Rc(ts)	f(t)	F	1/F	fpr(t)	tpr(t)	tdel	tact	fac(t)	Rexc	Σ Rexc
(min)	(mm)	(min)	(min)	(mm)	(mm/h)	(mm)	(mm)	(mm)	(1/mm)	(mm/h)	(min)	(min)	(min)	mm/h	mm	mm
1	2	3	4	5	6	7	8	9	10	11	12	13	14	15	16	17
0	0	0	0	0	0	0	0	0	0	37.5	0	0	0	0	0	0
0-10	0.5	5	5	0.25	3	0.25	0.25	0.25	4	68.64	0	0	0	0	0	0
	0.5	5	10	0.25	3	0.5	0.25	0.5	2	35.34	0	0	0	0	0	0
10.-20	0.5	5	15	0.25	3	0.75	0.25	0.75	1.33	24.24	0	0	0	0	0	0
	0.5	5	20	0.25	3	1	0.25	1	1	18.69	0	0	0	0	0	0
20-30	0.5	5	25	0.25	3	1.25	0.25	1.25	0.8	15.36	0	0	0	0	0	0
	0.5	5	30	0.25	3	1.5	0.25	1.5	0.67	13.14	0	0	0	0	0	0
30-40	0.5	5	35	0.25	3	1.75	0.25	1.75	0.57	11.55	0	0	0	0	0	0
	0.5	5	40	0.25	3	2	0.25	2	0.5	10.37	0	0	0	0	0	0
40-50	0.5	5	45	0.25	3	2.25	0.25	2.25	0.44	9.44	0	0	0	0	0	0
	0.5	5	50	0.25	3	2.5	0.25	2.5	0.4	8.7	0	0	0	0	0	0
50-60	3	0.5	50.5	0.15	18	2.65	0.15	2.65	0.38	8.32	14.5	36	14.5	8.32	0.08	0.08
	3	0.5	51	0.15	18	2.8	0.15	2.8	0.36	7.99	15.9	35.1	15.9	7.99	0.08	0.16
	3	0.5	51.5	0.15	18	2.95	0.15	2.95	0.34	7.68	17.4	34.1	17.4	7.68	0.09	0.25
	3	0.5	52	0.15	18	3.1	0.15	3.1	0.32	7.41	18.8	33.2	18.8	7.41	0.09	0.34
	3	0.5	52.5	0.15	18	3.25	0.15	3.25	0.31	7.16	20.3	32.2	20.3	7.16	0.09	0.43
	3	0.5	53	0.15	18	3.4	0.15	3.4	0.29	6.94	21.8	31.2	21.8	6.94	0.09	0.52
	3	0.5	53.5	0.15	18	3.55	0.15	3.55	0.28	6.73	23.4	30.1	23.4	6.73	0.09	0.62
	3	0.5	54	0.15	18	3.7	0.15	3.7	0.27	6.54	24.9	29.1	24.9	6.54	0.1	0.71
	3	0.5	54.5	0.15	18	3.85	0.15	3.85	0.26	6.37	26.5	28	26.5	6.36	0.1	0.81
	3	0.5	55	0.15	18	4	0.15	4	0.25	6.20	28.1	26.9	28.1	6.2	0.1	0.91
	3	0.5	55.5	0.15	18	4.15	0.15	4.15	0.24	6.05	29.6	25.9	29.6	6.05	0.1	1.01
	3	0.5	56	0.15	18	4.3	0.15	4.3	0.23	5.91	31.2	24.8	31.2	5.91	0.1	1.11
	3	0.5	56.5	0.15	18	4.45	0.15	4.45	0.23	5.78	32.8	23.7	32.8	5.78	0.1	1.21
	3	0.5	57	0.15	18	4.6	0.15	4.6	0.22	5.66	34.5	22.5	34.5	5.66	0.1	1.31
	3	0.5	57.5	0.15	18	4.75	0.15	4.75	0.21	5.55	36.1	21.4	36.1	5.55	0.1	1.41
	3	0.5	58	0.15	18	4.9	0.15	4.9	0.20	5.44	37.7	20.3	37.7	5.44	0.1	1.52
	3	0.5	58.5	0.15	18	5.05	0.15	5.05	0.20	5.34	39.3	19.2	39.3	5.34	0.11	1.62
	3	0.5	59	0.15	18	5.2	0.15	5.2	0.19	5.24	40.9	18.1	40.9	5.24	0.11	1.73
	3	0.5	59.5	0.15	18	5.35	0.15	5.35	0.19	5.15	42.5	17	42.5	5.15	0.11	1.84
	3	0.5	60	0.15	18	5.5	0.15	5.5	0.18	5.07	44.1	15.9	44.1	5.07	0.11	1.95

Table B16: Computation of Potential Runoff in storm (S3) and Light Clay soil

S3	Computation of rainfall excess in a Light Clay soil															
Time	R(ts)	T-step	T-cum	R(ts)	Ri(ts)	Rc(ts)	f(t)	F	1/F	fpr(t)	tpr(t)	tdel	tact	fac(t)	Rexc	Σ Rexc
(min)	(mm)	(min)	(min)	(mm)	(mm/h)	(mm)	(mm)	(mm)	(1/mm)	(mm/h)	(min)	(min)	(min)	mm/h	mm	mm
1	2	3	4	5	6	7	8	9	10	11	12	13	14	15	16	17
0	0	0	0	0	0	0	0	0	0	37.5	0	0	0	0	0	0
0-10	0.5	5	5	0.25	3	0.25	0.25	0.25	4	68.64	0	0	0	0	0	0
	0.5	5	10	0.25	3	0.5	0.25	0.5	2	35.34	0	0	0	0	0	0
10.-20	3.5	5	15	1.75	21	2.25	1.75	2.25	0.44	9.44	11	4.04	11	9.44	0.96	0.96
	3.5	0.5	15.5	0.18	21	2.43	0.18	2.43	0.41	8.91	12.5	3.01	12.5	8.91	0.1	1.06
	3.5	0.5	16	0.18	21	2.6	0.18	2.6	0.39	8.44	14.1	1.93	14.1	8.44	0.1	1.17
	3.5	0.5	16.5	0.18	21	2.78	0.18	2.78	0.36	8.04	15.7	0.8	15.7	8.04	0.11	1.28
	3.5	0.5	17	0.18	21	2.95	0.18	2.95	0.34	7.68	17.4	-0.4	17.8	7.61	0.11	1.39
	3.5	0.5	17.5	0.18	21	3.13	0.18	3.13	0.32	7.37	19.1	-1.6	20.7	7.11	0.12	1.50
	3.5	0.5	18	0.18	21	3.3	0.18	3.3	0.30	7.09	20.8	-2.8	23.7	6.69	0.12	1.62
	3.5	0.5	18.5	0.18	21	3.48	0.18	3.48	0.29	6.83	22.6	-4.1	26.7	6.34	0.12	1.75
	3.5	0.5	19	0.18	21	3.65	0.18	3.65	0.27	6.60	24.4	-5.4	29.8	6.04	0.12	1.87
	3.5	0.5	19.5	0.18	21	3.83	0.18	3.83	0.26	6.39	26.2	-6.7	33	5.77	0.13	2.00
	3.5	0.5	20	0.18	21	4	0.18	4	0.25	6.20	28.1	-8.1	36.1	5.54	0.13	2.13
20-30	1.5	0.5	20.5	0.08	9	4.08	0.08	4.08	0.25	6.13	28.9	-8.4	37.2	5.47	0.03	2.16
	1.5	0.5	21	0.08	9	4.15	0.08	4.15	0.24	6.05	29.6	-8.6	38.3	5.4	0.03	2.19
	1.5	0.5	21.5	0.08	9	4.23	0.08	4.23	0.24	5.98	30.4	-8.9	39.4	5.33	0.03	2.22
	1.5	0.5	22	0.08	9	4.3	0.08	4.3	0.23	5.91	31.2	-9.2	40.5	5.27	0.03	2.25
	1.5	0.5	22.5	0.08	9	4.38	0.08	4.38	0.23	5.85	32	-9.5	41.6	5.2	0.03	2.28
	1.5	0.5	23	0.08	9	4.45	0.08	4.45	0.23	5.78	32.8	-9.8	42.7	5.14	0.03	2.31
	1.5	0.5	23.5	0.08	9	4.53	0.08	4.53	0.22	5.72	33.6	-10	43.8	5.08	0.03	2.34
	1.5	0.5	24	0.08	9	4.6	0.08	4.6	0.22	5.66	34.5	-10	44.9	5.03	0.03	2.38
	1.5	0.5	24.5	0.08	9	4.68	0.08	4.68	0.21	5.60	35.3	-11	46	4.97	0.03	2.41
	1.5	0.5	25	0.08	9	4.75	0.08	4.75	0.21	5.55	36.1	-11	47.1	4.92	0.03	2.44
	1.5	0.5	25.5	0.08	9	4.83	0.08	4.83	0.21	5.49	36.9	-11	48.2	4.87	0.03	2.48
	1.5	0.5	26	0.08	9	4.9	0.08	4.9	0.20	5.44	37.7	-12	49.3	4.82	0.03	2.51
	1.5	0.5	26.5	0.08	9	4.98	0.08	4.98	0.20	5.39	38.5	-12	50.5	4.77	0.04	2.55
	1.5	0.5	27	0.08	9	5.05	0.08	5.05	0.20	5.34	39.3	-12	51.6	4.73	0.04	2.58
	1.5	0.5	27.5	0.08	9	5.13	0.08	5.13	0.20	5.29	40.1	-13	52.7	4.68	0.04	2.62
	1.5	0.5	28	0.08	9	5.2	0.08	5.2	0.19	5.24	40.9	-13	53.8	4.64	0.04	2.66
	1.5	0.5	28.5	0.08	9	5.28	0.08	5.28	0.19	5.20	41.7	-13	54.9	4.6	0.04	2.69
	1.5	0.5	29	0.08	9	5.35	0.08	5.35	0.19	5.15	42.5	-14	56	4.55	0.04	2.73
	1.5	0.5	29.5	0.08	9	5.43	0.08	5.43	0.18	5.11	43.3	-14	57.1	4.51	0.04	2.77
	1.5	0.5	30	0.08	9	5.5	0.08	5.5	0.18	5.07	44.1	-14	58.2	4.48	0.04	2.81
30-40	5.5	0.5	30.5	0.28	33	5.78	0.28	5.78	0.17	4.92	47.1	-17	63.6	4.3	0.24	3.05
	5.5	0.5	31	0.28	33	6.05	0.28	6.05	0.17	4.79	50	-19	69	4.15	0.24	3.29
	5.5	0.5	31.5	0.28	33	6.33	0.28	6.33	0.16	4.67	52.9	-21	74.3	4.01	0.24	3.53
	5.5	0.5	32	0.28	33	6.6	0.28	6.6	0.15	4.56	55.8	-24	79.6	3.89	0.24	3.77
	5.5	0.5	32.5	0.28	33	6.88	0.28	6.88	0.15	4.46	58.7	-26	84.8	3.78	0.24	4.01
	5.5	0.5	33	0.28	33	7.15	0.28	7.15	0.14	4.37	61.5	-28	90	3.69	0.24	4.26
	5.5	0.5	33.5	0.28	33	7.43	0.28	7.43	0.14	4.28	64.3	-31	95.1	3.6	0.25	4.50
	5.5	0.5	34	0.28	33	7.7	0.28	7.7	0.13	4.20	67.1	-33	100	3.51	0.25	4.75
	5.5	0.5	34.5	0.28	33	7.98	0.28	7.98	0.13	4.13	69.8	-35	105	3.44	0.25	4.99

	5.5	0.5	35	0.28	33	8.25	0.28	8.25	0.12	4.06	72.5	-38	110	3.37	0.25	5.24
	5.5	0.5	35.5	0.28	33	8.53	0.28	8.53	0.12	3.99	75.2	-40	115	3.3	0.25	5.49
	5.5	0.5	36	0.28	33	8.8	0.28	8.8	0.11	3.93	77.8	-42	120	3.24	0.25	5.73
	5.5	0.5	36.5	0.28	33	9.08	0.28	9.08	0.11	3.88	80.4	-44	124	3.19	0.25	5.99
	5.5	0.5	37	0.28	33	9.35	0.28	9.35	0.11	3.82	83	-46	129	3.14	0.25	6.23
	5.5	0.5	37.5	0.28	33	9.63	0.28	9.63	0.10	3.77	85.5	-48	134	3.09	0.25	6.48
	5.5	0.5	38	0.28	33	9.9	0.28	9.9	0.10	3.72	88	-50	138	3.04	0.25	6.73
	5.5	0.5	38.5	0.28	33	10.2	0.28	10.2	0.10	3.68	90.5	-52	142	3	0.25	6.98
	5.5	0.5	39	0.28	33	10.5	0.28	10.5	0.10	3.63	92.9	-54	147	2.96	0.25	7.23
	5.5	0.5	39.5	0.28	33	10.7	0.28	10.7	0.09	3.59	95.3	-56	151	2.92	0.25	7.48
	5.5	0.5	40	0.28	33	11	0.28	11	0.09	3.55	97.6	-58	155	2.89	0.25	7.73
40-50	0.5	2	42	0.1	3	11.1	0.1	11.1	0.09	3.54	0	0	0	0	0	7.73
	0.5	2	44	0.1	3	11.2	0.1	11.2	0.09	3.53	0	0	0	0	0	7.73
50-60	0.5	2	46	0.1	3	11.3	0.1	11.3	0.09	3.51	0	0	0	0	0	7.73
	0.5	2	48	0.1	3	11.4	0.1	11.4	0.09	3.50	0	0	0	0	0	7.73
60-70	0.5	2	50	0.1	3	11.5	0.1	11.5	0.09	3.49	0	0	0	0	0	7.73
	0.5	2	52	0.1	3	11.6	0.1	11.6	0.09	3.48	0	0	0	0	0	7.73

Table B17: Computation of Potential Runoff in storm (S4) and Light Clay soil

S4	**Computation of rainfall excess in a Light Clay soil**															
Time	R(ts)	T-step	T-cum	R(ts)	Ri(ts)	Rc(ts)	f(t)	F	1/F	fpr(t)	tpr(t)	tdel	tact	fac(t)	Rexc	Σ Rexc
(min)	(mm)	(min)	(min)	(mm)	(mm/h)	(mm)	(mm)	(mm)	(1/mm)	(mm/h)	(min)	(min)	(min)	mm/h	mm	mm
1	2	3	4	5	6	7	8	9	10	11	12	13	14	15	16	17
0	0	0	0	0	0	0	0	0	0	37.5	0	0	0	0	0	0
0-10	0.5	5	5	0.25	3	0.25	0.25	0.25	4	68.64	0	0	0	0	0	0
	0.5	5	10	0.25	3	0.5	0.25	0.5	2	35.34	0	0	0	0	0	0
10.-20	2	5	15	1	12	1.5	1	1.5	0.67	13.14	0	0	0	0	0	0
	2	2	17	0.4	12	1.9	0.4	1.9	0.53	10.8	8.11	8.89	8.11	10.8	0.04	0.04
	2	0.5	17.5	0.1	12	2	0.1	2	0.5	10.37	8.89	8.61	8.89	10.4	0.01	0.05
	2	0.5	18	0.1	12	2.1	0.1	2.1	0.48	9.97	9.7	8.3	9.7	9.97	0.02	0.07
	2	0.5	18.5	0.1	12	2.2	0.1	2.2	0.46	9.61	10.5	7.96	10.5	9.61	0.02	0.09
	2	0.5	19	0.1	12	2.3	0.1	2.3	0.44	9.28	11.4	7.61	11.4	9.28	0.02	0.11
	2	0.5	19.5	0.1	12	2.4	0.1	2.4	0.42	8.98	12.3	7.23	12.3	8.98	0.03	0.14
	2	0.5	20	0.1	12	2.5	0.1	2.5	0.4	8.7	13.2	6.84	13.2	8.7	0.03	0.17
20-30	5.5	0.5	20.5	0.28	33	2.78	0.28	2.78	0.36	8.04	15.7	4.8	15.7	8.04	0.21	0.37
	5.5	0.5	21	0.28	33	3.05	0.28	3.05	0.33	7.50	18.4	2.65	18.4	7.5	0.21	0.59
	5.5	0.5	21.5	0.28	33	3.33	0.28	3.33	0.30	7.05	21.1	0.41	21.1	7.05	0.22	0.80
	5.5	0.5	22	0.28	33	3.6	0.28	3.6	0.28	6.67	23.9	-1.9	25.8	6.44	0.22	1.02
	5.5	0.5	22.5	0.28	33	3.88	0.28	3.88	0.26	6.34	26.8	-4.3	31	5.93	0.23	1.25
	5.5	0.5	23	0.28	33	4.15	0.28	4.15	0.24	6.05	29.6	-6.6	36.3	5.53	0.23	1.48
	5.5	0.5	23.5	0.28	33	4.43	0.28	4.43	0.23	5.80	32.6	-9.1	41.7	5.2	0.23	1.71
	5.5	0.5	24	0.28	33	4.7	0.28	4.7	0.21	5.58	35.5	-12	47	4.92	0.23	1.94
	5.5	0.5	24.5	0.28	33	4.98	0.28	4.98	0.20	5.39	38.5	-14	52.5	4.69	0.24	2.18
	5.5	0.5	25	0.28	33	5.25	0.28	5.25	0.19	5.21	41.4	-16	57.9	4.49	0.24	2.42
	5.5	0.5	25.5	0.28	33	5.53	0.28	5.53	0.18	5.05	44.4	-19	63.3	4.31	0.24	2.66
	5.5	0.5	26	0.28	33	5.8	0.28	5.8	0.17	4.91	47.3	-21	68.7	4.16	0.24	2.90
	5.5	0.5	26.5	0.28	33	6.08	0.28	6.08	0.17	4.78	50.3	-24	74	4.02	0.24	3.14
	5.5	0.5	27	0.28	33	6.35	0.28	6.35	0.16	4.66	53.2	-26	79.3	3.9	0.24	3.38
	5.5	0.5	27.5	0.28	33	6.63	0.28	6.63	0.12	4.55	56.1	-29	84.6	3.79	0.24	3.62

	5.5	0.5	28	0.28	33	6.9	0.28	6.9	0.15	4.45	58.9	-31	89.8	3.69	0.24	3.87
	5.5	0.5	28.5	0.28	33	7.18	0.28	7.18	0.14	4.36	61.8	-33	95	3.6	0.25	4.11
	5.5	0.5	29	0.28	33	7.45	0.28	7.45	0.13	4.28	64.6	-36	100	3.51	0.25	4.36
	5.5	0.5	29.5	0.28	33	7.73	0.28	7.73	0.13	4.20	67.3	-38	105	3.44	0.25	4.61
	5.5	0.5	30	0.28	33	8	0.28	8	0.13	4.12	70.1	-40	110	3.37	0.25	4.85
40-50	0.5	5	35	0.25	3	8.25	0.25	8.25	0.12	4.06	0	0	0	0	0	4.85
	0.5	5	40	0.25	3	8.5	0.25	8.5	0.12	4.00	0	0	0	0	0	4.85
50-60	0.5	5	45	0.25	3	8.75	0.25	8.75	0.11	3.94	0	0	0	0	0	4.85
	0.5	5	50	0.25	3	9	0.25	9	0.11	3.89	0	0	0	0	0	4.85

Table B18: Computation of Potential Runoff in storm (T1) and Light Clay soil

T1	**Computation of rainfall excess in a Light Clay soil**															
Time	R(ts)	T-step	T-cum	R(ts)	Ri(ts)	Rc(ts)	f(t)	F	1/F	fpr(t)	tpr(t)	tdel	tact	fac(t)	Rexc	Σ Rexc
(min)	(mm)	(min)	(min)	(mm)	(mm/h)	(mm)	(mm)	(mm)	(1/mm)	(mm/h)	(min)	(min)	(min)	mm/h	mm	mm
1	2	3	4	5	6	7	8	9	10	11	12	13	14	15	16	17
0	0	0	0	0	0	0	0	0	0	37.5	0	0	0	0	0	0
0-10	7	0.5	0.5	0.35	42	0.35	0.35	0.35	2.86	49.61	0	0	0	0	0	0
	7	2	2.5	1.4	42	1.75	1.4	1.75	0.57	11.55	6.97	-4.5	11.4	9.26	1.09	1.09
	7	0.5	3	0.35	42	2.1	0.35	2.1	0.48	9.97	9.7	-6.7	16.4	7.88	0.28	1.38
	7	0.5	3.5	0.35	42	2.45	0.35	2.45	0.41	8.84	12.7	-9.2	21.9	6.93	0.29	1.67
	7	0.5	4	0.35	42	2.8	0.35	2.8	0.36	7.99	15.9	-12	27.9	6.22	0.3	1.97
	7	0.5	4.5	0.35	42	3.15	0.35	3.15	0.32	7.33	19.3	-15	34.2	5.68	0.3	2.27
	7	0.5	5	0.35	42	3.5	0.35	3.5	0.29	6.80	22.9	-18	40.7	5.25	0.31	2.58
	7	0.5	5.5	0.35	42	3.85	0.35	3.85	0.26	6.37	26.5	-21	47.5	4.9	0.31	2.88
	7	0.5	6	0.35	42	4.2	0.35	4.2	0.24	6.00	30.2	-24	54.4	4.62	0.31	3.20
	7	0.5	6.5	0.35	42	4.55	0.35	4.55	0.22	5.70	33.9	-27	61.3	4.37	0.31	3.51
	7	0.5	7	0.35	42	4.9	0.35	4.9	0.20	5.44	37.7	-31	68.3	4.17	0.32	3.82
	7	0.5	7.5	0.35	42	5.25	0.35	5.25	0.19	5.21	41.4	-34	75.4	3.99	0.32	4.14
	7	0.5	8	0.35	42	5.6	0.35	5.6	0.18	5.01	45.2	-37	82.4	3.83	0.32	4.46
	7	0.5	8.5	0.35	42	5.95	0.35	5.95	0.17	4.84	48.9	-40	89.4	3.7	0.32	4.78
	7	0.5	9	0.35	42	6.3	0.35	6.3	0.16	4.68	52.6	-44	96.3	3.58	0.32	5.10
	7	0.5	9.5	0.35	42	6.65	0.35	6.65	0.15	4.54	56.3	-47	103	3.47	0.32	5.42
	7	0.5	10	0.35	42	7	0.35	7	0.14	4.42	60	-50	110	3.37	0.32	5.74
10.-20	2	0.5	10.5	0.1	12	7.1	0.1	7.1	0.14	4.39	61	-50	111	3.35	0.07	5.81
	2	0.5	11	0.1	12	7.2	0.1	7.2	0.14	4.35	62	-51	113	3.33	0.07	5.89
	2	0.5	11.5	0.1	12	7.3	0.1	7.3	0.14	4.32	63	-52	115	3.31	0.07	5.96
	2	0.5	12	0.1	12	7.4	0.1	7.4	0.14	4.29	64	-52	116	3.29	0.07	6.03
	2	0.5	12.5	0.1	12	7.5	0.1	7.5	0.13	4.26	65.1	-53	118	3.27	0.07	6.10
	2	0.5	13	0.1	12	7.6	0.1	7.6	0.13	4.23	66.1	-53	119	3.25	0.07	6.18
	2	0.5	13.5	0.1	12	7.7	0.1	7.7	0.13	4.20	67.1	-54	121	3.23	0.07	6.25
	2	0.5	14	0.1	12	7.8	0.1	7.8	0.13	4.18	68.1	-54	122	3.21	0.07	6.32
	2	0.5	14.5	0.1	12	7.9	0.1	7.9	0.13	4.15	69.1	-55	124	3.2	0.07	6.40
	2	0.5	15	0.1	12	8	0.1	8	0.13	4.12	70.1	-55	125	3.18	0.07	6.47
	2	0.5	15.5	0.1	12	8.1	0.1	8.1	0.12	4.10	71.1	-56	127	3.16	0.07	6.54
	2	0.5	16	0.1	12	8.2	0.1	8.2	0.12	4.07	72	-56	128	3.15	0.07	6.62
	2	0.5	16.5	0.1	12	8.3	0.1	8.3	0.12	4.05	73	-57	130	3.13	0.07	6.69
	2	0.5	17	0.1	12	8.4	0.1	8.4	0.12	4.02	74	-57	131	3.12	0.07	6.77
	2	0.5	17.5	0.1	12	8.5	0.1	8.5	0.12	4.00	75	-57	132	3.1	0.07	6.84
	2	0.5	18	0.1	12	8.6	0.1	8.6	0.12	3.98	75.9	-58	134	3.09	0.07	6.91

	2	0.5	18.5	0.1	12	8.7	0.1	8.7	0.12	3.95	76.9	-58	135	3.07	0.07	6.99
	2	0.5	19	0.1	12	8.8	0.1	8.8	0.11	3.93	77.8	-59	137	3.06	0.07	7.06
	2	0.5	19.5	0.1	12	8.9	0.1	8.9	0.11	3.91	78.8	-59	138	3.04	0.07	7.14
	2	0.5	20	0.1	12	9	0.1	9	0.11	3.89	79.7	-60	139	3.03	0.07	7.21
20-30	0.5	5	25	0.25	3	9.25	0.25	9.25	0.11	3.84	0	0	0	0	0	7.21
	0.5	5	30	0.25	3	9.5	0.25	9.5	0.11	3.79	0	0	0	0	0	7.21
30-40	0.5	5	35	0.25	3	9.75	0.25	9.75	0.10	3.75	0	0	0	0	0	7.21

Table B19: Computation of Potential Runoff in storm (T3) and Light Clay soil

T3	**Computation of rainfall excess in a Light Clay soil**															
Time	R(ts)	T-step	T-cum	R(ts)	Ri(ts)	Rc(ts)	f(t)	F	1/F	fpr(t)	tpr(t)	tdel	tact	fac(t)	Rexc	Σ Rexc
(min)	(mm)	(min)	(min)	(mm)	(mm/h)	(mm)	(mm)	(mm)	(1/mm)	(mm/h)	(min)	(min)	(min)	mm/h	mm	mm
1	2	3	4	5	6	7	8	9	10	11	12	13	14	15	16	17
0	0	0	0	0	0	0	0	0	0	70	0	0	0	0	0	0
0-10	1	5	5	0.5	6	0.5	0.5	0.5	2	35.34	0	0	0	0	0	0
	1	5	10	0.5	6	1	0.5	1	1	18.69	0	0	0	0	0	0
10.-20	1.5	5	15	0.75	9	1.75	0.75	1.75	0.57	11.55	0	0	0	0	0	0
	1.5	5	20	0.75	9	2.5	0.75	2.5	0.4	8.7	13.2	6.84	13.2	8.7	0.03	0.03
20-30	0.5	5	25	0.25	3	2.75	0.25	2.75	0.36	8.10	0	0	0	0	0	0.03
	0.5	5	30	0.25	3	3	0.25	3	0.33	7.59	0	0	0	0	0	0.03
30-40	2.5	5	35	1.25	15	4.25	1.25	4.25	0.24	5.96	30.7	4.29	30.7	5.96	0.75	0.78
	2.5	5	40	1.25	15	5.5	1.25	5.5	0.18	5.07	44.1	-4.1	48.2	4.87	0.84	1.62
40-50	4	5	45	2	24	7.5	2	7.5	0.13	4.26	65.1	-20	85.1	3.78	1.69	3.31
	4	5	50	2	24	9.5	2	9.5	0.11	3.79	84.4	-34	119	3.26	1.73	5.04
50-60	0.5	5	55	0.25	3	9.75	0.25	9.75	0.10	3.75	0	0	0	0	0	5.04
	0.5	2	57	0.1	3	9.85	0.1	9.85	0.10	3.73	0	0	0	0	0	5.04
	0.5	2	59	0.1	3	9.95	0.1	9.95	0.10	3.71	0	0	0	0	0	5.04
60-70	0.5	2	61	0.1	3	10.1	0.1	10.1	0.1	3.70	0	0	0	0	0	5.04
	0.5	2	63	0.1	3	10.2	0.1	10.2	0.10	3.68	0	0	0	0	0	5.04
	0.5	2	65	0.1	3	10.3	0.1	10.3	0.10	3.66	0	0	0	0	0	5.04
	0.5	2	67	0.1	3	10.4	0.1	10.4	0.10	3.65	0	0	0	0	0	5.04
	0.5	2	69	0.1	3	10.5	0.1	10.5	0.10	3.63	0	0	0	0	0	5.04
70-80	0.5	2	71	0.1	3	10.6	0.1	10.6	0.10	3.62	0	0	0	0	0	5.04
	0.5	2	73	0.1	3	10.7	0.1	10.7	0.09	3.60	0	0	0	0	0	5.04
	0.5	2	75	0.1	3	10.8	0.1	10.8	0.09	3.59	0	0	0	0	0	5.04
	0.5	2	77	0.1	3	10.9	0.1	10.9	0.09	3.58	0	0	0	0	0	5.04
	0.5	2	79	0.1	3	11	0.1	11	0.09	3.56	0	0	0	0	0	5.04
80-90	1	5	84	0.5	6	11.5	0.5	11.5	0.09	3.49	101	-17	119	3.26	0.23	5.27
	1	5	89	0.5	6	12	0.5	12	0.08	3.43	105	-16	122	3.22	0.23	5.50
90-100	0.5	2	91	0.1	3	12.1	0.1	12.1	0.08	3.42	0	0	0	0	0	5.50
	0.5	2	93	0.1	3	12.2	0.1	12.2	0.08	3.41	0	0	0	0	0	5.50
	0.5	2	95	0.1	3	12.3	0.1	12.3	0.08	3.40	0	0	0	0	0	5.50
	0.5	2	97	0.1	3	12.4	0.1	12.4	0.08	3.39	0	0	0	0	0	5.50
	0.5	2	99	0.1	3	12.5	0.1	12.5	0.08	3.38	0	0	0	0	0	5.50
100-110	0.5	2	101	0.1	3	12.6	0.1	12.6	0.08	3.37	0	0	0	0	0	5.50
	0.5	2	103	0.1	3	12.7	0.1	12.7	0.08	3.36	0	0	0	0	0	5.50
	0.5	2	105	0.1	3	12.8	0.1	12.8	0.08	3.35	0	0	0	0	0	5.50
	0.5	2	107	0.1	3	12.9	0.1	12.9	0.08	3.34	0	0	0	0	0	5.50

	0.5	2	109	0.1	3	13	0.1	13	0.08	3.323	0	0	0	0	0	5.50

Table B20: Computation of Potential Runoff in storm (T4) and Light Clay soil

T4	Computation of rainfall excess in a Light Clay soil															
Time	R(ts)	T-step	T-cum	R(ts)	Ri(ts)	Rc(ts)	f(t)	F	1/F	fpr(t)	tpr(t)	tdel	tact	fac(t)	Rexc	Σ Rexc
(min)	(mm)	(min)	(min)	(mm)	(mm/h)	(mm)	(mm)	(mm)	(1/mm)	(mm/h)	(min)	(min)	(min)	mm/h	mm	mm
1	2	3	4	5	6	7	8	9	10	11	12	13	14	15	16	17
0	0	0	0	0	0	0	0	0	0	37.5	0	0	0	0	0	0
0-10	0.5	5	5	0.25	3	0.25	0.25	0.25	4	68.64	0	0	0	0	0	0
	0.5	5	10	0.25	3	0.5	0.25	0.5	2	35.34	0	0	0	0	0	0
10.-20	0.5	5	15	0.25	3	0.75	0.25	0.75	1.333	24.24	0	0	0	0	0	0
	0.5	5	20	0.25	3	1	0.25	1	1	18.69	0	0	0	0	0	0
20-30	1	5	25	0.5	6	1.5	0.5	1.5	0.67	13.14	0	0	0	0	0	0
	1	5	30	0.5	6	2	0.5	2	0.5	10.37	0	0	0	0	0	0
30-40	0.5	5	35	0.25	3	2.25	0.25	2.25	0.44	9.44	0	0	0	0	0	0
	0.5	5	40	0.25	3	2.5	0.25	2.5	0.4	8.7	0	0	0	0	0	0
40-50	0.5	5	45	0.25	3	2.75	0.25	2.75	0.36	8.10	0	0	0	0	0	0
	0.5	5	50	0.25	3	3	0.25	3	0.33	7.59	0	0	0	0	0	0
50-60	0.5	5	55	0.25	3	3.25	0.25	3.25	0.31	7.16	0	0	0	0	0	0
	0.5	5	60	0.25	3	3.5	0.25	3.5	0.29	6.80	0	0	0	0	0	0
60-70	2.5	5	65	1.25	15	4.75	1.25	4.75	0.21	5.55	36.1	28.9	36.1	5.55	0.79	0.79
	2.5	5	70	1.25	15	6	1.25	6	0.17	4.82	49.5	20.5	49.5	4.82	0.85	1.64

Table B21: Computation of Potential Runoff in storm (T6) and Light Clay soil

T6	Computation of rainfall excess in a Light Clay soil															
Time	R(ts)	T-step	T-cum	R(ts)	Ri(ts)	Rc(ts)	f(t)	F	1/F	fpr(t)	tpr(t)	tdel	tact	fac(t)	Rexc	Σ Rexc
(min)	(mm)	(min)	(min)	(mm)	(mm/h)	(mm)	(mm)	(mm)	(1/mm)	(mm/h)	(min)	(min)	(min)	mm/h	mm	mm
1	2	3	4	5	6	7	8	9	10	11	12	13	14	15	16	17
0	0	0	0	0	0	0	0	0	0	37.5	0	0	0	0	0	0
0-10	2	5	5	1	12	1	1	1	1	18.69	0	0	0	0	0	0
	2	5	10	1	12	2	1	2	0.5	10.37	8.89	1.11	8.89	10.4	0.14	0.14
10.-20	3.5	5	15	1.75	21	3.75	1.75	3.75	0.27	6.48	25.4	-10	35.9	5.56	1.29	1.42
	3.5	5	20	1.75	21	5.5	1.75	5.5	0.18	5.07	44.1	-24	68.2	4.17	1.4	2.83
20-30	11	5	25	5.5	66	11	5.5	11	0.09	3.55	97.6	-73	170	2.77	5.27	8.10
	11	5	30	5.5	66	16.5	5.5	16.5	0.06	3.05	138	-108	245	2.36	5.3	13.4
30-40	4.5	5	35	2.25	27	18.8	2.25	18.8	0.05	2.93	151	-116	266	2.27	2.06	15.46
	4.5	5	40	2.25	27	21	2.25	21	0.05	2.83	162	-122	284	2.2	2.07	17.53
40-50	1.5	5	45	0.75	9	21.8	0.75	21.8	0.05	2.81	166	-121	286	2.2	0.57	18.09
	1.5	5	50	0.75	9	22.5	0.75	22.5	0.04	2.78	169	-119	288	2.19	0.57	18.66
50-60	0.5	0.5	50.5	0.03	3	22.5	0.03	22.5	0.04	2.78	169	-119	288	2.19	0.01	18.67
	0.5	0.5	51	0.03	3	22.6	0.03	22.6	0.04	2.78	169	-118	288	2.19	0.01	18.67
	0.5	0.5	51.5	0.03	3	22.6	0.03	22.6	0.04	2.78	169	-118	287	2.19	0.01	18.68
	0.5	0.5	52	0.03	3	22.6	0.03	22.6	0.04	2.78	170	-118	287	2.19	0.01	18.69
	0.5	0.5	52.5	0.03	3	22.6	0.03	22.6	0.04	2.78	170	-117	287	2.2	0.01	18.69
	0.5	0.5	53	0.03	3	22.7	0.03	22.7	0.04	2.78	170	-117	287	2.2	0.01	18.7
	0.5	0.5	53.5	0.03	3	22.7	0.03	22.7	0.04	2.77	170	-116	286	2.2	0.01	18.71
	0.5	0.5	54	0.03	3	22.7	0.03	22.7	0.04	2.77	170	-116	286	2.2	0.01	18.71
	0.5	0.5	54.5	0.03	3	22.7	0.03	22.7	0.04	2.77	170	-116	286	2.2	0.01	18.72
	0.5	0.5	55	0.03	3	22.8	0.03	22.8	0.04	2.77	170	-115	285	2.2	0.01	18.73
	0.5	0.5	55.5	0.03	3	22.8	0.03	22.8	0.04	2.77	170	-115	285	2.2	0.01	18.73

	0.5	0.5	56	0.03	3	22.8	0.03	22.8	0.04	2.77	170	-114	285	2.2	0.01	18.74
	0.5	0.5	56.5	0.03	3	22.8	0.03	22.8	0.04	2.77	171	-114	285	2.2	0.01	18.75
	0.5	0.5	57	0.03	3	22.9	0.03	22.9	0.04	2.77	171	-114	284	2.2	0.01	18.75
	0.5	0.5	57.5	0.03	3	22.9	0.03	22.9	0.04	2.77	171	-113	284	2.21	0.01	18.76
	0.5	0.5	58	0.03	3	22.9	0.03	22.9	0.04	2.77	171	-113	284	2.21	0.01	18.77
	0.5	0.5	58.5	0.03	3	22.9	0.03	22.9	0.04	2.77	171	-113	284	2.21	0.01	18.77
	0.5	0.5	59	0.03	3	23	0.03	23	0.04	2.77	171	-112	283	2.21	0.01	18.78
	0.5	0.5	59.5	0.03	3	23	0.03	23	0.04	2.77	171	-112	283	2.21	0.01	18.79
	0.5	0.5	60	0.03	3	23	0.03	23	0.04	2.76	171	-111	283	2.21	0.01	18.79
60-70	0.5	0.5	60.5	0.03	3	23	0.03	23	0.04	2.76	171	-111	282	2.21	0.01	18.8
	0.5	0.5	61	0.03	3	23.1	0.03	23.1	0.04	2.76	172	-111	282	2.21	0.01	18.81
	0.5	0.5	61.5	0.03	3	23.1	0.03	23.1	0.04	2.76	172	-110	282	2.21	0.01	18.81
	0.5	0.5	62	0.03	3	23.1	0.03	23.1	0.04	2.76	172	-110	282	2.21	0.01	18.82
	0.5	0.5	62.5	0.03	3	23.1	0.03	23.1	0.04	2.76	172	-109	281	2.21	0.01	18.83
	0.5	0.5	63	0.03	3	23.2	0.03	23.2	0.04	2.76	172	-109	281	2.22	0.01	18.83
	0.5	0.5	63.5	0.03	3	23.2	0.03	23.2	0.04	2.76	172	-109	281	2.22	0.01	18.84
	0.5	0.5	64	0.03	3	23.2	0.03	23.2	0.04	2.76	172	-108	280	2.22	0.01	18.85
	0.5	0.5	64.5	0.03	3	23.2	0.03	23.2	0.04	2.76	172	-108	280	2.22	0.01	18.85
	0.5	0.5	65	0.03	3	23.3	0.03	23.3	0.04	2.76	172	-107	280	2.22	0.01	18.86
	0.5	0.5	65.5	0.03	3	23.3	0.03	23.3	0.04	2.76	173	-107	280	2.22	0.01	18.86
	0.5	0.5	66	0.03	3	23.3	0.03	23.3	0.04	2.76	173	-107	279	2.22	0.01	18.87
	0.5	0.5	66.5	0.03	3	23.3	0.03	23.3	0.04	2.75	173	-106	279	2.22	0.01	18.88
	0.5	0.5	67	0.03	3	23.4	0.03	23.4	0.04	2.75	173	-106	279	2.22	0.01	18.88
	0.5	0.5	67.5	0.03	3	23.4	0.03	23.4	0.04	2.75	173	-105	278	2.22	0.01	18.89
	0.5	0.5	68	0.03	3	23.4	0.03	23.4	0.04	2.75	173	-105	278	2.23	0.01	18.9
	0.5	0.5	68.5	0.03	3	23.4	0.03	23.4	0.04	2.75	173	-105	278	2.23	0.01	18.9
	0.5	0.5	69	0.03	3	23.4	0.03	23.4	0.04	2.75	173	-104	278	2.23	0.01	18.91
	0.5	0.5	69.5	0.03	3	23.5	0.03	23.5	0.04	2.75	173	-104	277	2.23	0.01	18.92
	0.5	0.5	70	0.03	3	23.5	0.03	23.5	0.04	2.75	173	-103	277	2.23	0.01	18.92

Table B22: Computation of Potential Runoff in storm (M2) and Light Clay soil

M2	**Computation of rainfall excess in a Light Clay soil**															
Time	R(ts)	T-step	T-cum	R(ts)	Ri(ts)	Rc(ts)	f(t)	F	1/F	fpr(t)	tpr(t)	tdel	tact	fac(t)	Rexc	Σ Rexc
(min)	(mm)	(min)	(min)	(mm)	(mm/h)	(mm)	(mm)	(mm)	(1/mm)	(mm/h)	(min)	(min)	(min)	mm/h	mm	mm
1	2	3	4	5	6	7	8	9	10	11	12	13	14	15	16	17
0	0	0	0	0	0	0	0	0	0	37.5	0	0	0	0	0	0
0-10	0.5	5	5	0.25	3	0.25	0.25	0.25	4	68.64	0	0	0	0	0	0
	0.5	5	10	0.25	3	0.5	0.25	0.5	2	35.34	0	0	0	0	0	0
10.-20	1	5	15	0.5	6	1	0.5	1	1	18.69	0	0	0	0	0	0
	1	5	20	0.5	6	1.5	0.5	1.5	0.67	13.14	0	0	0	0	0	0
20-30	1	5	25	0.5	6	2	0.5	2	0.5	10.37	0	0	0	0	0	0
	1	5	30	0.5	6	2.5	0.5	2.5	0.4	8.7	0	0	0	0	0	0
30-40	0.5	5	35	0.25	3	2.75	0.25	2.75	0.36	8.10	0	0	0	0	0	0
	0.5	5	40	0.25	3	3	0.25	3	0.33	7.59	0	0	0	0	0	0
40-50	0.5	5	45	0.25	3	3.25	0.25	3.25	0.31	7.16	0	0	0	0	0	0
	0.5	5	50	0.25	3	3.5	0.25	3.5	0.29	6.80	0	0	0	0	0	0
50-60	3	5	55	1.5	18	5	1.5	5	0.2	5.37	38.7	16.3	38.7	5.37	1.05	1.05
	3	5	60	1.5	18	6.5	1.5	6.5	0.15	4.60	54.7	5.25	54.7	4.6	1.12	2.17

Table B23: Computation of Potential Runoff in storm (M4) and Light Clay soil

M4	Computation of rainfall excess in a Light Clay soil															
Time	R(ts)	T-step	T-cum	R(ts)	Ri(ts)	Rc(ts)	f(t)	F	1/F	fpr(t)	tpr(t)	tdel	tact	fac(t)	Rexc	Σ Rexc
(min)	(mm)	(min)	(min)	(mm)	(mm/h)	(mm)	(mm)	(mm)	(1/mm)	(mm/h)	(min)	(min)	(min)	mm/h	mm	mm
1	2	3	4	5	6	7	8	9	10	11	12	13	14	15	16	17
0	0	0	0	0	0	0	0	0	0	70	0	0	0	0	0	0
0-10	1	5	5	0.5	6	0.5	0.5	0.5	2	35.34	0	0	0	0	0	0
	1	5	10	0.5	6	1	0.5	1	1	18.69	0	0	0	0	0	0
10.-20	2	5	15	1	12	2	1	2	0.5	10.37	8.89	6.11	8.89	10.4	0.14	0.14
	2	0.5	15.5	0.1	12	2.1	0.1	2.1	0.48	9.97	9.7	5.8	9.7	9.97	0.02	0.15
	2	0.5	16	0.1	12	2.2	0.1	2.2	0.46	9.61	10.5	5.46	10.5	9.61	0.02	0.17
	2	0.5	16.5	0.1	12	2.3	0.1	2.3	0.44	9.28	11.4	5.11	11.4	9.28	0.02	0.20
	2	0.5	17	0.1	12	2.4	0.1	2.4	0.42	8.98	12.3	4.73	12.3	8.98	0.03	0.22
	2	0.5	17.5	0.1	12	2.5	0.1	2.5	0.4	8.7	13.2	4.34	13.2	8.7	0.03	0.25
	2	0.5	18	0.1	12	2.6	0.1	2.6	0.39	8.44	14.1	3.93	14.1	8.44	0.03	0.28
	2	0.5	18.5	0.1	12	2.7	0.1	2.7	0.37	8.21	15	3.5	15	8.21	0.03	0.31
	2	0.5	19	0.1	12	2.8	0.1	2.8	0.36	7.99	15.9	3.06	15.9	7.99	0.03	0.34
20-30	3	5	24	1.5	18	4.3	1.5	4.3	0.23	5.91	31.2	-7.2	38.5	5.39	1.05	1.39
	3	5	29	1.5	18	5.8	1.5	5.8	0.17	4.91	47.3	-18	65.7	4.24	1.15	2.54

Table B24: Computation of Potential Runoff in storm (M6) and Light Clay soil

M6	Computation of rainfall excess in a Light Clay soil															
Time	R(ts)	T-step	T-cum	R(ts)	Ri(ts)	Rc(ts)	f(t)	F	1/F	fpr(t)	tpr(t)	tdel	tact	fac(t)	Rexc	Σ Rexc
(min)	(mm)	(min)	(min)	(mm)	(mm/h)	(mm)	(mm)	(mm)	(1/mm)	(mm/h)	(min)	(min)	(min)	mm/h	mm	mm
1	2	3	4	5	6	7	8	9	10	11	12	13	14	15	16	17
0	0	0	0	0	0	0	0	0	0	37.5	0	0	0	0	0	0
0-10	17.5	5	5	8.75	105	8.75	8.75	8.75	0.11	3.94	77.4	-72	150	2.94	8.51	8.51
	17.5	5	10	8.75	105	17.5	8.75	17.5	0.06	2.99	144	-134	277	2.23	8.56	17.07
10.-20	12.5	5	15	6.25	75	23.8	6.25	23.8	0.04	2.74	175	-160	334	2.05	6.08	23.15
	12.5	5	20	6.25	75	30	6.25	30	0.03	2.60	197	-177	375	1.95	6.09	29.24
20-30	7.5	5	25	3.75	45	33.8	3.75	33.8	0.03	2.53	208	-183	391	1.91	3.59	32.83
	7.5	5	30	3.75	45	37.5	3.75	37.5	0.03	2.48	218	-188	405	1.88	3.59	36.42
30-40	2	5	35	1	12	38.5	1	38.5	0.03	2.48	220	-185	405	1.88	0.84	37.26
	2	5	40	1	12	39.5	1	39.5	0.03	2.46	222	-182	404	1.88	0.84	38.11
40-50	1	5	45	0.5	6	40	0.5	40	0.03	2.46	223	-178	401	1.89	0.34	38.45
	1	5	50	0.5	6	40.5	0.5	40.5	0.03	2.45	224	-174	398	1.9	0.34	38.79
50-60	1.5	5	55	0.75	9	41.3	0.75	41.3	0.02	2.44	226	-171	396	1.9	0.59	39.38
	1.5	5	60	0.75	9	42	0.75	42	0.02	2.44	227	-167	394	1.9	0.59	39.97
60-70	0.5	0.5	60.5	0.03	3	42	0.03	42	0.02	2.44	227	-167	394	1.91	0.01	39.98
	0.5	0.5	61	0.03	3	42.1	0.03	42.1	0.02	2.44	227	-166	394	1.91	0.01	39.99
	0.5	0.5	61.5	0.03	3	42.1	0.03	42.1	0.02	2.44	227	-166	393	1.91	0.01	40
	0.5	0.5	62	0.03	3	42.1	0.03	42.1	0.02	2.44	227	-165	393	1.91	0.01	40.01
	0.5	0.5	62.5	0.03	3	42.1	0.03	42.1	0.02	2.44	227	-165	392	1.91	0.01	40.02
	0.5	0.5	63	0.03	3	42.2	0.03	42.2	0.02	2.44	227	-164	392	1.91	0.01	40.03
	0.5	0.5	63.5	0.03	3	42.2	0.03	42.2	0.02	2.44	228	-164	392	1.91	0.01	40.04
	0.5	0.5	64	0.03	3	42.2	0.03	42.2	0.02	2.44	228	-164	391	1.91	0.01	40.05
	0.5	0.5	64.5	0.03	3	42.2	0.03	42.2	0.02	2.43	228	-163	391	1.91	0.01	40.06

	0.5	0.5	65	0.03	3	42.3	0.03	42.3	0.02	2.43	228	-163	390	1.91	0.01	40.06
	0.5	0.5	65.5	0.03	3	42.3	0.03	42.3	0.02	2.43	228	-162	390	1.91	0.01	40.07
	0.5	0.5	66	0.03	3	42.3	0.03	42.3	0.02	2.43	228	-162	390	1.91	0.01	40.08
	0.5	0.5	66.5	0.03	3	42.3	0.03	42.3	0.02	2.43	228	-161	389	1.92	0.01	40.09
	0.5	0.5	67	0.03	3	42.4	0.03	42.4	0.02	2.43	228	-161	389	1.92	0.01	40.1
	0.5	0.5	67.5	0.03	3	42.4	0.03	42.4	0.02	2.43	228	-160	388	1.92	0.01	40.11
	0.5	0.5	68	0.03	3	42.4	0.03	42.4	0.02	2.43	228	-160	388	1.92	0.01	40.12
	0.5	0.5	68.5	0.03	3	42.4	0.03	42.4	0.02	2.43	228	-160	388	1.92	0.01	40.13
	0.5	0.5	69	0.03	3	42.5	0.03	42.5	0.02	2.43	228	-159	387	1.92	0.01	40.14
	0.5	0.5	69.5	0.03	3	42.5	0.03	42.5	0.02	2.43	228	-159	387	1.92	0.01	40.15
	0.5	0.5	70	0.03	3	42.5	0.03	42.5	0.02	2.43	228	-158	386	1.92	0.01	40.15

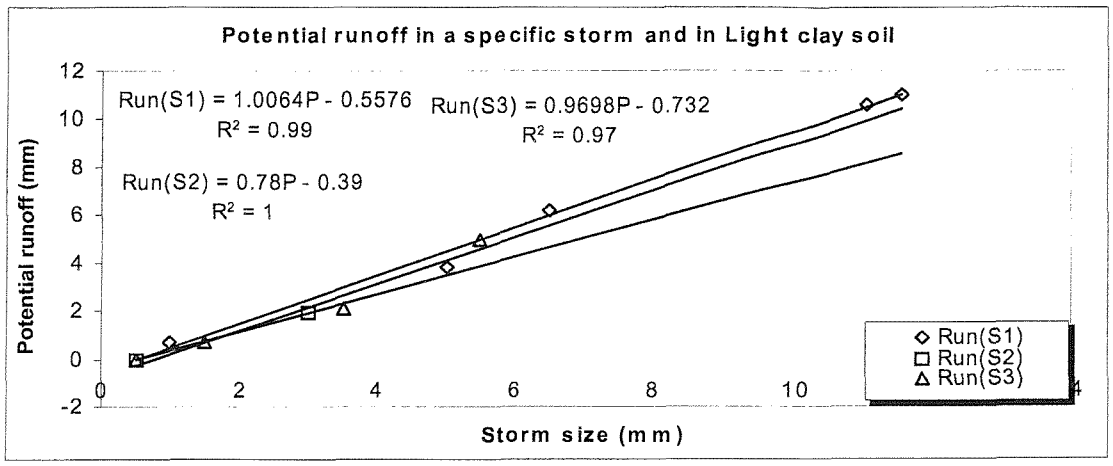

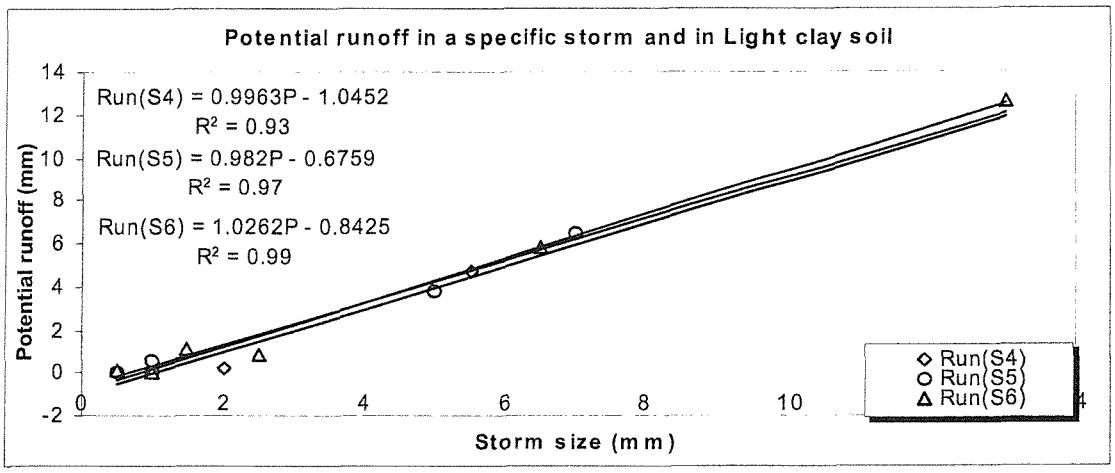

Figure B9: Storm size and Potential Runoff relationship in Light clay soil (For storms S1, S2, S3, S4, S5, S6)

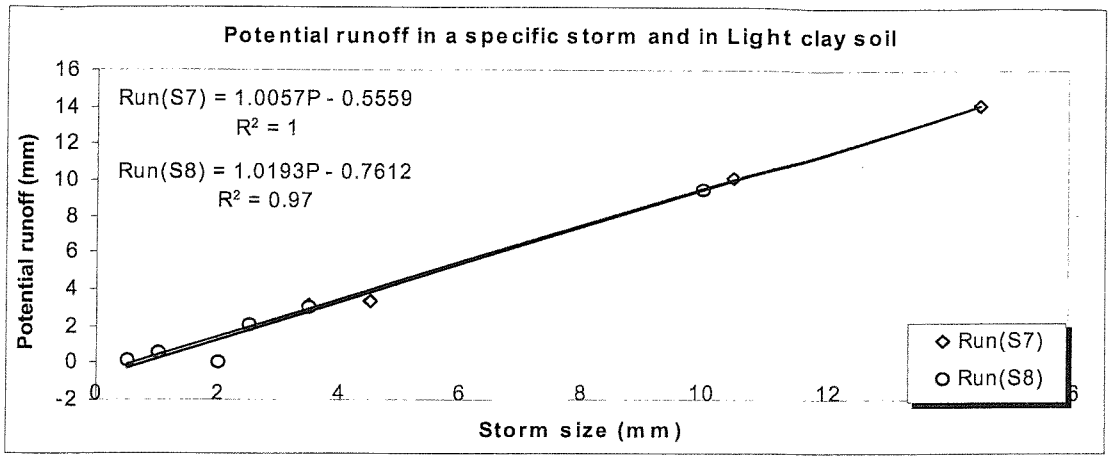

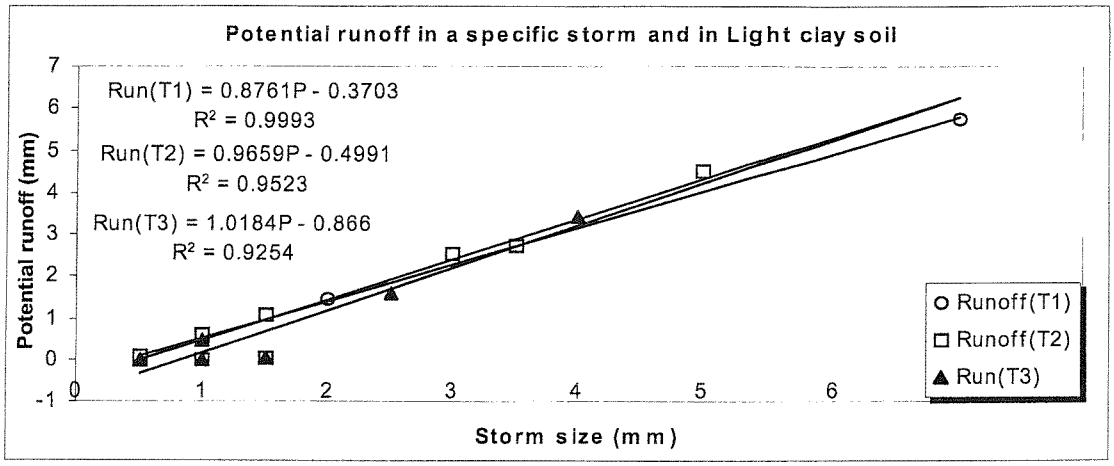

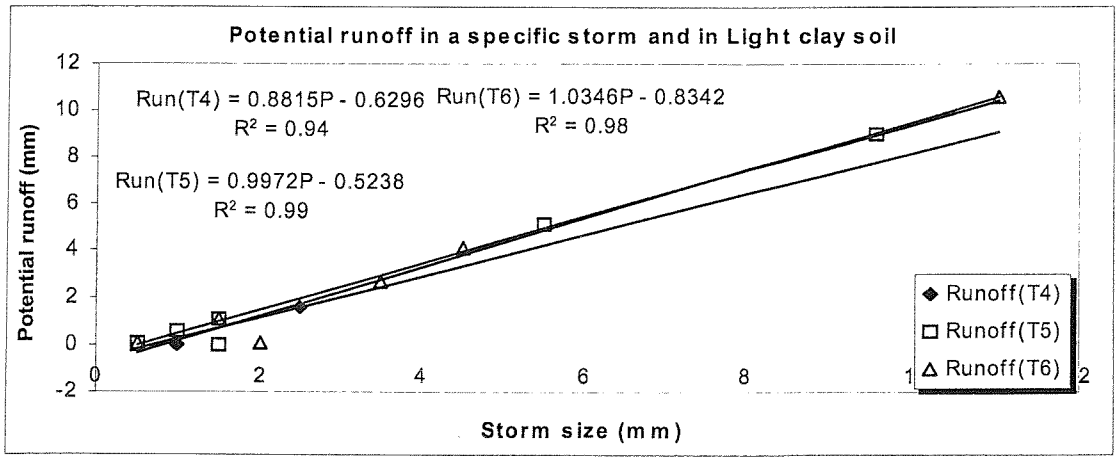

Figure B10: Storm size and Potential Runoff relationship in Light clay soil (For storms S7, S8, T1, T2, T3, T4, T5 and T6)

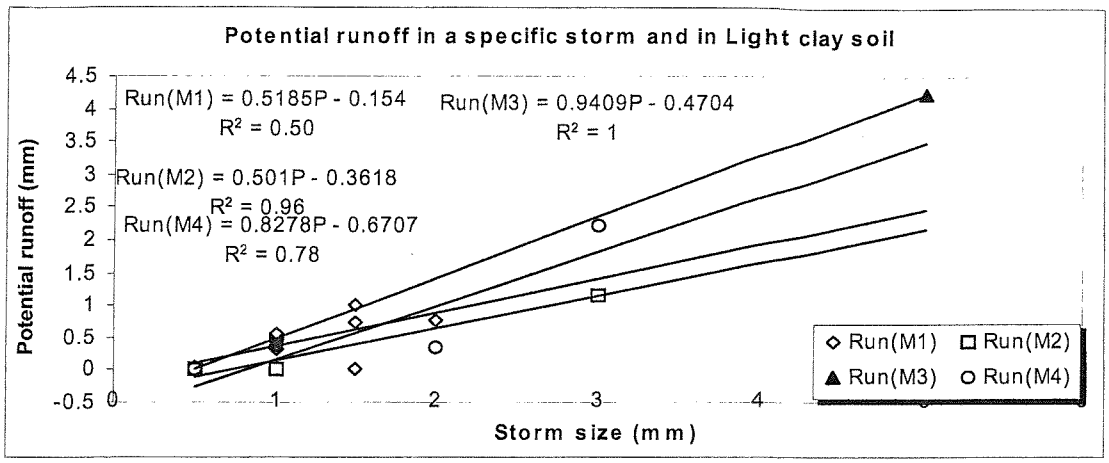

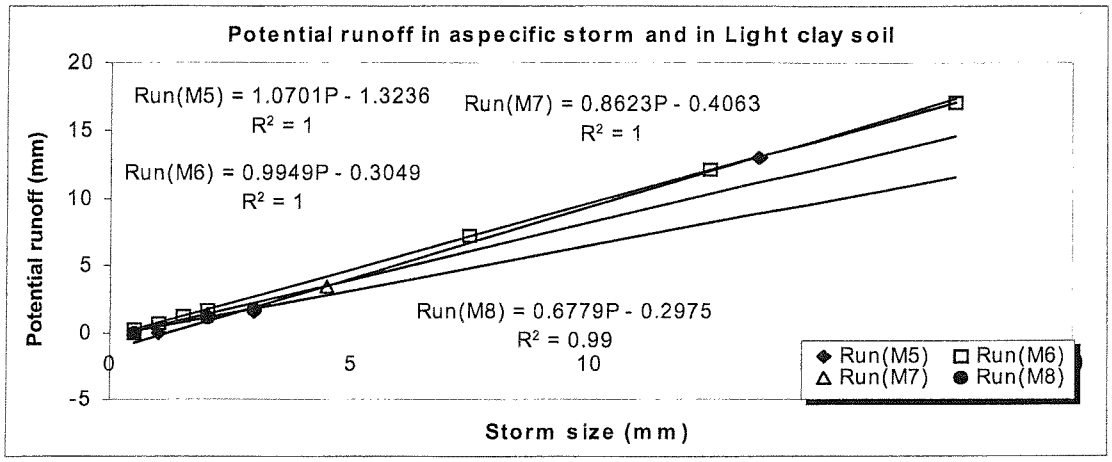

Figure B11: Storm size and Potential Runoff relationship in Light clay soil (For storms M1, M2, M3, M4, M5, M6, M7 and M8)

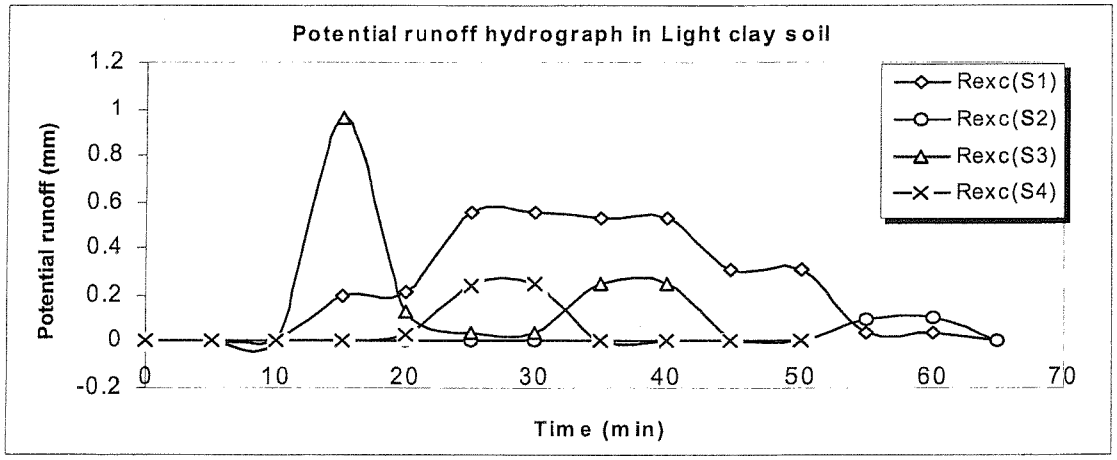

Figure B12: Potential runoff Hydrograph in Light clay soil (For storms S1, S2, S3, and S4)

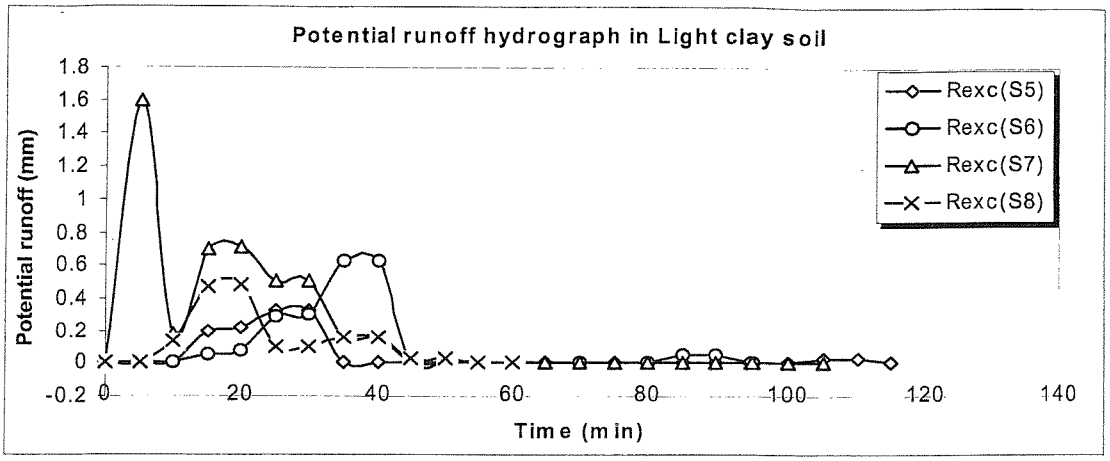

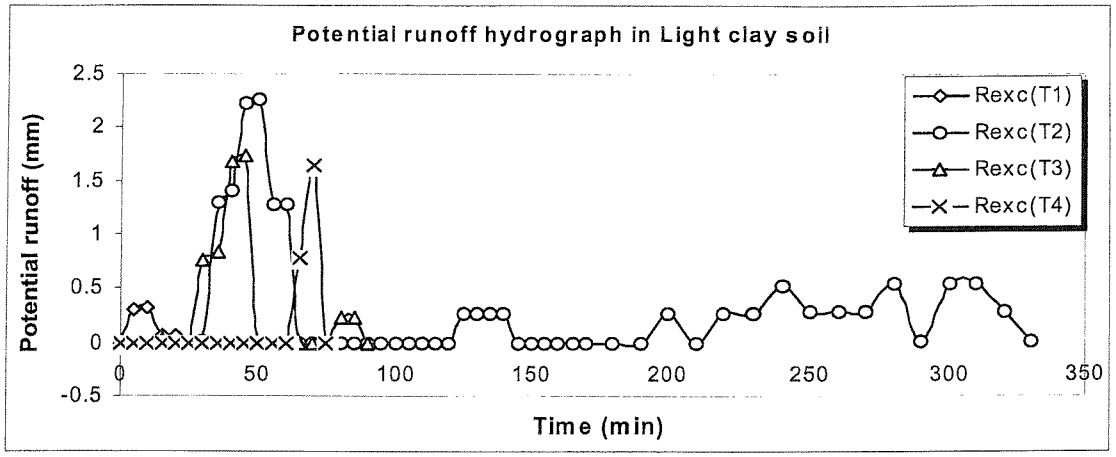

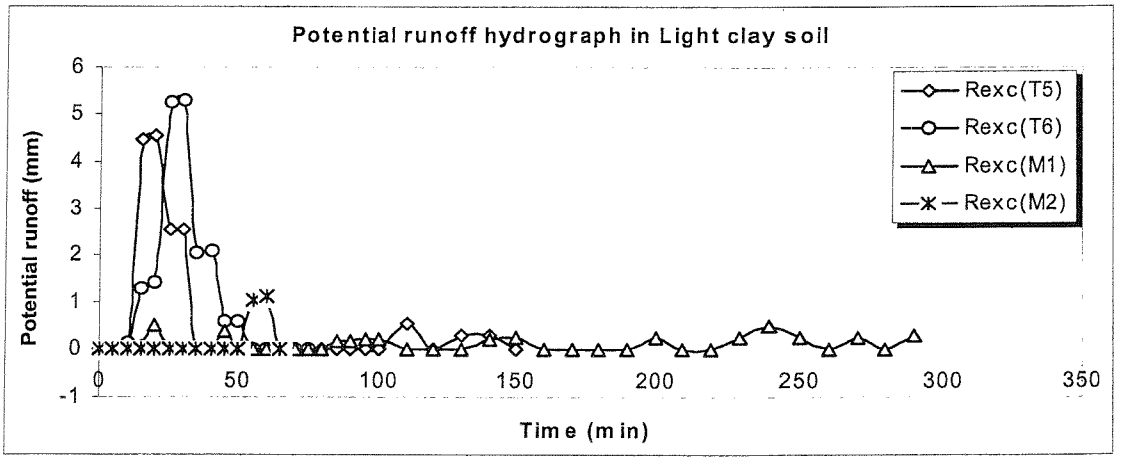

Figure B13: Potential runoff Hydrograph in Light clay soil (For storms S5, S6, S7, S4, T1, T2, T3, T4, T5 T,6, M1 and M2)

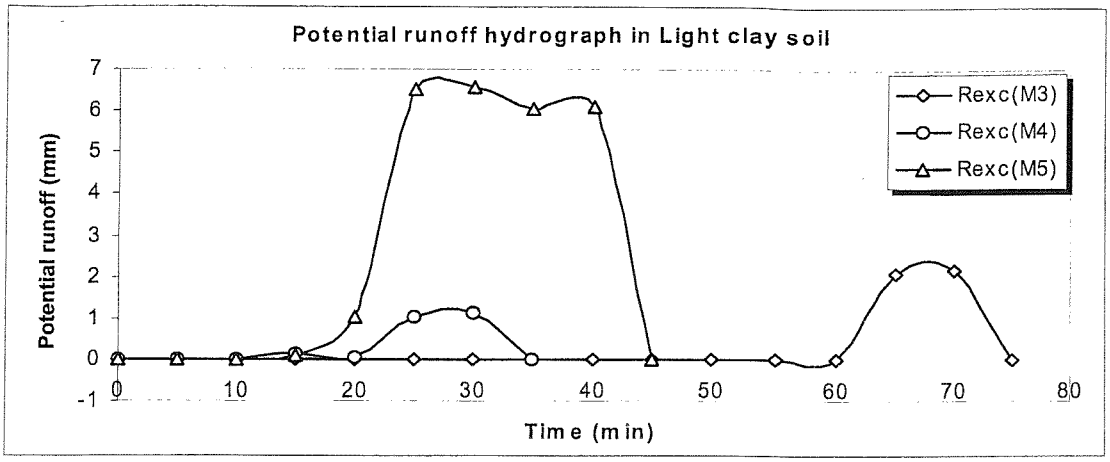

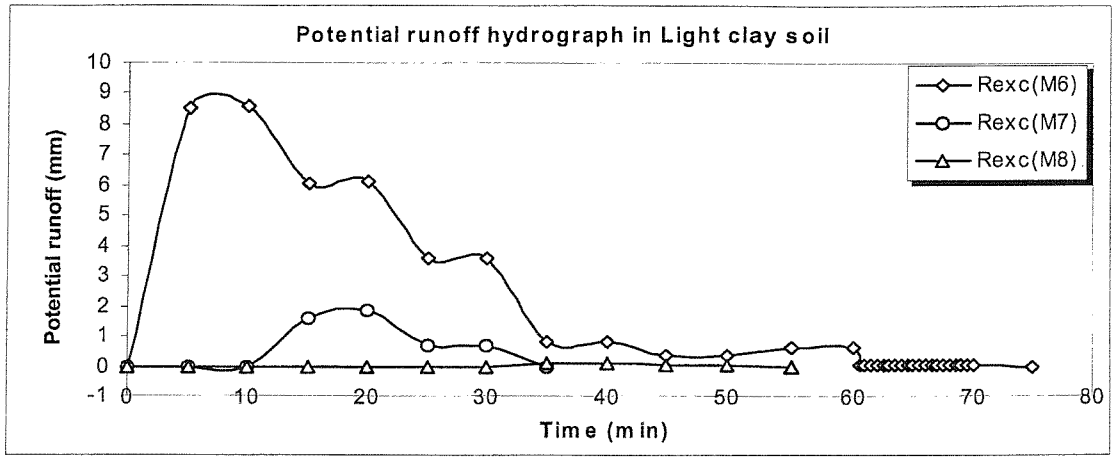

Figure B14: Potential runoff Hydrograph in Light clay soil (For storms M3, M4, M5, M6, M6 and M8)

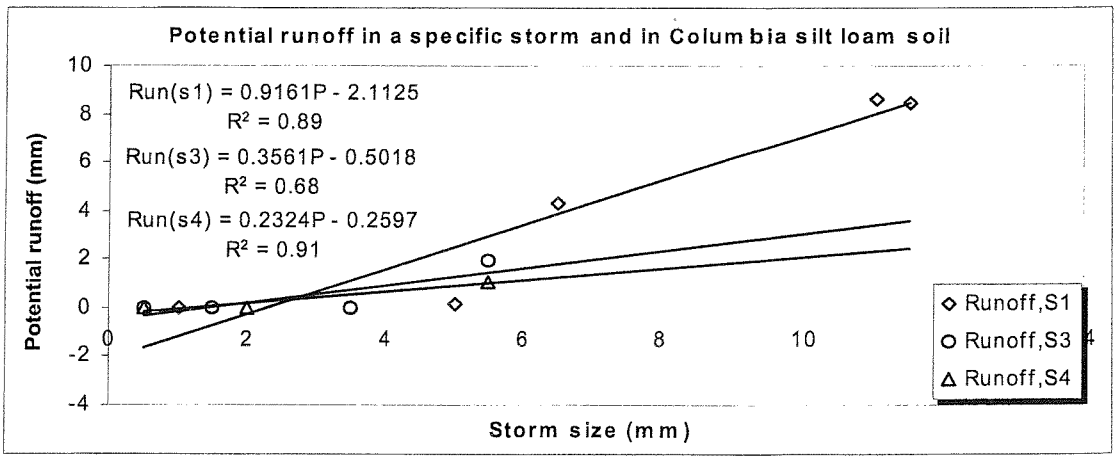

Figure B15: Storm size and Potential Runoff relationship in Light clay soil (For storms S1, S3, S4)

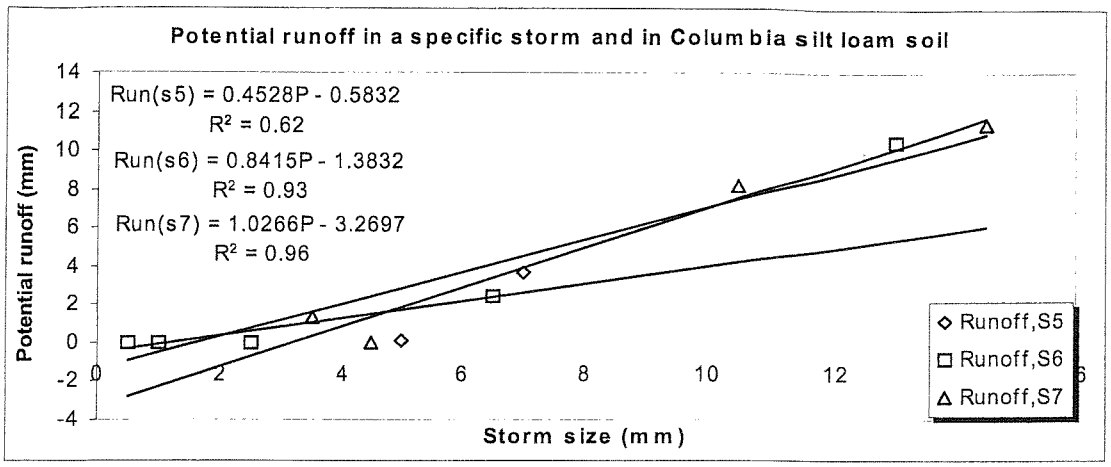

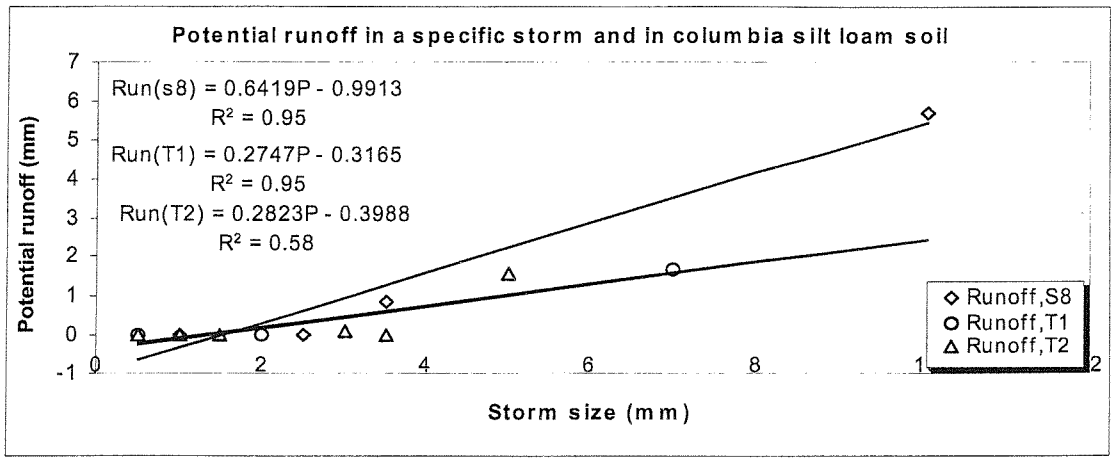

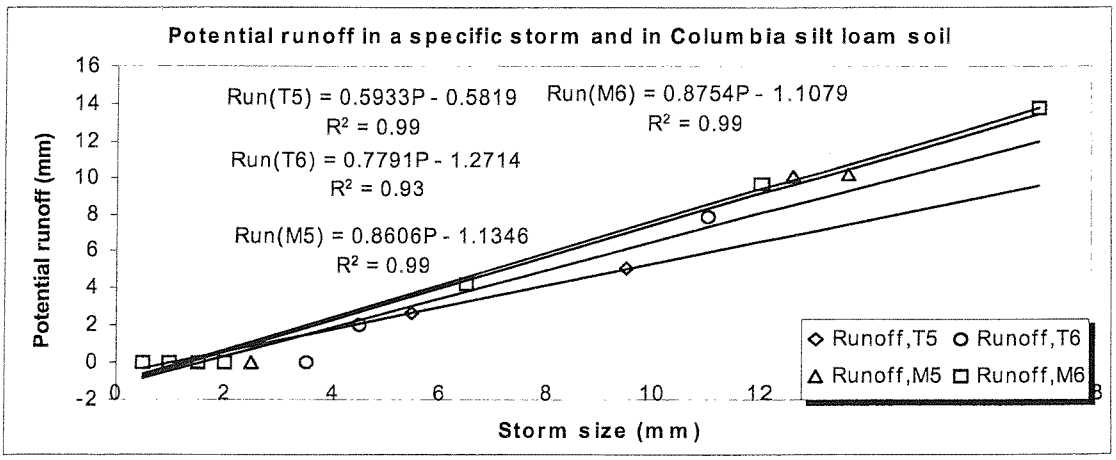

Figure B16: Storm size and Potential Runoff relationship in Light clay soil (For storms S5, S6, S7, S8, T1, T2, T5, T6, M5 and M6)

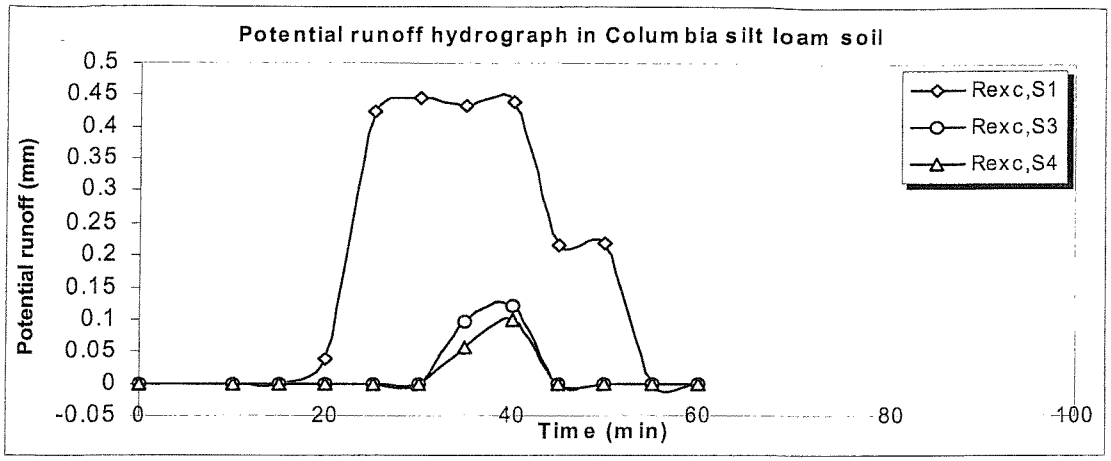

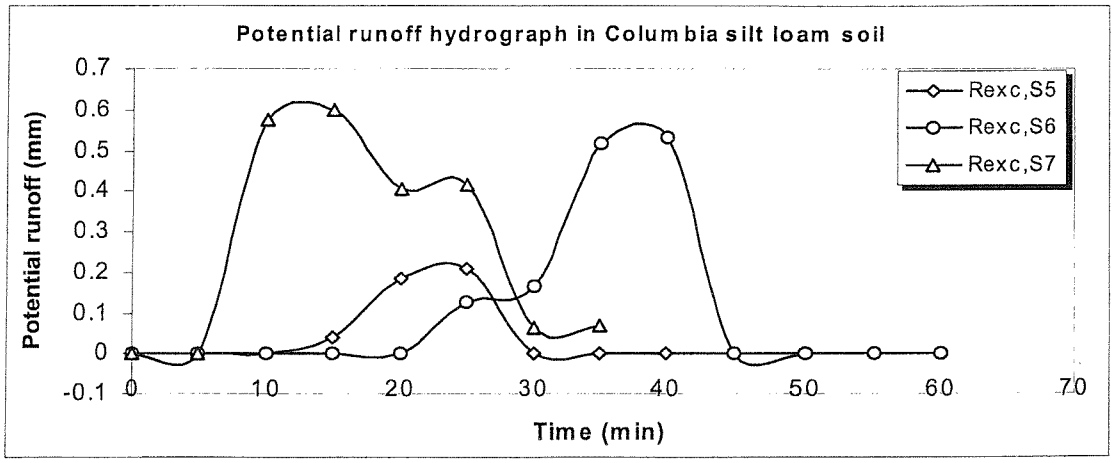

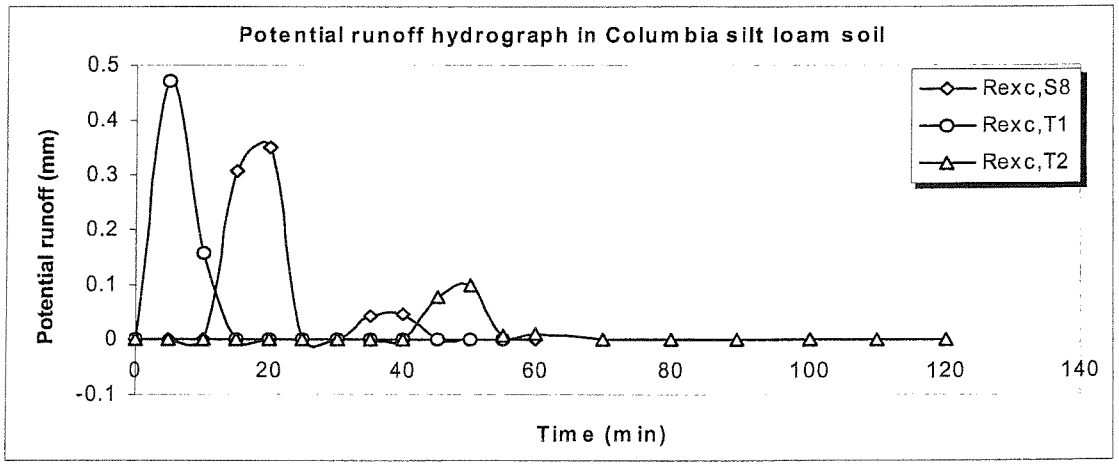

Figure B17: Potential runoff Hydrograph in Light clay soil (For storms S1, S3, S4, S5, S6, S7, S8, T1, and T2)

Appendix C: Simulation Model Equations

In this appendix a set of equations with boundary conditions is used to solve Richard equation in section 3.3.3 (Van Dam and Feddes, 2000). The implicit, backward, finite difference solution as discussed in section 3.3.3, reads (Equation.3.34).

$$C_i^{j+1.k-1}\left(h_i^{j+1,k}-h_i^{j+1,k-1}\right)+\theta_i^{j+1,k-1}-\theta_i^{j}= \tag{C1}$$

$$=\frac{\Delta t^j}{\Delta z_i}\left[K^j_{i-(1/2)}\left(\frac{h_{i-1}^{j+1,k}-h_i^{j+1,k}}{\Delta z_u}\right)+K^j_{i-(1/2)}-K^j_{i+(1/2)}\left(\frac{h_i^{j+1,k}-h_{i+1}^{j+1,k}}{\Delta z_l}\right)-K^j_{i+(1/2)}\right]-\Delta t^i S_i^j$$

The above equation can be written to the following:

$$\left(-\frac{\Delta t^j}{\Delta z_i\Delta z_u}K^j_{i-(1/2)}\right)h_{i-1}^{j+1,k}+\left[C_i^{j+1,k-1}+\left(\frac{\Delta t^j}{\Delta z_i\Delta z_u}K^j_{i-(1/2)}\right)+\left(\frac{\Delta t^j}{\Delta z_i\Delta z_u}K^j_{i+(1/2)}\right)\right]h_i^{j+1,k} \tag{C2}$$

$$+\left(-\frac{\Delta t^j}{\Delta z_i\Delta z_l}K^j_{i+(1/2)}\right)h_{i+1}^{j+1,k}=C_i^{j+1,k-1}h_i^{j+1,k-1}-\theta_i^{j+1,k-1}+\theta_i^j+\frac{\Delta t^j}{\Delta z_i}\left(K^j_{i-(1/2)}-K^j_{i+(1/2)}\right)-\Delta t^j S_i^j=f_i$$

This equation can be reduced to the following equation:

$$\alpha h_{i-1}^{j+1,k}+\beta h_i^{j+1,k}+\gamma h_{i+1}^{j+1,k}=f_i \tag{C3}$$

The system of equations between soil surface and soil profile and for each node point can be written as:

$$\beta_1 h_1^{j+1,k}+\gamma_1 h_2^{j+1,k}=C_1^{j+1,k-1}h_1^{j+1,k-1}+\frac{\Delta t^j}{\Delta z_1}\left(-q_{sur}-K^j_{1+(1/2)}\right)-\Delta t^j S_1^j=f_1 \tag{C4}$$

$$\alpha_2 h_1^{j+1,k}+\beta_2 h_2^{j+1,k}+\gamma_2 h_3^{j+1,k}=C_2^{j+1,k-1}h_2^{j+1,k-1}+\frac{\Delta t^j}{\Delta z_2}\left(K^j_{2-(1/2)}-K^j_{2+(1/2)}\right)-\Delta t^j S_2^j=f_2$$

$$\alpha_3 h_2^{j+1,k}+\beta_3 h_3^{j+1,k}+\gamma_3 h_4^{j+1.k}=C_3^{j+1,k-1}h_3^{j+1,k-1}+\frac{\Delta t^j}{\Delta z_3}\left(K^j_{3-(1/2)}-K^j_{3+(1/2)}\right)-\Delta t^j S_3^j=f_3$$

$$\alpha_{n-1} h_{n-2}^{j+1,k}+\beta_{n-1} h_{n-1}^{j+1,k}+\gamma_{n-1} h_n^{j+1,k}=C_{n-1}^{j+1,k-1}h_{n-1}^{j+1,k-1}+\frac{\Delta t^j}{\Delta z_{n-1}}\left(K^j_{(n-1)-(1/2)}-K^j_{(n-1)+(1/2)}\right)-\Delta t^j S_{n-1}^j=f_{n-1}$$

$$\alpha_n h_{n-1}^{j+1,k}+\beta_n h_n^{j+1,k}=C_n^{j+1,k-1}h_n^{j+1,k}+\frac{\Delta t^j}{\Delta z_n}\left(K^j_{n-(1/2)}-K^j_{n+(1/2)}\right)-\Delta t^j S_n^j=f_n$$

C.1. Intermediate node points

Rearrangement of C_1 to C_2 results in the coe3fficients:

$$\alpha_i = -\frac{\Delta t^j}{\Delta z_i \Delta z_u} K^j_{i-1/2} \qquad (C_5)$$

$$\beta_i = C_i^{j+1,k-1} + \frac{\Delta t^j}{\Delta z_i \Delta z_u} K^j_{i-(1/2)} + \frac{\Delta t^j}{\Delta z_i \Delta z_l} K^j_{i+(1/2)} \qquad (C_6)$$

$$\gamma_i = -\frac{\Delta t^j}{\Delta z_i \Delta z_l} K^j_{i+(1/2)} \qquad (C_7)$$

$$f_i = C_i^{j+1,k-1} h_i^{j+1,k-1} - \theta_i^{j+1,k-1} + \theta_i^j + \frac{\Delta t^j}{\Delta z_i}\left(K^j_{i-(1/2)} - K^j_{i+(1/2)}\right) - \Delta t^j S_i^j \qquad (C_8)$$

C.2. Top node Point

C.2.1. Soil Surface Infiltration (q_{sur}), boundary condition

For the solution of top nodal point (i=1) the right hand side of equation C_1 is transformed to:

$$\frac{\Delta t^j}{\Delta z_i}\left[-q_{sur} - K^j_{1(1/2)}\left(\frac{h_1^{j+1,k} - h_2^{j+1,k}}{\Delta z_l}\right) - K^j_{1(1/2)}\right] - \Delta t^j S_i^j \qquad (C_9)$$

Where:

$$q_{sur} = K^j_{1-(1/2)}\left[\left(\frac{h_{1-(1/2)}^{j+1,k} - h_i^{j+1,k}}{\Delta z_u}\right) + 1\right] \qquad (C_{10})$$

Rearrangements of C_1 to the first line of C_2 give the coefficients:

$$\beta_1 = C_1^{j+1,k-1} + \frac{\Delta t^j}{\Delta z \Delta l} K^j_{1(1/2)} \qquad (C_{11})$$

$$\gamma_1 = -\frac{\Delta t^j}{\Delta z_1 \Delta z l} K^j_{1(1/2)} \qquad (C_{12})$$

$$f_1 = C_1^{j+1,k-1} h_1^{j+1,k-1} - \theta_1^{j+1,k-1} + \theta_1^j + \frac{\Delta t^j}{\Delta z_1}\left(-q_{sur} - K^j_{1(1/2)}\right) - \Delta t^j S_1^j \qquad (C_{13})$$

When taking compartments of equal size, for example $\Delta z_u = \Delta z_l = \Delta z$, the coefficient of equation C_3 (α, β, γ,) then become:

$$\alpha = 0 \qquad (C_{14})$$

$$\beta_1 = C_1^{j+1,k-1} + \frac{\Delta t^j}{(\Delta z_1)^2} K^j_{1(1/2)} \qquad (C_{15})$$

$$\gamma_1 = -\frac{\Delta t^j}{(\Delta z_1)^2} K^j_{1(1/2)} \qquad (C_{16})$$

C.2.3. Bottom node

When the flux through the bottom of the unsaturated zone is known, the right hand side of equation C_1 transforms to:

$$\frac{\Delta t^j}{\Delta z_n}\left[K^j_{n-(1/2)}\left(\frac{h^{j+1,k}_{n-1} - h^{j+1,k}_n}{\Delta z_u} \right) + K^j_{n-(1/2)} + q_{bot} \right] - \Delta t^j S^j_n \qquad (C_{17})$$

Rearrangements of C_1 to the last line of C_2 gives the coefficients:

$$\alpha_n = -\frac{\Delta t^j}{\Delta z_n \Delta z_u} K^j_{n-(1/2)} \qquad (C_{18})$$

$$\beta_n = C^{j,+1,k-1}_n + \frac{\Delta t^j}{\Delta z_n \Delta z_u} K^j_{n-(1/2)} \qquad (C_{19})$$

$$\gamma_n = 0 \qquad (C_{20})$$

$$f_n = C^{j+1,k-1}_n h^{j+1,k-1}_n - \theta^{j+1,k-1}_n + \theta^j_n + \frac{\Delta t^j}{\Delta z_n}\left(K^j_{n-(1/2)} + q_{bot} \right) - \Delta t^j S^j_n \qquad (C_{21})$$

Where: q_{bot} = hydraulic conductivity as follow:

$$q_{bot} = -K\left(h^j_n\right) \qquad (C_{22})$$

For the bottom of the soil profile in infiltration of Micro-Catchment system is assumed that $\frac{\partial h}{\partial z} = 0$, which means that the water is allowed to drain fully so that q ($z=-z_b$, t)$=-K(h)$, where z_b is bottom of soil profile (Belmans and Feddes 1983, Hills, 1989).

Appendix D: Generating Daily Rainfall Pattern (Tables & Figures)

Table D.1. Observed and Exponential distribution of rainfall in Shiraz (Iran).

				(X-Xm)^2	observed	cumulative distribution	
uper,class), l	xi	fi(x)	Xi*fi	(2-Xm)^2	fraction(Oi/T)	Observed	Exponential
1	**2**	**3**	**4**	**5**	**6**	**7**	**8**
2	1	172	172	53.38	0.37	0.37	0.22
4	3	53	159	28.15	0.11	0.49	0.39
6	5	43	215	10.93	0.09	0.58	0.53
8	7	36	252	1.71	0.08	0.66	0.63
10	9	30	270	0.48	0.07	0.72	0.71
12	11	24	264	7.26	0.05	0.78	0.78
14	13	14	182	22.03	0.03	0.81	0.83
16	15	12	180	44.81	0.03	0.83	0.86
18	17	8	136	75.59	0.02	0.85	0.89
20	19	12	228	114.36	0.03	0.88	0.92
22	21	10	210	161.14	0.02	0.90	0.94
24	23	11	253	215.91	0.02	0.92	0.95
26	25	6	150	278.69	0.01	0.93	0.96
28	27	4	108	349.47	0.01	0.94	0.97
30	29	6	174	428.24	0.01	0.96	0.98
32	31	4	124	515.02	0.01	0.97	0.98
34	33	1	33	609.79	0	0.97	0.99
36	35	1	35	712.57	0	0.97	0.99
38	37	0	0	823.35	0	0.97	0.99
40	39	3	117	942.12	0.01	0.98	0.99
42	41	3	123	1068.9	0.01	0.98	0.99
44	43	0	0	1203.67	0	0.98	1
46	45	2	90	1346.45	0	0.99	1
48	47	0	0	1497.23	0	0.99	1
50	49	2	98	1656	0	0.99	1
52	51	0	0	1822.78	0	0.99	1
54	53	0	0	1997.55	0	0.99	1
56	55	0	0	2180.33	0	0.99	1
58	57	1	57	2371.11	0	0.99	1
60	59	1	59	2569.88	0	1	1
62	61	0	0	2776.66	0	1	1
64	63	0	0	2991.43	0	1	1
66	65	1	65	3214.21	0	1	1
68	67	0	0	3444.99	0	1	1
70	69	0	0	3683.76	0	1	1
72	71	0	0	3930.54	0	1	1
74	73	0	0	4185.31	0	1	1
76	75	1	75	4448.09	0	1	1
		461	3829	51783.9			
Xmea =	8.306		λ =	0.120397			

Table D2: Observed and exponential distribution of rainfall in Esfahan rain gage station (Iran)

					Cumulative distribution	
Upper class,I	xi	fi(0i)	Xi*fi	Oi/T	Observed	Exponential
1	2	3	4	5	6	7
2	1	196	196	0.53	0.53	0.45
4	3	79	237	0.21	0.74	0.70
6	5	45	225	0.12	0.86	0.83
8	7	17	119	0.05	0.91	0.91
10	9	10	90	0.03	0.94	0.95
12	11	10	110	0.03	0.96	0.97
14	13	2	26	0.01	0.97	0.98
16	15	3	45	0.01	0.98	0.99
18	17	2	34	0.01	0.98	1
20	19	0	0	0	0.98	1
22	21	3	63	0.01	0.99	1
24	23	2	46	0.01	0.99	1
26	25	0	0	0	0.99	1
28	27	0	0	0	0.99	1
30	29	0	0	0	0.99	1
32	31	1	31	0.00	1	1
34	33	1	33	0.00	1	1
Total		374	1259			
Xmea =	3.36631		λ =	0.297061		

Table D3: Observed and exponential distribution of rainfall in Kashan rain gage station (Iran)

				observed	cumulative distribution	
up,class),I	xi	fi(x)	Xi*fi	fraction(Oi/T)	Observed	Exponential
1	2	3	4	5	6	7
2	1	156	156	0.44	0.44	0.40
4	3	80	240	0.23	0.67	0.64
6	5	50	250	0.14	0.81	0.78
8	7	33	231	0.09	0.90	0.87
10	9	14	126	0.04	0.94	0.92
12	11	9	99	0.03	0.97	0.95
14	13	4	52	0.01	0.98	0.97
16	15	6	90	0.02	0.99	0.98
18	17	2	34	0.01	1	0.99
20	19	4	76	0.01	1.01	0.99
22	21	2	42	0.01	1.02	1
24	23	0	0	0	1.02	1
26	25	0	0	0	1.02	1
28	27	0	0	0	1.02	1
30	29	0	0	0	1.02	1
32	31	1	31	0	1.02	1
		361	1427			
Xmean =	3.952909		λ =	0.252978	3.952909	

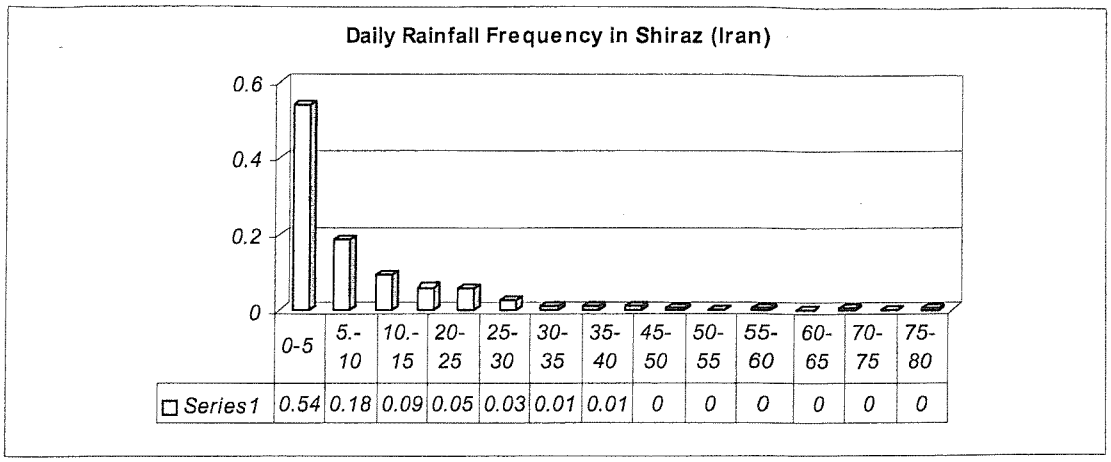

Figure D1: Relative frequency of rainfall in Shiraz (Iran)

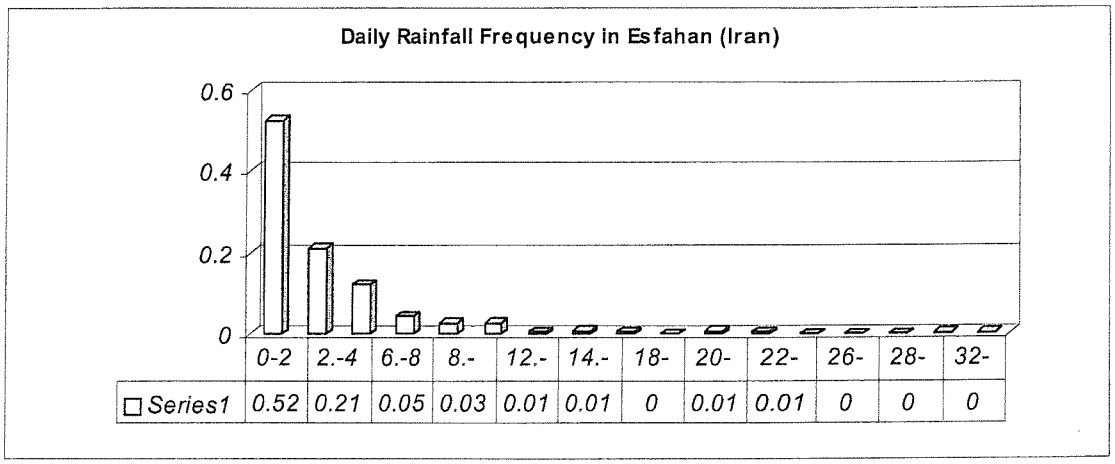

Figure D2: Relative frequency of rainfall in Esfahan (Iran)

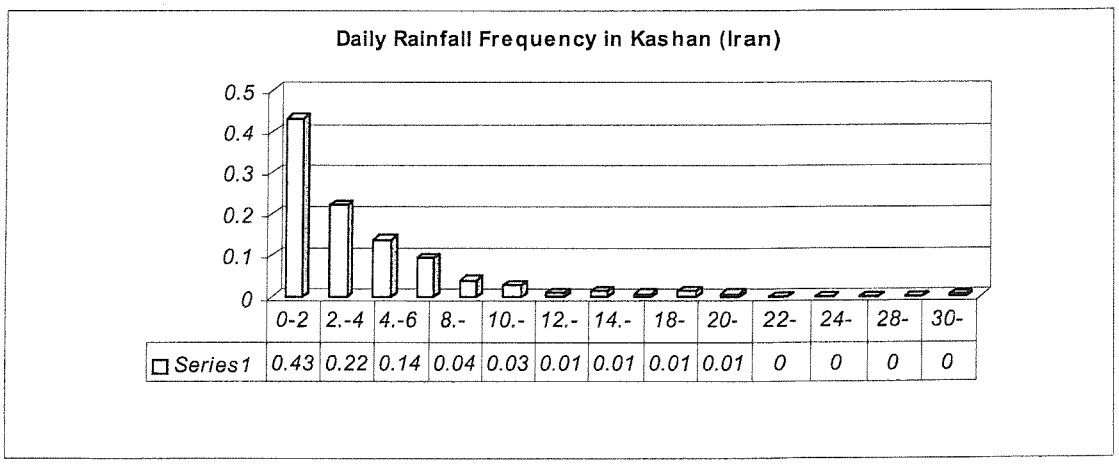

Figure D3: Relative frequency of rainfall in Kashan (Iran)

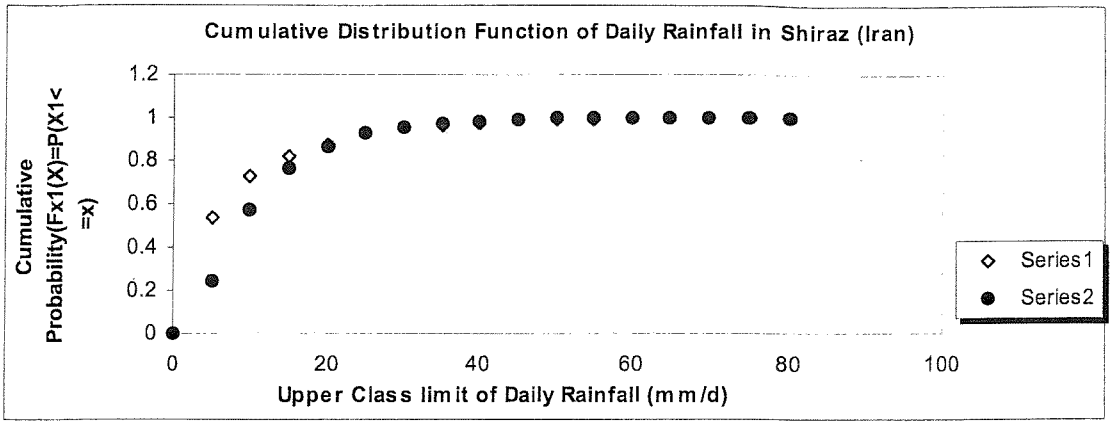

Figure D4: Observed (series 1) and exponential (series 2) cumulative daily rainfall distribution in Shiraz (Iran).

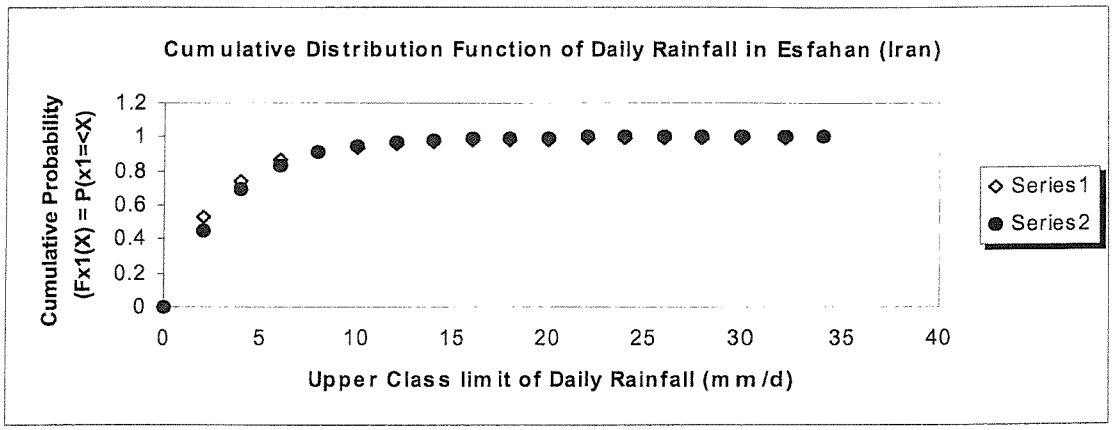

Figure D5: Observed (series 1) and exponential (series 2) cumulative daily rainfall distribution in Esfahan (Iran).

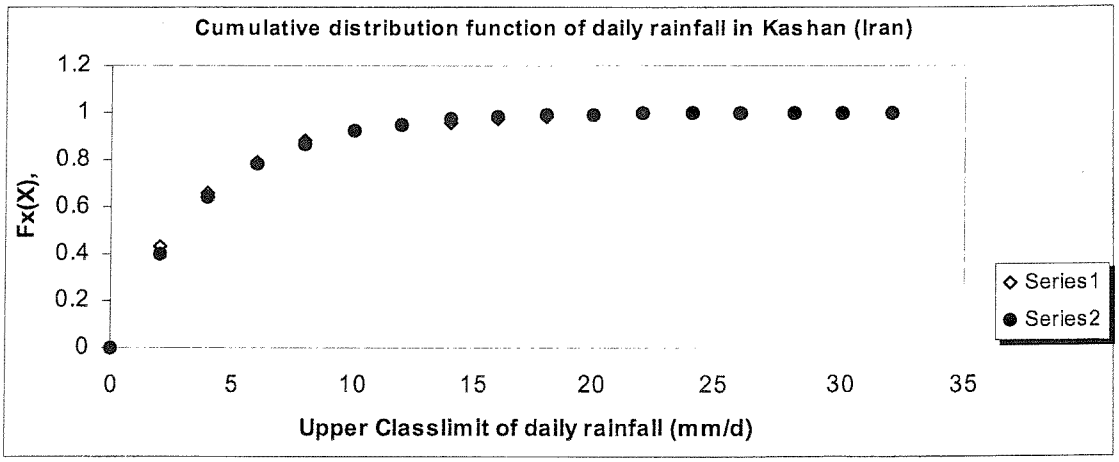

Figure D6: Observed (series 1) and exponential (series 2) cumulative daily rainfall distribution in Kashan (Iran).

Table D4: Historical rainfall data in Shiraz (Iran)

year	1987	1988	1989	1990	1991	1992	1993	1994	1995	1996	Ave
Jan	9.1	136	15.8	105	220	109	126	20.7	15.1	145	90.1
Feb	19.2	113	24.6	115	45	31	98.5	7.6	162	82	69.7
Mar	99.5	49.5	39.6	10.3	66.3	47.5	88.7	110	42.4	123	67.7
Apr	11.6	44.5	24.2	20	7.1	13.3	17.7	11.7	60.8	28.8	24
May	0.6	0	0	0	0	17.4	0.5	29	3.3	1.2	5.2
Jun	0	0	0	0	0	0	0	0	3	2.2	0.52
Jul	0.2	0	0	0	0	0	0	0	0.1	0.6	0.09
Aug	0	0	0	0	0	4	0.2	0	0	22.5	2.67
Sep	0	0	0	0	0	0.1	0	0.1	0	0	0.02
Oct	19.5	0	0	0	7.9	0	1.7	2.2	28	2.7	6.2
Nov	0	0	37.3	12.7	0	2.3	8	109	4	2.2	17.5
Dec	33.4	89.7	89	17.8	75	244	0.1	80.7	175	12.4	81.6
sum	193	432	231	280	421	468	341	371	493	423	365

Table D5: Historical rainfall data in Esfahan (Iran)

year	1987	1988	1989	1990	1991	1992	1993	1994	1995	1996	Ave
Jan	0	4.3	11.8	23.7	18	24.4	41.4	1.9	0.7	21.1	14.7
Feb	2	18.7	10.3	21.3	5.4	16.3	41.2	0	9.4	21.1	14.6
Mar	17.4	33.4	32.1	9.1	44.8	25.2	39.9	0	7	56	26.5
Apr	3.5	9.7	8.2	5.4	9	9.1	21.4	2	26.4	10.5	10.5
May	6.2	0	2	0.6	0.6	22.5	10.1	0	25.3	19.1	8.64
Jun	0	0	5	0	0	8.4	0	0	10.9	0.2	2.45
Jul	8.4	0.5	0	5	0	1.4	0	0	0	1.3	1.66
Aug	0	0	0	0	0	4	0.1	0	0	0	0.41
Sep	0	0	0	0	0	0	0	0	0	0	0
Oct	15.1	0.7	0	0	9.1	0	0.2	22.5	2.1	0	4.97
Nov	1.1	2.6	18.6	0	7.3	0	44.5	43.3	0	5.4	12.3
Dec	7.3	1	51.2	12.4	28.2	11.2	0	6.2	41.2	13.2	17.2
sum	61	70.9	139	77.5	122	123	199	75.9	123	148	114

Table D6: Historical rainfall data in Kashan (Iran)

year	1987	1988	1989	1990	1991	1992	1993	1994	1995	1996	Ave
Jan	0	17.7	32.3	38.3	17.6	45.8	30.8	12.6	0.1	22.7	21.8
Feb	2.1	22.2	17.9	16.1	5.4	20	25.5	18.3	12	72.2	21.2
Mar	33.6	12.1	12.2	9.9	33	53.8	24.5	28.7	19	54.1	28.1
Apr	0.2	20.9	1	1	0	21.7	27.8	10.2	25.7	26.2	13.5
May	19.1	0	0	1.1	3	61.3	29.8	9	35.1	34.8	19.3
Jun	0	0	0	0	0	0	0	0	0	5	0.5
Jul	4.1	1	0	0.2	0	0	0	0	0	0.7	0.6
Aug	0	0	0	0	0	0.3	0	0	0	0	0.03
Sep	0	1	0	0	0	0	0	0	1	0	0.2
Oct	19.1	1.1	0	2.3	6	0	0	4.2	0	0	3.27
Nov	7	5.1	17.1	0	12	4.3	17.7	16.3	0	0	7.95
Dec	15.5	0.9	19.8	14	25.4	22.5	0	4.7	8.2	4	11.5
sum	101	82	100	82.9	102	230	156	104	101	220	128

Table D7: Comparison of Generated rainfall with historic data in three stations of Iran (Kashan, Shiraz and Esfahan)

	Kashan	Kashan	Kashan	Shiraz	Shiraz	Shiraz	Esfahan	Esfahan	Esfahan
Month	historic Rainfall	Generated Rainfall	Error	historic Rainfall	Generated Rainfall	Error	historic Rainfall	Generated Rainfall	Error
	(ave 10 years)	(ave 100 years)	%	(ave 10 years)	(ave 100 years)	%	(ave 10 years)	(ave 100 years)	%
Jan	21.79	21.82	0.02	90.14	91.33	2.06	14.73	19.53	19.43
Feb	21.17	21.21	0.03	69.69	61.78	1.92	14.57	16.79	23.08
Mar	28.09	32.04	3.09	67.68	78.16	1.17	26.49	28.20	30.36
Apr	13.47	13.66	0.15	23.97	44.09	3.28	10.52	12.22	13.60
May	19.32	19.16	0.12	5.2	0	2.27	8.64	8.53	7.93
Jun	0.5	0	0.39	0.52	0	1.21	2.45	2.87	0
Jul	0.6	0	0.47	0.09	0	0	1.66	1.32	0
Aug	0.03	0	0.02	2.67	0	1.96	0.41	1.02	0
Sep	0.2	0	0.16	0.02	0	0	0	0	0
Oct	3.27	0	2.56	6.2	0	1.72	4.97	8.13	10.25
Nov	7.95	11.14	2.50	17.53	23.34	0.02	12.28	10.90	10.40
Dec	11.5	20.21	6.81	81.64	91.52	2.80	17.19	17.18	17.51

Table D8: Comparison of Generated daily wet days with historic data in three stations of Iran (Kashan, Shiraz and Esfahan)

	Kashan	Kashan	Kashan	Shiraz	Shiraz	Shiraz	Esfahan	Esfahan	Esfahan
Month	historic wet days	Generated wet days	Error	historic wet days	Generated wet days	Error	historic wet days	Generated wet days	Error
	(ave 10 years)	(ave 100 years)	%	(ave 10 years)	(ave 100 years)	%	(ave 10 years)	(ave 100 years)	%
Jan	3.2	2	7.10	5.4	6	1.36	2.4	2	2.68
Feb	2.4	2	2.37	5.3	6	4.19	1.9	3	7.38
Mar	3.7	4	1.78	6	5	0.48	3.6	4	2.68
Apr	2.1	3	5.32	2.2	2	1.20	1.7	2	2.01
May	1.9	2	0.59	0.5	0	1.48	0.9	1	0.67
Jun	0.1	0	0.59	0.2	0	0.60	0.3	0	2.01
Jul	0	0	0	0	0	0	0.2	0	1.34
Aug	0	0	0	0.2	0	1.12	0.1	0	0.67
Sep	0	0	0	0	0	0	0	0	0
Oct	0.6	0	3.55	0.3	0	0.84	0.7	1	2.01
Nov	1.2	1	1.18	1.4	1	0.52	1	1	0
Dec	1.7	2	1.78	5.5	5	1.88	2.1	2	0.67

Table D9: Generated Pattern of daily rainfall in three climatic stations of Iran (Shiraz, Esfahan and Kashan)

Daily Rainfall				Daily Rainfall				Daily Rainfall			
Day	Shiraz	Esfahan	Kashan	Day	Shiraz	Esfahan	Kashan	Day	Shiraz	Esfahan	Kashan
1	0	0	0	123	0	0	0	245	0	0	0
2	25.21	0	9.05	124	0	0	0	246	0	0	0
3	14.42	0	0	125	0	0	0	247	0	0	0
4	0	0	0	126	0	7.93	6.80	248	0	0	0
5	0	0	0	127	0	0	0	249	0	0	0
6	0	0	0	128	0	0	0	250	0	0	0
7	0	0	0	129	0	0	12.36	251	0	0	0
8	0	0	0	130	0	0	0	252	0	0	0
9	0	0	0	131	0	0	0	253	0	0	0
10	0	0	0	132	0	0	0	254	0	0	0
11	0	12.18	0	133	0	0	0	255	0	0	0
12	0	7.25	0	134	0	0	0	256	0	0	0
13	0	0	0	135	0	0	0	257	0	0	0
14	0	0	0	136	0	0	0	258	0	0	0
15	0	0	0	137	0	0	0	259	0	0	0
16	16.12	0	0	138	0	0	0	260	0	0	0
17	0	0	0	139	0	0	0	261	0	0	0
18	0	0	0	140	0	0	0	262	0	0	0
19	0	0	0	141	0	0	0	263	0	0	0
20	0	0	0	142	0	0	0	264	0	0	0
21	0	0	0	143	0	0	0	265	0	0	0
22	12.04	0	0	144	0	0	0	266	0	0	0
23	14.19	0	0	145	0	0	0	267	0	0	0
24	9.35	0	12.77	146	0	0	0	268	0	0	0
25	0	0	0	147	0	0	0	269	0	0	0
26	0	0	0	148	0	0	0	270	0	0	0
27	0	0	0	149	0	0	0	271	0	0	0
28	0	0	0	150	0	0	0	272	0	0	0
29	0	0	0	151	0	0	0	273	0	0	0
30	0	0	0	152	0	0	0	274	0	0	0
31	0	0	0	153	0	0	0	275	0	0	0
32	0	0	0	154	0	0	0	276	0	0	0
33	0	0	0	155	0	0	0	277	0	0	0
34	0	0	0	156	0	0	0	278	0	0	0
35	15.33	7.88	10.97	157	0	0	0	279	0	0	0
36	6.13	6.66	0	158	0	0	0	280	0	0	0
37	4.77	0	0	159	0	0	0	281	0	0	0
38	0	0	0	160	0	0	0	282	0	0	0
39	0	0	0	161	0	0	0	283	0	0	0
40	0	0	0	162	0	0	0	284	0	0	0
41	0	0	0	163	0	0	0	285	0	0	0
42	0	0	0	164	0	0	0	286	0	0	0
43	0	0	0	165	0	0	0	287	0	0	0
44	0	0	0	166	0	0	0	288	0	0	0

45	0	0	0	167	0	0	0	289	0	0	0
46	0	0	0	168	0	0	0	290	0	0	0
47	0	0	0	169	0	0	0	291	0	0	0
48	0	8.54	0	170	0	0	0	292	0	0	0
49	0	0	0	171	0	0	0	293	0	0	0
50	0	0	0	172	0	0	0	294	0	0	0
51	18.11	0	0	173	0	0	0	295	0	0	0
52	4.10	0	0	174	0	0	0	296	0	0	0
53	0	0	0	175	0	0	0	297	0	0	0
54	13.35	0	0	176	0	0	0	298	0	0	0
55	0	0	0	177	0	0	0	299	0	0	0
56	0	0	10.24	178	0	0	0	300	0	0	0
57	0	0	0	179	0	0	0	301	0	0	0
58	0	0	0	180	0	0	0	302	0	0	0
59	0	0	0	181	0	0	0	303	0	10.25	0
60	9.76	0	0	182	0	0	0	304	0	0	0
61	0	0	0	183	0	0	0	305	0	10.4	0
62	23.83	0	0	184	0	0	0	306	0	0	0
63	18.34	7.44	0	185	0	0	0	307	0	0	0
64	0	0	10.09	186	0	0	0	308	0	0	0
65	0	0	0	187	0	0	0	309	0	0	0
66	0	0	4.95	188	0	0	0	310	0	0	0
67	0	0	0	189	0	0	0	311	0	0	0
68	0	0	0	190	0	0	0	312	0	0	0
69	0	0	0	191	0	0	0	313	0	0	0
70	0	0	0	192	0	0	0	314	0	0	0
71	0	8.54	0	193	0	0	0	315	0	0	0
72	0	0	0	194	0	0	0	316	23.34	0	0
73	0	0	0	195	0	0	0	317	0	0	0
74	0	0	0	196	0	0	0	318	0	0	0
75	0	0	0	197	0	0	0	319	0	0	0
76	0	0	0	198	0	0	0	320	0	0	11.14
77	0	0	0	199	0	0	0	321	0	0	0
78	0	0	0	200	0	0	0	322	0	0	0
79	0	0	0	201	0	0	0	323	0	0	0
80	0	8.80	0	202	0	0	0	324	0	0	0
81	14.4	0	6.98	203	0	0	0	325	0	0	0
82	11.83	5.60	0	204	0	0	0	326	0	0	0
83	0	0	10.01	205	0	0	0	327	0	0	0
84	0	0	0	206	0	0	0	328	0	0	0
85	0	0	0	207	0	0	0	329	0	0	0
86	0	0	0	208	0	0	0	330	0	0	0
87	0	0	0	209	0	0	0	331	0	0	0
88	0	0	0	210	0	0	0	332	0	0	0
89	0	0	0	211	0	0	0	333	0	0	0
90	0	0	0	212	0	0	0	334	0	0	0
91	0	0	0	213	0	0	0	335	0	0	0
92	0	0	0	214	0	0	0	336	0	0	0
93	0	0	0	215	0	0	0	337	16.26	0	0

94	29.47	0	0	216	0	0	0	338	11.86	7.33	0
95	14.62	0	0	217	0	0	0	339	0	0	0
96	0	0	0	218	0	0	0	340	0	0	0
97	0	0	0	219	0	0	0	341	0	0	0
98	0	0	0	220	0	0	0	342	29.27	0	0
99	0	0	0	221	0	0	0	343	7.30	0	0
100	0	0	0	222	0	0	0	344	0	0	0
101	0	10.16	0	223	0	0	0	345	0	0	0
102	0	3.43	0	224	0	0	0	346	0	0	9.55
103	0	0	0	225	0	0	0	347	0	0	0
104	0	0	0	226	0	0	0	348	0	0	0
105	0	0	8.12	227	0	0	0	349	0	10.19	0
106	0	0	0	228	0	0	0	350	0	0	0
107	0	0	0	229	0	0	0	351	0	0	0
108	0	0	0	230	0	0	0	352	0	0	0
109	0	0	0	231	0	0	0	353	0	0	0
110	0	0	0	232	0	0	0	354	0	0	0
111	0	0	0	233	0	0	0	355	0	0	0
112	0	0	0	234	0	0	0	356	0	0	0
113	0	0	0	235	0	0	0	357	0	0	0
114	0	0	0	236	0	0	0	358	0	0	0
115	0	0	0	237	0	0	0	359	0	0	0
116	0	0	2.84	238	0	0	0	360	0	0	0
117	0	0	2.70	239	0	0	0	361	0	0	0
118	0	0	0	240	0	0	0	362	0	0	0
119	0	0	0	241	0	0	0	363	0	0	0
120	0	0	0	242	0	0	0	364	0	0	10.66
121	0	0	0	243	0	0	0	365	26.83	0	0
122	0	0	0	244	0	0	0				

Bibliography:

Abraham, N. and Tiwari, K. N. (1999), "Modelling hydrological process in hill slope watershed of humid Tropics". J. Irrigation and Drainage Engineering, 125 (4). 203-211.

Allen, R. G, (1996), "Assessing Integrity of Weather Data for Reference Evapotranspiration Estimation". J. Irrigation and Drain Engineering, 122(2), pp, 97-106.

Allen, R. G., Pereira, L. S., Raes, D., and Smith, M. (1998), "Crop evapotranspiration (guidelines for computer crop water requirements)."FAO Irrig. And Drain. Paper No. 65, Food and Agricultural Organization of the Unite Nations, Rome.

Atkinson. D, (1991), "Plant root growth (An ecological perspective)", Oxford, London.

Basha, H. A. (1999). "One-dimensional non-linear steady infiltration." J. Water resources research, Vol. 35 (6). PP. 1697-1704.

Belmans, C., Wesseling, J. G. and Feddes, R. A. (1983), "Simulation model of the water balance of a croped soil: SWATER. J. Hydrol. Vol. 63.PP. 271-286.

Ben-Asher, J., Oron. G., and Button. B. J, (1985), " Estimation of runoff volume for agriculture in arid lands". J. Dry land resources & technology, 2, PP, 76-91.

Ben-hur. M (1991), The effects of dispersants, stabilisers and slope length on runoff and water-harvesting farming. Aust. J. Soil Res., 29, 553-563.

Binh. N. D., Murty. V. V. N., Hoan. D. X., (1994), "Evaluation of the possibility for rainfed agriculture using a soil moisture simulation model" J. Agricultural water management. 26. PP. 187-199.

Boers, T. M., and J. Ben-Asher. (1982). " A review of rainwater harvesting." Agric. Water Manage., Vol. 5. PP. 145-158.

Boers. Th. M, Degraaf. M, Feddes. R. A and Ben-Asher. J. (1986). " A linear regression model combined with a soil water balance model to design micro-catchments for water harvesting in arid zones", Agricultural water management, vol. 11. PP 187-206.

Bogardi. Janson J, Duckstein. L and Rumambo. Omar H, (1988), " Practical generation of synthetic rainfall event time series in a semi-arid climatic zone". Journal of hydrology, 103. PP. 357-373

Bonta, J. V. (1997), " Determination of watershed curve number using derived distributions", J. Irrigation and Drainage Engineering (ASCE), 123, 1, pp. 28-36.

Botta. E. F. F, and Wubs. F. W., (1993), " The convergence behaviour of iterative methods on severely stretched grids", Int. J. Numer. Meth. Engng. Vol. 36, PP, 3333-3350.

Brutsaert. W., and Chen. D. (1995), "Desorption and the two stages of drying of natural tall grass prairie", Water resour, Res., 19(2), pp. 1305-1313.

Buishand, T. A. (1978), " Some remarks on the use of daily rainfall models". J. Hydrology, 36, PP. 295-308.

Burman, R. D., Nixon, WY. P.R, and Pruit, W. O. (1981). "Water requirements." In design and operation of farm irrigation systems. By Jenson, M. E., American Society Agricultural engineers. PP. 189-232.

Celia, M.A., Bouloutas, E.T., Zarba, R.L., (1990), " A general mass conservative numerical solution for the unsaturated flow equation. Water Resources. Res. 26, pp. 1483-1496.

Celia,.M. A., L. R. Ahuja, and G. F. Pinder. (1987), " Orthogonal collocation and alternating-direction procedures for unsaturated flow problems, Adv. Water Resour. , 10, PP. 178-187.

Chang, Y. Y,. and Corapcioglu, M. Y. (1997), "Effect of root on water flow in unsaturated soils", J. Irrigation and Drainage Engineering, 123(3), pp.202-209.

Chin, Edwin H., (1977), "Modelling daily precipitation occurrence process with Markov Chain". J. Water resources research. 13(6). pp. 949-956.

Chow. V. T, Maidment, D. R.,and Mays, L. W . (1988)," Applied Hydrology" ed. be. MCGraw-Hill company. New York.

Ciuff, C. B. (1989). " Water Harvesting System in Arid Lands, Desalination (Elsvier Science publishers B. V., Amsterdam-Printed in the Netherlands), 72, pp. 149-159.

Cundy, Terrance W., and Tento. Scott. W. (1985). "Solution to the kinematics wave approach to overland flow routing with rainfall excess given by Philip's equation." J. Water resources research, Vol, 21 (8), PP. 1132-1140.

Dabney, S. M. (1998), " Cover crop impacts on watershed hydrology." J. Soil and Water conservation, 53(3), pp. 207-213.

Darcy, H. , (1956), " Les Fontaines Publiques de la Ville de Dijon", Dalmont, Paris.

Davey. K., and Rosindale. I., (1994), " An iterative solution scheme for systems of boundary element equations", Int. J. Numer. Meth. Engng. Vol. 37, PP, 1399-1411.

Delleur, J. W, Chang, T. J, Kavvas, M. L., (1989), "Simulation models of sequence of dry and wet days", Journal of Irrigation and Drainage Engineering, 115(3), PP. 344 – 357.

Diskin, M. H., (1972), "Application of a simple hydrologic model for rainfall-runoff relations of Dalton watershed". Water resources research. V 9 (4). PP. 927-936.

Diskin, M. H., Nazimov, N., (1995), "Linear reservoir with feedback regulated inlet as a model for the infiltration process", J. Hydrology, V. 172. pp. 313-330.

Diskin, M. H., Nazimov, N., (1996), "Ponding time and infiltration capacity variation during steady rainfall", J. Hydrology, V. 178, pp. 369-380.

Doorenbos J. and Pruitt W. O., (1977), "Crop Water Requirements", Irrigation and Drainage, paper 24, FAO, Rome, Italy.

Doorenbos, J., and Pruitt, W. O. (1977). "Guidelines for predicting crop water requirements." Irrig. And Drain. Paper 24 (Revised). Food and Agricultural Organisation of the United Nations, Rome.

Dunavant, D. A., (1985), " High Degree efficient symmetrical gaussian Quadrature Rules For The Triangle", Int. J. Num. Meth. Eng., VOL. 21, pp. 1129-1148.

Dunne, T., Zhang, W., and Aubry, B. F., (1991), "Effects of Rainfall, Vegetation, and Micro Topography on Infiltration and Runoff", Water resour, Res, V. 27(9). pp. 2271-2285.

Dunne, Thomas and Leopold, Luna B. (1978), Water in environmental planning" W. H. Freeman and company, San Francisco.

Erie, L. J., Franch, O. F., and Harries, K. (1965). "Consumptive use of water by crops. " Arizona tech. Bull. 169, University of Arizona, Tucson, Ariz.

Everson, C.S. (2001). "The water balance of a first order catchment in the montane grasslands of South Africa". J. Hydrology 241. 110-123.

FAO, (1981), "Arid zone hydrology". FAO Irrigation and drainage paper, No. 37, FAO, Rome.

Feddes, R. A., Kabat. P, Van Bakel. P.J. T., Bronswijk. J. J. B., Halbertsma. J, (1988), " Modelling soil water dynamics in the unsaturated zone-State of the art. J. Hydrology, 100, PP. 69-111.

Fisher, P. D. (1995), "An alternative plastic mulching system for improved water management in dry land maize production." J, Agricultural water management. 27, PP. 155-166.

Flug, M., (1982), "Production of annual crops on micro catchment, in proceedings of a workshop on rainfall collection for agriculture in arid and semi-arid regions, edited by G. R. Dutt, C. F. Hutchinson and M. A. Garduzo, Commonwealth Agriculture Bureaux, London.

Frasier, Gary W., (1989), Comment on " Statistic consideration in optimal design of a Micro-catchment layout of runoff water harvesting" by Gideon Oron and Gerda Enthoven. J. Water resources research. Vol. 25, No. 2, PP. 333-334.

Galarza . G. A., Carrera. J., And Medina. A., (1999), " Computational Techniques for Optimisation of problems involving non-linear transient simulations", Int. J. For numerical Method in Engng. Vol. 45. PP. 319-334.

Gottardi, G., and Venutelli, M. (1992). " Moving finite element model for one dimensional infiltration in unsaturated soil". Water Resources. Res., 28(12). PP. 3259-3267.

Gottardi. G., Venutelli. M, (1992), "Moving finite model for one-dimensional infiltration in unsaturated soil", J. Water resources research, vol. 28, No. 12, PP. 3259-3267.

Green, W. H., and Ampt, G. A. , (1911), "Studies on Soil Physics: I. Flow of Air and Water Through Soils", J. Agron. Sci., Vol. 4, pp. 1.

Haan. Charles. T (1979), " Statistical Methods in Hydrology". Iowa State University press.

Habib. R., and Lafolie. F., (1991), "Water and nitrate redistribution in soil as affected by root distribution and absorption", in Plant root growth, edited by Atkinson. D, University of Aberdeen. PP.131-146.

Hanks, R. J. (1991): " Soil Evaporation and Transpiration", in modelling plant and soil systems John Hanks and J. T. Ritchie, co-editors, Madison, Wisconsin USA.

Hartley, D. M. (1992), "Interpretation of Kostiakov infiltration parameters for Borders." J. J. Irrigation and Drain Enging, 118(1), pp. 156-165.

Hatfield, J. K., and Allen, R. G. (1996), "Evapotranspiration Estimates under Deficient Water Supplies." J. Irrigation and Drain Enging, 122(5), pp. 301-308.

Hatfield, J. L, (1990), "Methods of estimating evapotranspiration", in Irrigation of agricultural crops, Steward and Nilson, edited by Bruce, Niehaus, Kanemasu and Gilley. Madison, Wisconsin USA.

Haverkamp, R., Vauclin, M., Touma, J., Wierenga, P.J., Vachaud, G., (1977), "A comparison of numerical simulation models for one-dimensional infiltration". Soil Sci. Soc. Am. J. 41, PP. 285-294.

Hawkins, h. H (1993). " A symptotic determination of runoff curve number from data". J. Irrig. and Drain. Engin., ASCE, 119(2), 334-345.

Hawkins, r. H. (1982), " Interpretation of source area variability in rainfall runoff relationships, edited by V. P. Singh, pp. 303-324.

Hiler, E.A. and Clark, R.A., (1971), "Stress day index to characterise effects of water stress on crop yield". Trans. ASAE, 14: 757-761.

Hillel, D., (1980), " Applications of soil physics", Academic press.

Hills, R. G., Porro, I., Hudson, D. B., and Wierenga, P. J. (1989), " Modelling one-dimensional infiltration into very dry soils. I. Model development and evaluation". Wter Resour, Res., 25(6), 1259-1269.

Horton, R. E. , (1940), "An Approach Toward a Physical Interpretation of Infiltration Capacity", Soil Sci. Soc. Amer. Proc., Vol. 5, pp. 339.

Hotchkiss, Rollin. H., and McCallum, Brain. E. (1995). "Peak discharge foe small agricultural watersheds." J. Hydraulic engineering. Vol 121 (1). PP. 36-48.

Huang. K., Mohanty. B. P., van Genuchten. M. Th., (1996), " A new convergence criterion for the modified picard iteration method to solve the variably saturated flow equation", J. Hydrology. Vol, 178. PP, 69-91.

Idso, S. B., Reginato, R. J., Jackson, B. A. Kimball, and Nakayama, F. S. (1974), "The three stages of drying of a field soil", Soil Sci. Soc. AM. Proc., 38, pp. 831-836.
Ithaca, N. Y.

James, L.G., (1988), " Principles of farm irrigation system design" John Wiley & sons, Washington, U.S.A.,

Jenson D. T., Hargreaves, G. H., Temesgen, B. and Allen, R. G. (1997), "Computation of ETO under non-ideal conditions." J. Irrigation and Drainage Enging, 123(5), pp. 394-400.

Jenson M.E., (1980), "Design and operation of farm irrigation systems". The American society of agricultural engineers. U.S.A.

Jimoh. O. D, Webster. P., (1996), " The optimum order of a Markov Chain model for daily rainfall in Nigeria". Journal of Hydrology 185, PP. 45-69.

Johnson, W. M. , and C. H. Niederhof. (1941), "Some relationships of plant cover to runoff, erosion, and infiltration on granitic soils, J. For. , 39, pp. 854-858.

Kahlown. Muhammad Akram and Hamilton. Joel R. (1996), "Sailaba Irrigation Practices and Prospects", J, Arid soil research and rehabilitation, 10. pp. 179-191.

Karl Wood, Sheikh Suleman, M. Hussain Shah, Bashir, Murry Liegh (1995), Rainwater harvesting for increasing livestock for age on arid rangelands of Pakistan. J. Range Manage, 48, 523-527.

Katul, Gabriel., Todd, Philip., and Pataki, Diane. (1997). " Soil water depletion by oak trees and the influence of root water uptake on the moisture content spatial statistics." J, Water resources research. Vol. 33 (4). PP. 611-623.

Kempt, Paul. R., Reynolds. J. F., Pachepsky. Y. and Chen. Jia-Lin. (1997). "A comparative modelling study of soil water dynamics in a desert ecosystem." J. Water resources research. Vol. 33 (1). PP.73-90.

Kostiakov, A. N. , (1932), " On the dynamics of the coefficients of water percolation in soils and on the necessity of studying it from a dynamic point of view for purposes of amelioration", Trans. Com. Int. Soil Sci Soc. 6th, Moscow, Part A, pp. 17.

Kotsopoulos, S., and Babajimopoulos, C. (1997). "Analytical estimation of modified Penman equation parameters." J, Irrigation and Drainage engineering, Vol. 123 (4), PP. 253-256.

Kottegoda. N. T., (1980), " Statistic Water Resources Technology". MacMillan, London.

Kottegoda. Nathabandu T, and Rosso. Reins, (1998), " Statistics, Probability, and Reliability for Civil and Environmental Engineers. McGAW-HILL, New York, London.

Kronen. M. (1994), "Water harvesting and conservation techniques for small holder crop production systems", Soil & Tillage Research 32, pp. 71-86.

Lee, Jin., and Musiake, Katumi., (1994), " Constant time interval Hortonian infiltration model", J. Irrigation and Drainage Engineering, V. 120(2), pp. 250-265.

Lockington. D. A. (1994), "Falling rate evaporation and desorption estimates, J. Water resources research, vol, 30. No. 4, pp. 1071-1074.

Marino, Miguel A, and Tracy, John C. (1988). " Flow of water through root-soil environment." J, Irrigation and Drainage engineering, Vol. 114 (4), PP. 588-604.

Markar.M. S., and Mein. Russell. G., (1987), "Modelling of evapotranspiration from homogenous soils", J. Water resources research, Vol. 23, No. 10, pp. 2001-2007.

Marston, R. B. (1952), "Ground cover requirements for summer storm runoff control on aspen sites in Northern Utah, J. For. , 50, PP. 303-307.

Mathur, Shashi., and Rao, Sandhya (1999), " Modelling water uptake by plant roots" j. Irrigation and Drainage Engineering, Vol. 125, No. 3, pp. 159-165

McCuen, R. H. (1989), "Hydrologic analysis and design." Prentice-Hall, Inc., Englewood Cliffs, N. J.

Meisinger, J. J., Hargrove, W. L., Kelson, R. L. M., Williams, J. R., and Benson, V. W. (1991), "Effects of cover crops on groundwater quality, In: (Hargrove, W. L., ed), Cover for clean Water. J. Soil and Water conservation, Soc., Ankeny, I A. pp. 57-68.

Meshkat, M., Warner, Richard. C., and Workman Stephen. R., (1999), " Modelling of evapotranspiration reduction in drip irrigation system", J. Irrigation and Drainage Engng. Vol, 125(6). PP. 315-323.

Milly, P.CD., (1985), " A mass conservative procedure for time stepping in models of unsaturated flow. Adv. Water Resour. 8, pp. 32-36.

Mls, J. (1982), "Formation and solution of fundamental problems of vertical infiltration." Vodohosp. Cas, 30, PP, 304-313 (in Czech).

Moldenhauer, W. C., Barrows, and D. Swartzendruber. (1960), "influence of rainstorm characteristics in infiltration measurements", Trans. Int. Cong. Soil Sci., 7, pp. 426-432.

Monteith, J. L. (1965). " Evaporation and atmosphere." In: G. E. Fogg (Editor). The state and movement of water in living organisms, 19th Symp. Soc. EXP. Bio., 8-12 September 1964. Swansea. The Company of Biologists. Cambridge, PP. 206-234.

Montesinos, Pilar. Camacho, E. and Alvarez, S. (2001). " Seasonal furrow irrigation model with genetic algorithms (OPTIMEC)". J. Agricultural water management. 52. 1-16.

Mualem, Y. (1976), "A new model for predicting the hydraulic conductivity of unsaturated porous media". Water Resour. Res., 12, 613-522.

Musters, P.A.D., Bouten, W. (2000). "A Method for identifying optimum strategies of measuring soil water content for calibration a root water uptake model". J. Hydrology , 227. 273-286.

Nichols, W. D. (1992). " Energy budgets and resistance's to energy transport in sparsely vegetated rangeland." Agric. For. Meteorol., Vol. 60. PP. 221-247.

Nieber. J.L, and Feddes. R.A, (1999), " Solution for combined saturated and unsaturated flow" in Agricultural and drainage, edited by Skaggs. R.W, and Schilfgaarde. J.van. Number 38 in the series of Agronomy.

Novak. V., Simunek. J., and van Genuchten. M. Th., (2000), "Infiltration of water into soil with cracks", J, Irrigation and Drainage Engineering. Vol. 126, No. 1, PP. 41-47.

O'loughlin, G., Huber. W., and Chocat. B, (1997), "Rainfall-runoff processes and modelling" J. hydraulic research, v, 34. No. 6. Pp. 733-751.

Ogden , F. L., and Saghafian, B. (1997), "Green and Ampt Infiltration With Redistribution", J. Irrigation and Drainage Engineering, V. 123(5), pp. 366-393.

Oron, G., and Enthoven, G. (1987). " Stochastic consideration in optimal design of a micro-catchment layout of runoff water harvesting". J. Water Resou Res. 23 (7). 1131-1138.

Oron. G., Ben-Asher. J., and Issar. A. (1983). " Economic evaluation of water harvesting in Micro-Catchments." J. Water resources research. Vol. 19 (5), PP. 1099-1105.

Osborn, H. B. and Lane, L. J. (1972), "Optimum Gating of Thunderstorm Rainfall in Southern Arizona. Water Res, Res. V, 8, pp. 259-265.

Pandey Sushil (1991), The Economics of Water Harvesting and Supplementary Irrigation in the Semi-Arid Tropics of India. Agricultural Systems, 36, 207-220.

Pandit, A, and Gopalakrishnan, G. (1996). " Estimation of annual storm runoff coefficients by continuous simulation". J, Irrig and Drain, Engin; ASCE, Vol, 122, No. 4, PP. 211-220.

Parton, W. J., W. K. Lauenroth, and F. M. Smith. (1981). "Water losses from a short grass steppe." Agric. Meteorol., Vol. 76, PP. 510-520.

Penman, H. L. (1948). "Natural evaporation from open water, bare soil and grass." Proc. Royal Soc., Ser. A, London, 193, 120-145.

Pereira, Luis S, Perrier, Alain., Allen. Richard G., and Alves. Isabel (1999), "Evapotranspiration: Concepts and future trends", J, Irrigation and drainage Engineering, vol. 125, No. 2, PP. 45-51.

Phien, H.N. and Apichart, A., (1984), " Agricultural practices under rainfed conditions in Thailand" research report no. 165, Asian Institute of Technology, Bankok, Thailand.

Philip, J. R. , (1969), " Theory of Infiltration", Adv. Hydro science, Vol. 5, pp. 215.

Philip, J. R. (1957), "Theory of infiltration: 4. Sorbtivity and algebraic infiltration equations." Soil Sci. 84: 257-264.

Ponce, Victor. M., and Hawkins, R. H. (1996). " Runoff curve number; has it reached maturity". J of Irri and Drain, Eng, vol,1, No. 1, pp 11-19.

Prasad, R. (1988). "A linear root water uptake model." J. Hydrology., 99. PP. 297-306.

Press, W.H., Flannery, B. P., Teukolsky, S. A., Vetterling, W. T., (1989), "Numerical Recipes. The Art of Science Computing, Cambridge University press, Cambridge, P. 702.

Raes D., Lemmens H., van Aelst P., vanden Bulcke M. and Smith M., (1988), "IRSIS-Irrigation scheduling information system (2 vol.)". Laboratory of land management, Katholieke University, Leuven, Belgium.

Raudkivi Arved J. (1979), " Hydrology: an advanced introduction to hydrological processes and modelling". Pergamon press, Oxford. New York.

Reca, Juan, Roldan, Jose., Alcaide, Miguel, Lopez, Rafael and Camacho, Emilio. (2001), " Optimisation model for water allocation in deficit systems". I. Description of the model. J. Agricultural water management 48. 103-116.

Reca, Juan, Roldan, Jose., Alcaide, Miguel, Lopez, Rafael and Camacho, Emilio. (2001), " Optimisation model for water allocation in deficit systems". II. Application to the Bembezer irrigation system. J. Agricultural water management 48. 117-132.

Remson, I., Hornberger, G. M and Molz, F. J., (1971), "Numerical methods in subsurface hydrology. Wiley-Interscience, New York, N. Y, 389 pp.

Reynolds, W. D., and Walker, G. K. (1984). " Development and validation of a numerical model simulating evaporation." J. Soil Sci. AM. J. Vol. 48. PP. 969-969.

Ritchie, J, T, (1972), " Model for predicting evaporation from a row crop with incomplete cover". J. water resources research. Vol. 8, No. 5. PP. 1204-1213.

Ritchie, J, T, and Johnson, B. S. (1990), " Soil and plant factors affecting evaporation" in Irrigation of agricultural crops. Steward and Nilson, edited by Bruce, Niehaus, Kanemasu and Gilley. Madison, Wisconsin USA.

Rodier, J. A., (1985), "Aspects of arid zone hydrology", In: Facets of hydrology volume II, Edited by J. C. Rodda. John Wiley and Sones Ltd. PP., 205-246.

Rodriguez. A. (1996), "Sustainability and economic viability of cereals growth under alternative treatments of water-harvesting in highland Balochistan, Pakistan, J. sustainable Agriculture, 8, pp. 47-59.

Rodriguez. A., Shah. N.A., Afzal. M, Mustafa.U. (1996), "Is water -harvesting in valley floors a viable option for increasing cereal production in highland Balochestan, Pakistan? J. Expl Agric, 32, pp. 305-315.

Romano, N., Brunone, B., Santini, A., (1998), " Numerical analysis of one-dimensional unsaturated flow in layered soils". Adv. Water resource. 21, pp. 315-324.

Rubin, J., (1966), "Theory of rainfall uptake by soils initially drier than their field capacity and its applications, Water resour. Res., V. 2, pp. 739-750.

Russel, E.D. (1998), "Soil conditions and plant growth (eleventh edition)," edited by Alan Vild, Department of Soil science, University of Readying.

Rydzewski. J. R., (1987), "Irrigation development planning", an introduction for engineers, John Wiley and Sons Ltd., London, UK.

Salvadori. Mario, G, and Baron. Melvin, L., (1961), "Numerical Methods In Engineering", Englewood Cliffs, N. J. Prentice-Hall, INC. United States Of America. 300 PP.

Salvucci, .G. D. (1997). "Soil and moisture independent estimation of stage-two evaporation from potential evaporation and albedo or surface temperature." J. Water resources research. Vol. 33 (1). PP. 111-122.

Samir El-Askari. Khaled Mohamed, (1994), " A computerised irrigation scheduling package for personal computers running under Windows", MSc thesis of irrigation engineering. Published by University of Southampton.

Schreiber, H. A., and Kincaid, D. R. (1967), " Regression models for predicting on-site runoff from short-duration convective storms". J. Water resources research, V 3 (2), PP. 389-395.

Scoging, Helen (1992), "Modelling overland flow hydrology for dynamic hydraulics", in Overland flow, Hydraulics and erosion mechanics. ED, by Parson . Anthony J & Abrahams. D.

SCS national engineering handbook. (1985). "Section 4: Hydrology, Chapter4." Soil Conservation Service, USDA, Washington, D. C.

Sen Zekai, (1978), " Autorun analysis of hydrologic time series", J. Hydrology, 36, PP. 75 – 85.

Sen Zekai, (1980), " Statistical analysis of hydrologic critical droughts", Journal of hydraulics division, Proceedings of the American Society of Civil Engineering, 106(HYI), PP. 99 – 115.

Sharifi, F. (1997), "An investigation into rainfall runoff processes aiming at simulating runoff from ungaged catchments" in Proceedings of the 8th international conference of Rainwater catchment systems, April 25-29, 1997. Tehran, I. R. Iran. Vol.1. PP. 500-516.

Sharma. K, Pareek .O. P., and Singh. H.P, (1982), "Effect of runoff concentration on growth and yield of Jujube", J. Agricultural water management, No. 5. PP. 73-84.

Sharma. K. D. (1986), " Runoff behaviour of water harvesting micro-catchments" J. Agricultural water management, vol. 11. PP. 137-144.

Sharma. T. C. (1996), " Simulation of the Kenyan longest dry and wet spells and the largest rain-sums using a Markov model". Journal of Hydrology 178, PP. 55-67.

Sharon, D., (1981), " The distribution in space of local rainfall in the Namib desert", J. Climatol., 1, PP. 69-75.

Shuttleworth, W. J., and Gurney, J. S. (1990). "The theoretical relationship between foliage temperature and canopy resistance in sparse crops." Quaterly J. Royal Meteorological Soc., 116, PP. 497-519.

Simuneh, J., Wendroth, O.,and M. Th. Van Genuchten. (1998), " Parameter Estimation Analysis of the Evaporation Method for Determining Soil Hydraulic Properties". Soil Sci. Am. J. 62. PP. 894 - 905.

Singh, V.P. (1988 and 1989), "Hydrologic system, Volum1, Rainfall runoff modelling. And Volume 2, Watershed modelling, Prentice Hall, Englewood Cliffs, NJ.

Smith, R. E., Corradini, C., and Melone, F. (1993), "Modelling infiltration for multi storm runoff events". Water Resour. Res., 29(1), 133-144.

Soil Conservation Service (SCS). (1986). "Urban hydrology for small watersheds, SCS." Tech. Release 55, U. S. Dept. of Agr., Engrg. Div., Washington, D. C.

Spiegel-Roy, P., Mazigh and Evenari, M. (1977). " Response of Pistachio to low soil moisture conditions". J. Amer. Soc. Hort. Sci. 104(4). 470-473.

Srivastava, R. C. (2001), "Methodology for design of water harvesting system for high rainfall areas". J. Agricultural water management 47. 37-53.

Staple, W. J. (1971). "Boundary conditions and conductivities used in the isothermal model of evaporation from soil." J. Sol Sci. Soc. Am. Proc. Vol. 35. PP. 853-855.

Steenhuis, Tammo S. Winchell Michael, Rossing Jane Zollweg James A, and Walter Machael F. (1995), " SCS Runoff Equation Revisited for Variable-Source Runoff Areas, J. Irrigation and Drainage Engineering, 121(3), pp. 234-238.

Stern, R. D. (1980), " The calculation of probability distribution for models of daily precipitation", J. Arch. Met. Geoph. Biokl., Ser, B, 28, PP.137-147.

Stern, R. D. and Coe, R. (1984), " A model fitting analysis of daily rainfall data. J. Roy. Statistic. Soc., A 147, 1-34.

Tabor, Joseph. A. (1995), " Improving crop yields in the Sahel by means of water-harvesting", J. Arid Environments, 30, pp. 83-106.

Tan, B. Q., and O'Connor, K. M. (1996). "Application of an empirical infiltration equation in the SMAR conceptual model." J. Hydrology 185, PP. 275-295.

Teare. D., and Peat. M. M, (1983), "Crop – Water Relations", A Widley-Interscience Publication, John Wiley & Sons. New York, Chichester, Brisbane, Toronto and Singapore.

Tomlin, A. D., Shipitalo, M. J., Edvards, W. M., and Protz, R. (1995), " Earthworms and their influence on soil structure and infiltration." In: Hendrix, P. F, Earthworm ecology and biogeography in North America. Lewis pub., Boca Raton, FL. pp. 159-183.

US Department of Agriculture, (1972), in SCS National Engineering Handbook, Section 4, Hydrology, USDA Soil Conserve. Serv., Washington, D. C., 548pp.

Van Dam, J.C., and Feddes, R.A., (2000), " Numerical simulation of infiltration, evaporation and shallow ground levels with the Richards equation". J, Hydrology 233, pp. 72-85.

Van Dijk, Ahmed Mohamed Hassan. (1993), "Opportunities for Expanding Water Harvesting in Sub Saharan Africa*: The* Case of the Teras of Kassala". Gatekeeper Series No. 40, pp. 1-19.

Van Genuchten, M. Th. (1980) " A closed-form equation for predicting the hydraulic conductivity of unsaturated soils, Soil Sci, Soc, Am. J., 44, 892-898.

Vandervaere, Jean. P., Vauclin, M. Haverkamp, R., and Peugeot, C. (1998). " Prediction of crust-induced surface runoff with disc infiltration data." J. Soil Science. Vol. 163 (1). PP.9-21.

Wang, G. T., and Chen, Shulin. (1996), "A linear spatially distributed model for a surface rainfall-runoff system", J. Hydrology, 185, pp. 183-198.

Wang, G. T., Singh. V. P., and Yu. F. X. (1992), "A rainfall-runoff model for small watersheds", J. Hydrology, 138. Pp. 97-117.

Warrick, A. W., (1991), " Numerical approximations of Darcian flow through unsaturated soil., Water Resource. Research. 27. PP. 1215-1222.

Withers, B., and Vipond, S. (1980), " Irrigation design and practice, 2nd ED., Cornell University Press,

Woolhiser. D. A, Keefer. T. O., and Redmond. K. T. (1993), "Southern oscillation effects on daily precipitation in the south-western United States". J. Water resources research, 29(4). PP. 1287-1295.

Yair, A. (1983), " Hill slope hydrology water harvesting and Arial distribution of some ancient agricultural systems in the northern Negev desert", J. Arid Environments, 6, pp. 283-301.

Yair, A. and Lavee, H. (1985), " Runoff generation in arid and semi-arid zones." In: M. G. Anderson and T. P. Burt. ed, Hydrological Forecasting, Wiley. Chichester, pp. 183-220.

Ye. W., Bates, B. C., Viney, N. R., and Sivapalan, M. (1997), "Performance of conceptual rainfall-runoff models in low-yielding ephemeral catchments", J. water resources research, Vol. 33, No. 1, pp. 153-166.

Yen. Ben. Chie., and Lee. K. T. (1997). "Unit hydrograph derivation for ungaged Watersheds by stream-order laws." J. Hydrologic engineering, Vol. 2 (1), PP. 1-9.

Zali. Abbas-Ali and Jafari-Shabestari. Jamshid (1994), " Introduction to Probability and Statistics (In Persian language)". Tehran University (Iran).

Zarmi. Y., Asher. Ben., and Greengard. T. (1983). " Constant velocity kinematics analysis of infiltration micro-catchment hydrograph." J. Water resources research, Vol. 19 (1). PP. 277-283.

Zhang, Jinquan. Wu., and Yang, Jinzhong,. (1996), " Analysis of Rainfall-recharge relationships". J. Hydrology, 177. PP. 143-160.

Zhan-Qian, Lu., and Berliner, L. M. (1999), " Markov switching series models with application to a daily runoff series", J. Water resources research, 35(2), PP. 523 – 534.